University of Windsor
Scholarship at UWindsor

Electronic Theses and Dissertations

2000

Bond strength and characteristics of carbon fibre-reinforced plastic (CFRP) bars in concrete beams.

Ee Yeong. Lim
University of Windsor

Follow this and additional works at: http://scholar.uwindsor.ca/etd

Recommended Citation
Lim, Ee Yeong., "Bond strength and characteristics of carbon fibre-reinforced plastic (CFRP) bars in concrete beams." (2000). *Electronic Theses and Dissertations.* Paper 1323.

This online database contains the full-text of PhD dissertations and Masters' theses of University of Windsor students from 1954 forward. These documents are made available for personal study and research purposes only, in accordance with the Canadian Copyright Act and the Creative Commons license—CC BY-NC-ND (Attribution, Non-Commercial, No Derivative Works). Under this license, works must always be attributed to the copyright holder (original author), cannot be used for any commercial purposes, and may not be altered. Any other use would require the permission of the copyright holder. Students may inquire about withdrawing their dissertation and/or thesis from this database. For additional inquiries, please contact the repository administrator via email (scholarship@uwindsor.ca) or by telephone at 519-253-3000ext. 3208.

INFORMATION TO USERS

This manuscript has been reproduced from the microfilm master. UMI films the text directly from the original or copy submitted. Thus, some thesis and dissertation copies are in typewriter face, while others may be from any type of computer printer.

The quality of this reproduction is dependent upon the quality of the copy submitted. Broken or indistinct print, colored or poor quality illustrations and photographs, print bleedthrough, substandard margins, and improper alignment can adversely affect reproduction.

In the unlikely event that the author did not send UMI a complete manuscript and there are missing pages, these will be noted. Also, if unauthorized copyright material had to be removed, a note will indicate the deletion.

Oversize materials (e.g., maps, drawings, charts) are reproduced by sectioning the original, beginning at the upper left-hand corner and continuing from left to right in equal sections with small overlaps.

Photographs included in the original manuscript have been reproduced xerographically in this copy. Higher quality 6" x 9" black and white photographic prints are available for any photographs or illustrations appearing in this copy for an additional charge. Contact UMI directly to order.

ProQuest Information and Learning
300 North Zeeb Road, Ann Arbor, MI 48106-1346 USA
800-521-0600

BOND STRENGTH AND CHARACTERISTICS OF CARBON FIBRE REINFORCED PLASTIC (CFRP) BARS IN CONCRETE BEAMS

by
Ee Yeong Lim

A Thesis
Submitted to the Faculty of Graduate Studies and Research
through the Department of Civil and Environmental Engineering
in Partial Fulfillment of the Requirements for
the Degree of Master of Applied Science at the
University of Windsor

Windsor, Ontario, Canada

2000

© 2000 Ee Yeong Lim

National Library of Canada
Acquisitions and Bibliographic Services
395 Wellington Street
Ottawa ON K1A 0N4
Canada

Bibliothèque nationale du Canada
Acquisitions et services bibliographiques
395, rue Wellington
Ottawa ON K1A 0N4
Canada

Your file Votre référence

Our file Notre référence

The author has granted a non-exclusive licence allowing the National Library of Canada to reproduce, loan, distribute or sell copies of this thesis in microform, paper or electronic formats.

The author retains ownership of the copyright in this thesis. Neither the thesis nor substantial extracts from it may be printed or otherwise reproduced without the author's permission.

L'auteur a accordé une licence non exclusive permettant à la Bibliothèque nationale du Canada de reproduire, prêter, distribuer ou vendre des copies de cette thèse sous la forme de microfiche/film, de reproduction sur papier ou sur format électronique.

L'auteur conserve la propriété du droit d'auteur qui protège cette thèse. Ni la thèse ni des extraits substantiels de celle-ci ne doivent être imprimés ou autrement reproduits sans son autorisation.

0-612-62242-8

Canada

ABSTRACT

An experimental investigation of bond strength and characteristics of Carbon Fibre Reinforced Plastic (CFRP) bars in concrete beams has been conducted at the University of Windsor. A total of twenty-eight concrete T-beams reinforced with CFRP bars was tested statically as simply supported beams. Three types of CFRP bars were used and three different parameters affecting bond characteristics were considered in the test program, namely (1) pressure induced on the bar due to support condition, (2) embedment length and (3) transverse reinforcement.

Results indicated that the average bond strength of the three types of CFRP bars varied from each other and depended primarily on their surface conditions. It was found that the tensile force in the CFRP bars increased when the bond length increased, but the average bond strength decreased when the bond length increased. Confinement provided by transverse reinforcement increased the average bond strength of CFRP bars and the average bond strength varied as $\sqrt{f_c'}$ when other factors were constant. However, the results gave no satisfactory information about the influences of support conditions on bond strength.

It has also been concluded that the expressions for development length and bond strength of conventional steel reinforcing bar provided in the CSA and ACI codes cannot be directly applied for the use of CFRP bars due to their inherent physical and mechanical properties. Preliminary expressions for bond strength of the three types of CFRP bars were developed, as well as expressions for development length depending on the types of CFRP bars.

ACKNOWLEDGEMENTS

The author wishes to express his great gratitude to his advisors, Dr. George Abdel-Sayed, Professor Emeritus of Department of Civil and Environmental Engineering, and Dr. Murty K. S. Madugula, Professor of Department of Civil and Environmental Engineering, for their invaluable guidance, advice and financial support throughout this research project.

The author is also thankful to Glasform Inc., USA and DFI Pultruded Composite Inc., USA for providing CFRP bars used in the experimental investigation program.

Special thanks to laboratory technicians, Mr. Richard Clark and Mr. Lucian Pop, for their technical assistance and support. Gratitude and thanks are also extended to graduated students, Mr. Sameh Salib and Mr. William Tape.

Technical writing assistance provided by Mr. Ron Dumouchelle, Instructor of the Academic Writing Center, is also grateful acknowledged. Acknowledgement is also extended to committee members for reviewing this document.

In the end, the author wishes to express his very special thanks to his loving parents for their love, care and financial support during the whole period of study at the University of Windsor.

TABLE OF CONTENTS

ABSTRACT		iii
ACKNOWLEDGEMENTS		iv
LIST OF FIGURES		ix
LIST OF TABLES		xii
LIST OF SYMBOLS		xiv
CHAPTER 1	INTRODUCTION	1
1.1	General	1
1.2	Bond Strength	2
1.3	Bond Failure	3
1.4	Development Length	4
1.5	Objectives	4
1.6	Research Significance	5
CHAPTER 2	LITERATURE REVIEW	7
2.1	General	7
2.2	Fibre Materials	7
2.2.1	Carbon Fibre	7
2.2.2	Aramid Fibre	8
2.2.3	Glass Fibre	8
2.3	FRP Reinforcement	8
2.4	Bond Test of Reinforcement	9
2.5	Published Research Work	9
2.5.1	Plain and Deformed Steel Reinforcing Bars	9
2.5.2	High Yield Strength Reinforcing Bars	11
2.5.3	FRP Reinforcement	12
2.6	Code Requirements	20
2.6.1	CSA Code	20
2.6.2	ACI Code	22
2.6.3	JSCE Standard	23
CHAPTER 3	EXPERIMENTAL INVESTIGATION	27
3.1	General	27

3.2 Purposes 27
3.3 Materials 28
3.3.1 CFRP Bars 28
3.3.2 Concrete 29
3.4 Testing Instrumentation 29
3.4.1 Hydraulic Jack and Load Cell 29
3.4.2 Strain Indicator and Switch & Balance units 29
3.4.3 Strain Gauges and Strain Gauge Cement 30
3.4.4 Dial Gauges 30
3.5 Formwork and Casting of Beam Specimens 30
3.5.1 Preparation of Formwork 30
3.5.2 Casting of Beam Specimens 31
3.6 Test Program 32
3.6.1 Tension Test 32
3.6.2 Beam Test 32
3.6.2.1 Details of Beam Specimens 32
3.6.2.2 Pressure Induced on The Bar Due to Support Condition 33
3.6.2.3 Embedment Length 34
3.6.2.4 Transverse Reinforcement 34
3.7 Test Setup 35
3.7.1 Setup of Test Beams 35
3.7.2 Attachment of Measuring Devices 35
3.7.3 Loading Configuration 35
3.7.4 Compression Test 36
3.8 Data Collection 36
3.8.1 Strain Readings 36
3.8.2 Dial Gauge Readings 36
3.8.3 Identification of Cracks 36
3.8.4 Compressive Strength 37

CHAPTER 4 EXPERIMENTAL RESULTS 52

4.1 General 52
4.2 Calculations Required 52
4.2.1 Calculation of Tensile Force 52
4.2.2 Calculation of Mean Bond Strength 53
4.2.3 Determination of K_1 and K_2 53
4.3 Results of Tension Tests 53
4.4 Results of G1-D8 and G1-D10 CFRP Bars 54
4.4.1 Pullout Test (G1-D8 CFRP Bar) 54
4.4.2 Beam Test (G1-D8 CFRP Bar) 54
4.4.3 Beam Test (G1-D10 CFRP Bar) 55
4.4.4 Comparison of Pullout and Beam Tests Results 56
4.5 Results of G2-D9.79 CFRP Bar 56

4.6 Results of D1-D9.70 CFRP Bar 58
4.7 Results of Leadline CFRP Bar 59
4.8 Summary of Test Results 60

CHAPTER 5 DISCUSSION OF TEST RESUTLS 101

5.1 General 101
5.2 Results of Tension Test 101
5.3 Comparison of Pullout and Beam Specimens 101
5.4 Effect of Bar Diameter 102
5.5 Effect of Pressure Induced on The Bar Due to Support Condition 102
5.6 Effect of Embedment Length 103
5.7 Effect of Transverse Reinforcement 103
5.8 Effect of Concrete Compressive Strength 104
5.9 Empirical Expression for Bond Strength of CFRP Bar 105
5.10 Relationships Between Applied Load and Slip 105
5.11 Appearance of Concrete After Test 105

CHAPTER 6 CONCLUSIONS AND RECOMMENDATIONS 108

6.1 Conclusions 108
6.2 Recommendations for Further Study 109

REFERENCES 110

APPENDIX

A Calibration Data and Curve of Universal Flat Load Cell 116

B Stress-Strain Data and Curve of G2-D9.79 CFRP Bar 119

C Stress-Strain Data and Curve of D1-D9.70 CFRP Bar 123

D Crack Pattern of Beams Reinforced with G1-D8 CFRP Bar 127

E Crack Pattern of Beams Reinforced with G2-D9.79 CFRP Bar 130

F Crack Pattern of Beams Reinforced with D1-D9.70 CFRP Bar 136

G Applied Load vs. Slip Curve (G1-D8 Bar) 142

H Applied Load vs. Slip Curve (G2-D9.79 Bar) 151

I	Applied Load vs. Slip Curve (D1-D9.70 Bar)	176
J	Load-Deflection Curve (G2-D9.79 Bar)	205
K	Load-Deflection Curve (D1-D9.70 Bar)	210
L	Tensile Force vs. Bond Length (G2-D9.79 bar, Free-end Slip)	216
M	Bond Strength vs. Bond Length (G2-D9.79 bar, Free-end Slip)	221
N	Bond Strength vs. Free-end Slip (G2-D9.79 bar)	226
O	Tensile Force vs. Bond Length (G2-D9.79 bar, Loaded-end Slip)	231
P	Bond Strength vs. Bond Length (G2-D9.79 bar, Loaded-end Slip)	235
Q	Bond Strength vs. $\sqrt{f_c'}$ (G2-D9.79 bar, Free-end Slip)	238
R	Effect of Transverse Reinforcement on Bond Strength (G2-D9.79 bar)	242
S	Tensile Force vs. Bond Length (D1-D9.70 bar, Free-end Slip)	247
T	Bond Strength vs. Bond Length (D1-D9.70 bar, Free-end Slip)	251
U	Bond Strength vs. Free-end Slip (D1-D9.70 bar)	255
V	Bond Strength vs. $\sqrt{f_c'}$ (D1-D9.70 bar, Free-end Slip)	260
W	Effect of Transverse Reinforcement on Bond Strength (D1-D9.70 bar)	264
X	Results of the CFRP Bond Test (Jerrett and Ahmad 1995)	267
VITA AUCTORIS		269

LIST OF FIGURES

Figure		
1.1	Free body diagram of embedded length	6
1.2	Splitting of concrete along reinforcement	6
1.3	Bond stress due to flexure	6
2.1	Classification of FRP reinforcement according to material	25
2.2	Classification of FRP reinforcement according to shape	25
2.3	Classification of test method for bond of CFRM	26
3.1(a)	Type A CFRP bar (G1-D8 and G1-D10)	41
3.1(b)	Types B and C CFRP bars (G2-D9.79 and D1-D9.70)	41
3.2	Types of transverse reinforcement	41
3.3	Picture of a complete formwork	42
3.4	Setup of tension test	42
3.5(a)	Cross-section of beam specimen	43
3.5(b)	Configuration of Group A beam specimen	44
3.5(c)	Configuration of Group B beam specimen	44
3.5(d)	Configuration of Group C beam specimen	45
3.6	Picture of steel roller supports	46
3.7(a)	Plan view of steel I-beam section support	46
3.7(b)	Cross-section view of steel I-beam section support	47
3.8(a)	Picture of steel I-beam section supports (plan view)	47
3.8(b)	Picture of steel I-beam section supports (side view)	48

3.9 Location of measuring devices and loading configuration 49

3.10(a) Picture of complete test setup of Group A beam specimen 50

3.10(b) Picture of complete test setup of Group A beam specimen (side view) 50

3.11(a) Picture of complete test setup of Groups B and C beam specimens 51

3.11(b) Picture of complete test setup of Groups B and C beam specimens (side view) 51

4.1 Beam specimen for calculation of tensile force by pure bending 83

4.2 Tensile force vs. bond length (G1-D8 bar, pullout test) 84

4.3 Bond strength vs. bond length (G1-D8 bar, pullout test) 85

4.4 Bond strength vs. $\sqrt{f_c'}$ (G1-D8 bar, pullout test) 86

4.5 Tensile force vs. bond length (G1-D8 bar, beam test) 87

4.6 Bond strength vs. bond length (G1-D8 bar, beam test) 88

4.7 Bond strength vs. $\sqrt{f_c'}$ (G1-D8 bar, beam test) 89

4.8 Tensile force vs. bond length (G1-D10 bar, beam test) 90

4.9 Bond strength vs. bond length (G1-D10 bar, beam test) 91

4.10 Bond strength vs. $\sqrt{f_c'}$ (G1-D10 bar, beam test) 92

4.11 Comparison of tensile force vs. bond length (G2-D9.79 bar, free-end slip) 93

4.12 Comparison of bond strength vs. bond length (G2-D9.79 bar, free-end slip) 93

4.13 Comparison of tensile force vs. bond length (G2-D9.79 bar, loaded-end slip) 95

4.14 Comparison of bond strength vs. bond length (G2-D9.79 bar, loaded-end slip) 96

4.15 Comparison of bond strength vs. $\sqrt{f_c'}$ (G2-D9.79 bar, free-end slip) 97

4.16 Comparison of tensile force vs. bond length (D1-D9.70 bar, free-end slip) 98

4.17 Comparison of bond strength vs. bond length (D1-D9.79 bar, free-end slip) 99

4.18 Comparison of bond strength vs. $\sqrt{f_c'}$ (D1-D9.70 bar, free-end slip) 100

5.1 Appearance of concrete cover of beams reinforced with G2-D9.79 bar 107

5.2 Appearance of concrete cover of beams reinforced with D1-D9.70 bar 107

LIST OF TABLES

Table		
3.1	Physical properties of G2-D9.79 and D1-D9.70 CFRP bars	38
3.2	Mechanical properties of CFRP bars	38
3.3	Proportioning of concrete mix	38
3.4	Concrete compressive strength of beam specimens	39
3.5	Detail of beam specimens	40
4.1	Pullout test results of G1-D8 CFRP bar	62
4.2	Beam test results of G1-D8 CFRP bar	63
4.3	Effect of transverse reinforcement on bond strength (G1-D8 bar)	64
4.4	Beam test results of G1-D10 CFRP bar	65
4.5	Comparison of bond strength obtained from pullout and beam tests	66
4.6	Comparison of maximum tensile force of G2-D9.79 CFRP bar	67
4.7	Tensile force at free-end slip of 0.05, 0.10 and 0.25 mm (G2-D9.79 bar)	68
4.8	Bond strength at free-end slip of 0.05, 0.10 and 0.25 mm (G2-D9.79 bar)	69
4.9	Tensile force at loaded-end slip of 0.10 and 0.25 mm (G2-D9.79 bar)	70
4.10	Bond strength at loaded-end slip of 0.10 and 0.25 mm (G2-D9.79 bar)	71
4.11	Summary of calculations for G2-D9.79 CFRP bar at free-end slip	72
4.12	Summary of calculations for G2-D9.79 CFRP bar at loaded-end slip	73
4.13	Effect of support condition on bond strength (G2-D9.79 bar)	74
4.14	Effect of transverse reinforcement on bond strength (G2-D9.79 bar)	75
4.15	Comparison of maximum tensile force of D1-D9.70 CFRP bar	76
4.16	Tensile force at free-end slip of 0.05 and 0.10 mm (D1-D9.70 bar)	77

4.17 Bond strength at free-end slip of 0.05 and 0.10 mm (D1-D9.70 bar) 78

4.18 Summary of calculations for D1-D9.70 CFRP bar at free-end slip 79

4.19 Effect of support condition on bond strength (D1-D9.70 bar) 80

4.20 Effect of transverse reinforcement on bond strength (D1-D9.70 bar) 81

4.21 Summary of the test results of different types of CFRP bars 82

LIST OF SYMBOLS

ε	average strain of reinforcement
Σo	circumference of reinforcement
α_1	coefficient
α_2	modification factor for bond strength
ϕ	reduction factor
a	shear span
A_b	nominal cross-sectional area of reinforcement
A_t	area of transverse reinforcement
c	downward cover of main reinforcement or half of the space between the anchored reinforcement whichever is the smaller
d_b	nominal diameter of reinforcement
E_f	modulus of elasticity of reinforcement
E_o	standard modulus of elasticity
E_t	modulus of elasticity of transverse reinforcement
f_{bod}	design bond strength of concrete
f_c'	compressive strength of concrete
f_{ck}'	characteristic compressive strength of concrete
f_d	design tensile strength of reinforcement
f_f	tensile strength of the reinforcement
f_{fu}	ultimate tensile strength of reinforcement
f_s	stress developed in the reinforcement
f_y	yield strength of reinforcement
f_{yf}	effective yield strength of reinforcement
j	distance between resultant tensile and compressive forces
K_1	coefficient of bond strength
K_2	coefficient of development length
k_1	modification factor for bar location
k_2	modification factor for coating
k_3	modification factor for concrete density

k_4	modification factor for bar size
l_b	bond length
l_d	development length of reinforcement
l_{db}	basic development length of reinforcement
M	bending moment
P	applied load
s	distance between the centers of the transverse reinforcement
T	bar force to be anchored = tensile force
u	mean bond strength
u_{max}	maximum mean bond strength

CHAPTER 1

INTRODUCTION

1.1 General

Concrete is made by mixing cement, water, fine aggregate (sand), coarse aggregate, and frequently other additives (that modify properties). The hardened concrete without reinforcement is strong in compression, but it is weak in tension. Steel reinforcing bars are normally used in the tension side of concrete structures to overcome the tensile limitation.

Steel is a high strength material. When properly protected from ion attack, steel reinforcement can last for decades without exhibiting any visible signs of deterioration. However, it is not always possible to provide this kind of corrosion protection. Insufficient concrete cover, poor design or workmanship and presence of humidity and/or aggressive agents can lead to cracking of the concrete and corrosion of the steel reinforcing bars.

Much effort has been directed towards the design of new structures to reduce or eliminate the corrosion problems through the increase of the concrete cover, using epoxy coated steel and stainless steel. These methods are not cost-effective or efficient to solve the long-term corrosion problems. Another uncommon method is to use cathodic protection. This method significantly increases the cost and complexity of concrete system.

In recent years, advanced composite material (also known as Fibre Reinforced Plastic (FRP)) in concrete structures has been an alternative for concrete reinforcement. The FRP composites offer several significant benefits such as: (1) non-corrosive (2) high tensile strength (3) light weight (4) non-conductive (5) excellent fatigue resistance and (6) magnetic transparency.

Currently, standard codes and/or specifications for the application of FRP reinforcement in concrete structural design are being developed. Much research has been conducted to develop a database and to gain more confidence in using these promising composite materials. Researches have also been directed at the bond performance of FRP bars in concrete structures. The bond design relates to more reliable assessment of both the demand and supply sides of the anchorage/development design problem. Proper consideration of the conditions affecting bond is necessary to limit slippage of reinforcing bar relative to concrete. Bond strength and development length of reinforcement are briefly discussed in the following sections.

1.2 Bond Strength

Early design of reinforced concrete structures was based on the assumption that slip of reinforcement had to be prevented in order to minimize cracking, to develop flexural and shear strengths and to maintain the composite behaviour of reinforced concrete components. The transfer of axial force from a reinforcing bar to the surrounding concrete results in the development of shear-type stresses along the contact surface. The stress acting parallel to the bar along the interface is called bond stress and is

denoted by u per unit area of bar surface. The bond strength of a reinforcing bar can be established experimentally by measuring the force needed to produce excessive slippage or pullout of a bar embedded in concrete. If shear-type bond stresses, u, of constant magnitude are assumed to act uniformly on the bar's surface over the anchorage length l_b, equilibrium of the bar, as shown in Figure 1.1, gives

$$u\sum_o l_b = T$$

$$u = \frac{T}{\sum o l_b} = \frac{d_b f_s}{4 l_b} \qquad (1.1)$$

Past experience and investigations (Lutz and Gergely 1967) have concluded that the bond strength of steel is a function of bar diameter and that the average bond strength varied approximately in proportion to $\sqrt{f_c'}$. The bond strength may be written as follows.

$$u = \frac{K_1\sqrt{f_c'}}{d_b} \qquad (1.2)$$

where K_1 is a coefficient .

1.3 Bond Failure

Factors that contribute to bond strength are chemical adhesion, friction and bearing of the bar deformations (also referred to as ribs or lugs) against concrete. The mechanisms that initiate bond failure may involve a breakup of adhesion between the bar and the concrete, longitudinal splitting of the concrete around the bar, crushing of the concrete in front of the bar ribs, shearing of the concrete key between the ribs along a cylindrical surface surrounding the ribs, or any combinations of the above. When bond failure occurs, it results generally in splitting of concrete along the bars, either in vertical

planes as in Figure 1.2(a) or in horizontal plane, Figure 1.2(b). If the bars were greased or lubricated in concrete beam, the bars would slip longitudinally with respect to the adjacent concrete, which would experience tensile strain due to flexure, as shown in Figure 1.3.

1.4 Development Length

The development length, l_d, is the length necessary to introduce or develop a given stress into the bar through bond. The concept of development length is that a certain minimum length of bar is needed on either side of a point of maximum steel stress to prevent the bar from pulling out. The value of l_d may be obtained from Equation (1.1)

$$l_d = \frac{f_s d_b}{4u} \qquad (1.3)$$

Substituting Equation (1.1) into Equation (1.2), the development length of reinforcement can also be expressed as follows.

$$l_d = K_2 \frac{A_b f_s}{\sqrt{f_c'}} \qquad (1.4)$$

where K_2 is a coefficient.

1.5 Objectives

The purpose of the experimental program presented here is to investigate the bond strength and characteristics of carbon fibre reinforced plastic (CFRP) bars in concrete beams. The bond characteristics are examined using bond tests by beam specimens. The research program included the following specific tasks.

a. Development of an experimental expression for the bond strength of concrete beams reinforced with CFRP bar.

b. Development of an expression for the development length of concrete beams reinforced with CFRP bar.

c. Investigation of the effect of pressure induced on the bar due to support condition of concrete beams on bond strength.

d. Investigation of the effect of embedment length of CFRP bars on bond strength.

e. Investigation of the effect of transverse reinforcement on bond strength.

1.6 Research Significance

Currently, limited data are available on the bond behaviour of FRP bars in concrete members while design guidelines provided in CSA 23.3-M94 (and CSA 23.3-M84) and ACI 318-93 (and ACI 318-89) for steel cannot be directly used for FRP bars due to inherent differences in surface deformations and mechanical properties. Therefore, there is an urgent need to investigate the bond characteristics of FRP reinforcing bars in concrete structures. The experimental results contribute to the guidelines for future FRP development and its usage.

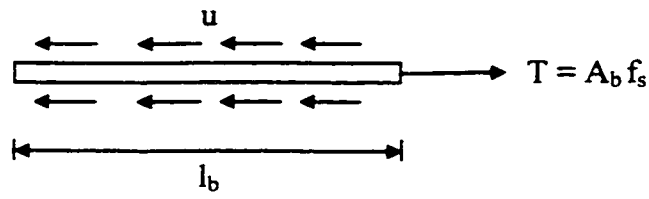

Figure 1.1: Free body diagram of embedded length l_b

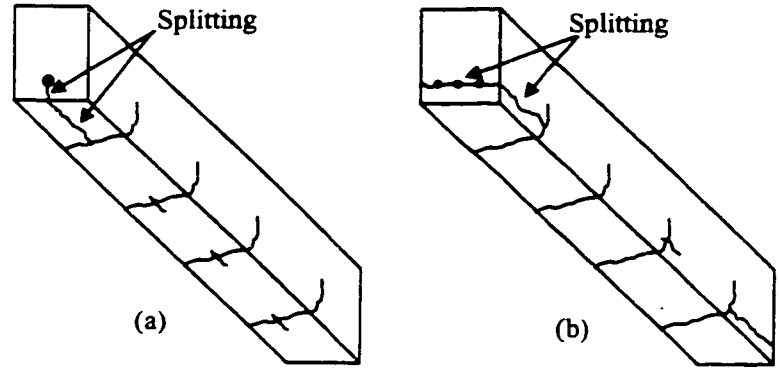

Figure 1.2: Splitting of concrete along reinforcement
(Source: Nilson, 1991)

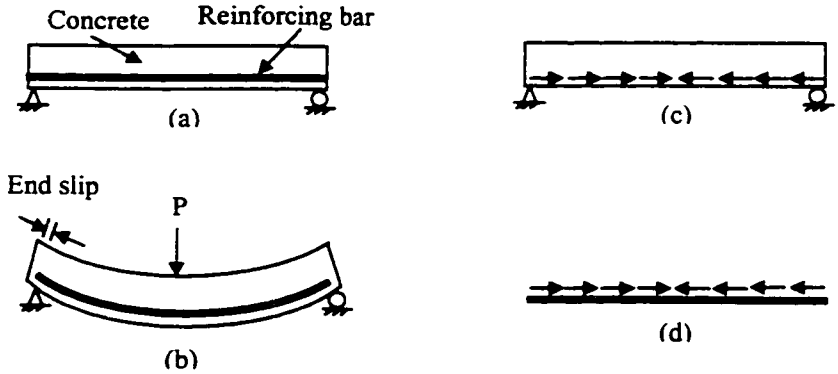

Figure 1.3: Bond stress due to flexure (a) beam before loading (b) unrestrained slip between concrete and reinforcement (c) bond forces acting on concrete (d) bond forces acting on reinforcement (Source: Nilson, 1991)

CHAPTER 2

LITERATURE REVIEW

2.1 General

This chapter briefly reviews FRP materials and their general characteristics. A review of published research work conducted to determine the bond characteristics of steel and FRP reinforcements is also included

2.2 Fibre Materials

At present, a number of fibre materials are studied for application in structural engineering. They include carbon fibres, aramid fibres and glass fibres. A brief discussion of each fibre is as follows. Figure 2.1 outlines the classification of FRP reinforcement according to material type.

2.2.1 Carbon Fibre

Carbon fibre is made from either petroleum or coal pitch and polyacrylic (PAN). Each fibre is between 5 and 20 μmm in diameter, and is an aggregate of imperfect fine graphite crystals. Its characteristics differ depending on the composition and orientation of the crystals. Commercially available carbon fibres are classified into pitch carbon and PAN carbon fibres: the pitch carbon being ordinary or high Young's modulus fibre; and the PAN carbon, high strength or high Young's modulus fibre.

2.2.2 Aramid Fibre

Three types of aramid fibres are available commercially bearing trade names such as Kevlar, Twaron and Technora. Kevlar and Twaron are aromatic polyamide fibres whose nuclei are bonded linearly by aramid. Technora, on the other hand, is an aromatic polyetheramide fibre whose nuclei are bonded by ether.

2.2.3 Glass Fibre

Two types of glass fibres are commercially available for use as continuous fibre materials, namely E-glass fibre and alkali-resistant glass fibre. The E-glass fibre contains large amounts of boric and aluminate, while the alkali-resistant glass fibre contains a considerable amount of zirconia, which serves to prevent corrosion by alkali attacks from cement matrixes.

2.3 FRP Reinforcement

When using continuous fibres such as carbon, aramid or glass as reinforcing materials for concrete, the fibres are bonded and processed by impregnating them with binding agents, for example, epoxy resins or vinyl ester resins. The fibres may be formed as one-dimensional bars, two-dimensional grids or three-dimensional textiles. As an alternative for steel reinforcement, the bars in general are processed by the pultrusion method, in which fibres are shaped while subjected to a specific tension to prevent static fracture by eliminating twists from the fibres and allowing uniform tensile stress. Further, to ensure good bonding with concrete, the fibres are braided, wound around the surface in

a spiral pattern or coated with sand. The classification of FRP reinforcement according to shape may be seen in Figure 2.2.

2.4 Bond Test of Reinforcement

Pullout and flexure beam tests are the two tests used by most researchers to determine bond performance of reinforcement in concrete members. A summary of test method for bond of continuous FRP bars may be seen in Figure 2.3.

2.5 Published Research Work

Standard guidelines for determination of bond strength in steel reinforced concrete members are well established and available elsewhere; however, these guidelines should be modified in the case of FRP reinforcement. FRP has no or slightly effectuate ridges (deformed surface) and has relatively high tensile strength. The following summarizes the work being done to determine the bond characteristics of steel and FRP reinforcements.

2.5.1 Plain and Deformed Steel Reinforcing Bars

For steel bars, two basic hypotheses were used to determine bond strength between the reinforcing bar and its surrounding concrete. The first hypothesis considered bond strength as a linear function of slip (Nilson 1971; Mirza and Houde 1979). Mathey and Watstein (1961) investigated bond in beams and pullout specimens and suggested that either a loaded-end slip of 0.25 mm (0.01 in.) or a free-end slip of 0.05 mm (0.002 in.) used to define the "critical" bond strength, depending on which of these slips

developed first. Slips greater than these limits were usually accompanied by large crack widths which may not be acceptable (Park and Paulay 1975). Ferguson et al. (1965) also concluded that the embedment length had only a minor effect on the stress attained by any steel bar until the loaded-end slip reached 0.25 mm (0.01 in.). The second hypothesis assumed that bond strength related only to the steel strength (Glanville 1913). Kankam (1997) tested double pullout test specimens reinforced with 25 mm diameter plain round mild steel, cold worked and hot-rolled ribbed bars to establish a fundamental relationship based on the two hypotheses. KanKam developed prediction models for each type of reinforcing bars.

Bond strength of plain rebars was lower than that of deformed rebars (Mo et al. 1996; Kankam 1997) since plain rebars had no surface deformation and no bearing component. It was reported that the maximum bond strength of plain rebar was $1.0 - 2.0$ MPa as compared to $6.0 - 6.7$ MPa high yield ribbed bars (Kankam 1997). Deformed bars were considered simply as plain bars with better bond properties. A comprehensive study of the mechanics of bond of deformed bars in concrete was conducted by Lutz and Gergely (1967). They noted that plain bars depended primarily on chemical adhesion and friction. However, deformed bars depended primarily on mechanical interlocking between concrete and steel (Treece and Jirsa 1989). Chemical adhesion and friction were secondary.

2.5.2 High Yield Strength Reinforcing Bars

Mathey and Watstein (1961) investigated bond of eighteen beam and eighteen pullout specimens consisting of deformed reinforcing bars with a nominal yield strength of 689.5 MPa (100 ksi). Two different diameters were used, 12.7 mm (0.5 in) and 25.4 mm (1 in.), and the embedment lengths ranged from 178 mm (7 in.) to 432 mm (17 in.) for 12.7 mm diameter bars and from 178 mm (7 in.) to 864 mm (34 in.) for 25.4 mm diameter bars. The test procedures and beam specimens were as described in the report of the ACI Committee 208 (1958). It was concluded that, for a bar of a given size, bond strength decreased with increase in the embedment length. The bond strength also decreased with an increase in the bar diameter for a given length-diameter ratio. The ultimate bond strengths in the pullout specimens agreed in general with the values obtained from beams with 12.7 mm diameter bars. However, for 25.4 mm diameter bars, the bond strengths in pullout specimens were significantly greater than the values obtained from beams.

A similar test was conducted by Ferguson et al. (1962). Bar diameters of 9.5 mm (0.375 in.), 22.2 mm (0.875 in.) and 34.9 mm (1.375 in.) having yield point of 517 MPa (75 ksi) were investigated. A total of seventy-six beams was investigated including variables such as strength of concrete, clear cover over bars, development length, bar size, effect of stirrups, etc. It was concluded that diagonal tension was a complicating factor when bars split out in bond. The developed bond strength was lower as the development length for larger bars was increased, but the bond strength showed to be primarily a function of length rather than bar size. Ultimate bond strength varied as $\sqrt{f_c'}$

when other factors were constant. Results also indicated that the width of the beam was a significant factor in ultimate bond strength developed.

2.5.3 FRP Reinforcement

A test method for evaluation of bond of FRP reinforcement and specific design guidelines has not yet been standardized (Mochizuki et al. 1993). It depends primarily on researchers' point of view and application. Recommendations for design and construction of concrete structures using continuous fibre reinforcing materials (CFRM) has been given by the Research Committee on CFRM, Japan Society of Civil Engineers (Machida 1993, 1997; Okamura et al. 1993; Sonobe et al. 1997). In the mean time, development of design guidelines has also been undertaken by the ACI Committee 440 (1996).

Abdel-Sayed et al. (1998) conducted bond tests by testing seven pullout and eighteen T-shaped beam specimens reinforced with either 8 or 10 mm diameter Glasform CFRP bars. The bond strengths of pullout and beam specimens were calculated based on a free-end slip of 0.10 mm. It was found that bond strengths, which were obtained from the pullout specimens reinforced with 8 mm diameter CFRP bars, ranged from 1.32 MPa (192 psi) to 4.31 MPa (625 psi). For beams reinforced with 8 mm diameter CFRP bars, the ultimate bond strength ranged from 3.30 MPa (479 psi) to 5.66 MPa (821 psi) and for 10 mm diameter CFRP bars, the ultimate bond strength ranged from 4.36 MPa (632 psi) to 5.02 MPa (728 psi). Comparison of the two tests showed that the ultimate bond strengths obtained from beam specimens were relatively higher than and more consistent than the bond strength obtained from the pullout tests. Abdel-Sayed noted that the results

obtained from pullout tests may not be directly applied for design but it could serve only as a guide for bond evaluation. A preliminary expression for bond strength of Glasform CFRP bars was suggested as follows.

$$u = \frac{2.45\sqrt{f_c'}}{d_b} \leq 470 psi \qquad \text{(U. S. Units)}$$

where u = bond strength (psi);

f_c' = compressive strength of concrete (psi);

d_b = nominal diameter of CFRP bar (in.).

A different way of testing for bond of CFRP bars was conducted by Jerrett and Ahmad (1995). The CFRP bars were manufactured by Mitsubishi Kasei Corporation under the trade name Leadline. The bond tests were conducted on three concrete slabs containing three smooth rods and three deformed rods each. The slabs thicknesses were 152 mm, 305 mm and 457 mm. The results showed that deformed rods, as compared to the smooth rods, had a higher load at which there was initial free end displacement and showed an ability to obtain significantly higher short-term loads after initial free end displacement. The reserve strength factor, defined as the ratio of ultimate load to the load at initial free end displacement, was 1.0 for the smooth rods and ranged from 3.5 to 9 for deformed rods. The loads of smooth and deformed rods at initial free end displacement and at ultimate load varied almost linearly with embedment length. The average bond strength for smooth rods at failure was 417 kPa (61 psi). For the deformed rods, the average bond strength at initial free end displacement was 1630 kPa (236 psi) and the average bond strength associated with the maximum load was 7440 kPa (1080 psi).

Bond strength of glass fibre reinforced plastic (GFRP) bars embedded in concrete beams was studied by Benmokrane et al. (1995, 1996, 1997) and Tighiouart et al. (1998). Four different nominal diameters of GFRP and steel rebars, namely 12.7 mm, 15.9 mm, 19.1 mm and 25.4 mm, were used in order to investigate the effect of bar diameter on the bond strength. Three embedment lengths, namely 6, 10 and 16 times bar diameter, were used in order to investigate the effect of embedment length on the bond strength. The bond tests were conducted by beam specimens in accordance with the RILEM specifications (RILEM 1978) for testing beams. It was generally believed that beam tests could realistically simulate the stress conditions of reinforced concrete elements subjected to bending. The direct pullout test was also conducted on a concrete wall (1200 x 760 x 400 mm) reinforced with the FRP bars placed at top, bottom and middle of the wall in order to investigate the top bar effect. Simple pullout specimens, according to ASTM C234, were also made by placing one GFRP rebar at the center of a 255 x 400 mm concrete cylinder. The anchorage length was kept at 380 mm.

According to the RILEM specifications (RILEM 1978), bond strength was quantified at different slips at each end of the reinforcement. The average bond strengths at 0.01 mm, 0.10 mm and 0.20 mm and the maximum bond strength with the corresponding type and diameter of the reinforcing bars were evaluated. Test results showed that the average bond strength of GFRP reinforcing bars decreased as the reinforcing bar diameter increased. The bond strength of GFRP reinforcing bars was lower (60 to 90 percent) than that of steel reinforcing bars (Larralde et al. 1993). The bond strength from beam tests was lower (55 to 95 percent) than that from pullout tests.

Furthermore, distributions of tensile and bond stresses along the embedment portion of GFRP reinforcing bars were nonlinear (Larralde et al. 1993). The bond stresses were exponentially distributed along the embedment length before debonding. The maximum bond stress moved progressively towards the free end of the reinforcing bars with increasing load. The basic equations of development length and bond strength, based on a free-end slip of 0.01 mm, for the use of GFRP bars were developed as shown in the following:

$$l_{db} = \frac{0.064 A_b f_f}{\sqrt{f_c'}} \text{ (SI Units)} \quad \text{and} \quad u = \frac{4.97\sqrt{f_c'}}{d_b} \text{ (SI Units)}$$

where l_{db} = basic development length (mm);

A_b = nominal cross-sectional area of GFRP bar (mm^2);

f_f = tensile strength of GFRP bar (MPa);

f_c' = compressive strength of concrete (MPa);

u = mean bond strength (MPa);

d_b = nominal diameter of GFRP bar (mm).

Daniali (1992) investigated bond strength of GFRP bars by testing thirty beams in accordance with the recommendation of the ACI Committee 208 (1958). These beams were reinforced with 12.7 mm (0.5 in.), 19.1 mm (0.75 in.) or 25.4 mm (1 in.) diameter FRP bars and 9.5 mm (0.375 in.) diameter FRP shear reinforcements having varying embedment lengths. Tension failure of reinforcement, pullout failure and splitting failure were observed during the tests. Daniali found that the cover splitting could be prevented by providing shear reinforcements in the constant moment regions. It was concluded that

the development length varied from 203 mm (8 in.) for 12.7 mm diameter bars to 762 mm (30 in.) for 25.4 mm diameter bars.

The average bond strength and development length of aramid FRP (AFRP) bar were around 13 MPa and 55 mm (Saafi and Toutanji 1998). Pleimann (1987, 1991) conducted pullout tests by examining the bond strength of glass, aramid FRP and steel bars. Three different diameters of GFRP bars, namely 6.35 mm (0.25 in.), 9.53 mm (0.375 in.) and 12.7 mm (0.5 in.) and one 9.53 mm (0.375 in.) diameter of AFRP were tested. Pleimann proposed that the development lengths of glass and aramid bars could be evaluated according to the following equations:

$$\text{For GFRP bar, } l_d = \frac{A_b f_{fu}}{42\sqrt{f_c'}} \quad \text{(SI Units)}$$

$$\text{For AFRP bar, } l_d = \frac{A_b f_{fu}}{49\sqrt{f_c'}} \quad \text{(SI Units)}$$

where l_d = development length of FRP reinforcement (mm);

A_b = cross-sectional area of FRP reinforcement (mm^2);

f_{fu} = ultimate tensile strength of FRP reinforcement (MPa);

f_c' = compressive strength of concrete (MPa).

A similar equation for basic development length of FRP rebars was developed by Faza and GangaRao (1993) by applying a reduction factor $\phi = 0.75$ to the ultimate tensile capacity of the rebar. Thus, a reduced bond strength value was assumed. They concluded that the ACI basic development equation should be modified to account for the use of FRP rebars. The modified development equation was as follows.

$$l_{db} = 0.028\frac{A_b f_{yf}}{\sqrt{f_c'}} \qquad \text{(SI Units)}$$

where l_{db} = basic development length of FRP bar (mm);

A_b = cross-sectional area of FRP bar (mm^2);

f_{yf} = effective yield strength of FRP bar (MPa) (taken as 80% of the ultimate strength of FRP bar);

f_c' = compressive strength of concrete (MPa).

It was noted that each of the above studies considered only a small number of parameters that influence bond performance of FRP bars. Thus, those studies may not result in comprehensive design guidelines. An extensive investigation of the bond strength of GFRP bars was conducted by Ehsani et al. (1993) and Ehsani et al. (1996). A total of one hundred and two specimens, including forty-eight beam specimens, eighteen pullout specimens and thirty-six hooked rebar specimens, was constructed and tested. Variables included in the study were concrete compressive strength, embedment length, clear concrete cover, rebar diameter, concrete cast depth, radius of bend and tail length. Based on the theoretical analysis of test results, it was recommended that the allowable slips at the loaded-end and free-end of GFRP bars be limited to 0.38 mm (0.015 in.) and 0.064 mm (0.0025 in.), respectively. A minimum development length of 381 mm (15 in.) must be provided. The equations for the basic development length and bond strength were presented in the following:

$$l_{dh} = \frac{0.022 A_b f_y}{\sqrt{f_c'}} \text{ (SI Units)} \qquad \text{and} \qquad u = \frac{14.25\sqrt{f_c'}}{d_b} \text{ (SI Units)}$$

where l_{db} = basic development of straight rebar (mm);

A_b = nominal cross-sectional area of rebar (mm^2);

f_c'= compressive strength of concrete (MPa);

f_y = tensile strength of rebar (MPa);

d_b = rebar diameter (mm).

Another study related to physical and mechanical properties of FRP rods was conducted by Khin et al. (1994). Three different types of FRP reinforcements, namely seven CFRP rods, four AFRP rods and one vinylon FRP rod, were examined by pullout tests according to the provisional testing procedures of Japan Society of Civil Engineers (JSCE). Test results indicated that the maximum bond strengths ranged from 4.3 MPa to 15.3 MPa for carbon rods, 7.7 MPa to 12.6 MPa for aramid rods and 9.2 MPa for vinylon rod. Khin et al. concluded that bond strength of FRP rods in concrete depended not only on the surface condition of the rods but also on the fibre type, fibre strength, spiral rod adhesion and spiral strength of spiral FRP rods.

Yamasaki et al. (1993) examined bond characteristics of three kinds of fibre materials (carbon, glass and aramid) of different deformed shapes (spiral, straight, sanded-straight, sand-braided, deformed and 7-piece stranded) by pullout tests. Bond strength at free end slip of 0.10 mm and maximum bond strength were determined for FRP bars of different raw materials and surface conditions. It was concluded that (1) the bond strength at initial slip and the maximum bond strength were more likely to differ with the surface of the continuous fibre bars than with the kinds of fibre materials; (2) the loaded-end slip could be roughly estimated from the free-end slip; (3) applying sand

particles to the surface of straight bars provided the bond strength equivalent to that of the deformed bar; (4) the bond strength of straight of bars almost equaled that of the round steel bars.

A similar study on different shape of surface and cross-section of FRP bars were conducted by Makitani et al. (1993). Results showed that the bond strength of FRP bars increased considerably if the surface of bars was processed in spiral type and covered by sand.

An experimental program consisting of three series of tests was conducted by Kanakubo et al. (1993) in order to investigate the bond performance of concrete members reinforced with FRP bars (carbon, glass and aramid). The first, second and third series of tests were simple bond test, cantilever type bond test and anti-symmetrical loading test, respectively. The test variables were the types of longitudinal bars, lateral reinforcement, percentage of lateral reinforcement and concrete type. The first series of test results showed that the bond splitting strength could be estimated using ratio of lug height to diameter of FRP bars. Results obtained from cantilever type bond tests indicated that the tendency of the bond splitting strength without lateral reinforcement was equal to that of the first test and the increment of the strength caused by lateral reinforcement could be evaluated in terms of its percentage and elastic modulus. Bond strength obtained from the anti-symmetrical loading test agreed with the results obtained from the former two tests. Thus, Kanakubo concluded that bond performance of beam could be predicted from results of the cantilever type of bond test.

Much of FRP research work has been conducted on GFRP for non-prestressed reinforcement. As pointed out by Erki and Rizkalla (1993), GFRP was the least expensive type of FRP reinforcement available in the market and was proposed for non-prestressed reinforcement. Surface treatments such as sand coating and external fiber windings were used to produce a rough or ribbed surface to improve the bond between the rebar and its surrounding concrete.

2.6 Code Requirements

The code requirements for bond and/or basic development length of concrete reinforcement are outlined in the following sections. Three different codes are included and examined, namely Canadian Standards Association specification (CSA standard A23.3-84 and A23.3-94 Design of Concrete Structures) and American Concrete Institute specification (ACI 318-89 Building Code Requirement for Reinforced Concrete and Commentary) and Japan Society of Civil Engineers (JSCE) recommendations for design and construction of concrete structures using continuous fibre reinforcing materials.

2.6.1 CSA Code

According to CAN3-A23.3-M84, the basic development length, l_{db}, in millimeters, of deformed steel bars and deformed wire in tension can be calculated as follows.

For 35.7 mm diameter bar and smaller, $l_{db} = \frac{0.019 A_b f_y}{\sqrt{f_c'}}$ but not less than $0.058 d_b f_y$

For 43.7 mm diameter bar, $l_{db} = \frac{26 f_y}{\sqrt{f_c'}}$

For 56.4 mm diameter bar, $l_{db} = \frac{34 f_y}{\sqrt{f_c'}}$

For deformed wire, $l_{db} = \frac{0.36 d_b f_y}{\sqrt{f_c'}}$

In the edition of CAN3-A23.3-M94, the development length, l_{db}, of deformed bars and wires in tension are given in the following form.

$$l_{db} = 0.45 k_1 k_2 k_3 k_4 \frac{f_y}{\sqrt{f_c'}} d_b$$

where k_1, k_2, k_3 and k_4 are modification factors for bar location, coating, concrete density and bar size, respectively.

The basic development length, l_{db}, may be modified by multiplying applicable modification factors. These modification factors are for top reinforcement, reinforcement with yield strength, f_y, great than 400 MPa, low density concrete, reinforcement direction and spacing, reinforcement in excess of that required by analysis and reinforcement enclosed with spiral reinforcement. These modification factors may be found in CSA specification clauses 12.2.3, 12.2.4 and 12.2.5. The development length, l_d, shall not be less than 300 mm.

The empirical expression for bond strength is as follows.

$$u = \frac{19.7\sqrt{f_c'}}{d_b} \quad \text{(SI Units)}$$

2.6.2 ACI Code

According to ACI 318M-89/318RM-89, the basic development length, l_{db}, can be calculated as follows.

SI Units:

For 35.7 mm diameter bar and smaller and deformed wire, $l_{db} = \frac{0.02 A_b f_y}{\sqrt{f_c'}}$

For 43.7 mm diameter bar, $l_{db} = \frac{25 f_y}{\sqrt{f_c'}}$

For 56.4 mm diameter bar, $l_{db} = \frac{40 f_y}{\sqrt{f_c'}}$

U.S Units:

For 35 mm (1.375 in.) diameter bar and smaller and deformed wire, $l_d = \frac{0.04 A_b f_y}{\sqrt{f_c'}}$

For 44.5 mm (1.75 in) diameter bar, $l_d = \frac{0.085 f_y}{\sqrt{f_c'}}$

For 57.2 mm (2.25 in.) diameter bar, $l_d = \frac{0.125 f_y}{\sqrt{f_c'}}$

There are modification factors to account for bar spacing, amount of cover and enclosing transverse reinforcement. These modification factors can be found in clauses 12.2.3.1 through 12.2.3.6. The development length, l_d, shall not be less than 300 mm (12 in.).

The empirical expression for bond strength is as follows.

$$u = \frac{9.5\sqrt{f_c'}}{d_b} \quad \text{(U. S. Units)}$$

2.6.3 JSCE Standard

According to the recommendations for design and construction of concrete structures using continuous fibre reinforcing materials of Japan Society of Civil Engineers (JSCE), the basic development length of tensile reinforcement types which undergo bond splitting failure may be calculated as follows.

$$l_d = \alpha_1 \frac{f_d}{4 f_{bod}} d_b \geq 20 d_b$$

where $f_{bod} = 0.28\alpha_2 f'^{2/3}_{ck} / \gamma_c (N/mm^2) \leq 3.2 N/mm^2$;

α_1 = coefficient;

α_2 = modification factor for bond strength;

f_d = design tensile strength of reinforcement (MPa);

d_b = diameter of reinforcement (mm);

f_{ck}' = characteristic compressive strength of concrete (MPa);

γ_c = 1.3

The value of α_1 depends on the value of k_c which can be calculated as follows.

$$k_c = \frac{c}{d_b} + \frac{15 A_t}{s d_b} * \frac{E_t}{E_o}$$

where c = downward cover of main reinforcement or half of the space between the anchored reinforcement whichever is the smaller (mm);

d_b = diameter of reinforcement (mm);

A_t = area of transverse reinforcement (mm^2);

s = distance between the centers of the transverse reinforcement (mm);

E_t = modulus of elasticity of transverse reinforcement (MPa);

E_o = standard modulus of elasticity (200 MPa).

In addition, the development length may also be modified by modification factors such as location of reinforcement.

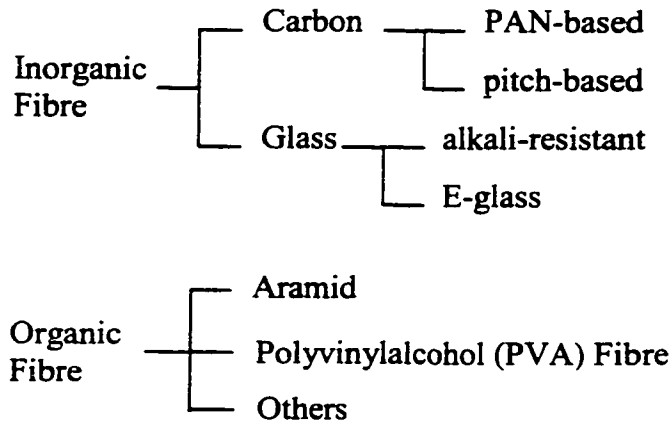

Figure 2.1: Classification of FRP reinforcement according to material
(Source: Fukuyama, 1999)

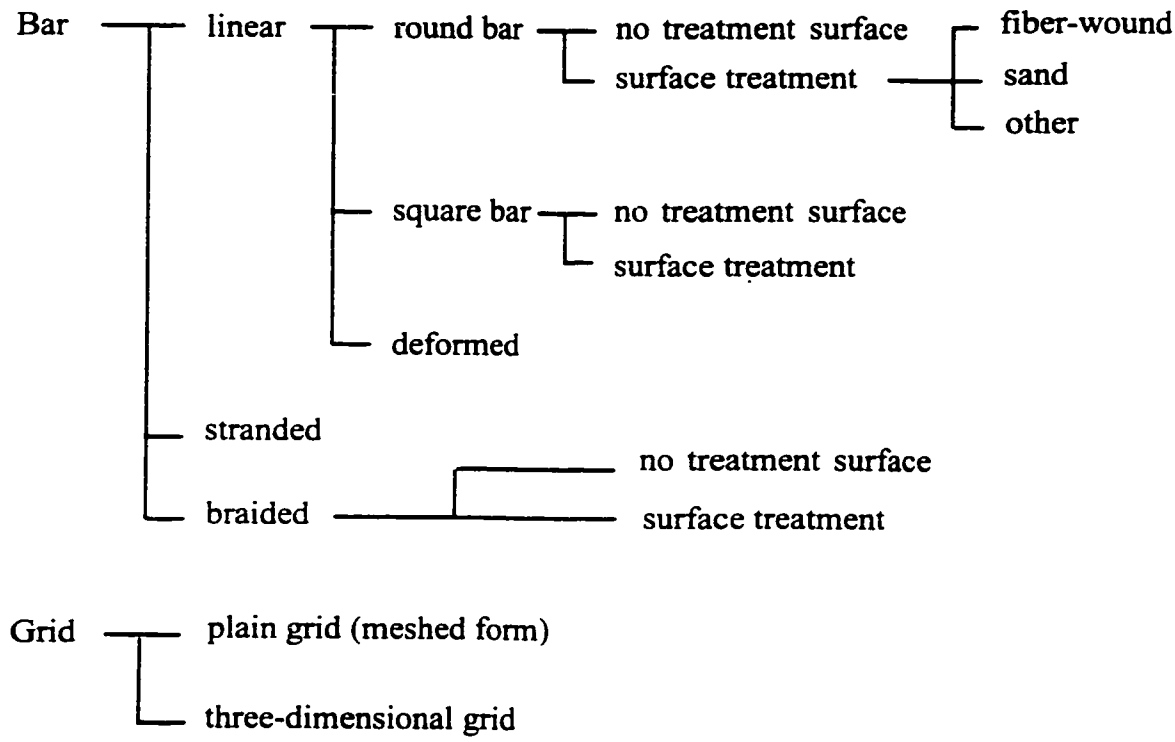

Figure 2.2: Classification of FRP reinforcement according to shape
(Source: Fukuyama, 1999)

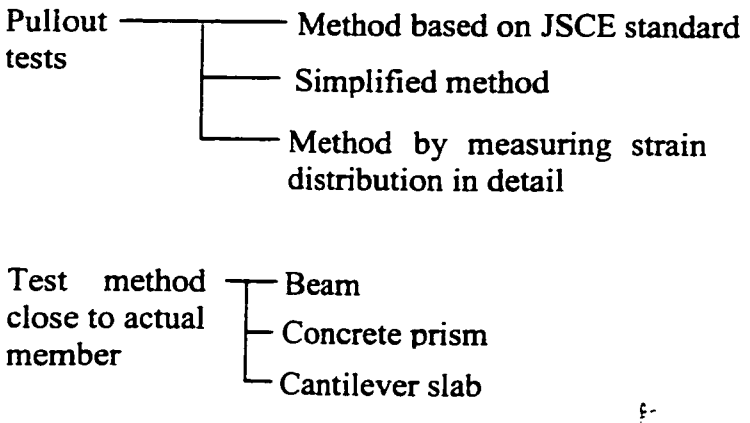

Figure 2.3: Classification of test method for bond of continuous fiber reinforcing material (Source: Machida, 1993)

CHAPTER 3

EXPERIMENTAL INVESTIGATION

3.1 General

Factors affecting bond properties depend on both the type of reinforcement and the concrete. These factors may be summarized as follows:

a. size and type of FRP bars (carbon, glass, aramid)

b. surface deformations (smooth, deformed, sand-coated, braided)

c. concrete compressive strength

d. concrete confinement (concrete cover and transverse reinforcement)

e. type of loading (static, cyclic, impact)

f. mechanical properties (tensile strength and modulus of elasticity)

g. type and volume of fibre

h. position of FRP bars (top bar effect)

i. embedment length of FRP bars

j. setup of test specimens (cantilever, simply supported)

k. type of bond tests (pullout test, bond beam test)

3.2 Purposes

The purpose of this experimental program is to investigate the bond strength and characteristics of Glasform and DFI CFRP bars using beam specimens. The mean bond strength of the CFRP bars was examined through concrete T-beam reinforced with a

CFRP bar. The following three parameters were investigated in this experimental research.

a. pressure induced on the bar due to support condition of beam specimen

b. embedment length of CFRP bar

c. transverse reinforcement

3.3 Materials

3.3.1 CFRP Bars

Three types of carbon fiber reinforced plastic (CFRP) bars were used in the tests, as shown in Figures 3.1(a) and (b). Types A (G1-D8 and G1-D10) and B (G2-D9.79) CFRP bars were manufactured by Glasform Inc., USA. These CFRP bars were manufactured by the pultrusion process and made up of continuous longitudinal carbon fibers bound together with a thermosetting resin. The indentation of type A CFRP bars was parallel to and along the length of the bar while type B CFRP bar was characterized by spiral indentation. Type C CFRP bar was manufactured by DFI Pultruded Composite Inc., USA. These CFRP bars were made of carbon fibers (fibers not preheated before passing through the die) with a carbon content of 65% by volume. The surface was characterized by spiral indentation along the length of the bar. The physical properties of types B and C CFRP bars are shown in Table 3.1 and the mechanical properties of types A, B and C CFRP bars are shown in Table 3.2.

3.3.2 Concrete

Concrete was made by mixing of fine aggregate (sand), 20 mm (0.75 in.) coarse aggregate (gravel), type III Portland cement (high-early-strength cement) and water. A minimum 7-day concrete compressive strength of 35 - 40 MPa (5100 - 5800 psi) was assumed and a water-cement of 0.55 was used in the mix design. Three 150 x 300 mm (6 x 12 in) standard concrete cylinders were prepared for each beam specimen and tested at the same day of bond beam test. The proportioning of concrete mix and compressive strength of beam specimens are presented in Tables 3.3 and 3.4, respectively.

3.4 Testing Instrumentation

3.4.1 Hydraulic Jack and Load Cell

A universal flat load cell of capacity 225 kN (50 000 lb) and a manually operated hydraulic jack were used in beam testing. The load cell was calibrated using universal testing machine to obtain the load-strain relationship required for beam testing. The load cell was wired to a strain indicator which gave readings in microstrain. The load-strain readings are presented in Table A.1 and the corresponding calibration curve is shown in Figure A.1.

3.4.2 Strain Indicator and Switch & Balance Unit

P-3500 digital strain indicator was used with electric resistance strain gauges. This strain indicator would accept full, half or quarter-bridge inputs and all required bridge completion components for 120-ohm and 350-ohm bridges were provided. SB-1 switch & balance unit, which provided an output of ten channels of strain gauge readings

on a single strain indicator, was used in beam testing. Both instruments were manufactured by Measurement Group, Inc., USA.

3.4.3 Strain Gauges and Strain Gauge Cement

PC-12 strain gauge cement was used to glue strain gauges on the surface of CFRP bar. The strain gauges used in beam testing were of type KFG-5-120-C1-11 KYOWA strain gauges. Both PC-12 strain gauge cement and strain gauges were manufactured by KYOWA Electronic Instruments Co. Ltd.

3.4.4 Dial Gauges

Mitutoyo shock proof dial gauges were used in the beam testing. These dial gauges were graduated in 0.01 mm with a range of 20 mm and 50 mm.

3.5 Formwork and Casting of Beam Specimens

3.5.1 Preparation of Formwork

A total of five wooden forms was prepared to cast the beam specimens. Two forms of length 1829 mm (72 in.) and three forms of length 2438 mm were cut and made by 15.9 mm (0.625 in.) thick plywood. Two types of transverse reinforcement (steel stirrups) were prepared, namely (a) Type A stirrups with a total length of 711 mm (28 in.) and (b) Type B with a total length of 558 mm (22 in.). Type A stirrups were used in the bonded part of reinforcement while Type B stirrups were used in the unbonded part of reinforcement. These two-leg steel stirrups were made from 6 mm (0.24 in.) diameter mild steel longitudinal bars with a minimum yield stress of 400 MPa (58 ksi). Steel

stirrups spaced at 152 mm (6 in.) were hung from two 6 mm diameter mild steel longitudinal bars and tied with mechanical wire and a CFRP bar was tied with these stirrups. Then the assembly was ready to set in to wood forms. The unbonded part of reinforcement was covered by 50.8 mm (2 in.) thick blue styrospan. Figures 3.2 and 3.3 show sketches of two types of transverse reinforcement and a completed formwork, respectively.

3.5.2 Casting of Beam Specimens

The quantities of concrete mix were measured accurately, loaded and mixed in a mechanical mixer. The concrete was placed into forms and vibrated with the aid of laboratory internal vibrator and then smoothed with a trowel. In order to prevent rapid moisture loss in the initial hardening process, plastic sheets were used to cover the surface of the beam specimens. The forms were removed 24-30 hours after casting, sprayed with intermittent water for the first 3 days and left to air dry until testing (7 days after casting). Three 150 x 300 mm (6 x12 in.) standard concrete cylinders were made for each beam specimen and cured under water for the first 3 days and left in the air until testing. The top and bottom of these concrete cylinders were capped with capping material prior to testing. Both concrete T-beams and concrete cylinders were cast and stored in the concrete laboratory at the University of Windsor.

3.6 Test Program

3.6.1 Tension Test

Tension tests were conducted on G2-D9.79 and D1-D9.70 CFRP bars in order to determine the modulus of elasticity of the CFRP bars. A typical tension specimen of length 864 mm (34 in.) was selected and gripped by anchorage system on both ends with 76 mm (3 in.) overhanging the anchorage system. Three strain gauges were placed on the surface of the bar, wired and connected to switch & balance unit to give the strain readings. Two tension specimens from each type of CFRP bar were tested using the universal testing machine. Typical setup of tension test is shown in Figure 3.4.

3.6.2 Beam Test

A total of twenty-eight concrete T-beams reinforced with G2-D9.79 and D1-D9.70 CFRP bars was tested in this experimental program. Three parameters affecting bond characteristics were considered in this test program, namely (1) pressure induced on the bar due to support condition of beam specimen (2) embedment length of CFRP bar and (3) transverse reinforcement.

3.6.2.1 Details of Beam Specimens

The total length of beam specimens was 1829 mm (72 in.) or 2438 mm (96 in.) with a depth of 356 mm (14 in.) and an effective depth of 312 mm (12.3 in). A clear cover of 38.1 mm (1.5 in) was selected to avoid splitting of the concrete cover. The beam specimens were grouped into Groups A, B and C. Beam specimens in Groups A and B were tested using steel I-beam section supports and steel roller supports, respectively

(The different support conditions will be discussed in the following sections). In addition to CFRP reinforcement, Group C beam specimens were also reinforced with transverse reinforcement (stirrups) and tested using steel roller supports. The beam specimens were designated by three sets of letters and numbers. The first set of letters and numbers refers to manufacturer and type of CFRP bar manufactured by the manufacturer, respectively. The second set of letters and numbers refers to the diameter of CFRP bar. The third set of letters and numbers refers to group of beam specimen and embedment length (in inches) of the CFRP bar, respectively. Configurations of beam specimens are shown in Figures 3.5(a), (b), (c) and (d). Detailed information about bond test beam specimens may be seen in Table 3.5.

3.6.2.2 Pressure Induced on The Bar Due to Support Condition

Two support conditions of beam specimens were considered in the test program, namely (1) steel roller supports and (2) steel I-beam section supports. The steel roller supports consisted of two 305 x 305 mm (12 x12 in.) square plates and one 63.5 mm (2.5 in) diameter by 305 mm (12 in.) long steel roller for each end of beam support. For 1829 mm (72 in.) beam specimens, the beam ends were set up on top of the horizontal steel rollers as simply supported with a span of 1727 mm (68 in.) and 50.8 mm (2 in.) overhanging the supports. For 2438 mm (96 in) beam specimens, the beams were set up in the same manner, but with a span of 2337 mm (94 in.) and 50.8 mm (2 in.) overhanging the supports. A 50 x 125 x 3 mm (2 x 5 x 0.12 in) thick steel plate was placed underneath the bottom of the beam specimens on both ends to avoid stress concentration on the supports. A photograph showing a pair of steel roller supports is shown in Figure 3.6.

In order to minimize stress disturbances (support reaction forces) and confinement effect (concrete cover), a pair of special supports was designed and called steel I-beam section supports. The steel I-beam section supports were fabricated by steel angles, steel columns and steel plates. The beams were set up in such a way that the web of the beams was held by the angles welded to the steel plate. Some thin steel splices were inserted into the space between the web and the angles to hold the beams as tight as possible. A sketch of plan and cross-sectional view of this special support may be seen in Figures 3.7(a) and (b). A photograph showing a pair of steel I-beam section supports may be seen in Figures 3.8(a) and (b).

3.6.2.3 Embedment Length

Five different embedment lengths of CFRP bar were used in this experimental research, namely 305 mm (12 in.), 457 mm (18 in.), 610 mm.(24 in.), 762 mm (30 in.) and 914 mm (36 in). The embedment lengths were used to establish a relationship between bond strength and embedment length of CFRP bar.

3.6.2.4 Transverse Reinforcement

Group C beam specimens were reinforced with steel stirrups along the length of the beams. The results obtained from Group C beam specimens may provide a comparison with Group B beam specimens. The use of steel stirrups may increase the shear resistance and limit the crack width of beam.

3.7 Test Setup

3.7.1 Setup of Test Beams

The beams were set up on testing bed of a testing frame by using either steel roller supports or steel I-beam section supports. The beams were then tested statically as a simply supported beam. Figure 3.9 shows a sketch of the location of measuring devices and loading configuration. Photographs showing a complete test setup of Group A and Groups B, C beam specimens may be seen in Figures 3.10 and 3.11. Detailed information of test setup is presented in the following sections.

3.7.2 Attachment of Measuring Devices

One strain gauge was glued to each of the rear and front faces of the CFRP bar (offset to the middle of the bar ± 50.8 mm (2 in.)) after the surface was cleaned by acetone, M-Prep conditioner A and neutralized by M-Prep neutralizer 5A. The strain gauges were wired and connected to switch & balance unit and strains were read from strain indicator. Two dial gauges were attached to both ends of the beams and other two were attached to the unbonded ends of the bar. Two dial gauges were also located at the mid-span of the beams.

3.7.3 Loading Configuration

All beams were tested statically as a simply supported beam. The central concentrated load was applied in the increment of 4.4 kN (1000 lb) at two equal loading points spaced at 610 mm (24 in.) by using a load spreader system. The load spreader system consisted of a 12.7 x 152 x 152 x 902 mm (0.5 x 6 x 6 x 35.5 in) steel HSS

section, a 30 x 180 mm (1.18 x 7.09 in) circular steel roller and a 25 x 25 x 300 mm (1 x 1 x 11.8 in) rectangular steel bar.

3.7.4 Compression Test

The compression tests of concrete cylinders were conducted using RIEHLE testing machine by applying the load constantly and slowly.

3.8 Data Collection

3.8.1 Strain Readings

The strains of CFRP bar were read from a strain indicator in microstrain for each load increment. The average value of two strain readings was used to calculate the tensile force of CFRP bar.

3.8.2 Dial Gauge Readings

Elongation and loaded-end slips of the bar were read from dial gauges 2 and 3 located at the unbonded ends of the bar and free-end slips of the bar were recorded from dial gauges 1 and 4 for each load increment. The mid-span deflections were also recorded by two dial gauges.

3.8.3 Identification of Crack

The transverse cracks within the shear span and constant moment zone were traced with a black marker and indicated the extent of the cracks at each load increment.

3.8.4 Compressive Strength

The compression tests were done on the same day of bond tests. The average value of three concrete cylinder compressive strengths indicated the strength of the concrete.

Table 3.1: Physical properties of G2-D9.79 and D1-D9.70 CFRP bars

Physical Properties	Type of CFRP Bar	
	Glasform2 (G2-D9.79)	DFI1 (D1-D9.70)
nominal diameter (mm)	9.79	9.70
pitch of indentation (mm)	35.0	9.49
width of indentation (mm)	7.45	3.08
depth of indentation (mm)	0.13	0.37
angle of indentation (degree)	45	70

Note:

The pitch and width of indentation of DFI1 CFRP bar may slightly differ from bar to bar due to inconsistency of indentation.

Table 3.2: Mechanical properties of CFRP bars

Properties of Reinforcement	Type of CFRP Bar			
	A		B	C
Designation	G1-D8	G1-D10	G2-D9.79	D1-D9.70
Manufacturer	Glasform	Glasform	Glasform	DFI
d_b (mm)	8	10	9.79	9.70
E_f (GPa)	159	157	158	177

Table 3.3: Proportioning of concrete mix

Components	kg/m
Cement	320
Sand	785
Gravel	1122
Water	173

Table 3.4: Concrete compressive strength of beam specimens

Type of Reinforcement	Beam Specimen	Compressive Strength (MPa)	Type of Reinforcement	Beam Specimen	Compressive Strength (MPa)
Glasform2 Dia. = 9.79 mm E_f = 158 GPa	G2-D9.79-A18	36	DFI1 Dia. = 9.70 mm E_f = 177 GPa	D1-D9.70-A12	41
	G2-D9.79-B18	36		D1-D9.70-B12	45
	G2-D9.79-C18	41		D1-D9.70-C12	42
	G2-D9.79-A24	44		D1-D9.70-A18	42
	G2-D9.79-B24	49		D1-D9.70-B18	52
	G2-D9.79-C24	43		D1-D9.70-C18	41
	G2-D9.79-A30	42		D1-D9.70-A24	31
	G2-D9.79-B30	48		D1-D9.70-B24	43
	G2-D9.79-C30	44		D1-D9.70-C24	44
	G2-D9.79-A36	44		D1-D9.70-A30	44
	G2-D9.79-B-36	45		D1-D9.70-B30	42
	G2-D9.79-C36	43		D1-D9.70-C30	41
	*G2-D9.79-B36(F1)	57		**D1-D9.70-B18Comp	42
	*G2-D9.79-B36(F2)	54		**D1-D9.70-C18Comp	48

Note:
The first set of letters and numbers refers to manufacturer and type of CFRP bar manufactured by the manufacturer, respectively.
The second set of letters and numbers refers to diameter of CFRP bar.
The third set of letters and numbers refers to group of beam specimen and embedment length (inches), respectively.
*CFRP bar was fully bonded by concrete. The letter and number in parenthesis referred to full length and beam number.
**Beams reinforced with CFRP bar and two 25.4 mm (1 in.) diameter compression steels.

Table 3.5: Detail of beam specimens

Type of Reinforcement	Beam Specimen	Length of Beam Specimen (mm)	Embedment Length (mm)	Transverse Reinforcement	Support Condition
Glasform 2 Dia. = 9.79 mm E_f = 158 GPa	G2-D9.79-A18	1829	457	No	Steel I-Beam
	G2-D9.79-B18	1829	457	No	Steel Roller
	G2-D9.79-C18	1829	457	stirrups @152 mm	Steel Roller
	G2-D9.79-A24	1829	610	No	Steel I-Beam
	G2-D9.79-B24	1829	610	No	Steel Roller
	G2-D9.79-C24	1829	610	stirrups @152 mm	Steel Roller
	G2-D9.79-A30	1829	762	No	Steel I-Beam
	G2-D9.79-B30	1829	762	No	Steel Roller
	G2-D9.79-C30	1829	762	stirrups @152 mm	Steel Roller
	G2-D9.79-A36	2438	914	No	Steel I-Beam
	G2-D9.79-B-36	2438	914	No	Steel Roller
	G2-D9.79-C36	2438	914	stirrups @152 mm	Steel Roller
	*G2-D9.79-B36(F1)	1829	914	No	Steel Roller
	*G2-D9.79-B36(F2)	1829	914	No	Steel Roller
DFI 1 Dia. = 9.70 mm E_f = 177 GPa	D1-D9.70-A12	1829	305	No	Steel I-Beam
	D1-D9.70-B12	1829	305	No	Steel Roller
	D1-D9.70-C12	1829	305	stirrups @152 mm	Steel Roller
	D1-D9.70-A18	1829	457	No	Steel I-Beam
	D1-D9.70-B18	1829	457	No	Steel Roller
	D1-D9.70-C18	1829	457	stirrups @152 mm	Steel Roller
	D1-D9.70-A24	1829	610	No	Steel I-Beam
	D1-D9.70-B24	1829	610	No	Steel Roller
	D1-D9.70-C24	1829	610	stirrups @152 mm	Steel Roller
	D1-D9.70-A30	1829	762	No	Steel I-Beam
	D1-D9.70-B30	1829	762	No	Steel Roller
	D1-D9.70-C30	1829	762	stirrups @152 mm	Steel Roller
	**D1-D9.70-B18Comp	1829	457	No	Steel Roller
	**D1-D9.70-C18Comp	1829	457	stirrups @152 mm	Steel Roller

Note:

The first set of letters and numbers refers to manufacturer and type of CFRP bar manufactured by the manufacturer, respectively.

The second set of letters and numbers refers to diameter of CFRP bar.

The third set of letters and numbers refers to group of beam specimen and embedment length (inches), respectively.

*CFRP bar was fully bonded by concrete. The letter and number in parenthesis referred to full length and beam number.

**Beams reinforced with CFRP bar and two 25.4 mm (1 in.) diameter compression steels.

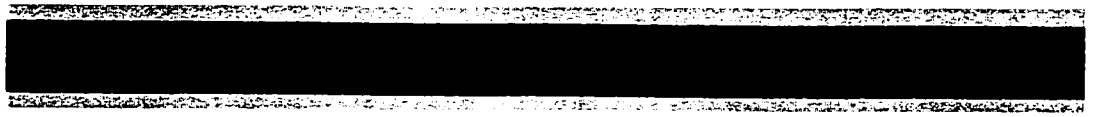

Glasform1, Diameter = 8 mm (0.315 in.)

Glasform1, Diameter = 10 mm (0.394 in.)

Figure 3.1(a): Type A CFRP bar (G1-D8 and G1-D10)

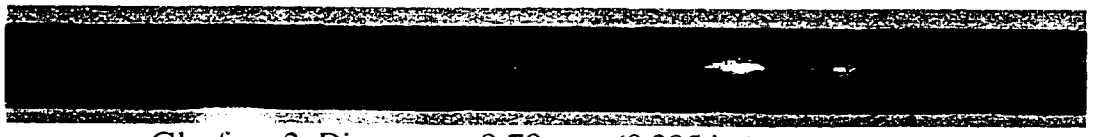

Glasform2, Diameter = 9.79 mm (0.385 in.)

DFI1, Diameter = 9.70 mm (0.382 in.)

Figure 3.1(b): Types B and C CFRP bars (G2-D9.79 and D1-D9.70)

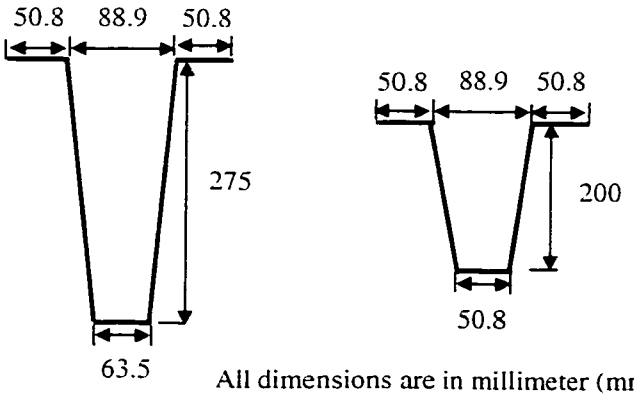

All dimensions are in millimeter (mm).

(a) Type A stirrup (b) Type B stirrup

Figure 3.2: Types of transverse reinforcement (a) Type A stirrup (b) Type B stirrup

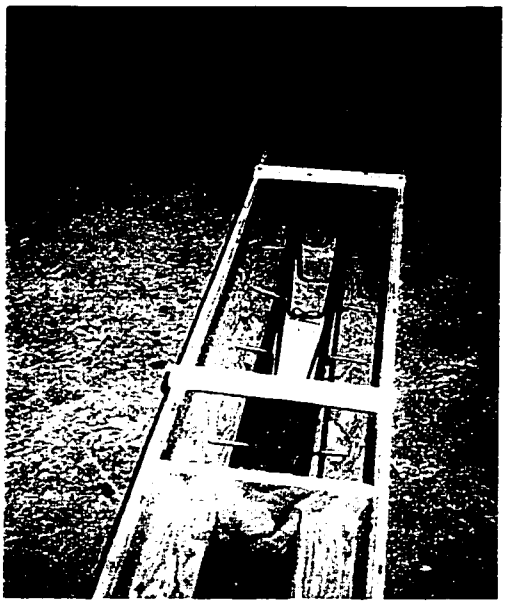

Figure 3.3: Picture of a complete formwork

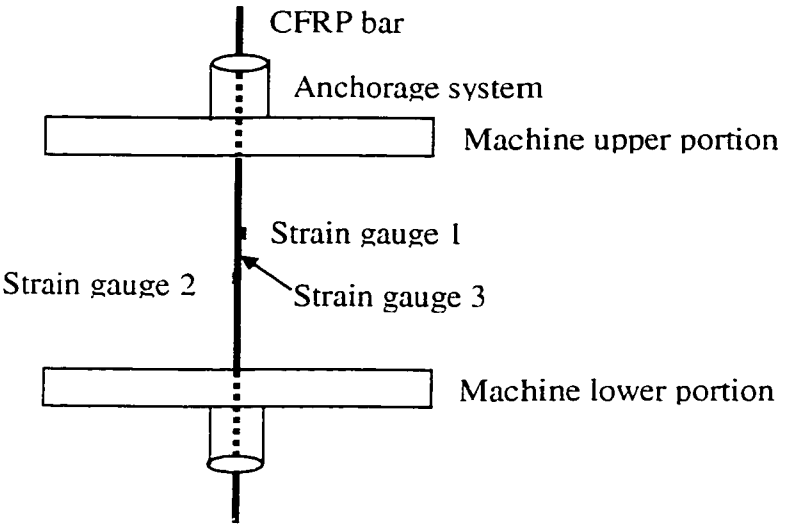

Figure 3.4: Setup of tension test

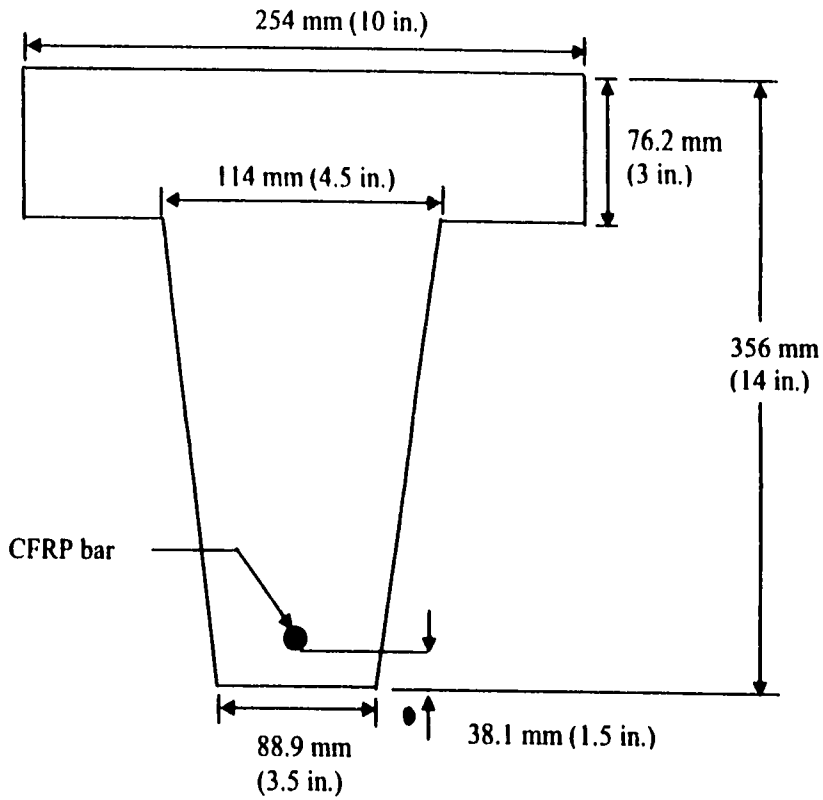

Figure 3.5(a): Cross-section of beam specimen

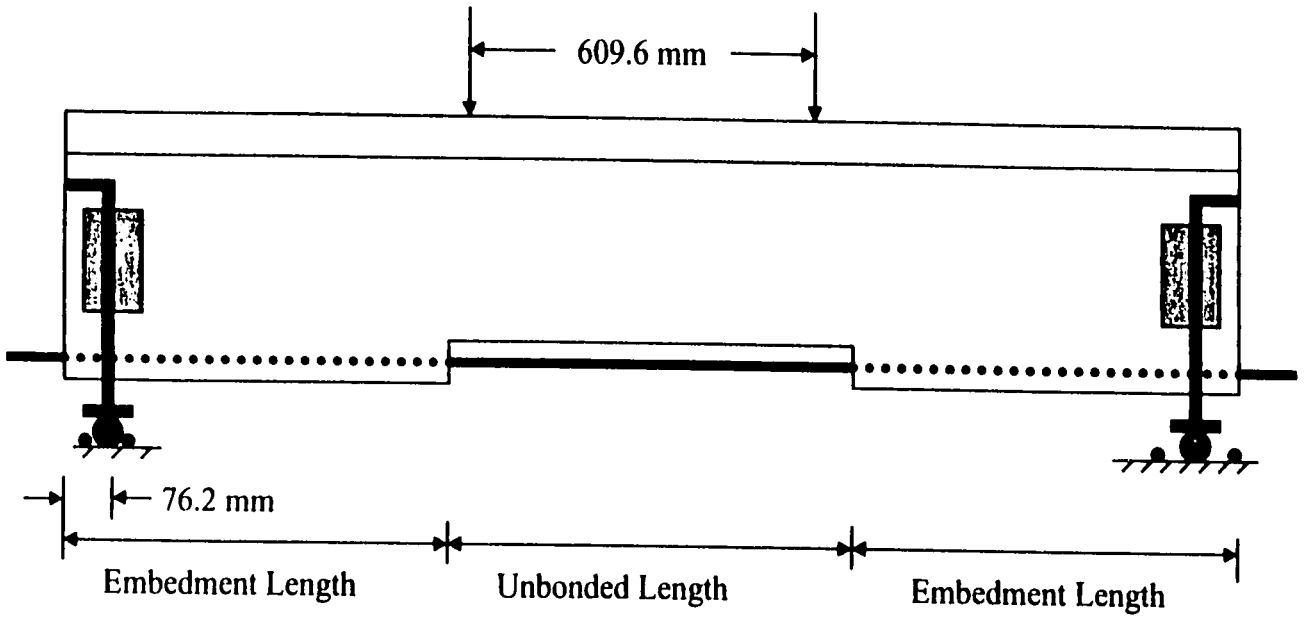

Figure 3.5(b): Configuration of Group A beam specimen

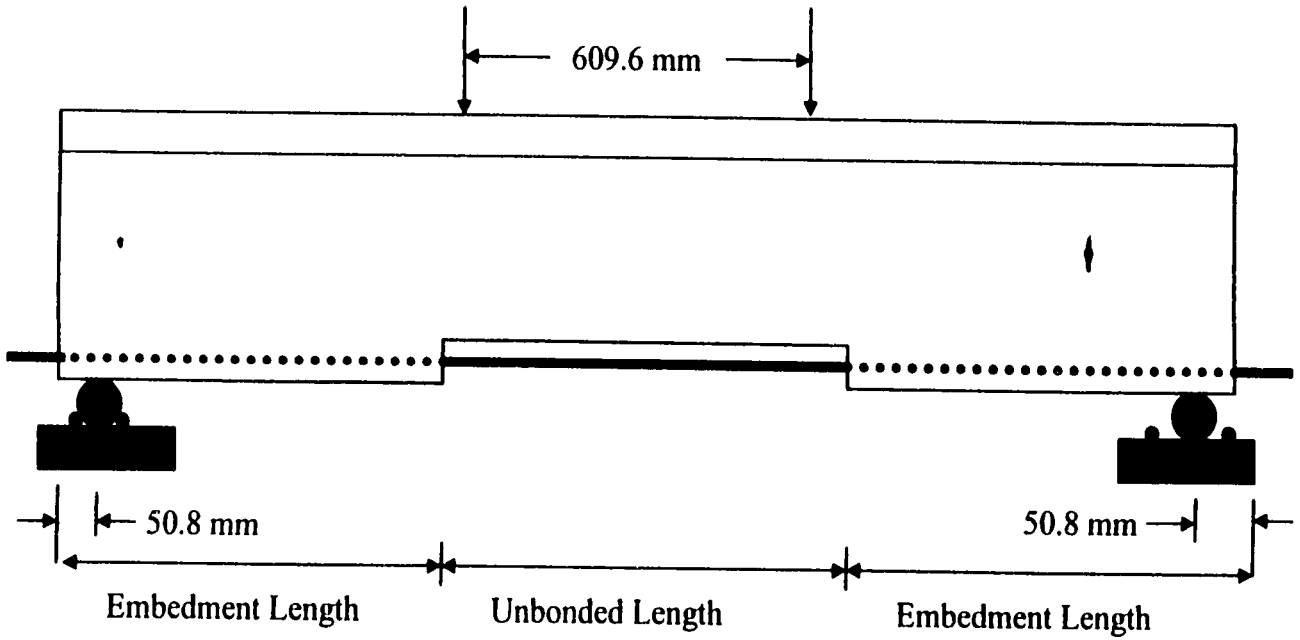

Figure 3.5(c): Configuration of Group B beam specimen

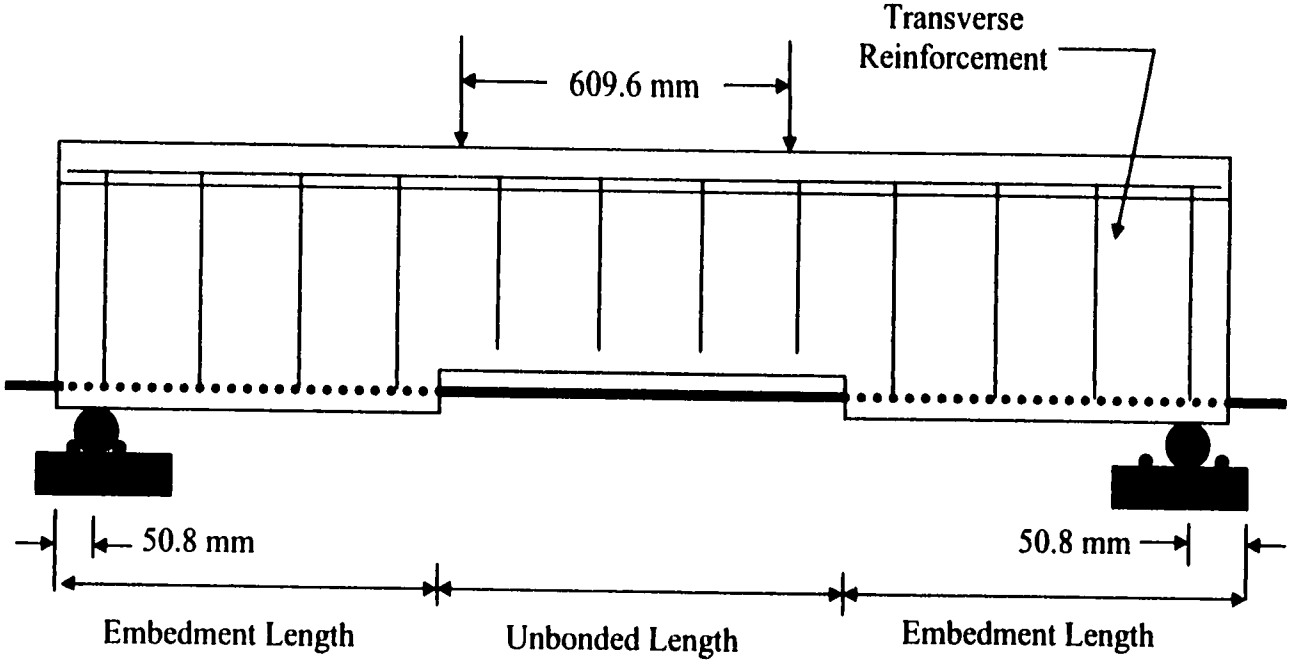

Figure 3.5(d): Configuration of Group C beam specimen

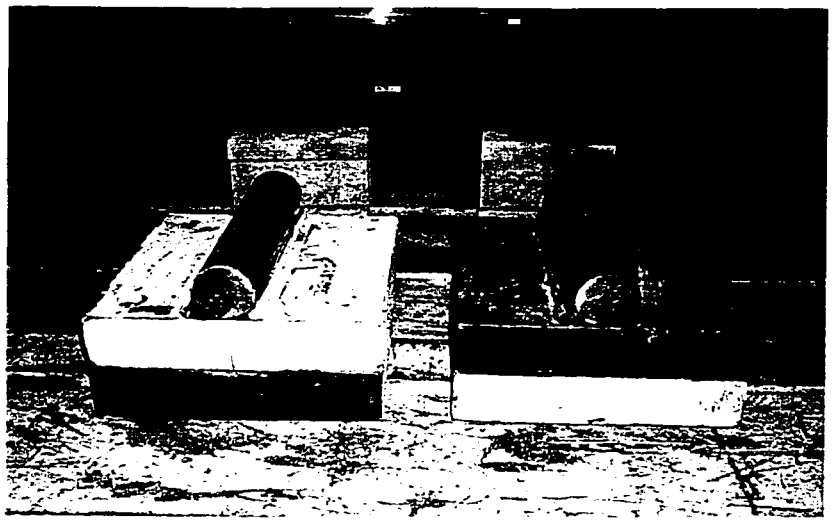

Figure 3.6: Picture of steel roller support

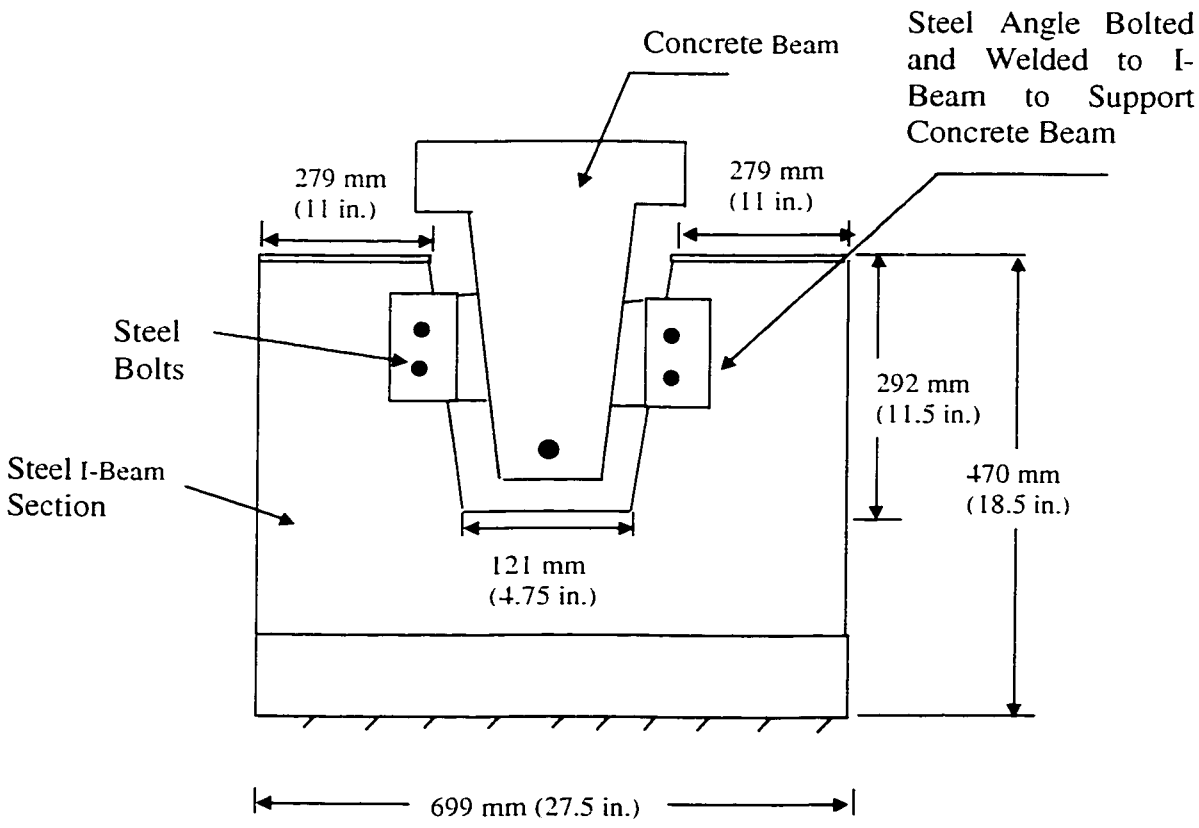

Figure 3.7(a): Plan view of steel I-beam section support

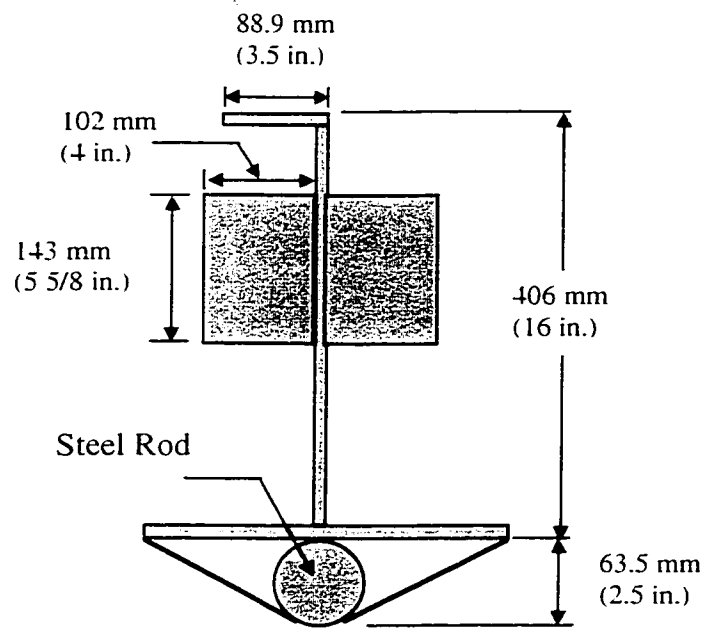

Figure 3.7(b): Cross-section of steel I-beam section support

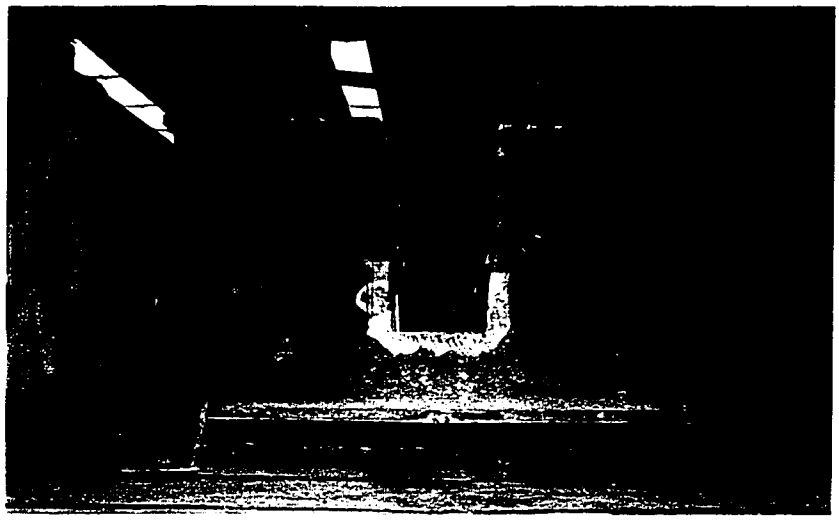

Figure 3.8(a): Picture of steel I-beam section supports (plan view)

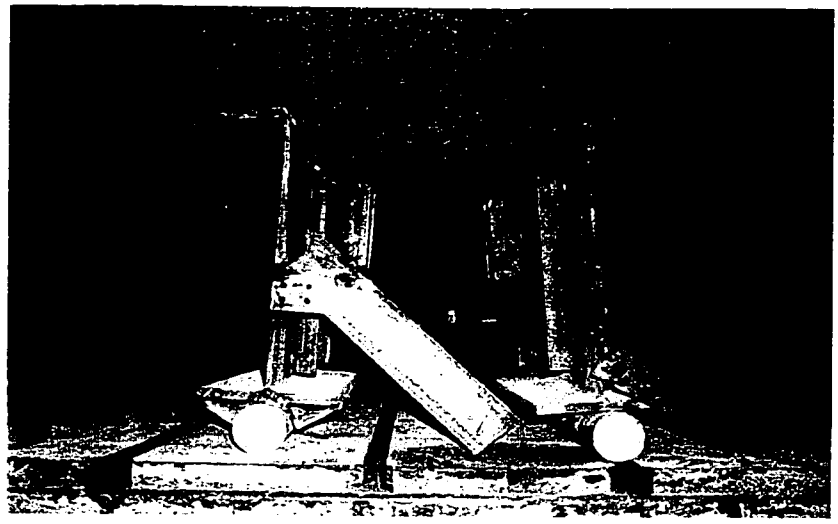

Figure 3.8(b): Picture of steel I-beam section supports (side view)

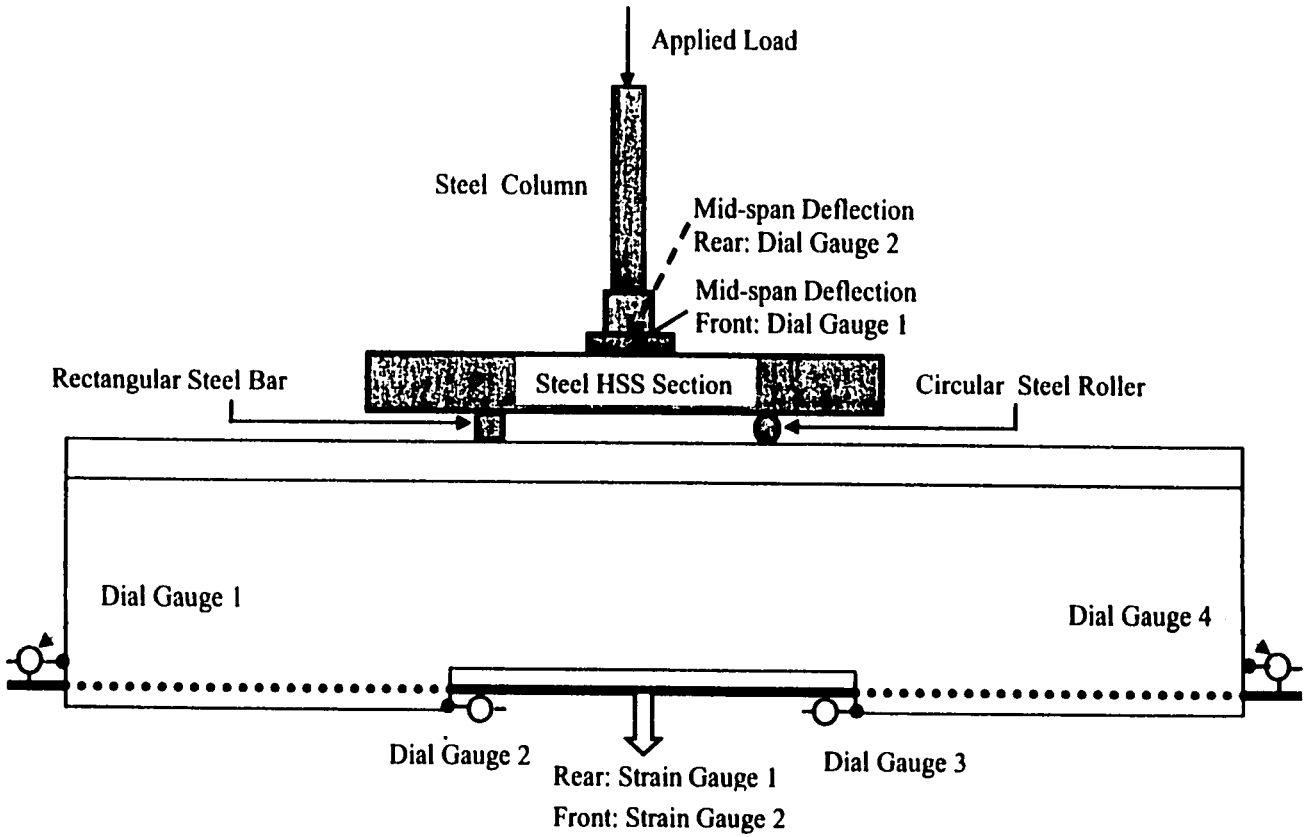

Figure 3.9: Location of measuring devices and loading configuration

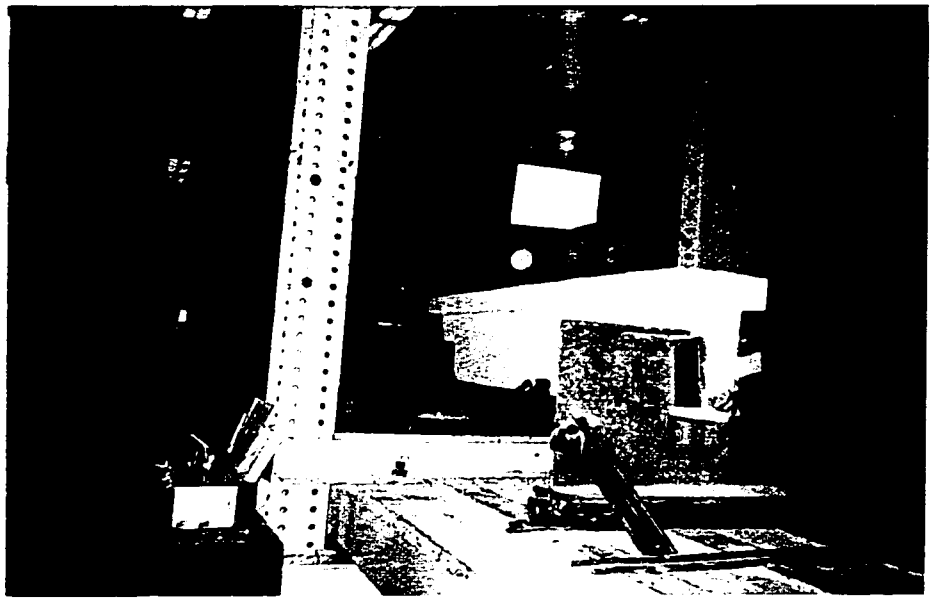

Figure 3.10(a): Picture of complete test setup of Group A beam specimen

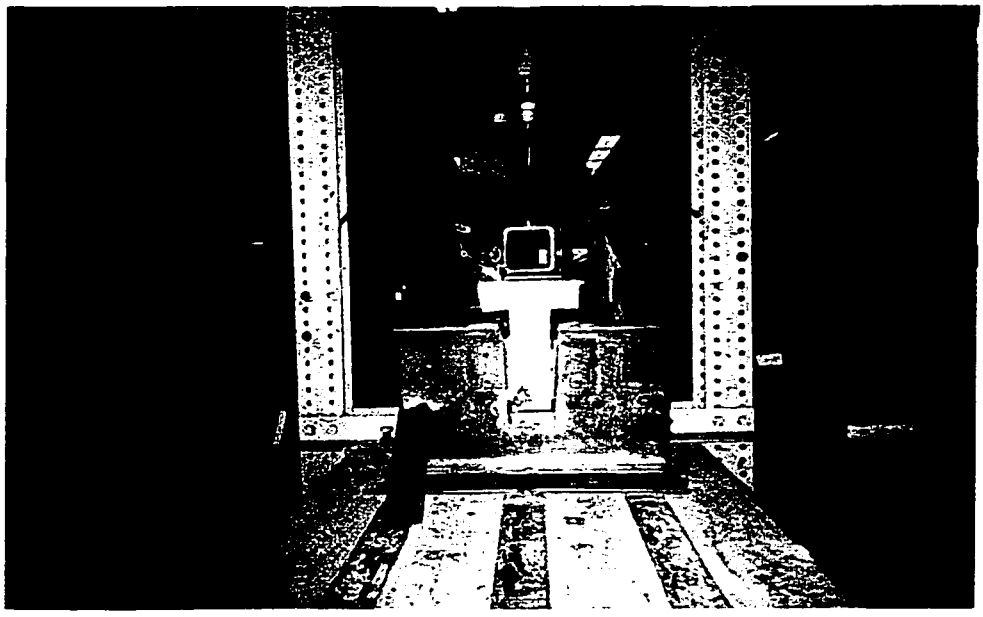

Figure 3.10 (b): Picture of complete test setup of Group A beam specimen (side view)

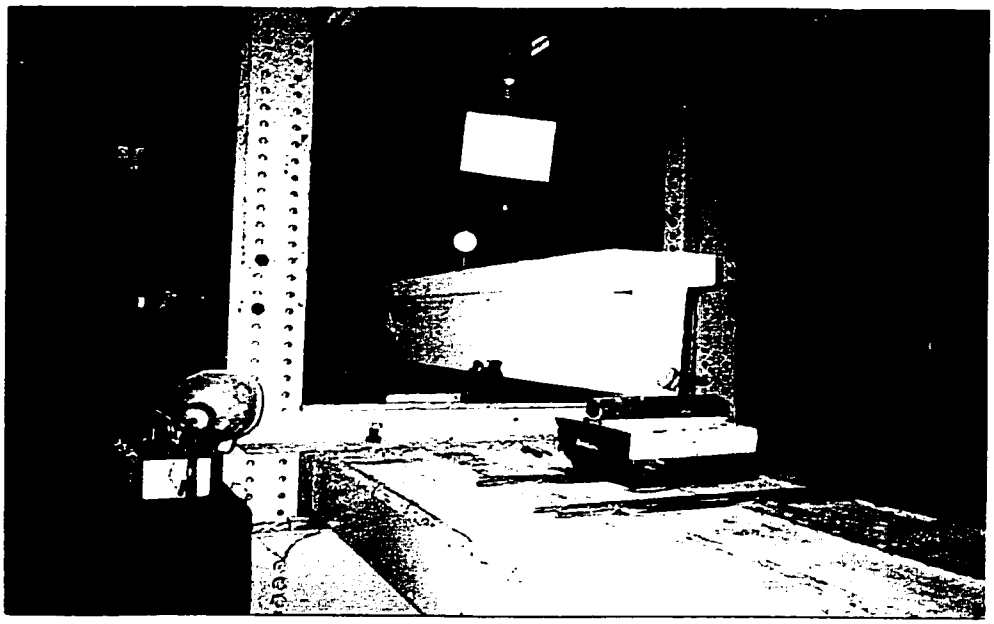

Figure 3.11 (a): Picture of complete test setup of Groups B and C beam specimens

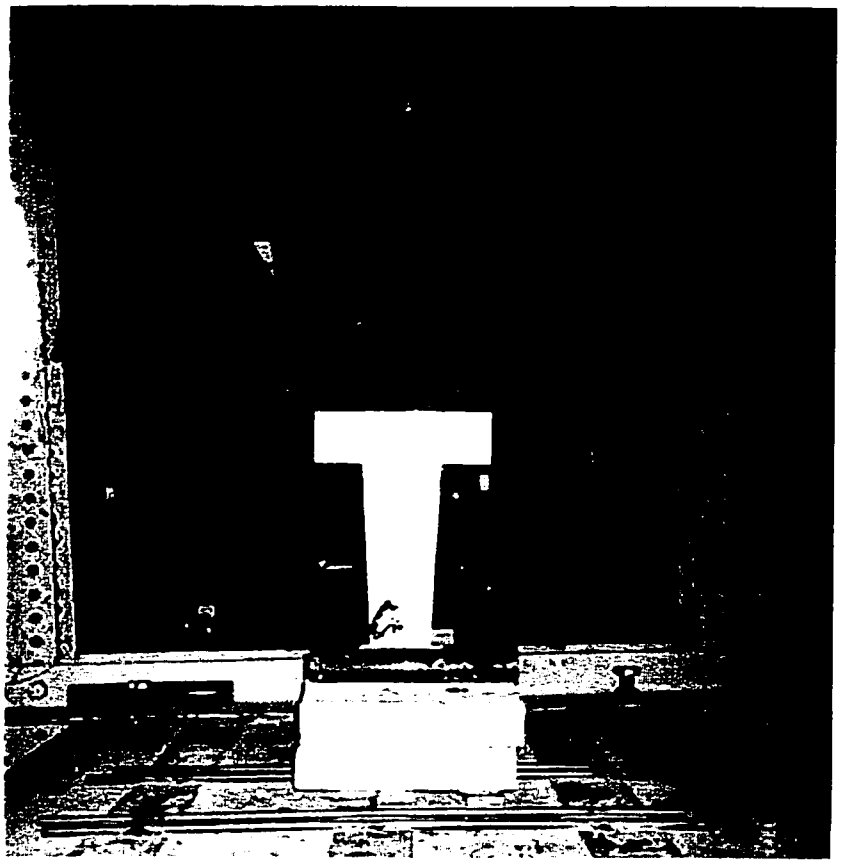

Figure 3.11(b): Picture of complete test setup of Groups B and C beam specimen (side view)

CHAPTER 4

EXPERIMENTAL RESULTS

4.1 General

This chapter presents all the results of the beam specimens by analyzing the experimental data. Data obtained from previous research work (Abdel-Sayed et al. 1998; Jerrett and Ahmad 1995) is also analyzed and the results serve as a comparison. Mechanical properties, such as modulus of elasticity, of Glasform2 and DFI1 CFRP bars were determined from tension tests and used in the calculations of beam specimens.

4.2 Calculations Required

4.2.1 Calculation of Tensile Force

The average tensile strain of CFRP bars obtained from the experiment was used to calculate tensile forces. The tensile force was the product of modulus of elasticity, average strain and cross-sectional area of CFRP bars.

$$T = E_f * \varepsilon * A_b \qquad (4.1)$$

The tensile force T acting on CFRP bar in beam specimens can also be calculated by pure bending moment $M = P * a$ due to two equal concentrated forces P.

$$T = \frac{P * a}{j} \qquad (4.2)$$

where a is shear span and j denotes the distance between resultant tensile and compressive forces as shown in Figure 4.1.

4.2.2 Calculation of Mean Bond Strength

The average bond strength of CFRP bar over the embedment length may be evaluated by Equation (1.1) by substituting the tensile force obtained from Equation (4.1).

$$u = \frac{T}{\sum ol_b} = \frac{T}{\pi * d_b * l_b} \qquad (4.3)$$

4.2.3 Determination of K_1 and K_2

Expression for average bond strength of CFRP bar may also be obtained directly from Equation (1.2), Section 1.2, by analysing the experimental results and determination of K_1 value. Expression of development length was then derived based on the developed average bond strength equation.

4.3 Results of Tension Tests

The modulus of elasticity of CFRP bar were determined by averaging the results obtained from two tension specimens for each type of CFRP bar. The average modulus of elasticity of G2-D9.79 and D1-D9.70 CFRP bars were 158 GPa (23 000 ksi) and 177 GPa (25 700 ksi), respectively. The ultimate breaking load of CFRP bars were not reported since the CFRP bars slipped or crushed within the grips. The stress-strain data and curves of G2-D9.79 and D1-D9.70 CFRP bars are presented in Appendixes B and C.

4.4 Results of G1-D8 and G1-D10 CFRP Bars

Bond strengths of G1-D8 and G1-D10 CFRP bars were determined by pullout and/or beam tests. The definition of bond failure was defined as a free-end slip of 0.10 mm.

4.4.1 Pullout Test (G1-D8 CFRP Bar)

A total of seven pullout specimens reinforced with G1-D8 CFRP bars was tested by varying the bond length of 60 mm, 80 mm and 120 mm (Abdel-Sayed et al. 1998). The test and analyzed results are summarized in Table 4.1. It was found that the bond strength ranged from 1.32 MPa to 4.31 MPa and the value of K_1 ranged from 1.93 to 6.76 with an average value of 3.68. The relationship between tensile force and bond length is shown in Figure 4.2. The effects of bond length and square root of concrete compressive strength (tensile strength of concrete) on bond strength are plotted and shown in Figures 4.3 and 4.4, respectively.

4.4.2 Beam Test (G1-D8 CFRP bar)

A total of fifteen beam specimens reinforced with G1-D8 CFRP bars was tested (Abdel-Sayed et. al 1998). The embedment length and concrete compressive strength were varied in order to establish the effects of these parameters on the bond strength. Transverse reinforcement (steel stirrups) was used in some beam specimens in order to prevent premature shear failure and to examine the effect of confinement provided by stirrups. Four types of failure modes were observed in the tests, namely shear (dowel), compression, tension and bond. It was found that the average bond strength ranged from

3.30 MPa to 5.66 MPa and the value of K_I ranged from 5.25 to 8.26 with an average value of 6.27. The bond test results of beam specimens are summarized in Table 4.2. Figures 4.5, 4.6 and 4.7 plot the relationships of tensile force vs. bond length, bond strength vs. bond length and bond strength vs. square root of concrete compressive strength, respectively. The applied load vs. free-end and loaded-end slips of beams G1-D8-B12 to G1-D8-B15 are shown in Appendix G. A sketch of crack pattern at failure of the four beams is shown in Appendix D.

A summary of the effect of transverse reinforcement on the bond strength of beam specimens is presented in Table 4.3. Bond strengths of five beam specimens with transverse reinforcement were compared to that of five beam specimens without additional transverse reinforcement. It was found that, in general, the transverse reinforcement increased the average bond strength.

4.4.3 Beam Test (G1-D10 CFRP bar)

The average bond strength of G1-D10 CFRP bar was determined by testing seven beam specimens (Abdel-Sayed et al. 1998). The observed modes of failure of the beam specimens were shear, compression and bond. The average bond strength was between 4.11 MPa and 5.02 MPa and the value of K_I was between 5.55 to 6.79 with an average value of 6.25. The beam test results are summarized in Table 4.4. The relationships of tensile force vs. bond length, bond strength vs. bond length and bond strength vs. square root of concrete compressive strength can be seen in Figures 4.8, 4.9 and 4.10, respectively.

4.4.4 Comparison of Pullout and Beam Tests Results

The bond strengths of G1-D8 CFRP bar were obtained from pullout and beam tests in the previous section. Table 4.5 presents a comparison of bond strength of pullout and beam specimens. It was found that the bond strength obtained from pullout specimens was relatively lower than that obtained from beam specimens.

4.5 Results of G2-D9.79 CFRP Bar

A total of fourteen beams reinforced with G2-D9.79 mm CFRP bar was tested. All beam specimens failed in bond with a free-end slip greater than 0.10 mm and with a vertical crack formed within the shear span or constant moment zone. Inclined flexural cracks formed within the shear span of beams G2-D9.79-C30 and G2-D9.79-C36 had reduced their bond length to 406 mm (16 in.) and 559 mm (22 in.), respectively. Two additional beams (G2-D9.79-B36(F1) and G2-D9.79-B36(F2)) with CFRP bar fully bonded by concrete were tested. It was observed that inclined flexural crack formed within the shear span of the two beams and free-end slip increased with the increase of crack width and applied load. Excessive slip occurring at one of the free-ends was observed in the tests. The bond strength were 2.61 MPa and 2.37 MPa for beams G2-D9.79-B36(F1) and G2-D9.79-B36(F2), respectively.

The tensile force of the CFRP bar was calculated by Equation (4.1) and compared to that obtained from pure bending moment, Equation (4.2). The results are presented in Table 4.6. Tensile forces and bond strengths at three levels of free-end slip of 0.05 mm, 0.10 mm and 0.25 mm, and two levels of loaded-end slip of 0.25 mm and

0.50 mm are calculated and presented in Tables 4.7, 4.8, 4.9 and 4.10, respectively. The tensile force vs. bond length and bond strength vs. bond length at three levels of free-end slip are shown in Figures 4.11 and 4.12, respectively. For loaded-end slip, the tensile force vs. bond length and bond strength vs. bond length can be seen in Figures 4.13 and 4.14, respectively. The bond strength at free-end slip vs. square root of concrete compressive strength can be seen in Figure 4.15.

A summary of calculations of tensile force, bond strength, the values of K_1 and K_2 for G2-D9.79 CFRP bar at free-end and loaded-end slips are presented in Tables 4.11 and 4.12, respectively. It was found that the average bond strength at free-end slip of 0.05 mm ranged from 1.19 MPa to 3.84 MPa and the value of K_1 ranged from 1.95 to 5.67 with an average of 3.16. For a free-end slip of 0.10 mm, the average bond strength ranged from 1.75 MPa to 4.14 MPa and the value of K_1 ranged from 2.45 to 6.12 with an average of 3.40. The tensile force, bond strength and the values of K_1 and K_2 at loaded-end slips of 0.25 mm and 0.50 mm were calculated and used to serve a comparison to that obtained from free-end slips.

The effect of support condition on bond strength is summarized in Table 4.13. It was found that bond strength obtained from steel I-beam section and steel roller supports varied from each other. Table 4.14 presents the effect of transverse reinforcement on bond strength of groups B and C beam specimens. It was noted that, in general, bond strength increased due to confinement provided by stirrups. Comparison of the bond strength between groups B and C beam specimens is shown in Appendix R.

4.6 Results of D1-D9.70 CFRP Bar

A total of fourteen beam specimens reinforced with D1-D9.70 CFRP was tested. Five out of fourteen beam specimens failed in bond / splitting of cover and nine beam specimens failure in compression. A vertical crack was formed within the constant moment zone for the beam specimens that failed in bond. However, the bond length of beam D1-D9.70-C24 was reduced to 279 mm (11 in.) due to inclined flexural crack formed within the shear span. Comparison of the maximum tensile force obtained from Equations (4.1) and (4.2) are presented in Table 4.15. Tensile force and bond strength at free-end slips of 0.05 mm and 0.10 mm are calculated and presented in Tables 4.16 and 4.17, respectively. The tensile force vs. bond length and bond strength vs. bond length at free-end slip can be seen in Figures 4.16 and 4.17, respectively. The bond strength at free-end slip vs. square root of concrete compressive strength can be seen in Figure 4.18.

A summary of calculations of tensile force, bond strength, the values of K_1 and K_2 for D1-D-9.70 CFRP bar at free-end slip is presented in Table 4.18. It was found that the average bond strength at free-end slip of 0.05 mm ranged from 4.56 MPa to 6.21 MPa and the value of K_1 ranged from 6.67 to 9.29 with an average value of 8.08. For a free-end slip of 0.10 mm, the average bond strength ranged from 4.67 MPa to 6.53 MPa and the value of K_1 ranged from 6.82 to 9.76 with an average value of 8.47.

The effect of support condition on bond strength is summarized in Table 4.19. It was found that bond strength obtained from steel I-beam section and steel roller supports varied from each other. The effect of transverse reinforcement on bond strength of groups

B and C beam specimens is summarized in Table 4.20. It was noted that, in general, bond strength increased due to confinement effect. Appendix W shows a comparison of bond strength between groups B and C beam specimens.

4.7 Results of Leadline CFRP Bar

Bond strength of Leadline CFRP bars was determined by Jerrett and Ahmad (1995). Results showed that the average bond strength for smooth rods at failure was 417 kPa. For deformed rods, the average bond strength at initial free-end displacement and maximum load were 1.63 MPa and 7.44 MPa, respectively. Results of their test is presented in Appendix X.

Further analysis was conducted in order to determine the value of K_I for bond strength expression. It was found that, for smooth rods, bond strengths were 0.483 MPa, 0.317 MPa and 0.453 MPa for bond length of 152 mm, 305 mm and 457 mm, respectively. The average value of K_I was 0.498 for smooth rod. The average bond strength at initial free-end displacement of deformed rods were 0.88 MPa, 1.91 MPa and 2.09 MPa for bond length of 152 mm, 305 mm and 457 mm and the average bond strength associated with maximum load were 7.81 MPa, 7.55 MPa and 7.35 MPa for bond length of 152 mm, 305 mm and 457 mm. For deformed rods, the average value of K_I was 9.04.

4.8 Summary of Test Results

Bond strength of different types of CFRP bars were determined in the previous section and summarized in Table 4.21. It should be noted that, bond strength of types G1-D8, G1-D10, G2-D9.79 and D1-D9.70 CFRP bars were determined based on a free-end slip of 0.10 mm. For smooth and deformed Leadline CFRP bars, the bond strength was calculated corresponding to maximum load.

Expressions for bond strength of different types of CFRP bars can be established by determining the corresponding value of K_I, Equation (1.2) in Section 1.2. It showed that expressions for bond strength of CFRP bars depended on the value of K_I. Therefore, the bond strength equation was modified for the use of CFRP bars as:

$$u = \frac{6.25\sqrt{f_c'}}{d_b} \quad \text{for G1-D8 and G1-D10 CFRP bars}$$

$$u = \frac{3.40\sqrt{f_c'}}{d_b} \quad \text{for G2-D9.79 CFRP bar}$$

$$u = \frac{8.47\sqrt{f_c'}}{d_b} \quad \text{for D1-D9.70 CFRP bar}$$

where u = mean bond strength (MPa);

f_c' = compressive strength of concrete (MPa);

d_b = nominal diameter of CFRP bar (mm).

These equations can be rearranged and presented in terms of development length, as shown in the following:

$$l_d = \frac{0.0509 A_b f_f}{\sqrt{f_c'}}$$ for G1-D8 and G1-D10 CFRP bars

$$l_d = \frac{0.0936 A_b f_f}{\sqrt{f_c'}}$$ for G2-D9.79 CFRP bar

$$l_d = \frac{0.0377 A_b f_f}{\sqrt{f_c'}}$$ for D1-D9.70 CFRP bar

where l_d = development length of CFRP bar (mm);

A_b = nominal cross-sectional area of CFRP bar (mm^2);

f_f = tensile strength of CFRP bar (MPa);

f_c' = compressive strength of concrete (MPa).

Table 4.1: Pullout test results of G1-D8 CFRP bar

Properties of Reinforcement	Pullout Specimen	l_b (mm)	f_c' (MPa)	P (kN)	u (MPa)	u*d/fc'^1/2 (K_1)
Glasform 1 Dia.= 8 mm E_f = 159 GPa f_{fu} = 1455 MPa	G1-D8-P1	60	26	4.98	3.27	5.13
	G1-D8-P2	60	30	2.22	1.49	2.18
	G1-D8-P3	80	26	8.68	4.31	6.76
	G1-D8-P4	80	30	2.67	1.32	1.93
	G1-D8-P5	80	30	5.78	2.86	4.18
	G1-D8-P6	120	30	4.45	1.48	2.16
	G1-D8-P7	120	30	7.12	2.35	3.43

Note:
The first set of letters and numbers refers to manufacturer and type of CFRP bar manufactered by the manufacturer, respectively.
The second of letters and numbers refers to diameter of CFRP bar.
The third set of letters and numbers refers to the number of pullout specimen.

Table 4.2: Beam test results of G1-D8 CFRP bar

Properties of Reinforcement	Beam Specimen	l_b (mm)	f_c' (MPa)	T (kN)	u (MPa)	$u*d/f_c\hat{}1/2$ (K_1)	Failure	Remark
Glasform1 Dia. = 8 mm E_f = 159 GPa f_{fu} = 1455 MPa	G1-D8-B1	381	35	54.2	5.66	7.65	Shear/Bond	Stirrups
	G1-D8-B2	457	17	48.5	4.22	8.26	Bond	
	G1-D8-B3	533	30	55.6	4.14	6.05	Bond	
	G1-D8-B4	610	30	60.5	3.94	5.76	Compression / Bond	
	G1-D8-B5	610	28	67.2	4.39	6.63	Bond	
	G1-D8-B6	762	35	74.4	3.88	5.25	Tension / Bond	
	G1-D8-B7	787	25	65.4	3.30	5.28	Bond	Stirrups
	G1-D8-B8	610	31	>79.8	>5.21	NA	Tension	
	G1D8-B9	686	30	>42.3	>2.45	NA	Shear (dowel)	
	G1-D8-B10	838	35	>68.8	>3.27	NA	Tension	
	G1-D8-B11	1092	30	>51.6	>1.88	NA	Shear (dowel)	
	G1-D8-B12	406	40	46.1	4.52	5.72	Bond	Stirrups
	G1-D8-B13	508	40	65.1	5.10	6.46	Bond	Stirrups
	*G1-D8-B14	584	43	67.3	4.58	5.59	Bond	Stirrups
	G1-D8-B15	419	43	>53.3	>5.06	NA	Tension	Stirrups

Note:
The first set of letters and numbers refers to manufacturer and type of CFRP bar manufactered by the manufacturer, respectively.
The second of letters and numbers refers to diameter of CFRP bar.
The third set of letters and numbers refers to the number of beam specimen.
*Bond strength was calculated based on 0.10 mm free-end slip, except beam G1-d8-B14 (which was based on 0.08 mm (max. free-end slip)).
All beam specimens were conducted by Abdel-Sayed et al. (1998), except beams G1-D8-B12 to G1-D8-G15.

Table 4.3: Effect of transverse reinforcement on bond strength (G1-D8 bar, beam test)

Properties of Reinforcement	Beam Specimen		l_b (mm)		u (MPa)	
	No Stirrups	Stirrups	No Stirrups	Stirrups	No Stirrups	Stirrups
Glasform 1 Dia.= 8 mm E_f = 159 GPa f_{fu} = 1455 MPa	G1-D8-B2	G1-D8-B1	457	381	4.22	5.66
	G1-D8-B3	G1-D8-B7	533	787	4.14	3.30
	G1-D8-B4	G1-D8-B12	610	406	3.94	4.52
	G1-D8-B5	G1-D8-B13	610	508	4.39	5.10
	G1-D8-B6	G1-D8-B14	762	584	3.88	4.79

Note:

The first set of letters and numbers refers to manufacturer and type of CFRP bar manufactered by the manufacturer, respectively.
The second of letters and numbers refers to diameter of CFRP bar.
The third set of letters and numbers refers to the number of beam specimen.

Table 4.4: Beam test results of G1-D10 CFRP bar

Properties of Reinforcement	Beam Specimen	l_b (mm)	f_c' (MPa)	T (kN)	u (MPa)	$u*d/f_c\text{^}1/2$ (K_1)	Failure
Glasform 1 Dia. = 10 mm E_f = 157 GPa f_{fu} = 1469 MPa	G1-D10-B1	330.2	35	50.1	4.82	6.51	Shear/Bond
	G1-D10-B2	330.2	36	50.9	4.90	6.53	Shear/Bond
	G1-D10-B3	406.4	35	52.6	4.11	5.55	Shear/Bond
	G1-D10-B4	457.2	35	62.7	4.36	5.89	Bond
	G1-D10-B5	457.2	35	72.2	5.02	6.79	Compression / Bond
	G1-D10-B6	495.3	35	>73.7	>4.73	NA	Shear
	G1-D10-B7	609.6	33	>63.0	>3.28	NA	Compression

Note:
The first set of letters and numbers refers to manufacturer and type of CFRP bar manufactered by the manufacturer, respectively.
The second of letters and numbers refers to diameter of CFRP bar.
The third set of letters and numbers refers to the number of beam specimen.

Table 4.5: Comparison of bond strength obtained from pullout and beam tests

Properties of Reinforcement	Specimens		l_b (mm)		u (MPa)	
	Pullout	Beam	Pullout	Beam	Pullout	Beam
Glasform 1 Dia.= 8 mm E_f = 159 GPa f_{fu} = 1455 MPa	G1-D8-P1	G1-D8-B1	60	381	3.27	5.66
	G1-D8-P2	G1-D8-B2	60	457	1.49	4.22
	G1-D8-P3	G1-D8-B3	80	533	4.31	4.14
	G1-D8-P4	G1-D8-B4	80	610	1.32	3.94
	G1-D8-P5	G1-D8-B5	80	610	2.86	4.39
	G1-D8-P6	G1-D8-B6	120	762	1.48	3.88
	G1-D8-P7	G1-D8-B7	120	787	2.35	3.30
		G1-D8-B12		406		4.52
		G1-D8-B13		508		5.10
		G1-D8-B14		584		4.79

Note:

The first set of letters and numbers refers to manufacturer and type of CFRP bar manufactered by the manufacturer, respectively.
The second of letters and numbers refers to diameter of CFRP bar.
The third set of letters and numbers refers to the number of pullout/beam specimen.

Table 4.6: Comparison of maximum tensile force of G2-D9.79 CFRP bar

Beam Specimen	T_{max} (kN)		Percent Difference
	Experiment	Theory	
G2-D9.79-A18	32.25	31.1	-3.59
G2-D9.79-B18	32.35	32.6	0.78
G2-D9.79-C18	37.38	36.7	-1.87
G2-D9.79-A24	44.24	45.6	2.96
G2-D9.79-B24	49.25	51.8	4.95
G2-D9.79-C24	47.32	50.5	6.35
G2-D9.79-A30	49.60	53.2	6.77
G2-D9.79-B30	60.20	57.1	-5.49
G2-D9.79-C30	59.19	63.0	6.09
G2-D9.79-A36	77.76	78.3	0.67
G2-D9.79-B36	71.55	69.3	-3.24
G2-D9.79-C36	72.49	75.6	4.13

Note:
The first set of letters and numbers refers to manufacturer and type of CFRP bar manufactured by the manufacturer, respectively.
The second set of letters and numbers refers to diameter of CFRP bar.
The third set of letters and numbers refers to group of beam specimen and embedment length (inches), respectively.

Table 4.7: Tensile force at free-end slip of 0.05, 0.10 and 0.25 mm (G2-D9.79 bar)

Beam Specimen	Tensile Force (kN) Free-end Slip (mm)				Tensile Force at Slip / Maximum Tensile Force		
	0.05	0.10	0.25	maximum	0.05/maximum	0.10/maximum	0.25/maximum
G2-D9.79-A18	16.77	26.86	28.88	32.25	0.520	0.83	0.895
G2-D9.79-B18	24.24	26.53	28.93	32.35	0.749	0.820	0.894
G2-D9.79-C18	24.47	27.40	31.62	37.38	0.654	0.733	0.846
G2-D9.79-A24	34.74	36.37	38.85	44.24	0.785	0.822	0.878
G2-D9.79-B24	31.32	32.74	35.68	49.25	0.636	0.665	0.724
G2-D9.79-C24	35.06	37.03	39.71	47.32	0.741	0.782	0.839
G2-D9.79-A30	40.70	43.15	46.44	49.60	0.821	0.870	0.936
G2-D9.79-B30	51.14	53.07	58.29	60.20	0.849	0.882	0.968
G2-D9.79-C30	52.64	54.61	57.59	59.19	0.889	0.923	0.973
*G2-D9.79-C16	47.99	51.73	56.58	59.20	0.811	0.874	0.956
G2-D9.79-A36	74.03	75.07		77.76	0.952	0.965	NA
G2-D9.79-B36	64.39	66.98	71.55	71.55	0.900	0.936	1.000
G2-D9.79-C36	57.20	58.93	63.38	72.49	0.789	0.813	0.874
*G2-D9.79-C22	45.06	46.70	51.15	60.05	0.750	0.778	0.852

Note:

The first set of letters and numbers refers to manufacturer and type of CFRP bar manufactured by the manufacturer, respectively.

The second set of letters and numbers refers to diameter of CFRP bar.

The third set of letters and numbers refers to group of beam specimen and embedment length (inches), respectively.

*reduced bond length.

Table 4.8: Bond strength at free-end slip of 0.05, 0.10 abd 0.25 mm (G2-D9.79 bar)

Beam Specimen	Bond Strength (MPa) Free-end Slip (mm)				Bond Strength at Slip / Maximum Bond Strength		
	0.05	0.10	0.25	maximum	0.05 / maximum	0.10 / maximum	0.25 / maximum
G2-D9.79-A18	1.19	1.91	2.06	2.30	0.520	0.833	0.895
G2-D9.79-B18	1.73	1.89	2.06	2.30	0.749	0.820	0.894
G2-D9.79-C18	1.74	1.95	2.25	2.66	0.654	0.733	0.846
G2-D9.79-A24	1.85	1.94	2.07	2.36	0.785	0.822	0.878
G2-D9.79-B24	1.67	1.75	1.91	2.63	0.636	0.665	0.724
G2-D9.79-C24	1.87	1.98	2.12	2.53	0.741	0.782	0.839
G2-D9.79-A30	1.74	1.84	1.98	2.12	0.821	0.870	0.936
G2-D9.79-B30	2.18	2.27	2.49	2.57	0.849	0.882	0.968
G2-D9.79-C30	2.25	2.33	2.46	2.53	0.889	0.923	0.973
*G2-D9.79-C16	3.84	4.14	4.53	4.74	0.811	0.874	0.956
G2-D9.79-A36	2.64	2.67	NA	2.77	0.952	0.965	NA
G2-D9.79-B36	2.29	2.38	2.55	2.55	0.900	0.936	1.000
G2-D9.79-C36	2.04	2.10	2.26	2.58	0.789	0.813	0.874
*G2-D9.79-C22	2.62	2.72	2.98	3.50	0.750	0.778	0.852

Note:
The first set of letters and numbers refers to manufacturer and type of CFRP bar manufactured by the manufacturer, respectively.
The second set of letters and numbers refers to diameter of CFRP bar.
The third set of letters and numbers refers to group of beam specimen and embedment length (inches), respectively.
*reduced bond length.

Table 4.9: Tensile force at loaded-end slip of 0.25 and 0.50 mm (G2-D9.79 bar)

Beam Specimen	Tensile Force(kN)			Tensile Force at Slip / Maximum Tensiel Force	
	Loaded-end Slip (mm)			Loaded-end Slip (mm)	
	0.25	0.50	maximum	0.25 / maximum	0.50 / maximum
G2-D9.79-A18	1.44	2.15	32.25	0.045	0.067
G2-D9.79-B18	7.87	15.57	32.35	0.243	0.481
G2-D9.79-C18	12.47	21.05	37.38	0.333	0.563
G2-D9.79-A24	8.79	17.57	44.24	0.199	0.397
G2-D9.79-B24	9.84	19.06	49.25	0.200	0.387
G2-D9.79-C24	9.28	18.69	47.32	0.196	0.395
G2-D9.79-A30	13.69	19.68	49.60	0.276	0.397
G2-D9.79-B30	13.16	23.31	60.20	0.219	0.387
G2-D9.79-C30	11.25	22.18	59.19	0.190	0.375
G2-D9.79-A36	7.42	28.46	77.76	0.095	0.366
G2-D9.79-B36	13.07	24.92	71.55	0.183	0.348
G2-D9.79-C36	13.75	22.76	72.49	0.190	0.314

Note:
The first set of letters and numbers refers to manufacturer and type of CFRP bar manufactured by the manufacturer, respectively.
The second set of letters and numbers refers to diameter of CFRP bar.
The third set of letters and numbers refers to group of beam specimen and embedment length (inches), respectively.

Table 4.10: Bond strength at loaded-end slip of 0.25 and 0.50 mm (G2-D9.79 bar)

Beam Specimen	Bond Strength (MPa)			Bond Strength at Slip / Maximum Bond Strength	
	Loaded-end Slip (mm)			Loaded-end Slip (mm)	
	0.25	0.50	maximum	0.25 / maximum	0.50 / maximum
G2-D9.79-A18	0.103	0.153	2.30	0.045	0.067
G2-D9.79-B18	0.560	1.108	2.30	0.243	0.481
G2-D9.79-C18	0.888	1.50	2.66	0.333	0.563
G2-D9.79-A24	0.469	0.938	2.36	0.199	0.397
G2-D9.79-B24	0.526	1.018	2.63	0.200	0.387
G2-D9.79-C24	0.496	0.998	2.53	0.196	0.395
G2-D9.79-A30	0.585	0.841	2.12	0.276	0.397
G2-D9.79-B30	0.562	0.996	2.57	0.219	0.387
G2-D9.79-C30	0.481	0.947	2.53	0.190	0.375
G2-D9.79-A36	0.264	1.013	2.77	0.095	0.366
G2-D9.79-B36	0.465	0.887	2.55	0.183	0.348
G2-D9.79-C36	0.490	0.810	2.58	0.190	0.314

Note:
The first set of letters and numbers refers to manufacturer and type of CFRP bar manufactured by the manufacturer, respectively.
The second set of letters and numbers refers to diameter of CFRP bar.
The third set of letters and numbers refers to group of beam specimen and embedment length (inches), respectively.

Table 4.11: Summary of calculations for G2-D9.79 CFRP bar at free-end slip

Beam Specimen	l_b (mm)	f_c' (MPa)	fc'^1/2 (MPa)	T (kN)		u (MPa)		u/fc'^1/2		u*d/fc'^1/2 (K_1)		$f_c'^{1/2}/u*pi*d$ (K_2)		Failure Mode
				Free-end Slip (mm)		Free-end Slip (mm)		Free-end Slip (mm)		Free-end Slip (mm)		Free-end Slip (mm)		
				0.05	0.10	0.05	0.10	0.05	0.10	0.05	0.10	0.05	0.10	
G2-D9.79-A18	457	36	6.00	16.77	26.86	1.19	1.91	0.199	0.319	1.95	3.12	0.1634	0.2851	Bond
G2-D9.79-B18	457	36	6.00	24.24	26.53	1.73	1.89	0.288	0.315	2.82	3.08	0.1130	0.4172	Bond
G2-D9.79-C18	457	41	6.40	24.47	27.40	1.74	1.95	0.272	0.305	2.66	2.98	0.1195	0.4077	Bond
G2-D9.79-A24	610	44	6.63	34.74	36.37	1.85	1.94	0.280	0.293	2.74	2.87	0.1163	0.5815	Bond
G2-D9.79-B24	610	49	7.00	31.32	32.74	1.67	1.75	0.239	0.250	2.34	2.45	0.1361	0.5825	Bond
G2-D9.79-C24	610	43	6.56	35.06	37.03	1.87	1.98	0.285	0.302	2.79	2.95	0.1139	0.5765	Bond
G2-D9.79-A30	762	42	6.48	40.70	43.15	1.74	1.84	0.268	0.284	2.63	2.78	0.1212	0.7179	Bond
G2-D9.79-B30	762	48	6.93	51.14	53.07	2.18	2.27	0.315	0.327	3.09	3.20	0.1031	0.7334	Bond
G2-D9.79-C30	762	44	6.63	52.64	54.61	2.25	2.33	0.339	0.352	3.32	3.44	0.0959	0.7336	Bond
*G2-D9.79-C16	406	44	6.63	47.99	51.73	3.84	4.14	0.580	0.625	5.67	6.12	0.0561	0.3766	Bond
G2-D9.79-A36	914	44	6.63	74.03	75.07	2.64	2.67	0.397	0.403	3.89	3.94	0.0818	0.9007	Bond
G2-D9.79-B36	914	45	6.71	64.39	66.98	2.29	2.38	0.342	0.355	3.35	3.48	0.0951	0.8780	Bond
G2-D9.79-C36	914	43	6.56	57.20	58.93	2.04	2.10	0.311	0.320	3.04	3.13	0.1047	0.8865	Bond
*G2-D9.79-C22	559	43	6.56	45.06	46.70	2.62	2.72	0.400	0.415	3.92	4.06	0.0812	0.5385	Bond

Note:

The first set of letters and numbers refers to manufacturer and type of CFRP bar manufactured by the manufacturer, respectively.

The second set of letters and numbers refers to diameter of CFRP bar.

The third set of letters and numbers refers to group of beam specimen and embedment length (inches), respectively.

*reduced bond length.

Table 4.12: Summary of calculations for G2-D9.79 CFRP bar at loaded-end slip

Beam Specimen	l_b (mm)	f_c' (MPa)	fc'^1/2 (MPa)	T (kN)		u (MPa)		u/fc'^1/2		u*d/fc'^1/2 (K_1)		$f_c'^{1/2}/u*pi*d$ (K_2)	
				Loaded-end Slip (mm)		Loaded-end Slip (mm)		Loaded-end Slip (mm)		Loaded-end Slip (mm)		Loaded-end Slip (mm)	
				0.25	0.50	0.25	0.50	0.25	0.50	0.25	0.50	0.25	0.50
G2-D9.79-A18	457	36	6.00	1.27	1.89	0.088	0.131	0.0147	0.0218	0.1434	0.2135	2.2191	0.3150
G2-D9.79-B18	457	36	6.00	6.89	13.7	0.479	0.949	0.0799	0.1581	0.7823	1.5480	0.4069	0.2363
G2-D9.79-C18	457	41	6.40	10.9	18.5	0.760	1.28	0.1187	0.2004	1.1617	1.9619	0.2740	0.2773
G2-D9.79-A24	610	44	6.63	7.74	15.4	0.402	0.803	0.0606	0.1211	0.5931	1.1855	0.5367	0.3133
G2-D9.79-B24	610	49	7.00	8.63	16.7	0.450	0.872	0.0643	0.1245	0.6290	1.2189	0.5060	0.3219
G2-D9.79-C24	610	43	6.56	8.14	16.4	0.424	0.854	0.0647	0.1303	0.6333	1.2754	0.5026	0.3098
G2-D9.79-A30	762	42	6.48	12.0	17.3	0.501	0.720	0.0773	0.1111	0.7564	1.0874	0.4208	0.5425
G2-D9.79-B30	762	48	6.93	11.6	20.5	0.481	0.852	0.0694	0.1230	0.6798	1.2042	0.4683	0.4412
G2-D9.79-C30	762	44	6.63	9.87	19.5	0.411	0.811	0.0620	0.1222	0.6070	1.1967	0.5244	0.3960
G2-D9.79-A36	914	44	6.63	6.49	25.0	0.226	0.867	0.0341	0.1308	0.3337	1.2802	0.9539	0.2434
G2-D9.79-B36	914	45	6.71	11.5	21.9	0.398	0.759	0.0594	0.1132	0.5814	1.1079	0.5475	0.4915
G2-D9.79-C36	914	43	6.56	12.1	20.0	0.503	0.832	0.0767	0.1269	0.7507	1.2425	0.4240	0.4727

Note:
The first set of letters and numbers refers to manufacturer and type of CFRP bar manufactured by the manufacturer, respectively.
The second set of letters and numbers refers to diameter of CFRP bar.
The third set of letters and numbers refers to group of beam specimen and embedment length (inches), respectively.

Table 4.13: Effect of support condition on bond strength (G2-D9.79 bar)

Beam Specimen	Bond Strength (MPa)				Percent Difference			
	Free-end Slip (mm)				Free-end Slip (mm)			
	0.05	0.10	0.25	maximum	0.05	0.10	0.25	maximum
G2-D9.79-A18	1.19	1.91	2.06	2.30	44.52	-1.24	0.17	0.30
G2-D9.79-B18	1.73	1.89	2.06	2.30				
G2-D9.79-A24	1.85	1.94	2.07	2.36	-9.82	-9.97	-8.17	11.32
G2-D9.79-B24	1.67	1.75	1.91	2.63				
G2-D9.79-A30	1.74	1.84	1.98	2.12	25.64	23.00	25.53	21.38
G2-D9.79-B30	2.18	2.27	2.49	2.57				
G2-D9.79-A36	2.64	2.67	NA	2.77	-13.02	-10.77	NA	-7.99
G2-D9.79-B36	2.29	2.38	2.55	2.55				

Note:
The first set of letters and numbers refers to manufacturer and type of CFRP bar manufactured by the manufacturer, respectively.
The second set of letters and numbers refers to diameter of CFRP bar.
The third set of letters and numbers refers to group of beam specimen and embedment length (inches), respectively.

Table 4.14: Effect of transverse reinforcement of bond strength (G2-D9.79 bar)

Beam Specimen	Bond Strength (MPa)				Percent Difference			
	Free-end Slip (mm)				Free-end Slip (mm)			
	0.05	0.10	0.25	maximum	0.05	0.10	0.25	maximum
G2-D9.79-B18	1.73	1.89	2.06	2.30	0.94	3.28	9.32	15.56
G2-D9.79-C18	1.74	1.95	2.25	2.66				
G2-D9.79-B24	1.67	1.75	1.91	2.63	11.92	13.08	11.30	-3.92
G2-D9.79-C24	1.87	1.98	2.12	2.53				
G2-D9.79-B30	2.18	2.27	2.49	2.57	2.94	2.90	-1.21	-1.68
G2-D9.79-C30	2.25	2.33	2.46	2.53				
G2-D9.79-B36	2.29	2.38	2.55	2.55	-11.17	-12.02	-11.42	1.32
G2-D9.79-C36	2.04	2.10	2.26	2.58				

Note:
The first set of letters and numbers refers to manufacturer and type of CFRP bar manufactured by the manufacturer, respectively.
The second set of letters and numbers refers to diameter of CFRP bar.
The third set of letters and numbers refers to group of beam specimen and embedment length (inches), respectively.

Table 4.15: Comparison of maximum tensile force of D1-D9.70 CFRP bar

Beam Specimen	T_{max} (kN)		Percent Difference
	Experiment	Theory	
D2-D9.70-A12	53.77	50.62	6.22
D1-D9.70-B12	53.91	53.02	1.68
D1-D9.70-C12	60.57	57.07	6.13
D1-D9.70-A18	62.11	58.40	6.35
D1-D9.70-B18	56.49	61.16	-7.64
D1-D9.70-C18	70.55	65.25	8.11
D1-D9.70-A24	67.01	69.30	-3.30
D1-D9.70-B24	77.32	73.39	5.35
D1-D9.70-C24	88.61	81.53	8.69
D1-D9.70-A30	62.57	61.83	1.20
D1-D9.70-B30	67.58	67.61	-0.04
D1-D9.70-C30	72.15	70.41	2.47
**D1-D9.70-B18Comp	62.15	73.39	-15.32
**D1-D9.70-C18Comp	103.53	101.95	1.55

Note:
The first set of letters and numbers refers to manufacturer and type of CFRP bar manufactured by the manufacturer, respectively.
The second set of letters and numbers refers to diameter of CFRP bar.
The third set of letters and numbers refers to group of beam specimen and embedment length (inches), respectively.
**Beams reinforced with CFRP bar and two 25.4 mm (1 in.) diameter compression steels.

Table 4.16: Tensile force at free-end slip of 0.05 and 0.10 mm

Beam Specimen	Tensile Force (kN)			Tensile Force at Slip / Maximum Tensile Force	
	Free-end Slip (mm)		maximum		
	0.05	0.10		0.05 / maximum	0.10 / maximum
D1-D9.70-A12	50.33	52.79	53.77	0.936	0.982
D1-D9.70-B12	51.48	53.22	53.91	0.955	0.987
D1-D9.70-C12	57.68	60.57	60.57	0.952	1.000
D1-D9.70-A18	NA	NA	62.11	NA	NA
D1-D9.70-B18	NA	NA	56.49	NA	NA
D1-D9.70-C18	NA	NA	70.54	NA	NA
D1-D9.70-A24	NA	NA	67.01	NA	NA
D1-D9.70-B24	70.87	73.49	77.32	0.917	0.950
*D1-D9.70-B21.5	61.74	66.76	77.31	0.799	0.864
D1-D9.70-C24	84.76	86.68	88.61	0.956	0.978
*D1-D9.70-C11	46.88	47.90	49.11	0.955	0.976
D1-D9.70-A30	NA	NA	62.57	NA	NA
*D1-D9.70-A21	NA	NA	58.40	NA	NA
*D1-D9.70-A22.5	NA	NA	58.40	NA	NA
D1-D9.70-B30	NA	NA	67.58	NA	NA
*D1-D9.70-B15	NA	NA	56.93	NA	NA
*D1-D9.70-B23	NA	NA	56.93	NA	NA
D1-D9.70-C30	69.37	70.80	72.15	0.961	0.981
*D1-D9.70-C16.5	65.16	66.32	68.50	0.951	0.968
*D1-D9.70-C21.5	68.10	68.41	75.08	0.907	0.911
**D1-D9.70-B18Comp	NA	NA	62.15	NA	NA
**D1-D9.70-B18Comp	81.85	90.94	103.53	0.791	0.878

Note: The first set of letters and numbers refers to manufacturer and type of CFRP bar manufactured by the manufacturer, respectively.
The second set of letters and numbers refers to diameter of CFRP bar.
The third set of letters and numbers refer to group of beam specimen and embedment length (inches), respectively.
*reduced bond length.
**Beams reinforced with CFRP bar and two 25.4 mm (1 in.) diameter compression steels.

Table 4.17: Bond strength at free-end slip of 0.05 and 0.10 mm (D1-D9.70 bar)

Beam Specimen	Bond Strength (MPa)			Bond Strength at Slip / Maximum Bond Strength	
	Free-end Slip (mm)		maximum		
	0.05	0.10		0.05 / maximum	0.10 / maximum
D1-D9.70-A12	5.42	5.68	5.79	0.936	0.982
D1-D9.70-B12	5.54	5.73	5.80	0.955	0.987
D1-D9.70-C12	6.21	6.52	6.52	0.952	1.000
D1-D9.70-A18	NA	NA	4.46	NA	NA
D1-D9.70-B18	NA	NA	4.05	NA	NA
D1-D9.70-C18	NA	NA	5.06	NA	NA
D1-D9.70-A24	NA	NA	3.61	NA	NA
D1-D9.70-B24	3.81	3.95	4.16	0.917	0.950
*D1-D9.70-B21.5	3.71	4.01	4.64	0.799	0.864
D1-D9.70-C24	4.56	4.67	4.77	0.956	0.978
*D1-D9.70-C11	5.51	5.63	5.77	0.955	0.976
D1-D9.70-A30	NA	NA	2.69	NA	NA
*D1-D9.70-A21	NA	NA	3.59	NA	NA
*D1-D9.70-A22.5	NA	NA	3.35	NA	NA
D1-D9.70-B30	NA	NA	2.91	NA	NA
*D1-D9.70-B15	NA	NA	4.90	NA	NA
*D1-D9.70-B23	NA	NA	3.20	NA	NA
D1-D9.70-C30	2.99	3.05	3.11	0.961	0.981
*D1-D9.70-C16.5	5.10	5.19	5.36	0.951	0.968
*D1-D9.70-C21.5	4.09	4.11	4.51	0.907	0.911
**D1-D9.70-B18Comp	NA	NA	4.46	NA	NA
**D1-D9.70-C18Comp	5.87	6.53	7.43	0.791	0.878

Note: The first set of letters and numbers refers to manufacturer and type of CFRP bar manufactured by the manufacturer, respectively.
The second set of letters and numbers refers to diameter of CFRP bar.
The third set of letters and numbers refers to group of beam specimen and embedment length (inches), respectively.
* reduced bond length.
**Beams reinforced with CFRP bar and two 25.4 mm (1 in.) diameter compression steels.

Table 4.18: Summary of calculations for D1-D9.70 CFRP bar at free-end slip

Beam Specimen	l_b (mm)	f_c' (MPa)	fc'^1/2 (MPa)	T (kN) Free-end Slip (mm)		u (MPa) Free-end Slip (mm)		u/fc'^1/2 Free-end Slip (mm)		u*d/fc'^1/2 (K_1) Free-end Slip (mm)		$f_c'^{1/2}/u*pi*d$ (K_2) Free-end Slip (mm)		Failure Mode
				0.05	0.10	0.05	0.10	0.05	0.10	0.05	0.10	0.05	0.10	
D1-D9.70-A12	305	41	6.40	50.33	52.79	5.42	5.68	0.85	0.89	8.21	8.61	0.0388	0.0370	Bond / Splitting
D1-D9.70-B12	305	45	6.71	51.48	53.22	5.54	5.73	0.83	0.85	8.01	8.28	0.0397	0.0384	Bond / Splitting
D1-D9.70-C12	305	42	6.48	57.68	60.57	6.21	6.52	0.96	1.01	9.29	9.76	0.0343	0.0326	Bond
D1-D9.70-A18	457	42	6.48	NA	NA	NA	NA	NA	NA	NA	NA	NA	NA	Compression
D1-D9.70-B18	457	52	7.21	NA	NA	NA	NA	NA	NA	NA	NA	NA	NA	Compression
D1-D9.70-C18	457	41	6.40	NA	NA	NA	NA	NA	NA	NA	NA	NA	NA	Compression
D1-D9.70-A24	610	31	5.57	NA	NA	NA	NA	NA	NA	NA	NA	NA	NA	Compression
D1-D9.70-B24	610	43	6.56	70.87	73.49	3.81	3.95	0.58	0.60	5.64	5.85	0.0564	0.0544	Compression
*D1-D9.70-B21.5	546	43	6.56	61.74	66.76	3.71	4.01	0.57	0.61	5.49	5.93	0.0580	0.0536	Compression
D1-D9.70-C24	610	44	6.63	84.76	86.68	4.56	4.67	0.69	0.70	6.67	6.82	0.0477	0.0467	Bond
*D1-D9.70-C11	279	44	6.63	46.88	47.90	5.51	5.63	0.83	0.85	8.05	8.23	0.0395	0.0387	Bond
D1-D9.70-A30	762	44	6.63	NA	NA	NA	NA	NA	NA	NA	NA	NA	NA	Compression / Splitting
*D1-D9.70-A21	533	44	6.63	NA	NA	NA	NA	NA	NA	NA	NA	NA	NA	Compression / Splitting
*D1-D9.70-A22.5	572	44	6.63	NA	NA	NA	NA	NA	NA	NA	NA	NA	NA	Compression / Splitting
D1-D9.70-B30	762	42	6.48	NA	NA	NA	NA	NA	NA	NA	NA	NA	NA	Compression
*D1-D9.70-B15	381	42	6.48	NA	NA	NA	NA	NA	NA	NA	NA	NA	NA	Compression
*D1-D9.70-B23	584	42	6.48	NA	NA	NA	NA	NA	NA	NA	NA	NA	NA	Compression
D1-D9.70-C30	762	41	6.40	69.37	70.80	2.99	3.05	0.47	0.48	4.52	4.62	0.0704	0.0689	Compression
*D1-D9.70-C16.5	419	41	6.40	65.16	66.32	5.10	5.19	0.80	0.81	7.73	7.86	0.0412	0.0405	Compression
*D1-D9.70-C21.5	546	41	6.40	68.10	68.41	4.09	4.11	0.64	0.64	6.20	6.23	0.0514	0.0511	Compression
**D1-D9.70-B18Comp	457	42	6.48	NA	NA	NA	NA	NA	NA	NA	NA	NA	NA	Compression / Splitting
**D1-D9.70-C18Comp	457	48	6.93	81.85	90.94	5.87	6.53	0.85	0.94	8.22	9.14	0.0387	0.0348	Bond

Note: The first set of letters and numbers refers to manufacturer and type of CFRP bar manufactured by the manufacturer, respectively.
The second set of letters and numbers refers to diameter of CFRP bar.
The third set of letters and numbers refers to group of beam specimen and embedment length (inches), respectively.
*reduced bond length.
**Beams reinforced with CFRP bar and two 25.4 mm (1 in.) diameter compression steels.

Table 4.19: Effect of support condition on bond strength (D1-D9.70 bar)

Beam Specimen	Bond Strength (MPa)			Percent Difference		
	Free-end Slip (mm)			Free-end Slip (mm)		
	0.05	0.10	maximum	0.05	0.10	maximum
D1-D9.70-A12	5.42	5.68	5.79	2.29	0.82	0.27
D1-D9.70-B12	5.54	5.73	5.80			
D1-D9.70-A18	NA	NA	4.46	NA	NA	-9.05
D1-D9.70-B18	NA	NA	4.05			
D1-D9.70-A24	NA	NA	3.61	NA	NA	15.38
D1-D9.70-B24	3.81	3.95	4.16			
D1-D9.70-A30	NA	NA	2.69	NA	NA	8.01
D1-D9.70-B30	NA	NA	2.91			

Note:

The first set of letters and numbers refers to manufacturer and type of CFRP bar manufactured by the manufacturer, respectively.
The second set of letters and numbers refers to diameter of CFRP bar.
The third set of letters and numbers refers to group of beam specimen and embedment length (inches), respectively.

Table 4.20: Effect of transverse reinforcement on bond strength (D1-D9.70 bar)

Beam Specimen	Bond Strength (MPa)			Percent Difference		
	Free-end Slip (mm)			Free-end Slip (mm)		
	0.05	0.10	maximum	0.05	0.10	maximum
D1-D9.70-B12	5.54	5.73	5.80	12.04	13.81	12.35
D1-D9.70-C12	6.21	6.52	6.52			
D1-D9.70-B18	NA	NA	4.05	NA	NA	24.88
D1-D9.70-C18	NA	NA	5.06			
D1-D9.70-B24	3.81	3.95	4.16	19.59	17.95	14.61
D1-D9.70-C24	4.56	4.67	4.77			
D1-D9.70-B30	NA	NA	2.91	NA	NA	6.76
D1-D9.70-C30	2.99	3.05	3.11			
**D1-D9.70-B18Comp	NA	NA	4.46	NA	NA	66.59
**D1-D9.70-C18Comp	5.87	6.53	7.43			

Note:

The first set of letters and numbers refers to manufacturer and type of CFRP bar manufactured by the manufacturer, respectively.

The second set of letters and numbers refers to diameter of CFRP bar.

The third set of letters and numbers refers to group of beam specimen and embedment length (inches), respectively.

**Beams reinforced with CFRP bar and two 25.4 mm (1 in.) diameter compression steels.

Table 4.21: Summary of the test results of different types of CFRP bars

Properties of Reinforcement	Type of CFRP Bar					
Designation	G1-D8	G1-D10	G2-D9.79	D1-D9.70	Leadline	Leadline
Manufacturer	Glasform	Glasform	Glasform	DFI	Mitsuibshi. Kasei	Mitsuibshi. Kasei
d_b (mm)	8	10	9.79	9.70	8 (Smooth)	8 (Deformed)
E_f (GPa)	159	157	158	177	147	147
f_{fu} (MPa)	1455	1469	NA	NA	94.3	94.3
Range of Bond Strength (MPa)	3.30 - 5.66	4.11 - 5.02	1.75 - 4.14	4.67 - 6.53	0.317 - 0.483	7.35 - 7.55
Ave. value of Bond Strength (MPa)	4.37	4.64	2.28	5.79	0.417	7.57
Range of K_1	5.25 - 8.26	5.55 - 6.79	2.45 - 6.12	6.82 - 9.76	0.379 - 0.577	8.78 - 9.33
Ave. value of K_1	6.27	6.25	3.40	8.47	0.498	9.04

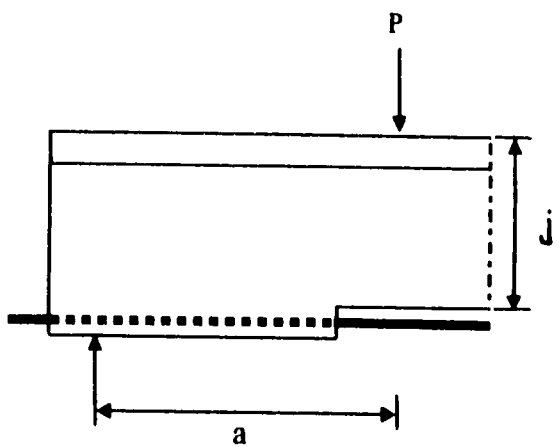

Figure 4.1: Beam specimen for calculation of tensile force by pure bending

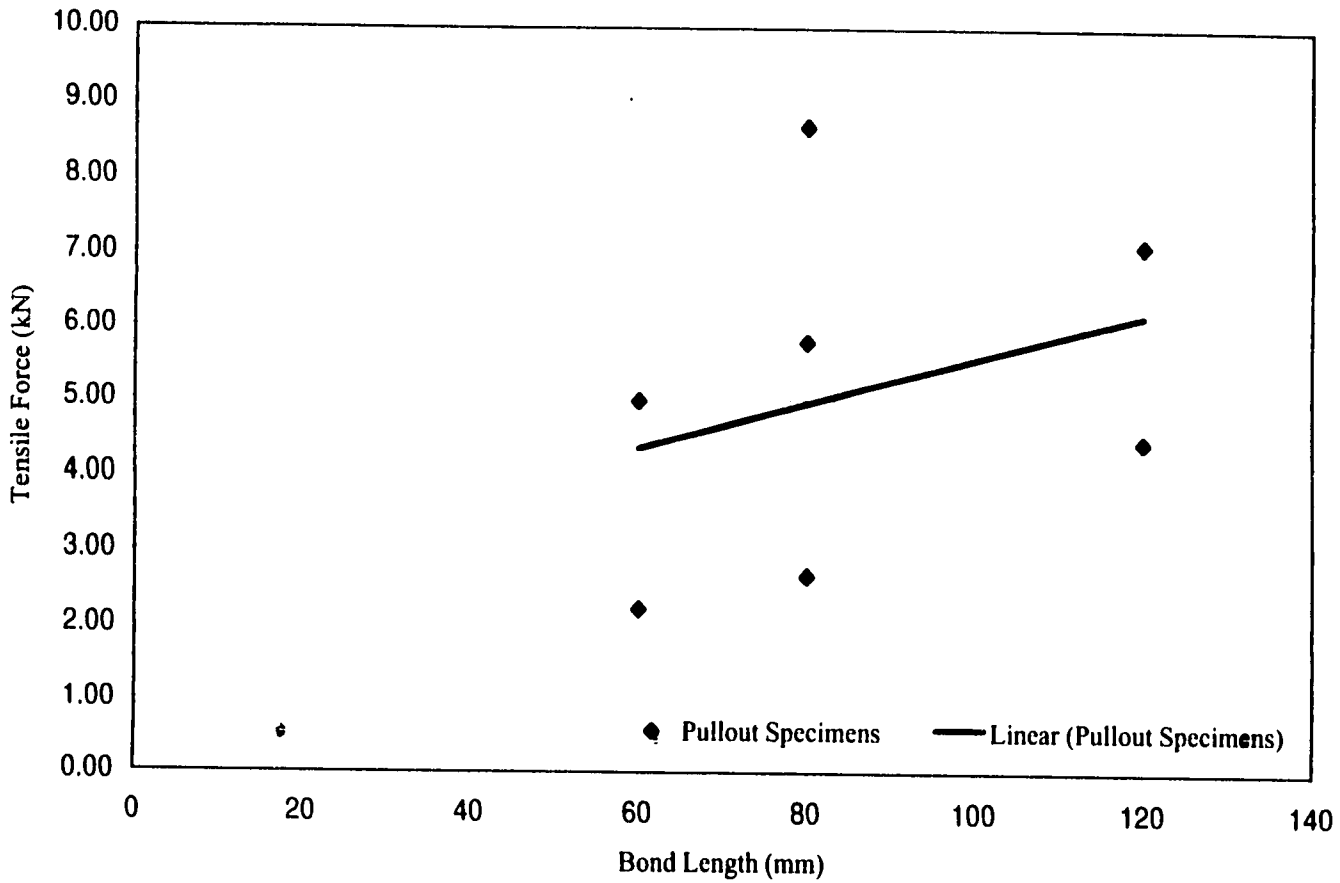

Figure 4.2: Tensile force vs. bond length (G1-D8 bar, pullout test)

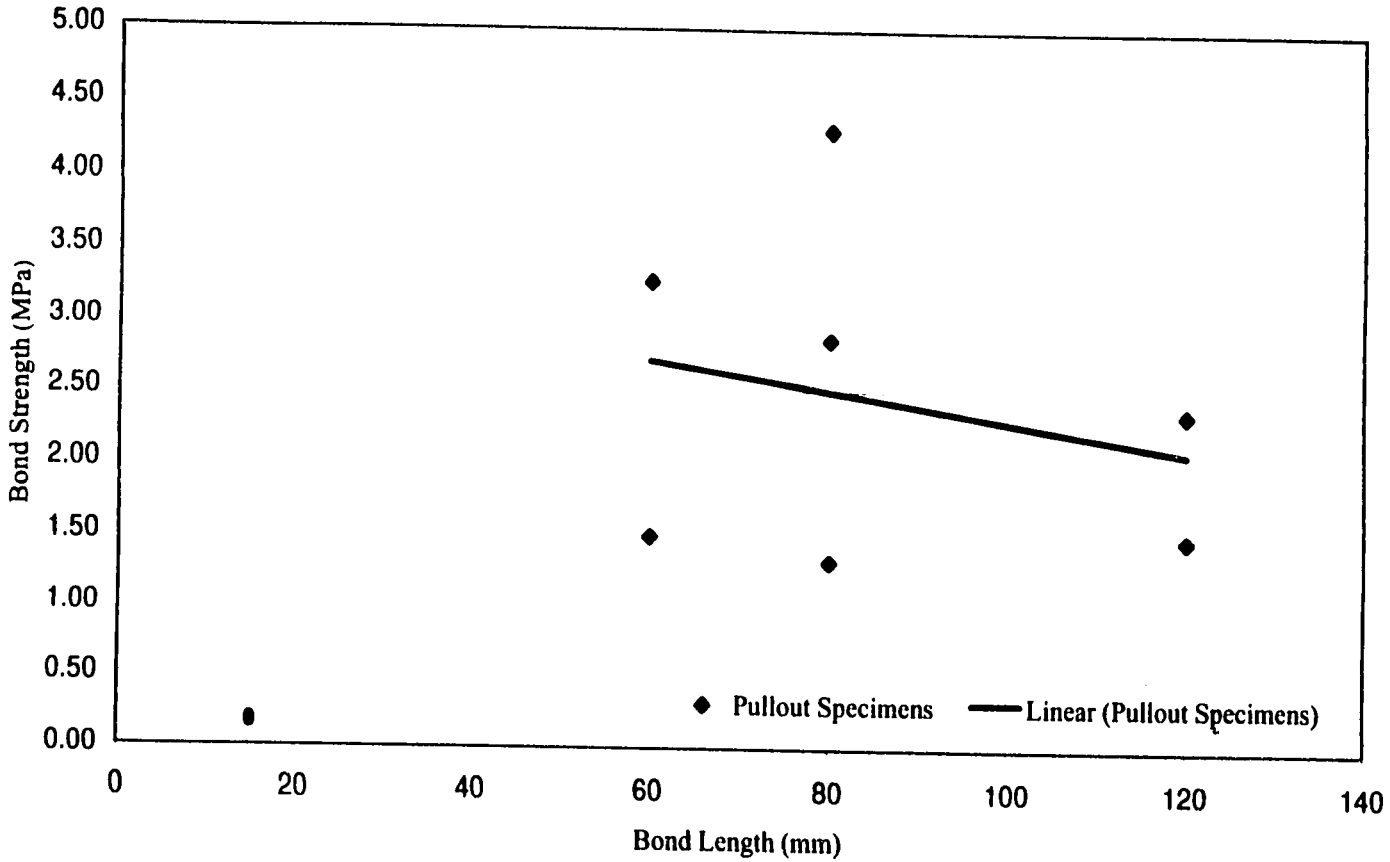

Figure 4.3: Bond strength vs. bond length (G1-D8 bar, pullout test)

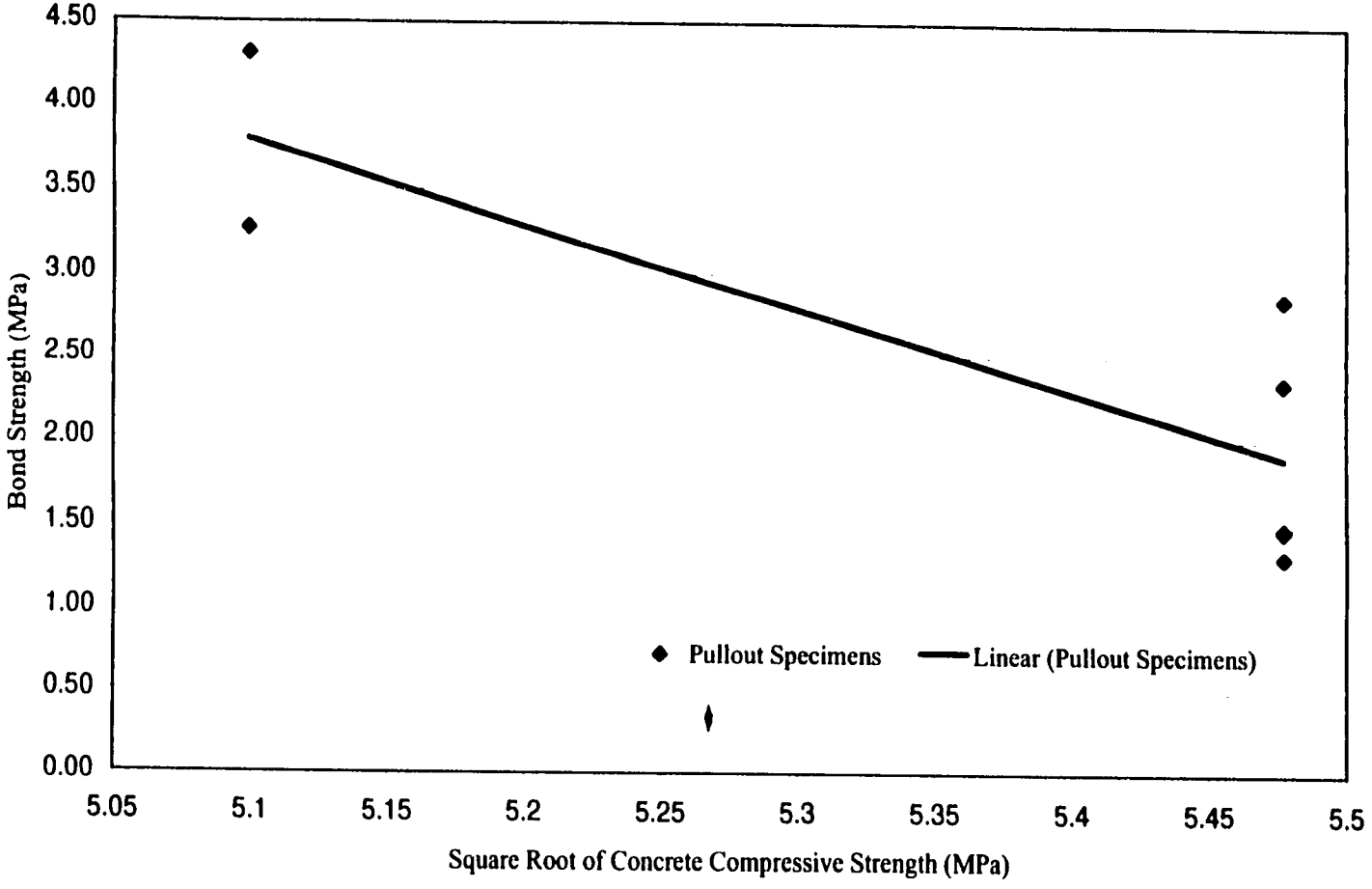

Figure 4.4: Bond strength vs. square root of concrete compressive strength (G1-D8 bar, pullout test)

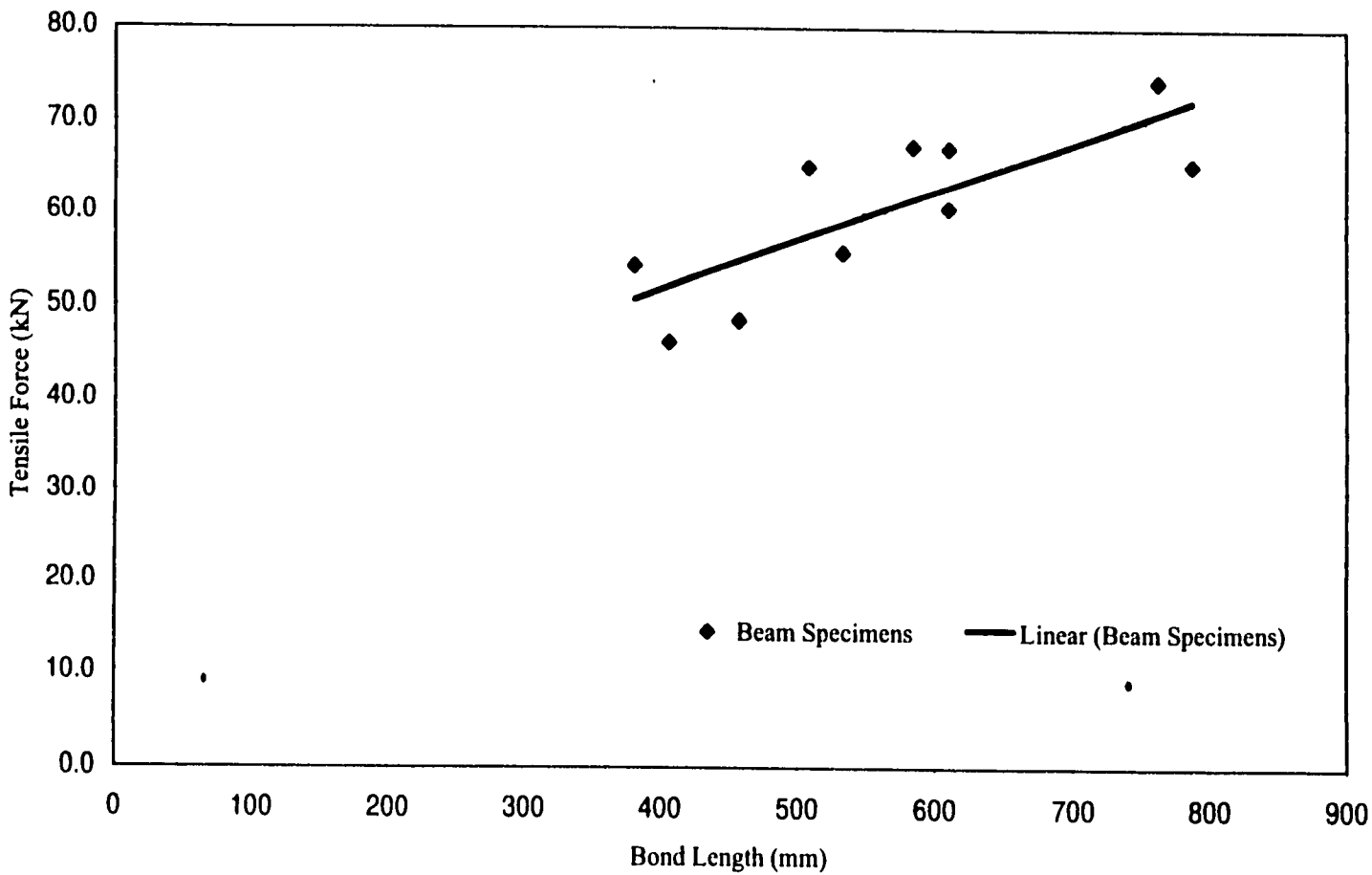

Figure 4.5: Tensile force vs. bond length (G1-D8 bar, beam test)

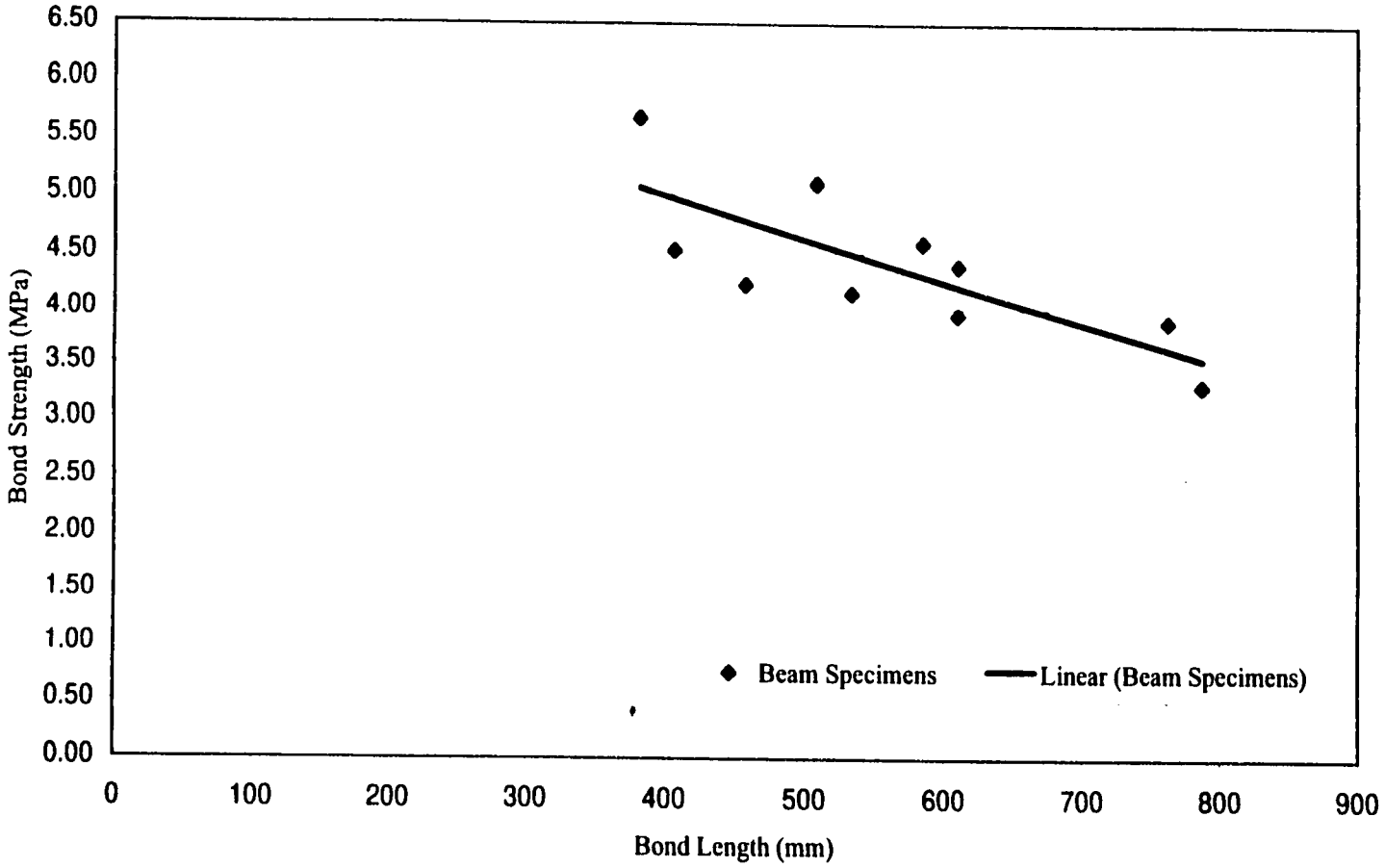

Figure 4.6: Bond strength vs. bond length (G1-D8 bar, beam test)

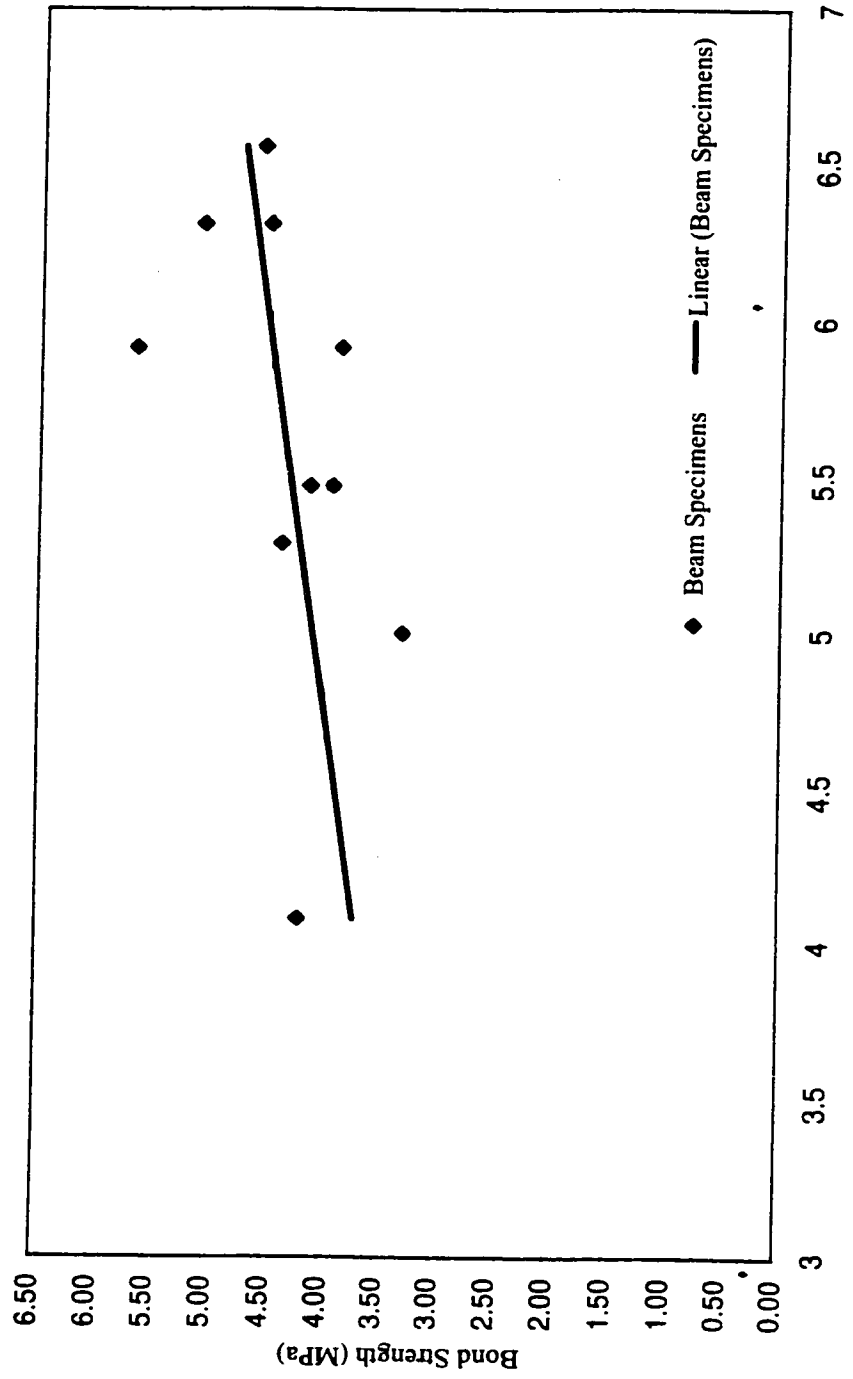

Figure 4.7: Bond strength vs. square root of concrete compressive strength (G1-D8 bar, beam test)

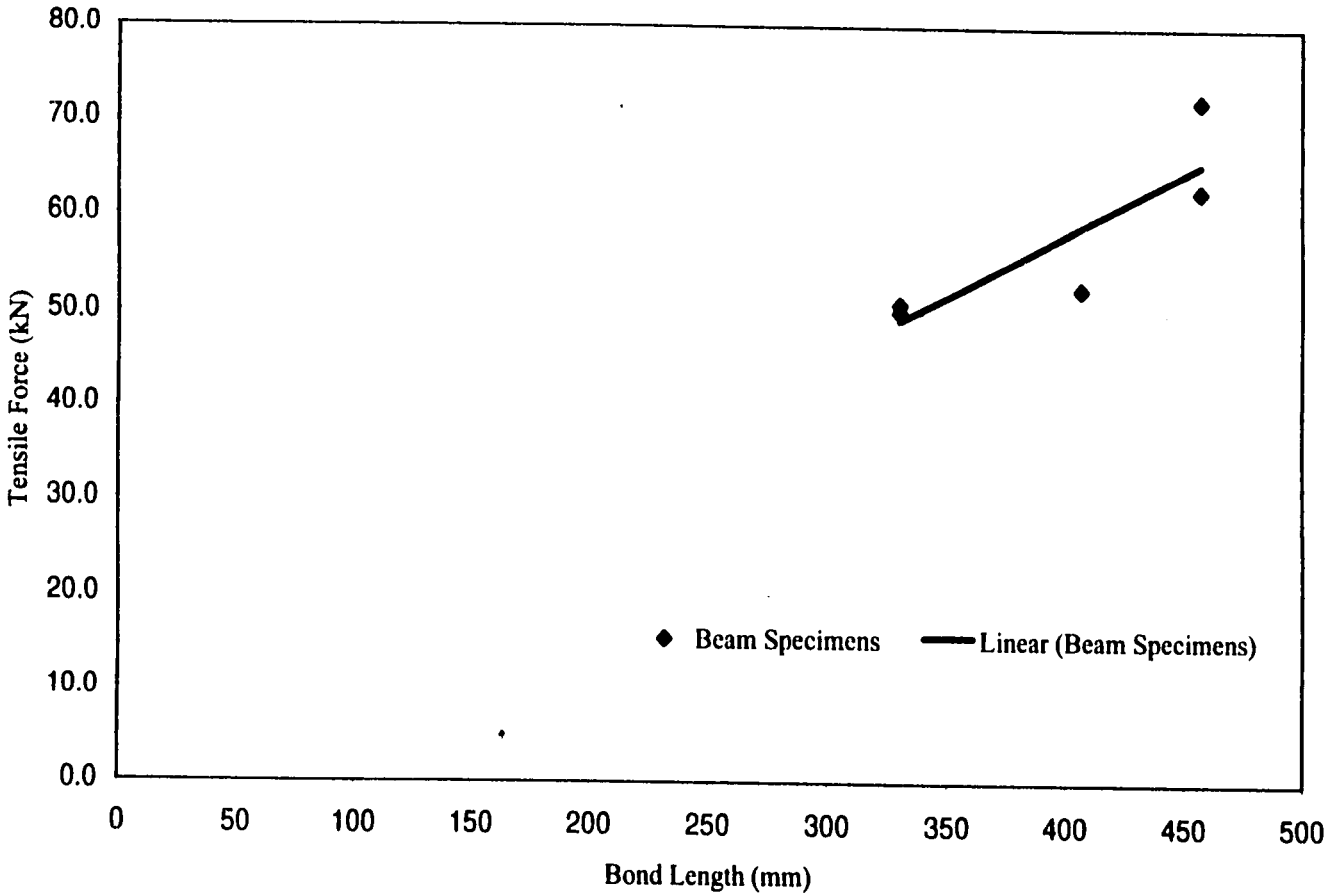

Figure 4.8: Tensile force vs. bond length (G1-D10 bar, beam test)

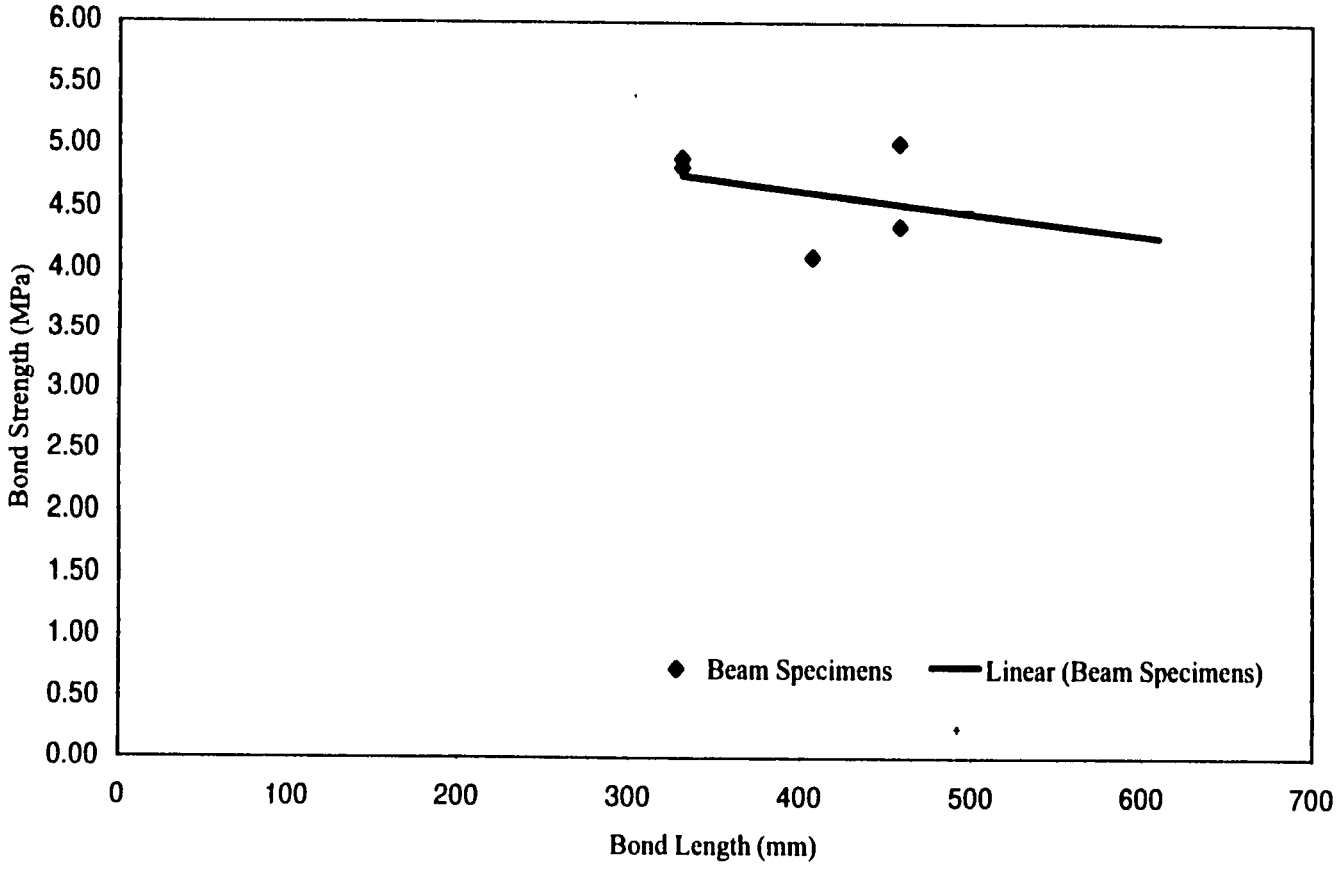

Figure 4.9: Bond strength vs. bond length (G1-D10, beam test)

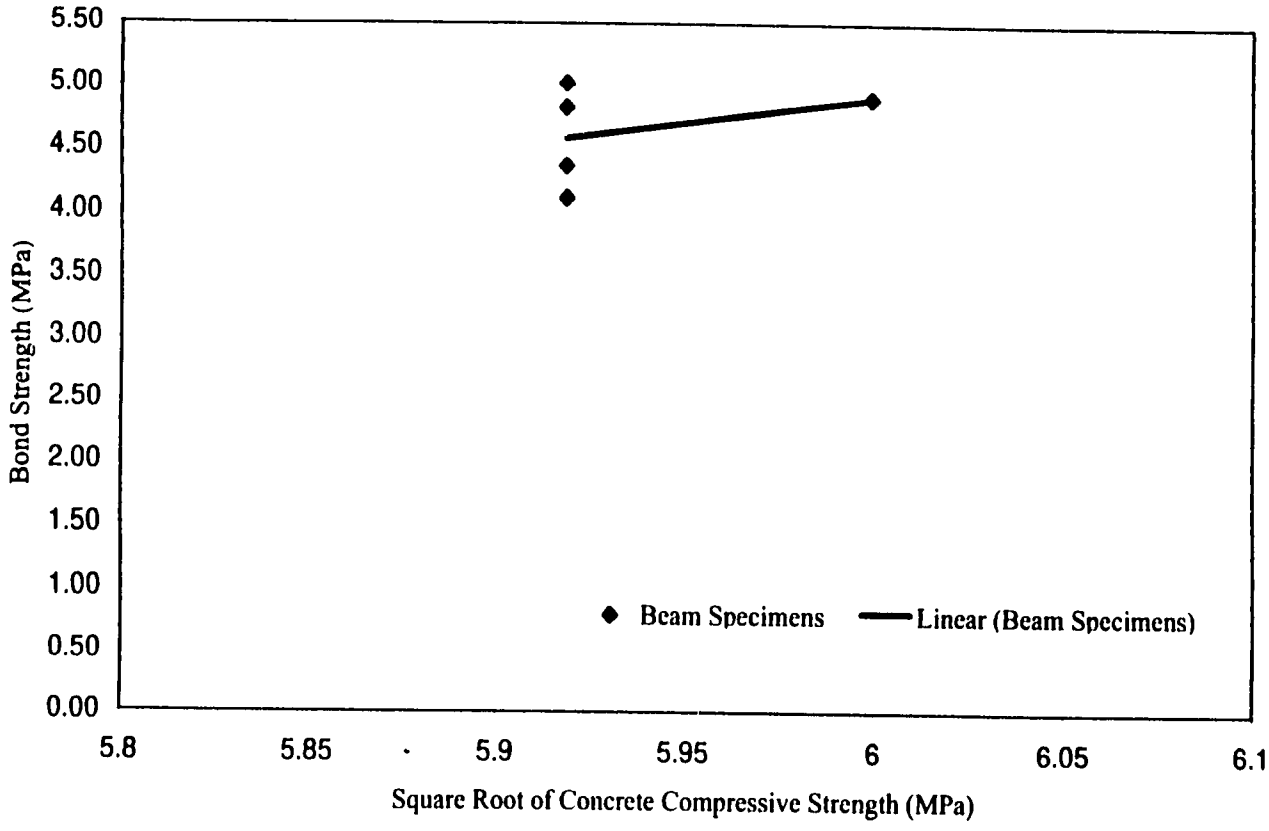

Figure 4.10: Bond strength vs. square root of concrete compressive strength (G1-D10 bar, beam test)

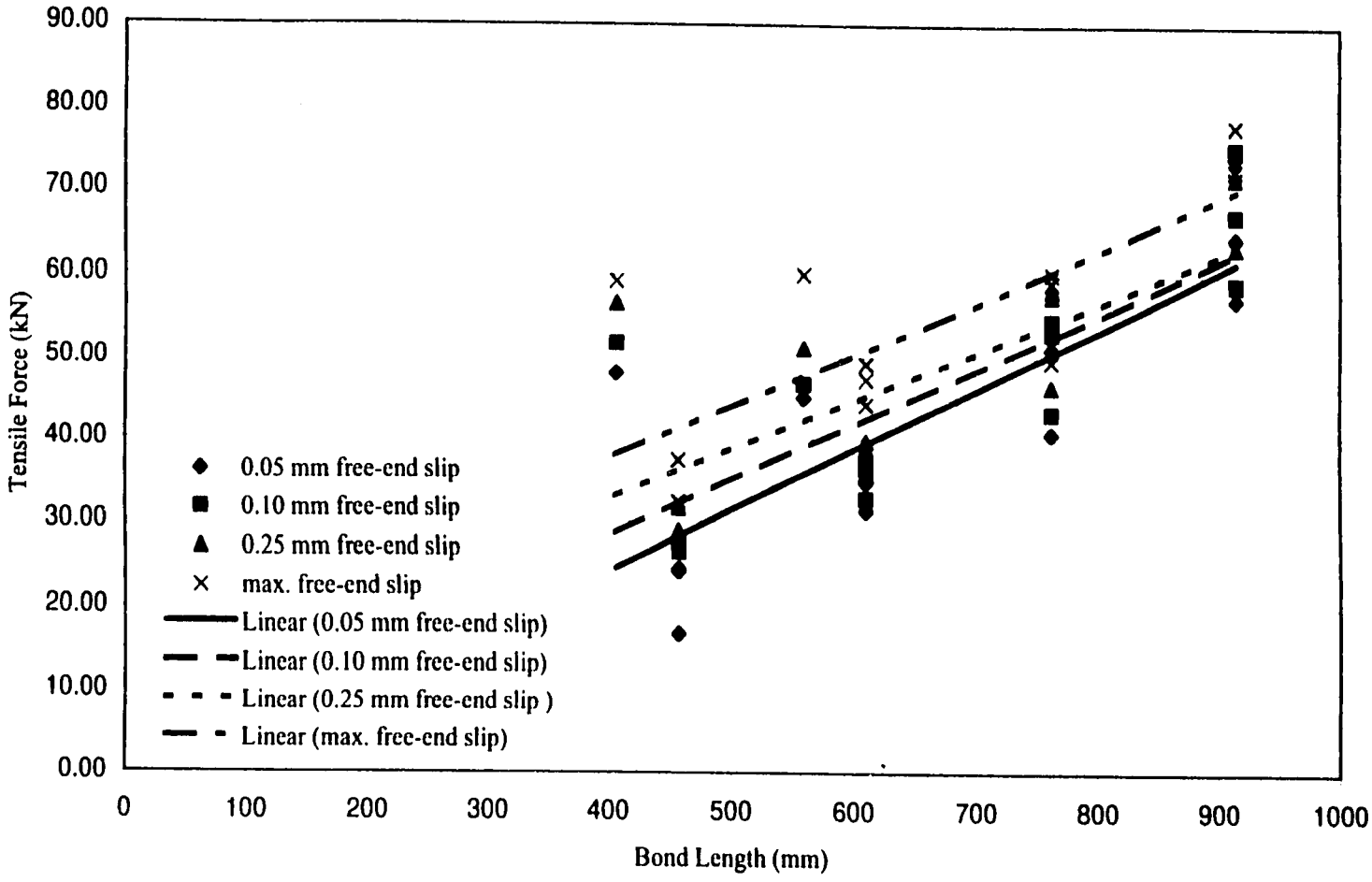

Figure 4.11: Comparison of tensile force vs. bond length (G2-D9.79 bar , free-end slip)

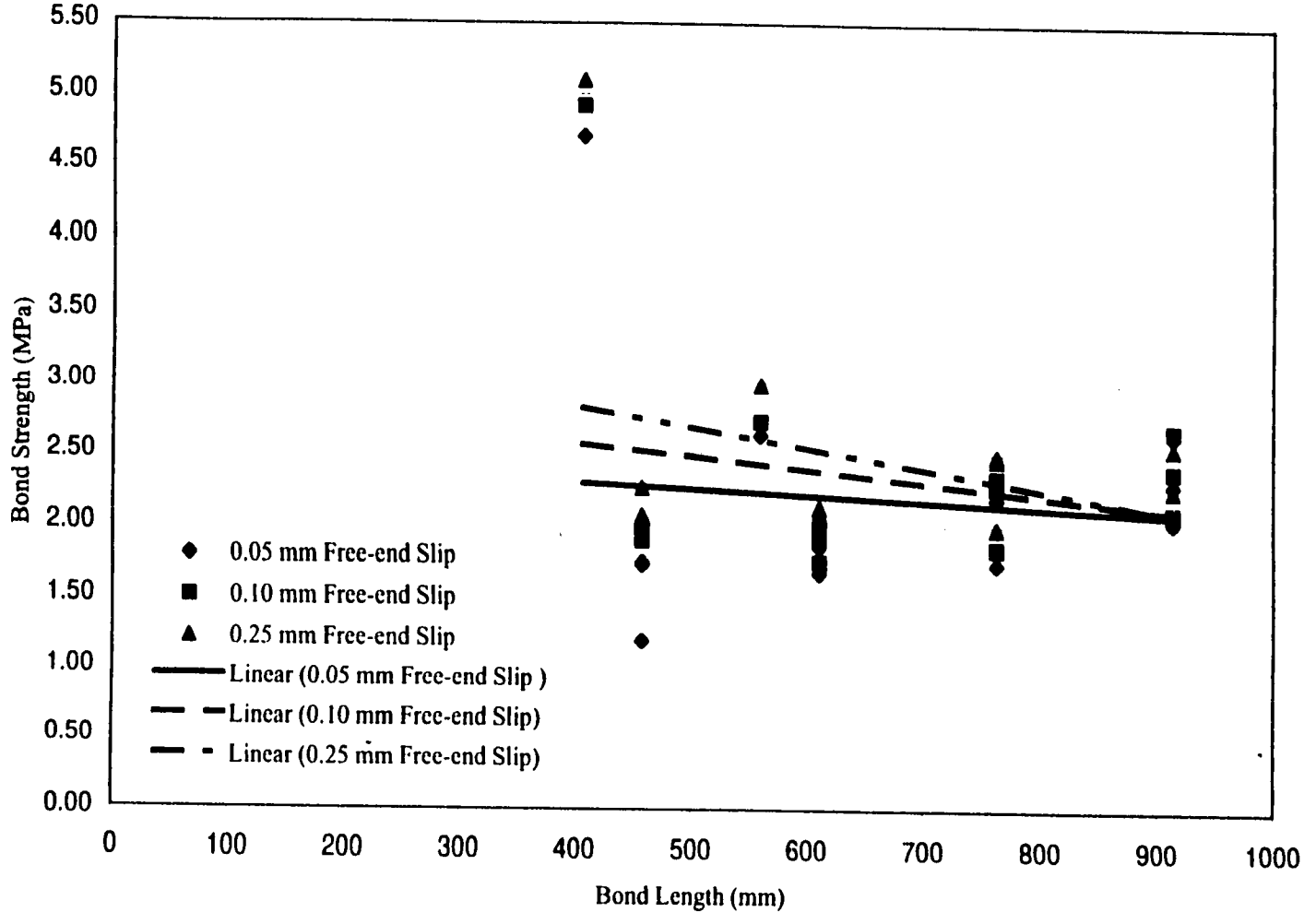

Figure 4.12: Comparison of bond strength vs. bond length (G2-D9.79 bar, free-end slip)

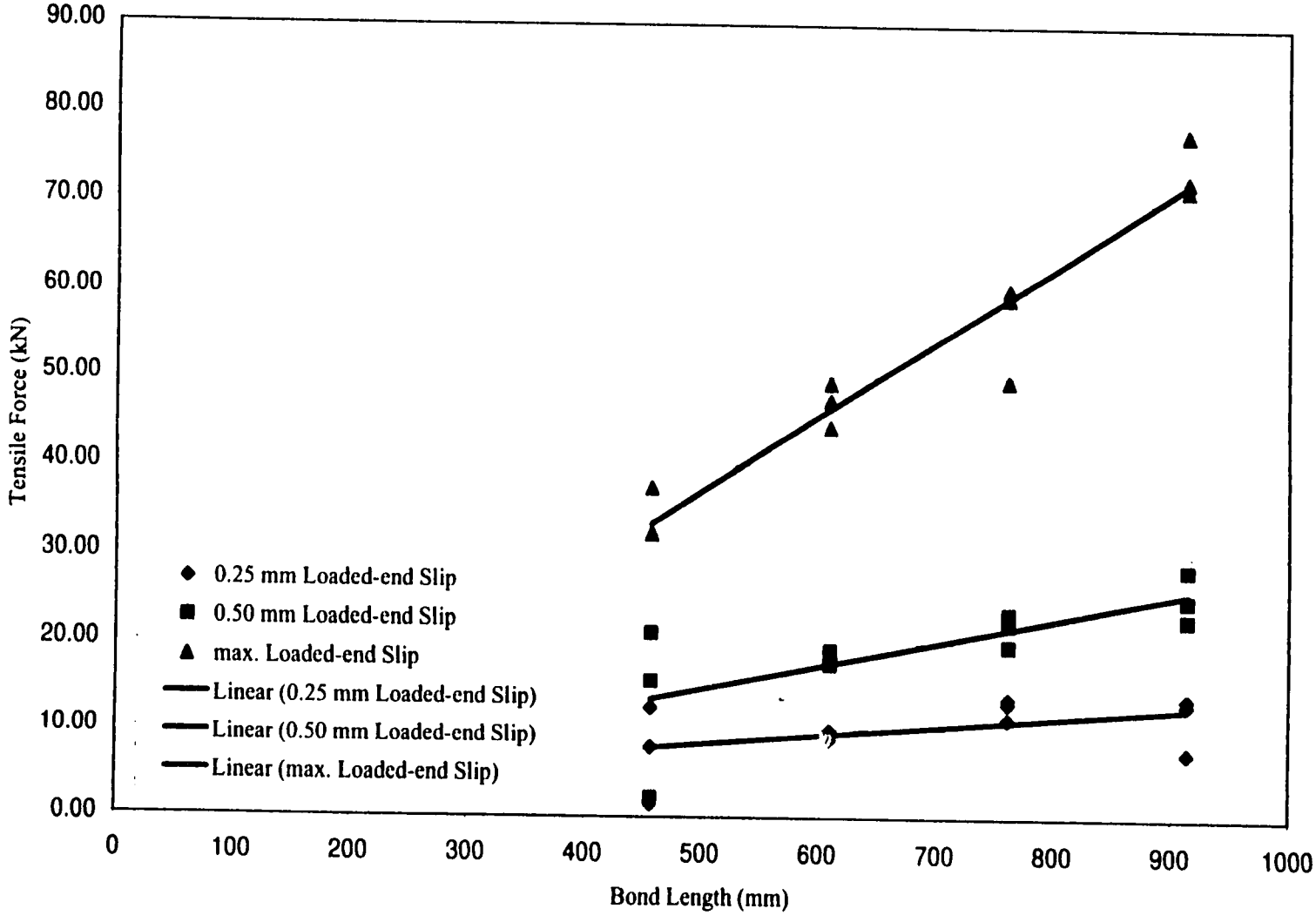

Figure 4.13: Comparsion of tensile force vs. bond length (G2-D9.79 bar, loaded-end slip)

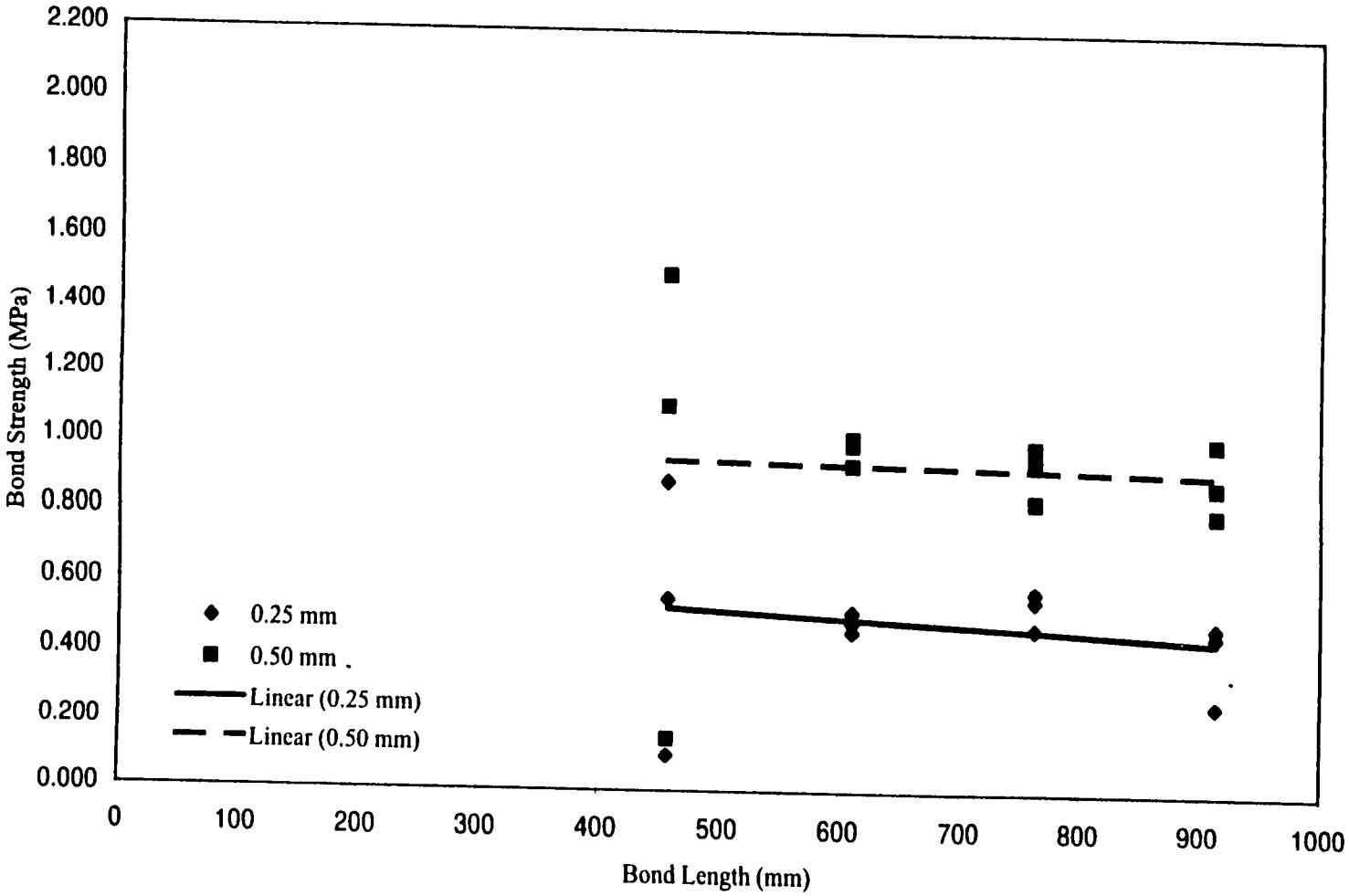

Figure 4.14: Comparison of bond strength vs. bond length (G2-D9.79, loaded-end slip)

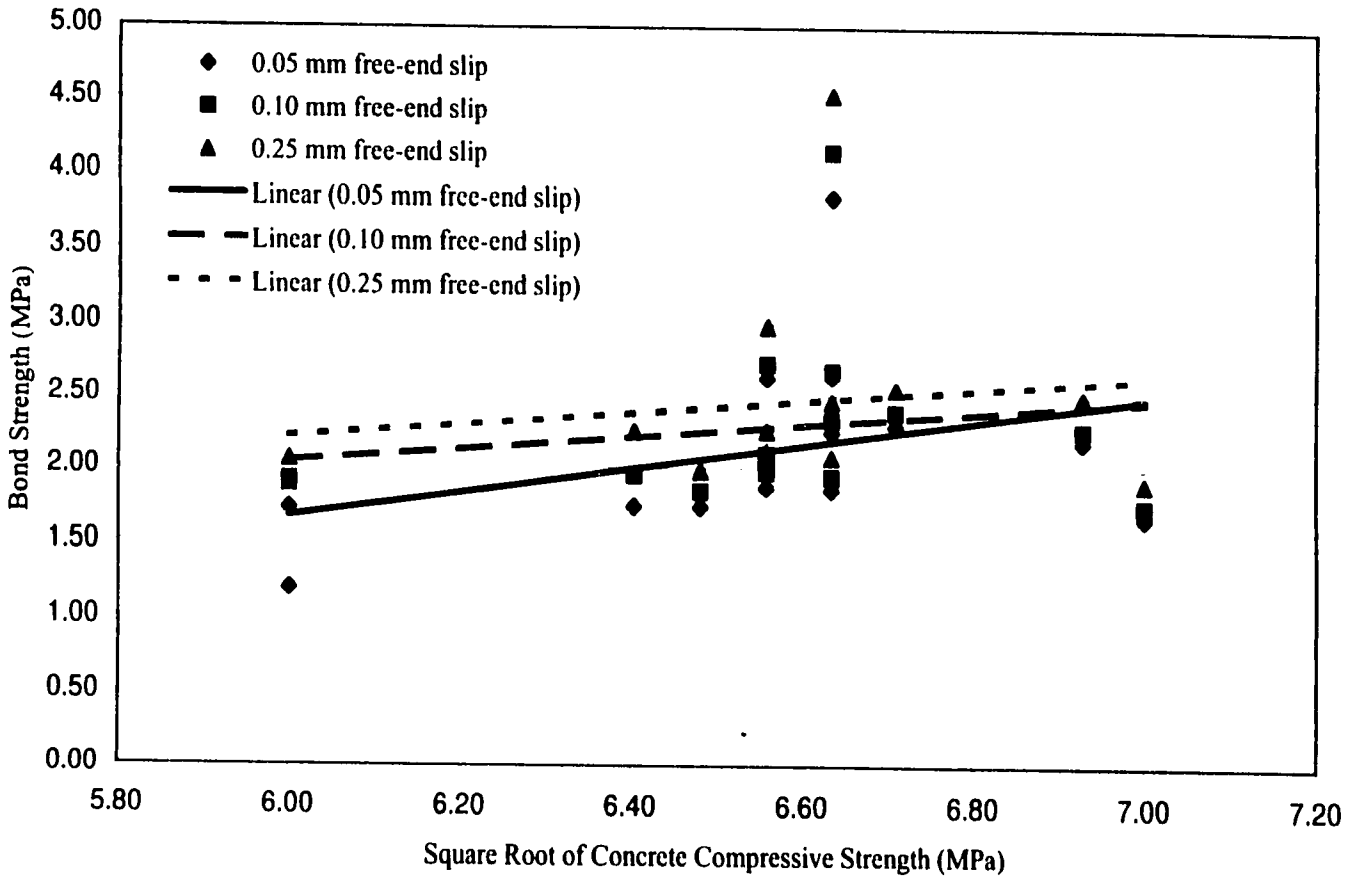

Figure 4.15 Comparison of bond strength vs square root of concrete compressive strength (G2-D9.79 bar, free-end slip)

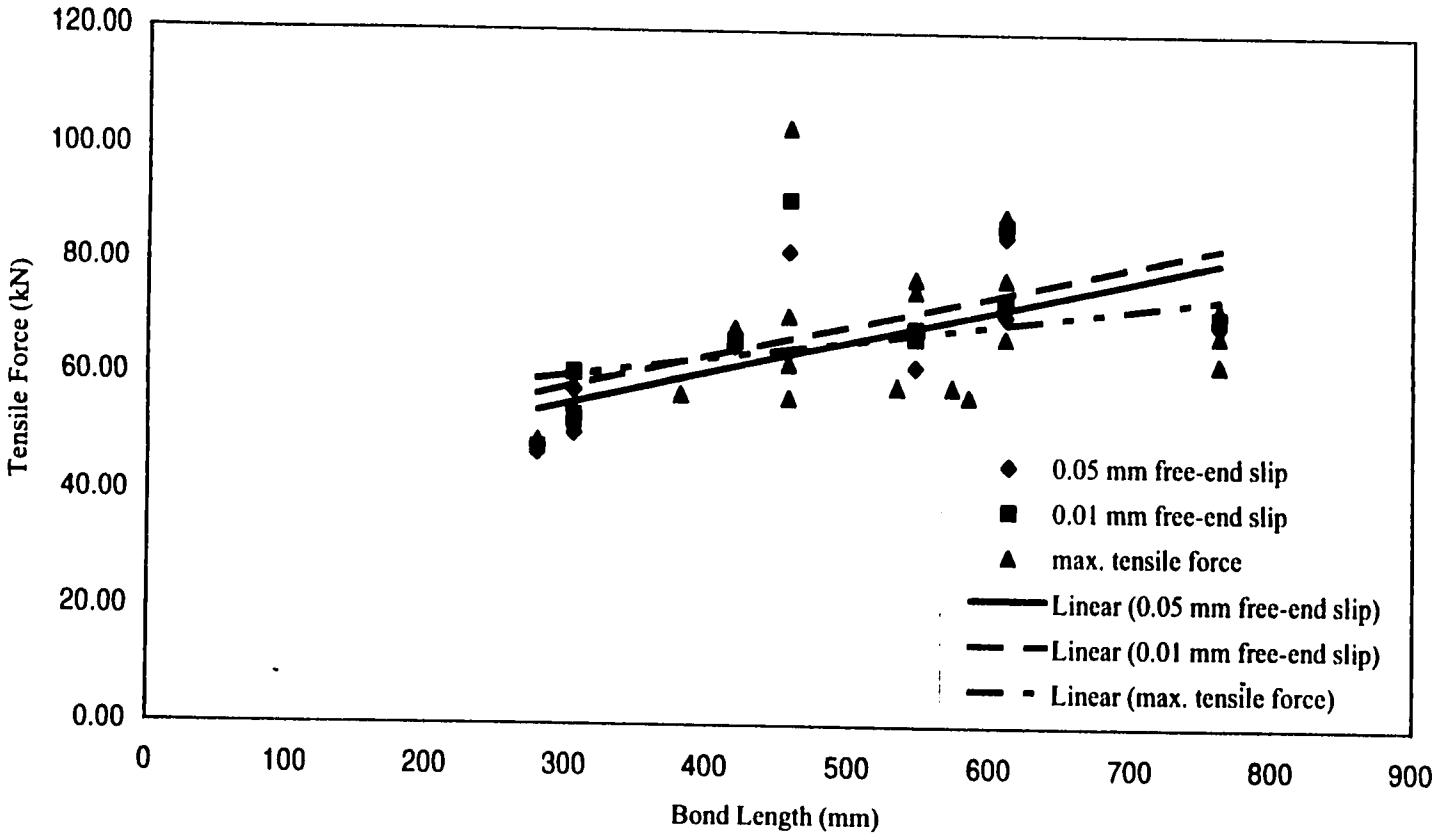

Figure 4.16: Comparison of tensile force vs. bond length (D1-D9.70 bar, free-end slip)

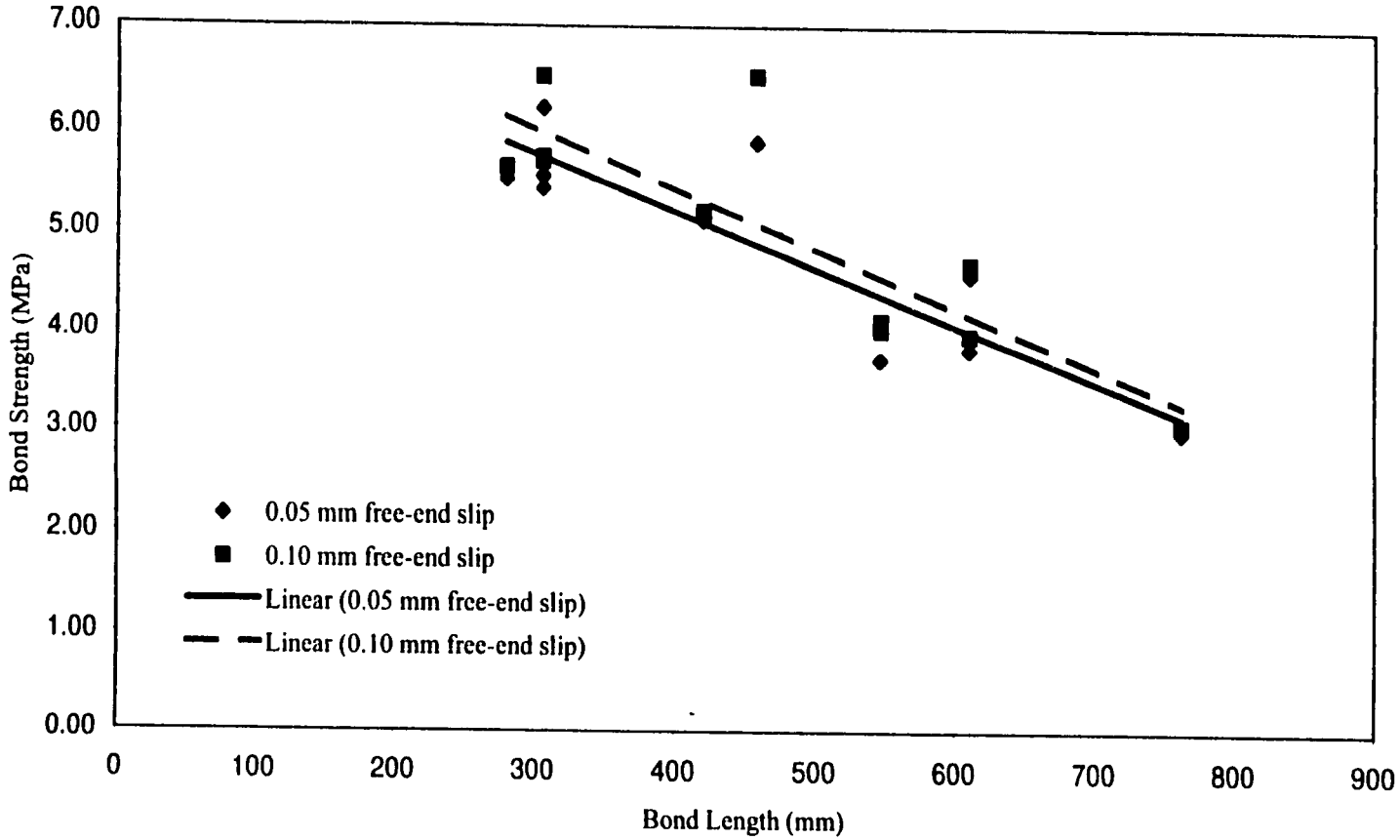

Figure 4.17: Comparison of bond strength vs. bond length (D1-D9.70, free-end slip)

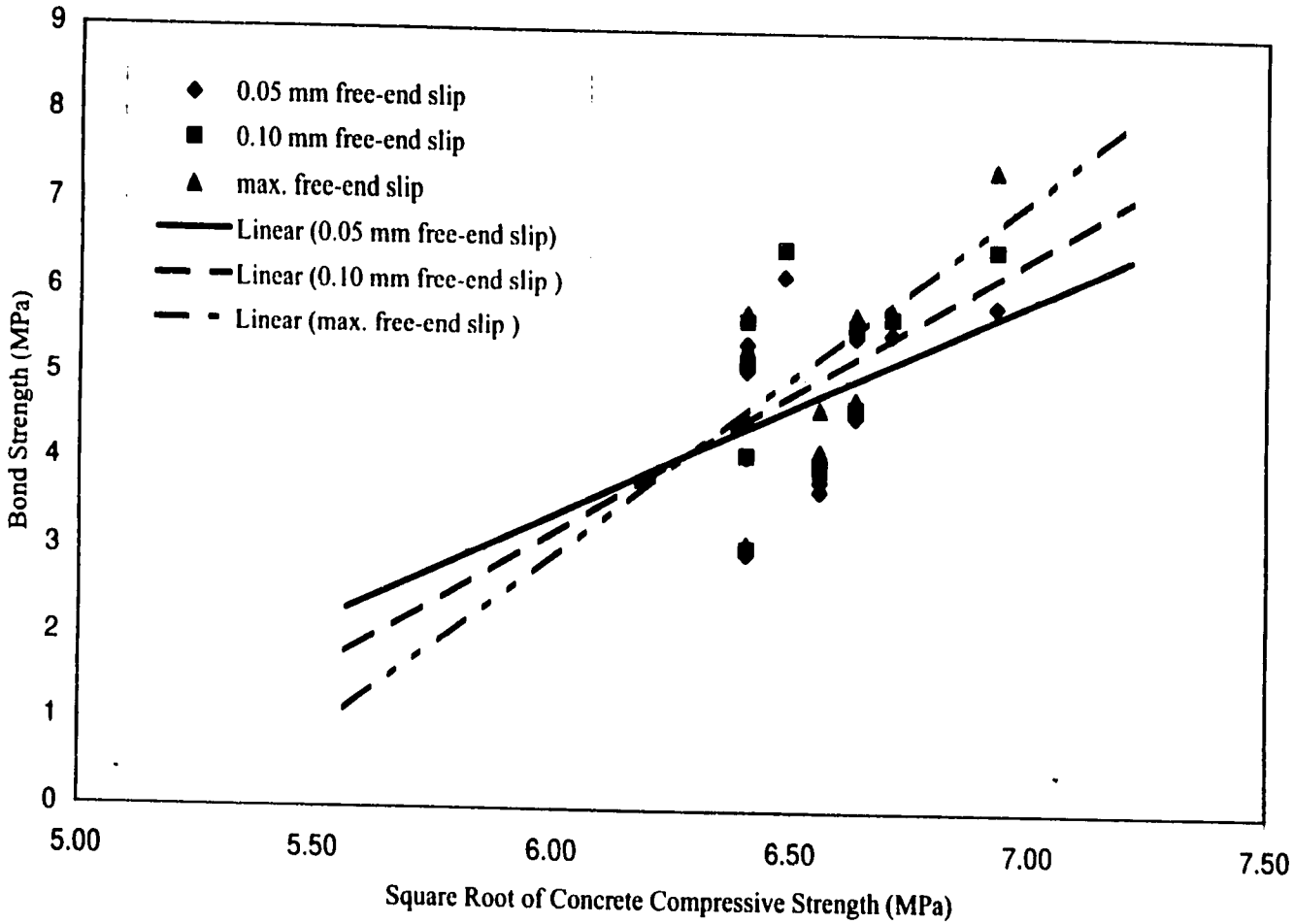

Figure 4.18: Comparison of bond strength vs. square root of concrete compressive stremgth (D1-D9.70 bar, free-end slip)

CHAPTER 5

DISCUSSION OF TEST RESULTS

5.1 General

This chapter discusses the results presented in Chapter 4 and the effects of three parameters, namely pressure induced on the bar due to support condition, embedment length and transverse reinforcement, on bond strength. Additional discussions of the effect of concrete compressive strength on bond strength, relationships between applied load and slip of beam specimens are also included.

5.2 Results of Tension Test

The stress-strain data obtained from the two tension specimens are consistent for G2-D9.79 CFRP bars, as well as D1-D9.70 CFRP bar. The modulus of elasticity of CFRP bars is lower than that of conventional steel reinforcing bars, approximately 79 to 88 percent of that of steel reinforcing bar. The ultimate breaking load is not reported since the CFRP bars slipped or crushed inside the grips.

5.3 Comparison of Pullout and Beam Specimens

Bond strengths obtained from pullout tests are inconsistent and varied from each other, as seen in Figures 4.2 and 4.3. In pullout specimens, the bar is subjected to tension while the concrete surrounding the bar is subjected to compression and, in beam specimens, the concrete surrounding the bar is under tension. This indicates that beam

test would be more realistic simulating the real behaviour of member in flexure and more suitable for such computations.

5.4 Effect of Bar Diameter

The values of bond strength presented in Tables 4.2 and 4.4 slightly indicate that bond strength decreases when the diameter of the bar increases. More test data are needed to verify this observation. In fact, the smaller bond strength of larger diameter can be explained by the bleeding of water in concrete. The larger the diameter of the bar, the higher the quantity of bleeding the water gets trapped beneath the bar. Thus, it creates a greater void and reduces the contact surface between the bar and the concrete and hence the bond.

5.5 Effect of Pressure Induced on The Bar Due to Support Condition

The use of steel I-beam section support, instead of steel roller support, was to eliminate the stress disturbance (support reaction forces) and confinement effect (concrete cover). But, the results in Tables 4.13 and 4.19 do not give a satisfactory comparison of bond strength by considering these two support conditions. In addition, there was difficulty in setting the test beams on the steel I-beam section support. It should be noted that the load-deflection curves of beams, tested by steel I-beam section support, are less steeper (larger deflection) due to slightly increased settlement of beams with the increase of applied load.

5.6 Effect of Embedment Length

Theoretical expression of the bond strength of reinforcing bar shows that the bond strength decreases as the embedment length of the reinforcing bar increases. This assumption was made to bond strength of constant magnitude acting uniformly on the reinforcing bar's surface over the anchorage length. This conclusion is confirmed by the results obtained from pullout and beam tests. As an example, Figures 4.5 and 4.6 show that as the embedment length (bond length) increases, the applied load approaches the tensile strength of the bar and the average bond strength reduces. Similar figures of tensile force vs. bond length and bond strength vs. bond length of all beam specimens are presented in Chapter 4.

In general, the distribution of tensile and bond strength along the embedment length of FRP reinforcement (Benmokrane et al. 1996) are similar to that of steel reinforcing bars (Jiang et al. 1984), which is non-linear. As a consequence of the non-linear distribution of bond strength, it is common to use mean bond strength for design purposes.

5.7 Effect of Transverse Reinforcement

With little confinement, beams reinforced with deformed bars fail in bond by splitting of the concrete because the small concrete cover cannot sustain the greater circumferencial tensile stress. As the confinement improved, commonly by the use of transverse reinforcement (stirrups), bond failure must occur by shearing of the concrete

keys instead of splitting. Thus, bond strength depends strongly on the amount of transverse reinforcement.

Table 4.3 presents the values of bond strength of beams reinforced with G1-D8 CFRP bar and with/without transverse reinforcement. It clearly indicates that the average bond strength increases due to confinement provided by transverse reinforcement. Similar results are observed for beams reinforced with G2-D9.79 and D1-D9.70 CFRP bars, as shown in Tables 4.14 and 4.20.

5.8 Effect of Concrete Compressive Strength

As mentioned in Section 1.3, bond strength of reinforcing bars depends on chemical adhesion, friction and bearing of the bar deformations against concrete. Bond failure may occur as a result of tensile splitting and shearing of concrete. In such cases, bond failure is proportional to the tensile strength of concrete (Ferguson and Thompson 1962) and is considered a key parameter (ACI 408 1992). The tensile strength of concrete is proportional to square root of the concrete compressive strength.

The relationships between bond strength and square root of concrete compressive strength are plotted for all beam specimens, as shown in the figures presented in Chapter 4. It clearly indicates that, in general, bond strength increases with the increase of concrete compressive strength.

5.9 Empirical Expression for Bond Strength of CFRP Bar

Expressions for bond strengths of different types of CFRP bars have been established by determining the corresponding value of K_1. It clearly indicates that the bond performance of D1-D9.70 CFRP bar is much better than that of G1-D8 and G1-D10 CFRP bars. Bond strength of G2-D9.79 CFRP bar is lower due to the glassy and smooth bar surface. Bond between the bar and its surrounding concrete depends primarily on chemical adhesion and friction.

5.10 Relationships Between Applied Load and Slip

The applied load vs. free-end and loaded-end slips of beams reinforced with G1-D8, G2-D9.79 and D1-D9.70 CFRP bars are shown in Appendixes G, H and I. Obviously, the loaded-end slip is greater than free-end slip. The loaded-end slip increases rapidly with the increase of applied load immediately after a vertical crack forms within the constant moment zone of the beams. Due to the low modulus of elasticity of CFRP bars, the measured loaded-end slip value includes the elongation of the bars. The free-end slip will not take place until the adhesion resistance between the bar and its surrounding concrete is broken.

5.11 Appearance of Concrete Cover After Test

After the test was completed, the bottom cover over the CFRP bar was removed to observe the contact surface between the bar and its surrounding concrete. The appearance of concrete cover of beams reinforced with G2-D9.79 and D1-D9.70 CFRP bars are shown in Figures 5.1 and 5.2, respectively. By observation of Figure 5.1, it may

be noted that the bond of G2-D9.79 CFRP bar depends primarily on friction and chemical adhesion. There are no signs of the concrete being crushed against the bar deformations. In addition, the contact surface between the CFRP bar and the concrete is glassy and smooth. All of these may explain the lower bond strength of the G2-D9.70 CFRP bar as proved by the test results

In contrast, test results show that D1-D9.70 CFRP bar has a better bond performance in concrete beams. This fact can be explained by observation of the physical properties of the bar and the appearance of concrete cover. Figure 5.2 shows the bond of D1-D9.70 CFRP bar depends on chemical adhesion, friction and bearing of the bar deformations. The contact surface between the bar and the surrounding concrete is not as glassy and smooth as that observed in Figure 5.1.

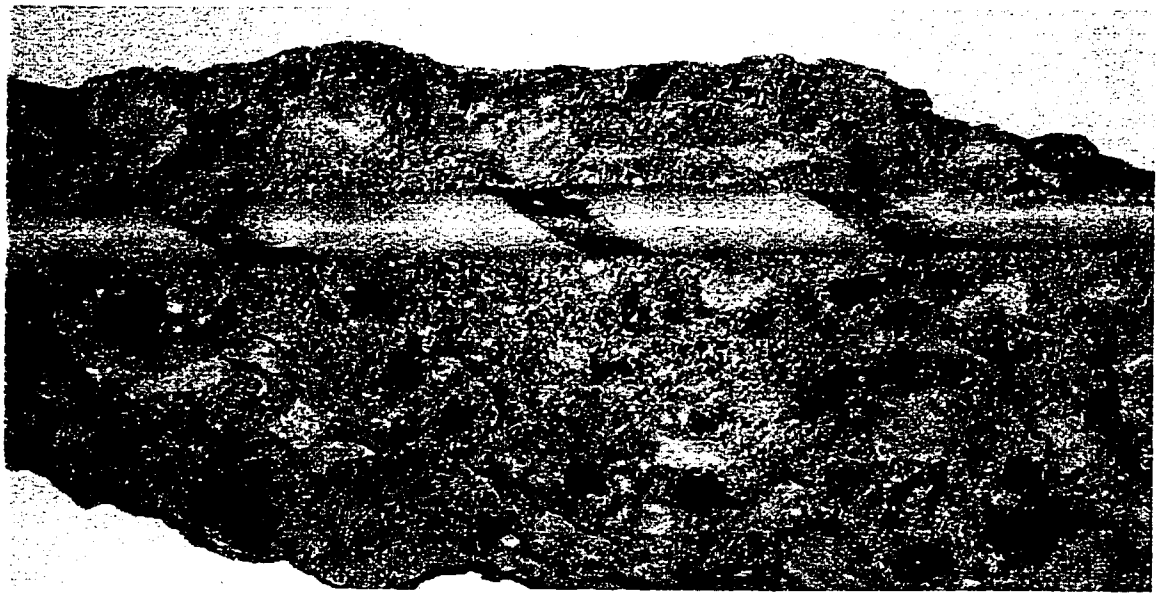

Figure 5.1: Appearance of concrete cover of beam reinforced with G2-D9.79 CFRP bar

Figure 5.2: Appearance of concrete cover of beam reinforced with D1-D9.70 CFRP bar

CHAPTER 6

CONCLUSIONS AND RECOMMENDATIONS

6.1 Conclusions

Bond performances of three types of CFRP bars in concrete beams were experimentally determined using beam specimens. Based on the test and analyzed results, the following conclusions can be drawn:

(1) The modulus of elasticity of CFRP bars is lower than that of steel reinforcing bar, approximately 79 to 88 percent of that of steel reinforcing bar.

(2) Bond strengths obtained from pullout tests are inconsistent. Therefore results may not be directly applied for design but can serve as a guide for bond evaluation.

(3) The average bond strength decreases when the diameter of the bar increases.

(4) The test results give no satisfactory information about the influences of support conditions on the bond strength.

(5) The tensile force in the CFRP bar increases when the bond length increases, but the average bond strength decreases when the bond length increases.

(6) The average bond strength increases due to confinement provided by transverse reinforcement.

(7) The average bond strength varied as $\sqrt{f_c'}$ when other factors were constant.

(8) Bond performance of CFRP bar depends strongly on its surface condition.

(9) The K_1 values of CFRP bars depend on types of CFRP bars. The values are calculated to be 6.25 for G1-D8 and G1-D10 CFRP bars, 3.40 for G2-D9.79 CFRP bars and 8.47 for D1-D9.70 CFRP bars.

(10) Bond performances of G1-D8, G1-D10 and D1-D9.70 CFRP bars are much better than the G2-D9.79 CFRP bar.

(11) The expressions for development length and bond strength of steel reinforcing bars provided in CSA and ACI codes should be modified for the use of CFRP bars due to inherent differences in surface deformations and mechanical properties.

6.2 Recommendations for Further Study

The experimental research investigated the effect of three parameters affecting the bond performance of CFRP bars in concrete beams. More test data and parameters are needed to contribute and develop the guidelines for future CFRP bar development and its usage. The following recommendations can be made for further study of bond performance of CFRP bars.

(1) Criteria for defining critical bond strength of CFRP bars based on either free-end or loaded-end slips has not yet been developed. An extended study in this area is needed.

(2) More pullout test data are needed in order to establish a sound comparison and relationships between beam tests and pullout tests.

(3) A detailed relationship between bond strength and concrete compressive strength should be established in order to realize the effect of low, normal and high strength concrete on bond performance.

(4) An extended study of the effect of physical and mechanical properties of different kinds of CFRP bars on bond strength is needed.

REFERENCES

"Comparing Concretes on the Basis of the Bond Developed with Reinforcing Steel", ASTM C234-91a, American Society of Testing and Materials.

"Epoxy-Coated Reinforcing Bars", ASTM A775/A775M-91b, American Society for Testing and Materials.

"Fiber Reinforced Plastic (FRP) Reinforcement for Concrete Structures: Properties and Application," Developments in Civil Engineering, A. Nanni, ed., Elsevier, 1993, 450 pp.

Abdel-Sayed, G., Salib, S., De Thomasis, J. and Grace, N. F. (1998). "Mechanical Properties and Structural Behaviour of Glasform CFRP Bars." Report for Glasform Incorporated, San Jose, California, Civ. Engrg. Dept., Univ. of Windsor, Windsor, 1-63.

ACI Committee 208. (1957). "Proposed Test Procedure to Determine Relative Bond Value of Reinforcing Bars." ACI J., 28(13), 89-104.

ACI Committee 208. (1958). "Test Procedure to Determine Relative Bond Value of Reinforcing Bars." ACI J., 30(1), 1-16.

ACI Committee 318. (1989). "Building Code Requirements for Reinforced Concrete (ACI 318-89) and Commentary (ACI 318R-89)." American Concrete Institute, Detroit.

ACI Committee 318. (1989). "Building Code Requirements for Reinforced Concrete (ACI 318-89) and Commentary (ACI 318R-89) (Metric Version)." American Concrete Institute, Detroit.

ACI Committee 408. (1964). "A Guide for Determination of Bond Strength in Beam Specimens." ACI J., Proceedings 61(2), 129-136.

ACI Committee 408. 91992). "State-of-the-art Report on Bond Under Cyclic Loads." American Concrete Institute, Detroit, 3-7.

ACI Committee 440R. (1996). "State-of-the-Art Report on Fiber Reinforced Plastic Reinforcement for Concrete Structures." American Concrete Institute, Detroit.

Alsayed, S. H. (1998). "Flexural Behaviour of Concrete Beams Reinforced with GFRP Bars." Cement and Concrete Composites, 20(1), 1-11.

Bakis, C. E., Uppuluri, V. S., Nanni, A. and Boothby, T.E. (1998). "Analysis of Bonding Mechanism of Smooth and Lugged FRP Rods Embedded in Concrete." Composites Science and Technology, 58(8), 1307-1319.

Benmokrane, B., Chaallal, O., and Masmoudi, R. (1995). "Glass Fiber Reinforced Plastic (GFRP) Rebars for Concrete Structures." Construction and Building Materials, 9(6), 353-364.

Benmokrane, B., Tighiouart, B., and Chaallal, O. (1996). "Bond Strength and Load Distribution of Composite GFRP Reinforcing Bars in Concrete." ACI Materials J., 93(3), 246-253.

Benmokrane, B., Tighiouart B. and Theriault M. (1997). " Bond Strength of Fiber Reinforced Plastic (FRP) Bars Embedded in Concrete Beams." Annual Conference of CSCE, May 27-30, Sherbrooke, 111-120.

Bond and Development of Reinforcement (A Tribute to Dr. Peter Gergely), International Symposium, SP-183, Roberto Leon, ed., American Concrete Institute, Detroit, 1998, 512 pp.

Bresler, B. (1974). "Reinforced Concrete Engineering." Wiley, New York.

CPCA. (1995). "Concrete Design Handbook." 2nd Edition, Canadian Portland Cement Association, Ottawa, Ontario.

Chaalla, O. and Benmokrane, B. (1996). "Fiber-reinforced Plastic Rebars for Concrete Applications." Composites Part B: Engineering, 27(3-4), 245-252.

CPCA. (1984). "Design and Control of Concrete Mixtures." (Canadian Metric Edition), Canadian Portland Cement Association, Ottawa, Ontario.

CSA. (1994). CAN/CSA-23.1-94, CAN/CSA-23.2-94 "Concrete Materials and Methods of Concrete Construction / Methods of Tests for Concrete. Standard." Canadian Standards Association, Rexdale, Ontario.

CSA. (1984). CAN3-A23.3-84 "Design of Concrete Structures for Building." Canadian Standards Association, Rexdale, Ontario.

CSA. (1994). CAN3-A23.3-94 "Design of Concrete Structures for Building." Canadian Standards Association, Rexdale, Ontario.

Daniali, S. (1992). "Development Length for Fiber Reinforced Plastic Bars." Advanced Composite Materials in Bridges and Structures, Proceedings of the 1st International Conference, Sherbrooke, 179-188.

Domenico, N. (1995). "Bond Properties of CFCC Prestressing Strands in Pretensioned Concrete Beams." M. Sc. Thesis, Department of Civil Engineering, University of Manitoba, Winnipeg, Manitoba.

Ehsani, M. R., Saadatmanesh, H. and Tao, S. (1993). "Bond of GFRP Rebars to Ordinary-Strength Concrete." Fiber-Reinforced-Plastic Reinforcement for Concrete Structures, SP-138, American Concrete Institute, Detroit, 333-345.

Ehsani, M. R., Saadatmanesh, H., and Tao, S. (1996). "Design Recommendations for Bond of GFRP Rebars to Concrete." Journal of Structural Engineering, 122(3), 247-254.

Erki, M. A., and Rizkalla, S. H. (1993). "FRP Reinforcement for Concrete Structures." Concrete Int.: Design and Construction, 15 (6), 48-53.

Esfahani, M. R. and Rangan, B. V. (1998). "Bond between Normal Strength and High-Strength Concrete (HSC) and Reinforcing Bars in Splices in Beams." ACI Structural Journal, 95(3), 272-280.

Esfahani, M. R. and Rangan, B. V. (1998). "Local Bond Strength of Reinforcing Bars in Normal Strength and High-Strength Concrete (HSC)." ACI Structural Journal, 95(2), 96-106.

Faza, S. S. and GangaRao, H. V. S. (1993). " Theoretical and Experimental Correlation of Behavoir of Concrete Beams Reinforced with Fiber Reinforeed Plastic Rebars." Fiber-Reinforced-Plastic Reinforcement for Concrete Structures, SP-138, American Concrete Institute, Detroit, 599-614.

Ferguson, P. M., Breen, J. E. and Thompson, J. N. (1965). "Pullout Tests on High-Strength-Reinforcing Bars." ACI J., 62(8), 933-949.

Ferguson, P. M., and Neils Thompson, J. (1962). "Development Length of High Strength Reinforcing Bars in Bond." ACI J., Proceedings 59(7), 887-971.

Fiber Reinforced Plastic Reinforcement for Concrete Structures, International Symposium, SP-138, A. Nanni and C. W. Dolan, eds., American Concrete Institute, Detroit, 1993, 977 pp.

Fukuyama, H. (1999). "Fibre-Reinforced Polymers in Japan." Structural Engineering International, 9(4), 263-266.

Glanville, W. H. (1913). "Studies in Reinforced Concrete Bond Resistance." Build. Res. Tech. Note No. 10, Dept. of Scientific and Industrial Res., Her Majesty's Stationary Ofc., London, England, vi-37.

Hadje-Ghaffari, H., Choi, O. C., Darwin, D., and McCabe, S. L. (1992). "Bond of Epoxy-coated Reinforcement to Concrete: Cover, Casting Position, Slump and Consolidation." Struct. Engrg. and Engrg. Mat., SL Rep. 92-3, Univ. of Kansas, Lawrence, Kans.

Jerrett, C. V. and Ahmad S. H. (1995). "Bond Tests of Carbon Fiber Reinforced Plastic (CFRP) Rods, Non-metallic (FRP) Reinforcement for concrete Structures." Proceedings of the Second International RILEM Symposium (FRPRCS-2), London: E. and F. N. Spon., 1180-191.

Jiang, D. H., Shah, S. P., and Andonian, A. T. (1984). " Study of the Transfer of Tensile Forces by Bond." ACI J. Proceedings 81(3), 251-259.

Kanakubo, T., Yonemaru, Y., Fukuyama, H., Fujisawa, M. and Sonobe, Y. (1993). "Bond Performance of Concrete Members Reinforced with FRP Bars." Fiber-Reinforced-Plastic Reinforcement for Concrete Structures, SP-138, American Concrete Institute, Detroit, 767-788.

Kankam, K. C. (1997). "Relationship of Bond Stress, Steel Stress and Slip in Reinforced Concrete." Journal of Structural Engineering, 123(1), 79-85.

Larralde, J., and Silva-Rodriguez, R. (1993). "Bond and Slip of FRP Reinforcing Bars in Concrete." Journal of Materials in Civil Engineering, 5(1), 30-40.

Leet, K. (1997). "Reinforced Concrete Design." McGraw-Hill, New York.

Lutz, Leory A., and Gergely, P. (1967). "Mechanics of Bond and Slip of Deformed Bars in Concrete." ACI J., Proceedings 64(11), 711-721.

Machida, A., (1993). "State-of-the-art Report on Continuous Fiber Reinforcing Materials." Japan Society of Civil Engineers.

Machida, A., (1997). "Recommendations for Design and Construction of Concrete Structures Using Continuous Fiber Reinforcing Materials." Japan Society of Civil Engineers.

Makitani, E., Irisawa, I. and Nishiura, N. (1993). "Investigation of Bond in Concrete Member with Fiber Reinforced Plastic Bars." Fiber-Reinforced-Plastic Reinforcement for Concrete Structures, SP-138, American Concrete Institute, Detroit, 315-331.

Marshall Industries Composites, Inc. (2000). Introduction. Retrieved Jan. 15, 2000 from the World Wide Web: http://www.c-bar.com/intcbar.htm.

Mathey, R. G. and Watstein, D. (1961). "Investigation of Bond Strength in Beam and Pull-Out Specimens with High-Yield Strength Deformed Bars." Journal of the American Concrete Institute, Proceedings 57(9), 1071-1090.

Mirza, S. M. and Houde, J. (1979). "Study of Bond Stress-Slip Relationship in Reinforced Concrete." ACI J. 76(1), 19-46.

Mo, Y. L., and Chan, J. (1996). "Bond and Slip of Plain Rebars in Concrete." Journal of Materials in Civil Engineering, 8(4), 208-211.

Mochizuki, S., Matsuzaki, Y. and sugita, M. (1993). "Evaluation Items and Methods of FRP Reinforcement as Structural Elements." Fiber-Reinforced-Plastic Reinforcement for Concrete Structures, SP-138, American Concrete Institute, Detroit, 117-131.

Mosley, W. H. and Bungey, J. H. (1976). "Reinforced Concrete Design." Unwin Brothers Limited, Great Britain.

Nilson, A. H. (1971). "Bond Stress-Slip Relationship in Reinforced Concrete." Rep. No. 345, Dept. of Struct. Engrg., Cornell Univ., Ithaca, N.Y.

Nilson, Arthur H., and Winter, G. (1986). "Design of Concrete Structures." McGraw-Hill, New York.

Nilson, Arthur H., and Winter, G. (1991). "Design of Concrete Structures." McGraw-Hill, New York.

Okamura, H., Kakuta Y., Uomoto T. and Mutsuyoshi H. (1993). "Design Concept for Conrete Members Using Continuous Fiber Reinforcing Materials." Fiber-Reinforced-Plastic Reinforcement for Concrete Structures, SP-138, American Concrete Institute, Detroit, 549-559.

Park, R. and Paulay, T. (1975). "Reinforced Concrete Structures." John Wiley & Sons, New York, 401-404.

Pleimann, L. G. (1987). "Tension and Bond Pull-out Tests of Deformed Fiberglass Rods." Final Report for Marshall-Vega Corporation, Marshall, Arkansas, Civ. Engrg. Dept., Univ. of Arkansas, Fayetteville,
Ark., 5-11.

Pleimann, L. G. (1991). "Strength , Modulus of Elasticity and Bond of Deformed FRP Rods." Adv. Composites Mat. in Civ. Engrg. Struct., Proc., of the Specialty Conf., Mat. Engrg. Div., ASCE, 99-110.

RILEM/CEB/FIP. (1978). "Test of the bond Strength of Reinforcement of Concrete: test by bending." Recommendation RC.5, 5 pp.

Saafi, M. and Toutanji, H. (1998). "Flexural Capacity of Prestressed Concrete Beams Reinforced with Aramid Fiber Reinforced Polymer (AFRP) Rectangular Tendons." Construction and Building Materials, 12(5), 245-249.

Sonobe Y, Fukuyama H, Okamoto T, Kani N, Kimura K, Kobayashi K, Masuda Y, Matsuzaki Y, Mochizuki S, Nagasaka T, Shimizu A, Tanano H, Tanigaki M,

Teshigawara M. (1997). Design Guidelines of FRP Reinforced Concrete Building Structures. ASCE J Comp Construct; 1(3):90.

Soretz, S. (1972). "A Comparison of Beam Tests and Pullout Tests." Materiaux and Constructions, 5(28), 261-264.

Tao, S. (1994). "Bond of Glass-Fiber-Reinforced-Plastic Reinforcing Bars to Concrete." PhD dissertation, Department of Civil Engineering, University of Arizona, Tucson.

Tighiouart, B., Benmokrane, B., and Gao, D. (1998). "Investigation of Bond in Concrete Member with Fibre Reinforced Polymer (FRP) Bars." Construction and Building Materials, 12(8), 453-462.

Treece, R. A. and Jirsa, J. O. (1989). "Bond Strength of Epoxy-Coated Reinforcing Bars." ACI Materials Journal, 86(2), 167-189.

Yamasaki, Y., Masuda, Y., Tanano, H. and Shimizu, A. (1993). " Fundamental Properties of Continuous Fiber Bars." Fiber-Reinforced-Plastic Reinforcement for Concrete Structures, SP-138, American Concrete Institute, Detroit, 715-730.

Yeih, W., Huang, R., Chang, J. J. and Yang, C. C. (1997). "A Pullout Test for Determining Interface Properties between Rebar and Concrete." Advance Cement Based Materials, 5(2), 57-65.

Appendix A

Calibration Data and Curve of Universal Flat Load Cell

Table A.1: Calibration data of universal flat load cell

Universal Flat Load Cell (222 kN)	
No. 3 365 689	
Oct. 13, 1999	
Load (kN)	Strain Reading (microstrain)
0	0
10	173
20	344
30	514
40	686
50	860
60	1032
70	1205
80	1379
90	1551
100	1725
110	1897
120	2070
130	2242
140	2417
150	2589
160	2762
170	2934
180	3109
190	3280
200	3453
210	3626
220	3799
230	3970

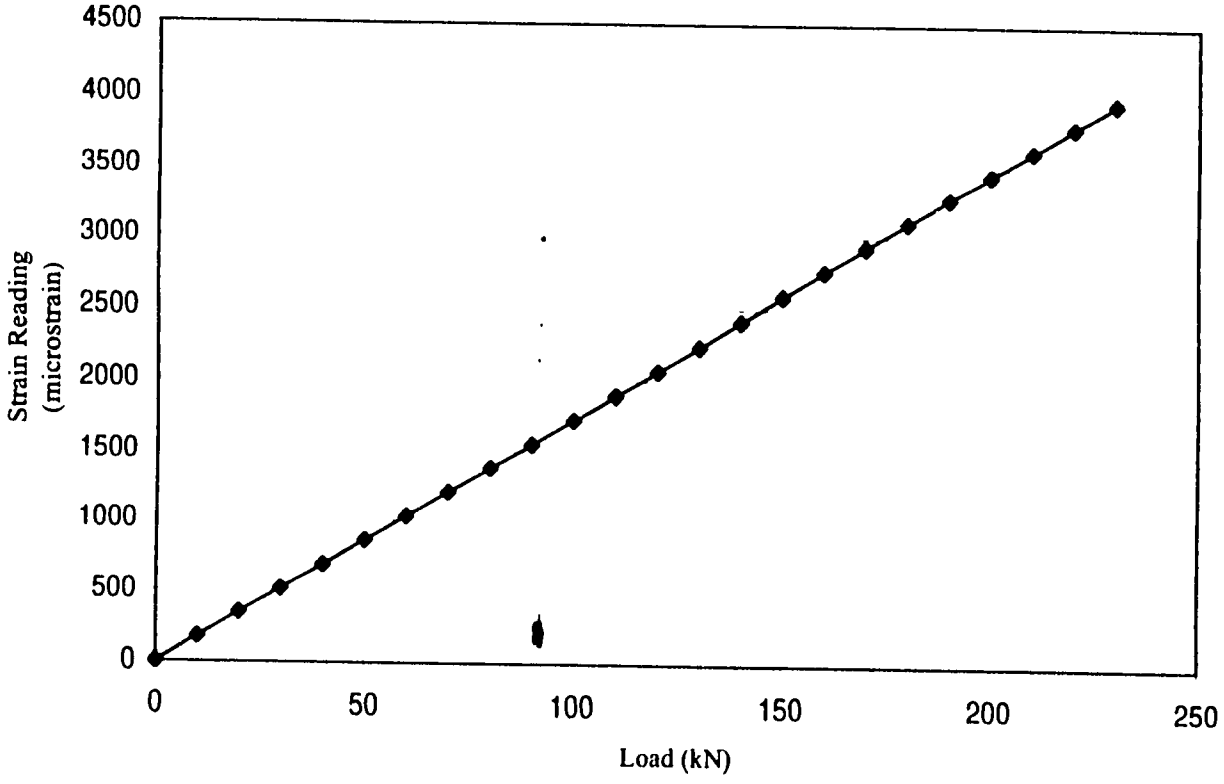

Figure A.1: Calibration curve of universal flat load cell

Appendix B

Stress-Strain Data and Curve of G2-D9.79 CFRP Bar

Table B.1: Stress-strain data of G2-D9.79 CFRP bar

Test 1	
Stress (MPa)	Strain (mm/mm)
0	0
29.54	0.000194
59.08	0.000393
88.62	0.000587
118.17	0.000791
147.71	0.000968
177.25	0.001158
206.79	0.001351
236.33	0.001548
265.87	0.001725
295.42	0.001921
324.96	0.002093
354.50	0.002283
384.04	0.002471
413.58	0.002650
443.12	0.002834
472.66	0.003015
502.21	0.003197
531.75	0.003379
561.29	0.003557
590.83	0.003728
620.37	0.003892
649.91	0.004046
679.46	0.004231
709.00	0.004413
738.54	0.004565

Test 2	
Stress (MPa)	Strain (mm/mm)
0	0
29.54	0.000210
59.08	0.000393
88.62	0.000596
118.17	0.000788
147.71	0.000981
177.25	0.001187
206.79	0.001374
236.33	0.001557
265.87	0.001752
295.42	0.001938
324.96	0.002132
354.50	0.002314
384.04	0.002505
413.58	0.002692
443.12	0.002874
472.66	0.003061
502.21	0.003246
531.75	0.003434
561.29	0.003622
590.83	0.003799
620.37	0.003974
649.91	0.004239
679.46	0.004413

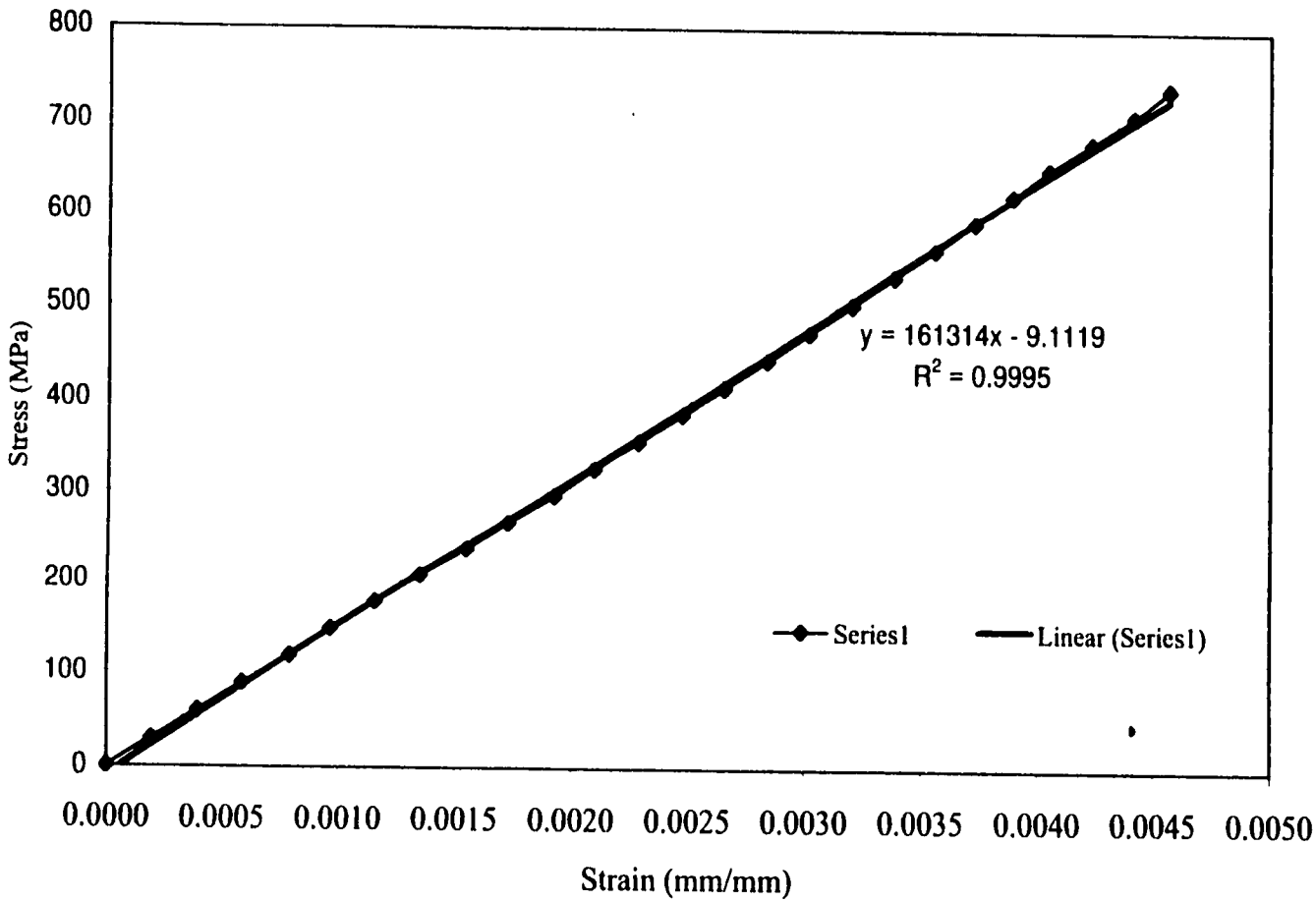

Figure B.1: Stress-strain curve of G2-D9.79 CFRP bar (Test 1)

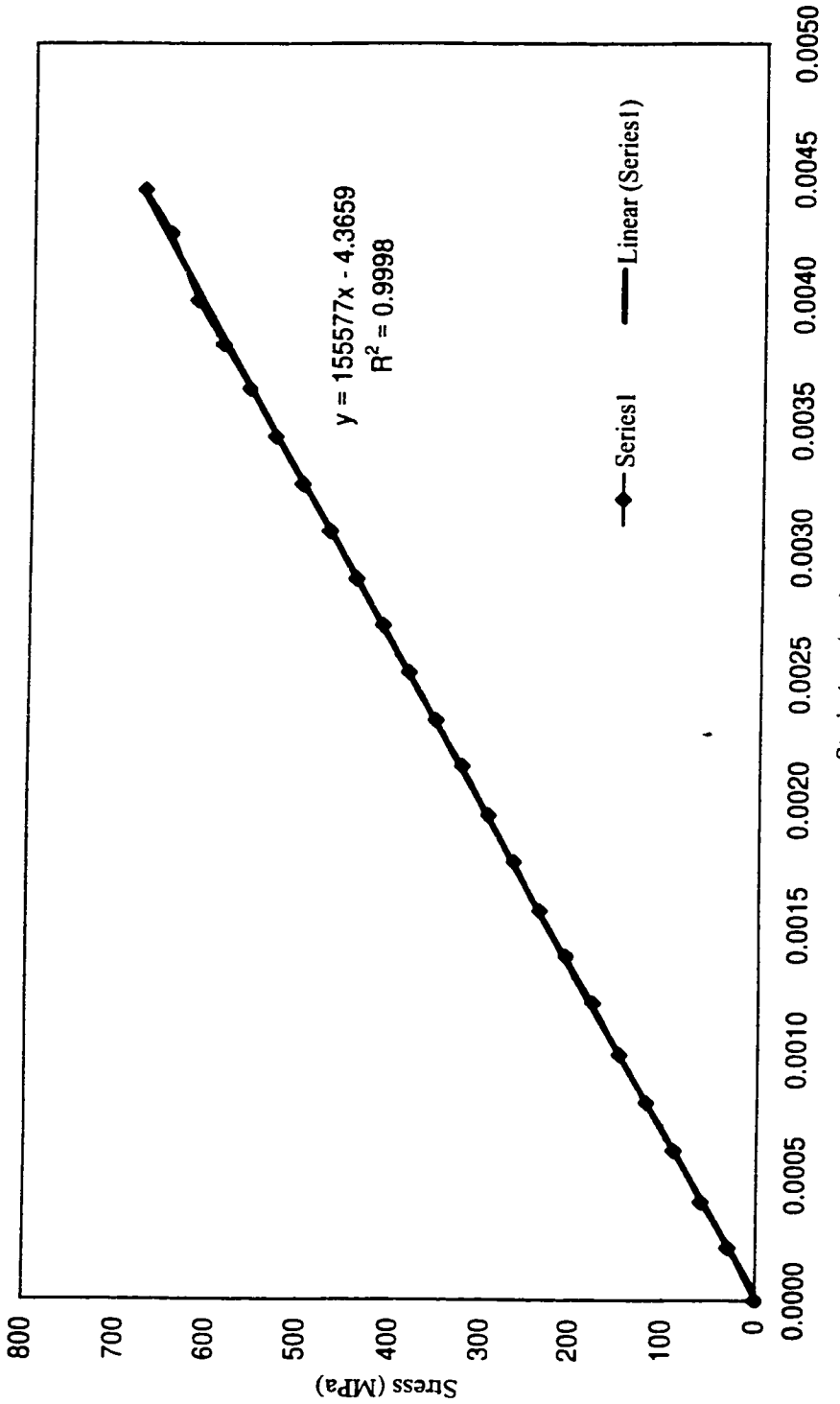

Figure B.2: Stress-strain curve of G2-D9.79 CFRP bar (Test 2)

Appendix C

Stress-Strain Data and Curve of D1-D9.70 CFRP Bar

Table C.1: Stress-strain data of D1-D9.70 CFRP bar

Test 1	
Stress (MPa)	Strain (mm/mm)
0	0.000000
30.11	0.000173
60.22	0.000350
90.33	0.000534
120.44	0.000709
150.55	0.000858
180.66	0.001053
210.76	0.001217
240.87	0.001395
270.98	0.001570
301.09	0.001734
331.20	0.001903
361.31	0.002071
391.42	0.002241
421.53	0.002406
451.64	0.002577
481.75	0.002753
511.86	0.002912
541.97	0.003101

Test 2	
Stress (MPa)	Strain (mm/mm)
0	0
30.11	0.000198
60.22	0.000375
90.33	0.000550
120.44	0.000727
150.55	0.000905
180.66	0.001071
210.76	0.001256
240.87	0.001428
270.98	0.001601
301.09	0.001763
331.20	0.001938
361.31	0.002108
391.42	0.002265
421.53	0.002434
451.64	0.002605
481.75	0.002775
511.86	0.002932
541.97	0.003102
572.07	0.003266
602.18	0.003430
632.29	0.003583
662.40	0.003747
692.51	NA
722.62	0.004066
752.73	0.004228
782.84	0.004376
812.95	0.004527
843.06	0.004925

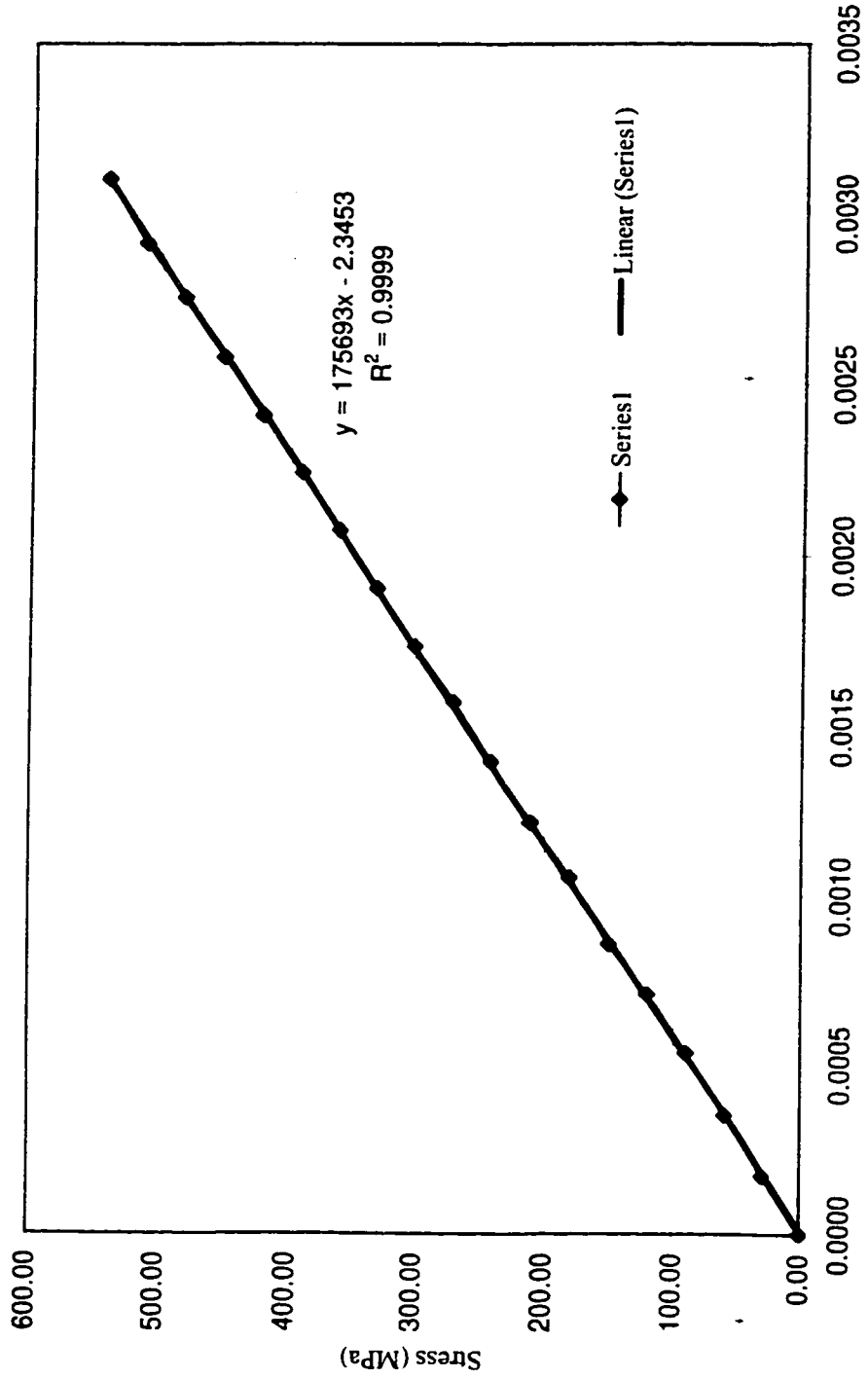

Figure C.1: Stress-strain curve of D1-D9.70 CFRP bar (Test 1)

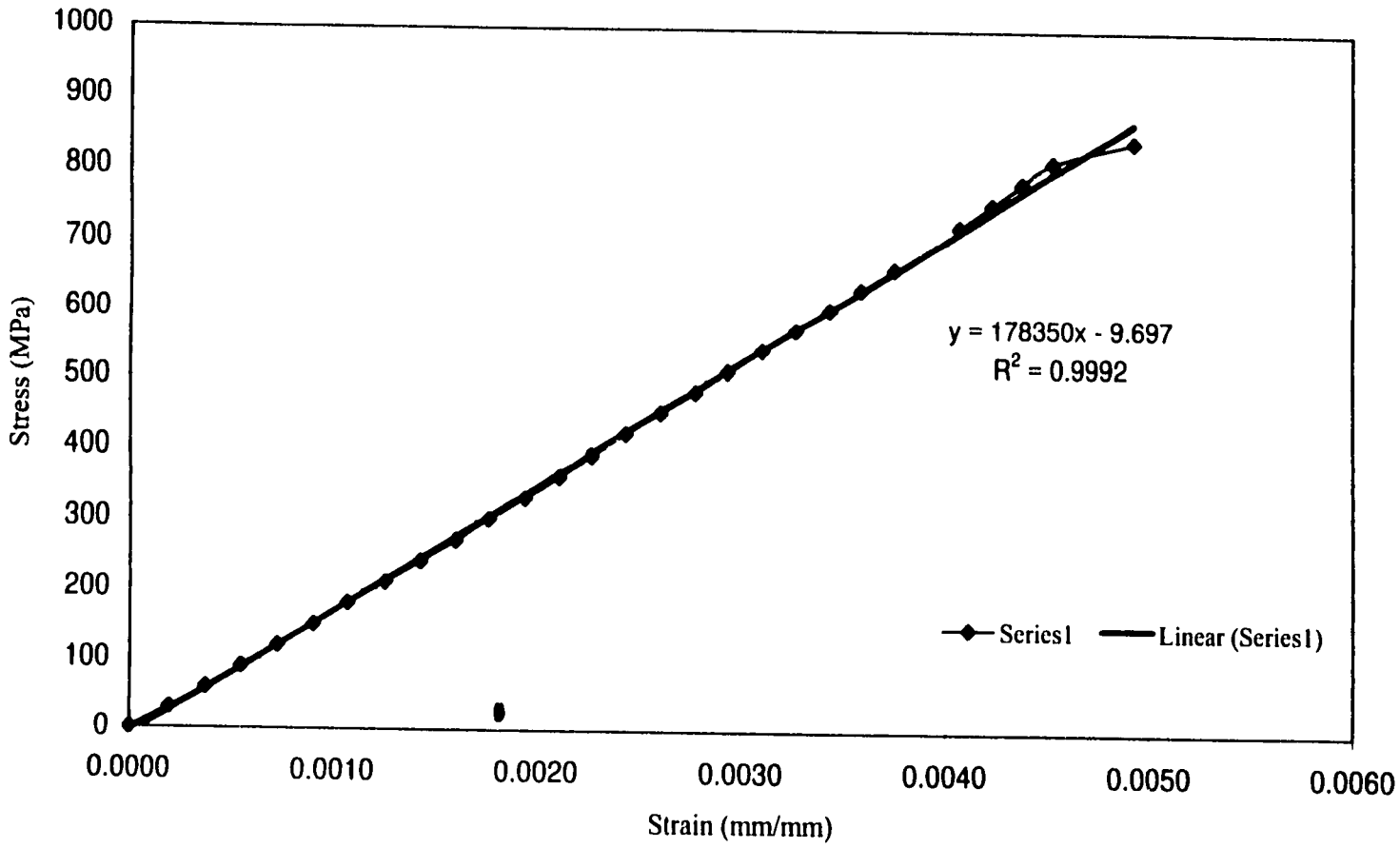

Figure C.2: Stress-strain curve of D1-D9.70 CFRP bar (Test 2)

Appendix D

Crack Pattern of Beams Reinforced with G1-D8 CFRP Bar

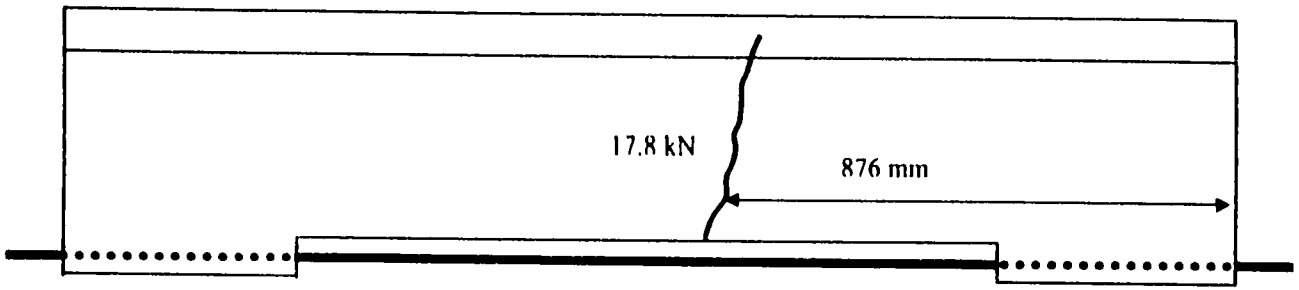

Figure D.1: Crack pattern of beam G1-D8-B12

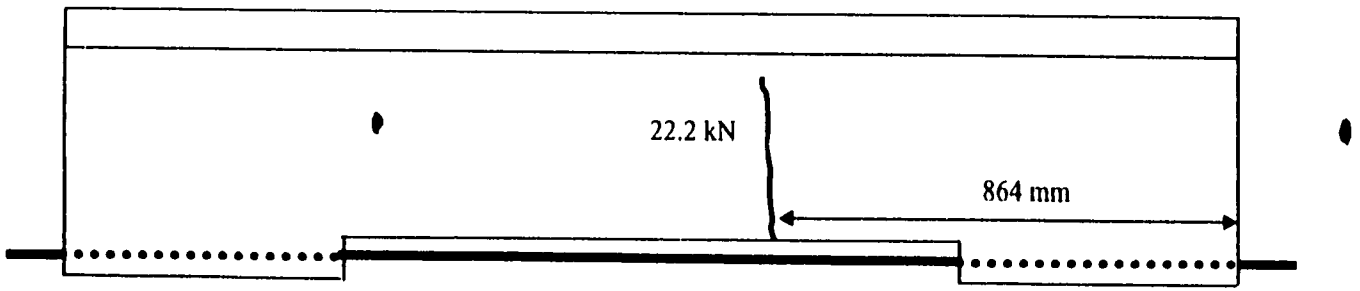

Figure D.2: Crack pattern of beam G1-D8-B13

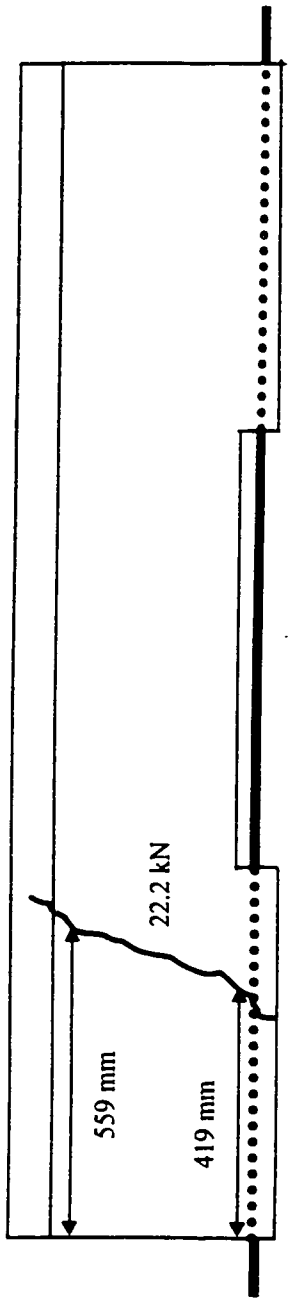

Figure D.3: Crack pattern of beam G1-D8-B14

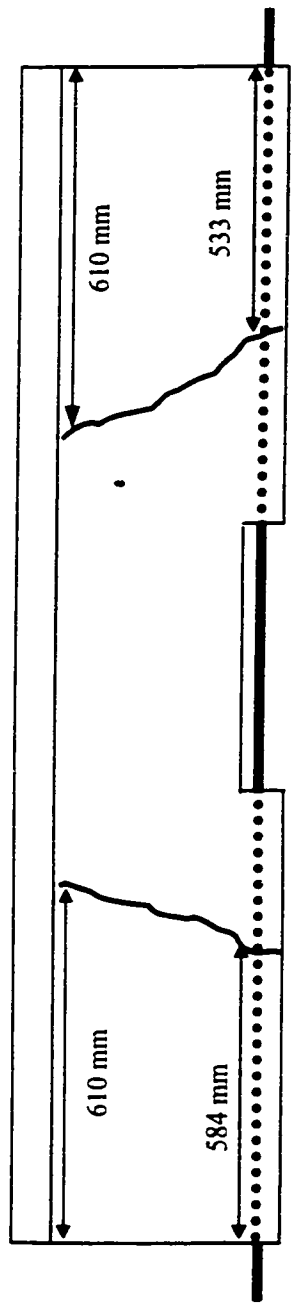

Figure D.4: Crack pattern of beam G1-D8-B15

Appendix E

Crack Pattern of Beams Reinforced with G2-D9.79 CFRP Bar

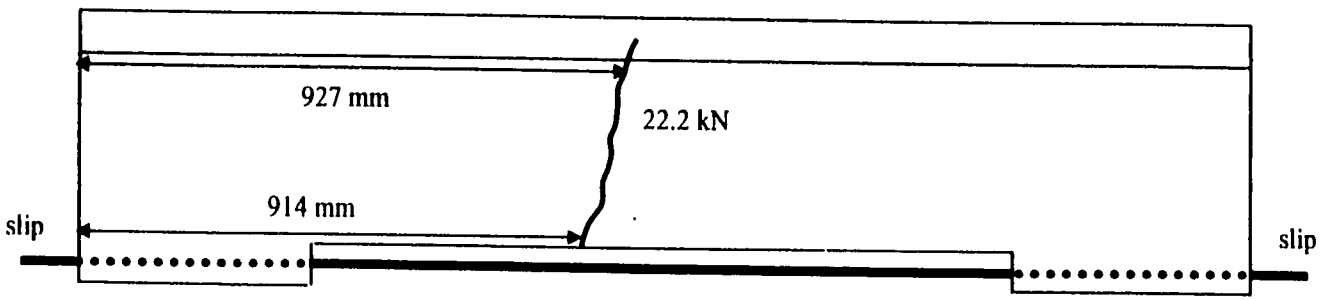

Figure E.1: Crack pattern of beam G2-D9.79-A18

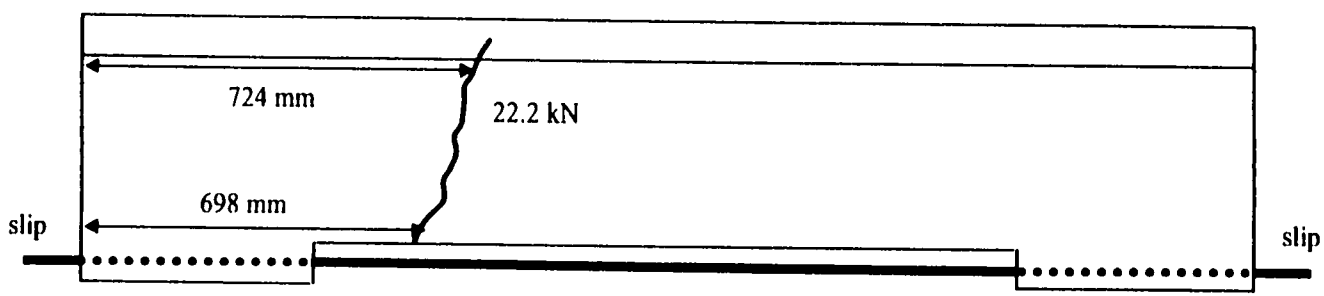

Figure E.2: Crack pattern of beam G2-D9.79-B18

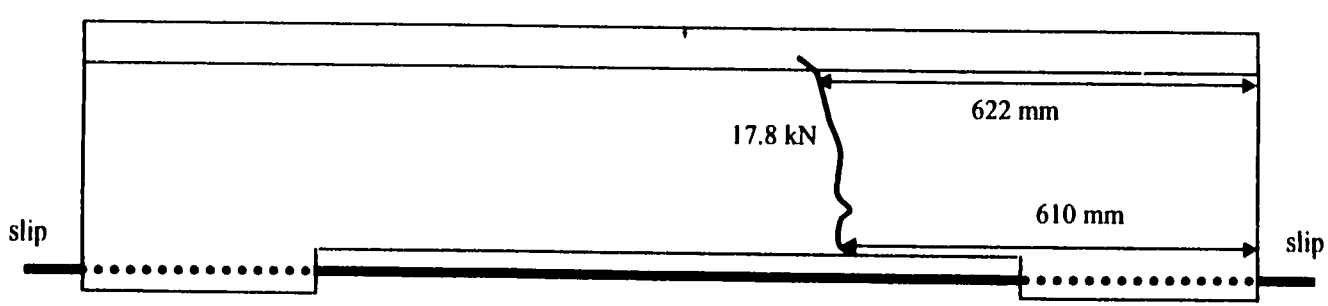

Figure E.3: Crack pattern of beam G2-D9.79-C18

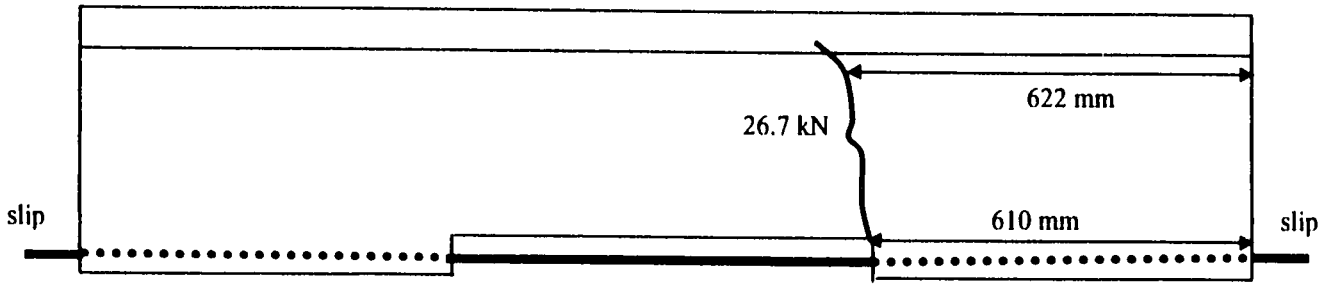

Figure E.4: Crack pattern of beam G2-D9.79-A24

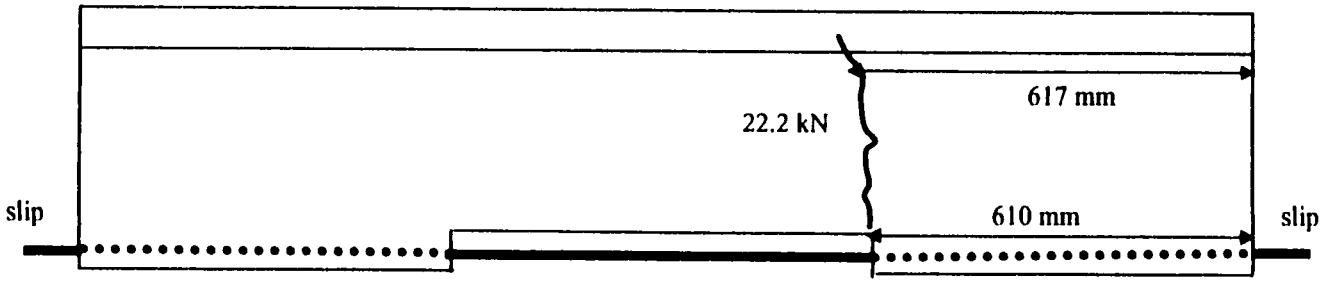

Figure E.5: Crack pattern of beam G2-D9.79-B24

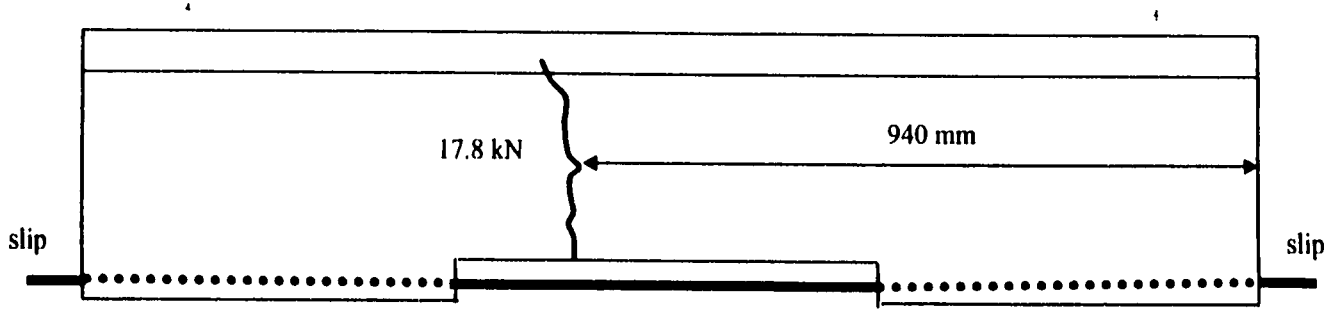

Figure E.6: Crack pattern of beam G2-D9.79-C24

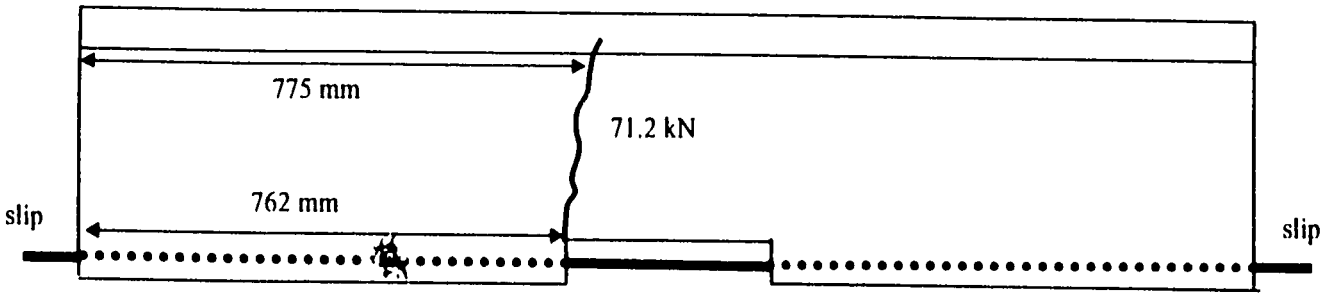

Figure E.7: Crack pattern of beam G2-D9.79-A30

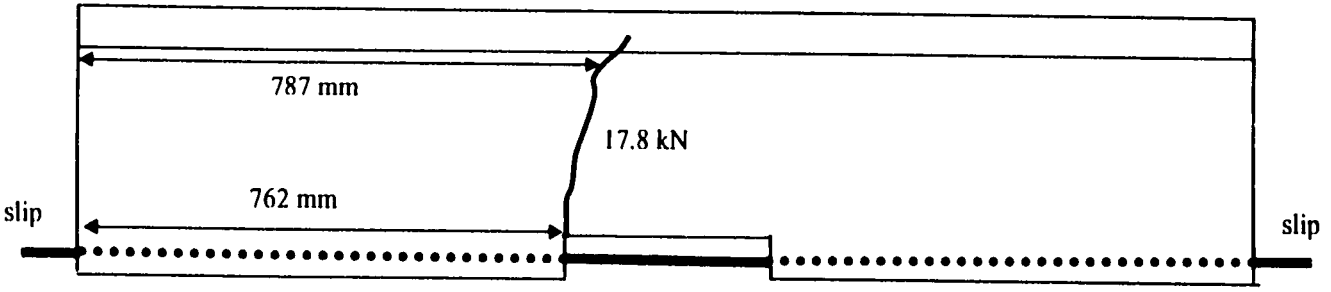

Figure E.8: Crack pattern of beam G2-D9.79-B30

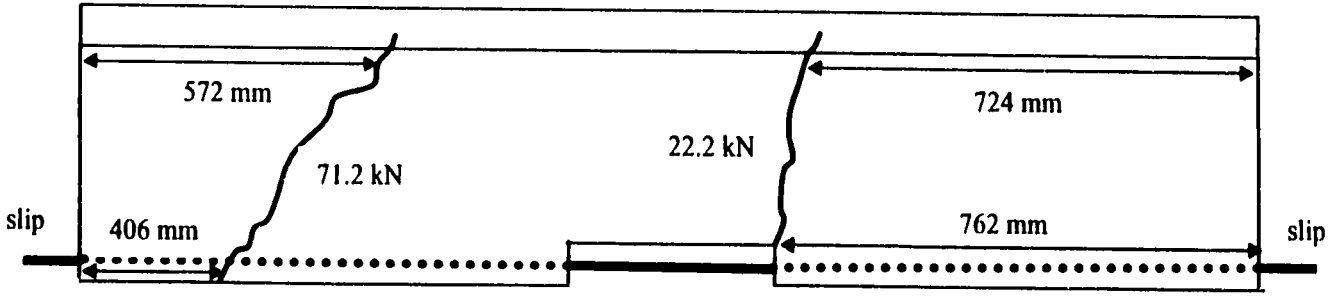

Figure E.9: Crack pattern of beam G2-D9.79-C30

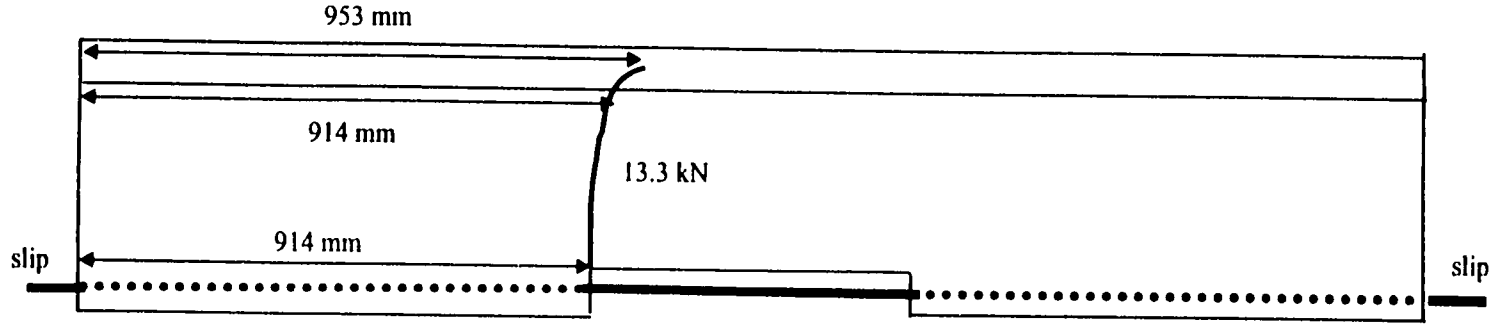

Figure E.10: Crack pattern of beam G2-D9.79-A36

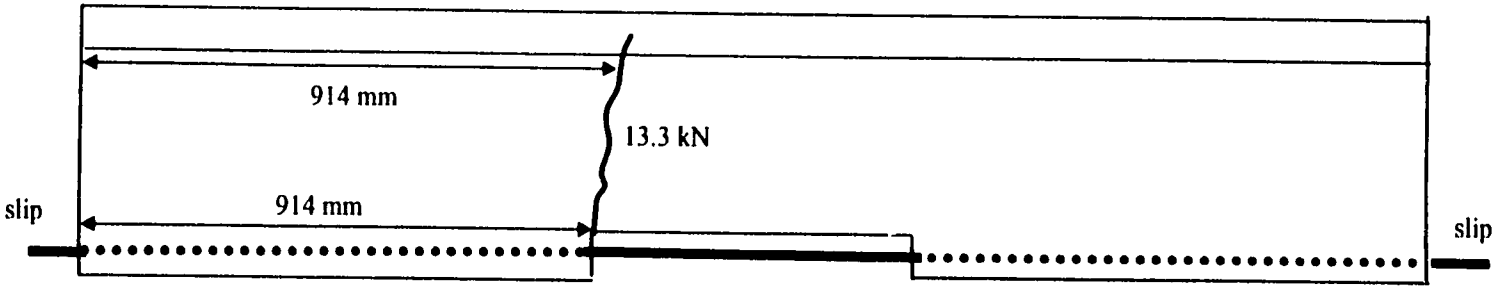

Figure E.11: Crack pattern of beam G2-D9.79-B36

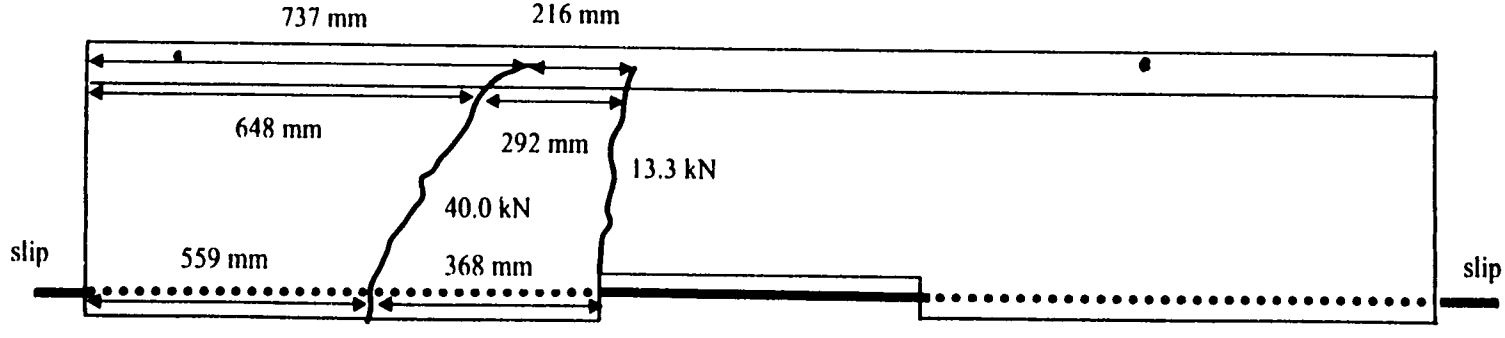

Figure E.12: Crack pattern of beam G2-D9.79-C36

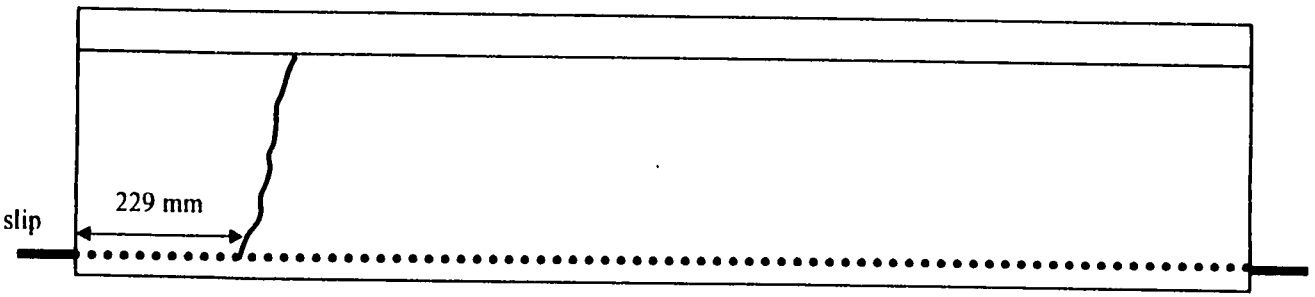

Figure E.13: Crack pattern of beam G2-D9.79-B36(F1)

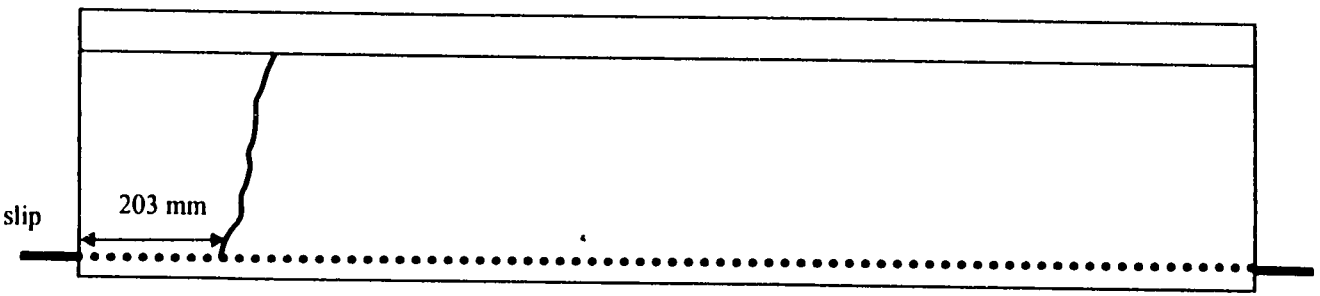

Figure E.14: Crack pattern of beam G2-D9.79-B36(F2)

Appendix F

Crack Pattern of Beams Reinforced with D1-D9.70 CFRP Bar

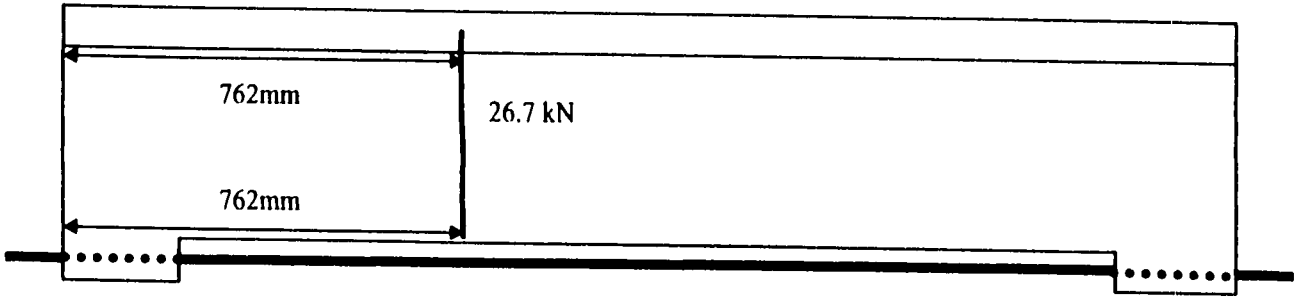

Figure F.1: Crack pattern of beam D1-D9.70-A12

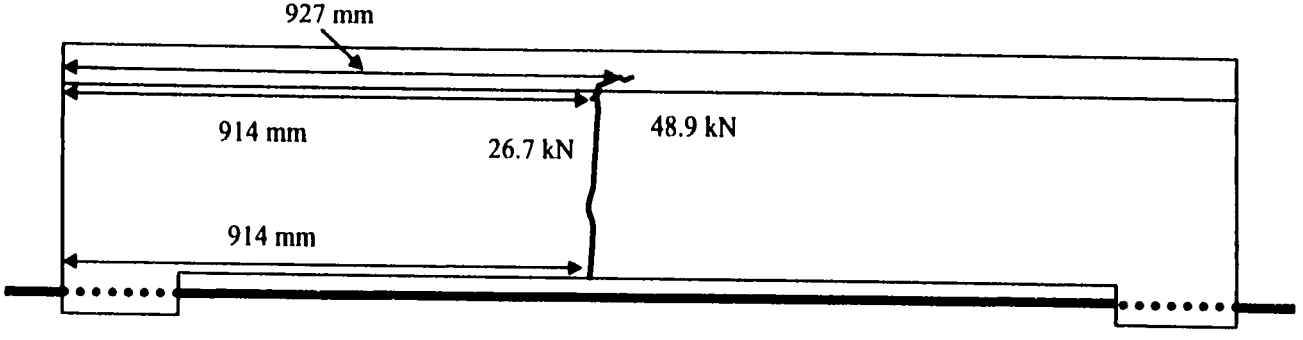

Figure F.2: Crack pattern of beam D1-D9.70-B12

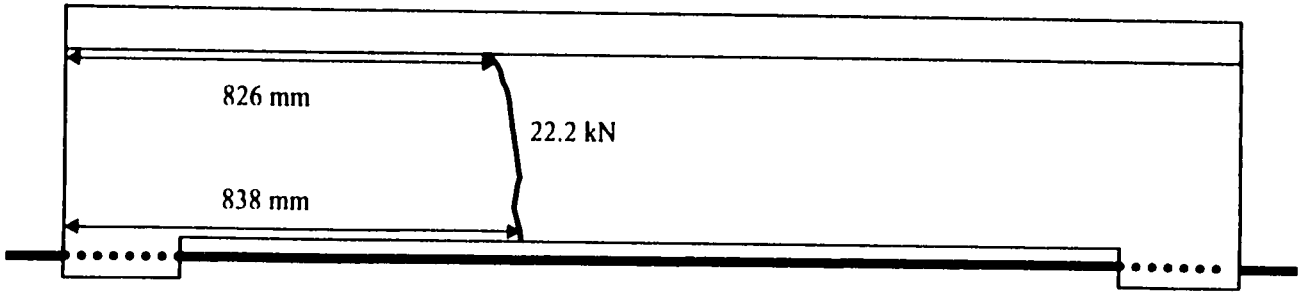

Figure F.3: Crack pattern of beam D1-D9.70-C12

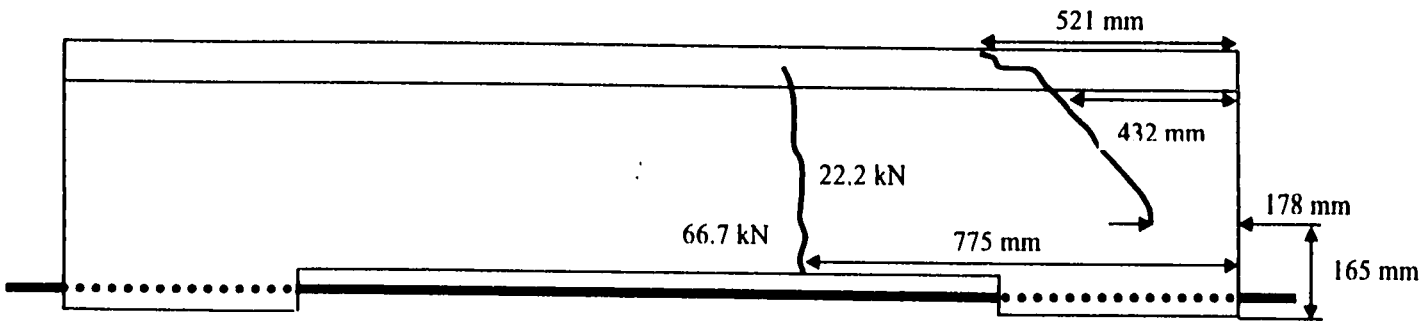

Figure F.4: Crack pattern of beam D1-D9.70-A18

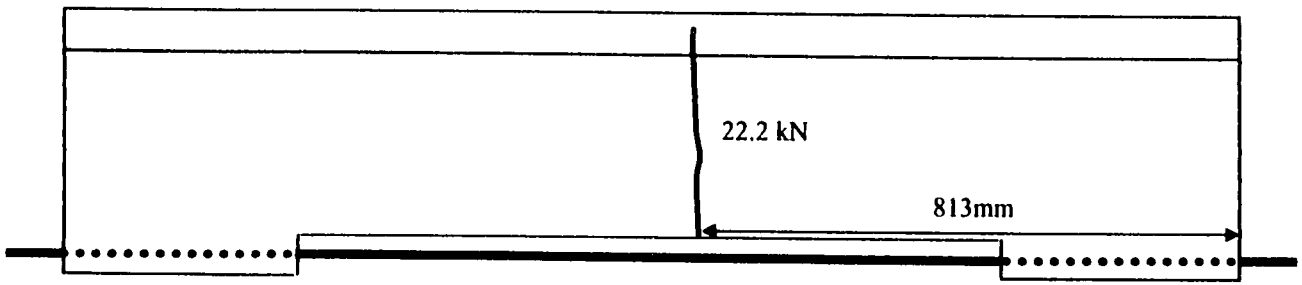

Figure F.5: Crack pattern of beam D1-D9.70-B18

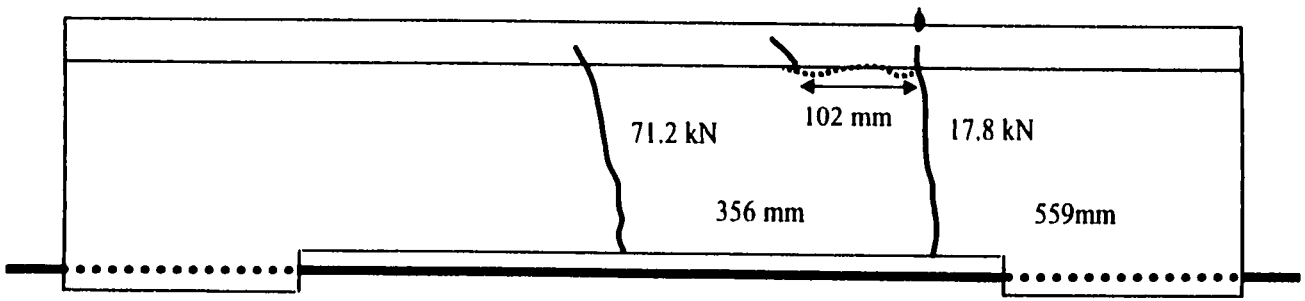

Figure F.6: Crack pattern of beam D1-D9.70-C18

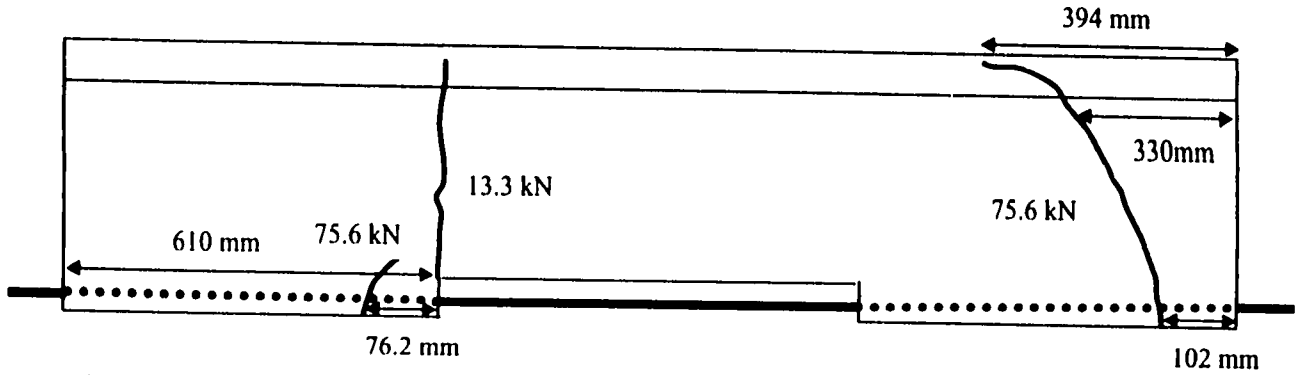

Figure F.7: Crack pattern of beam D1-D9.70-A24

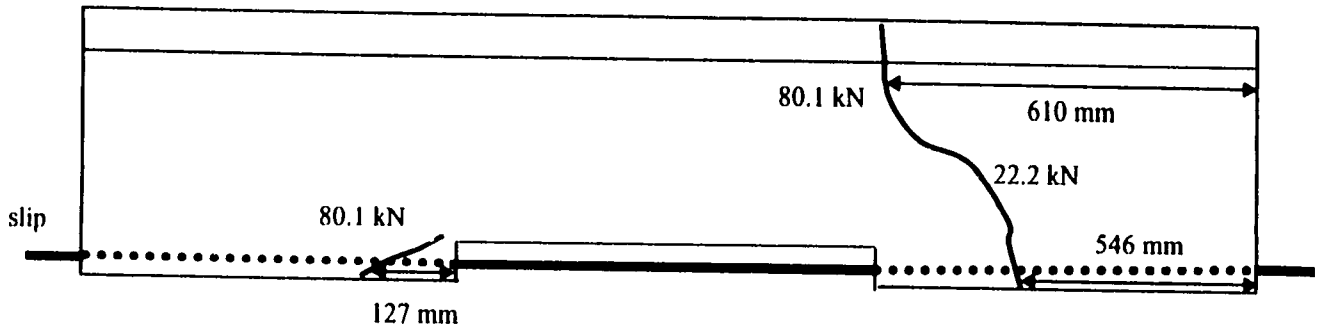

Figure F.8: Crack pattern of beam D1-D9.70-B24

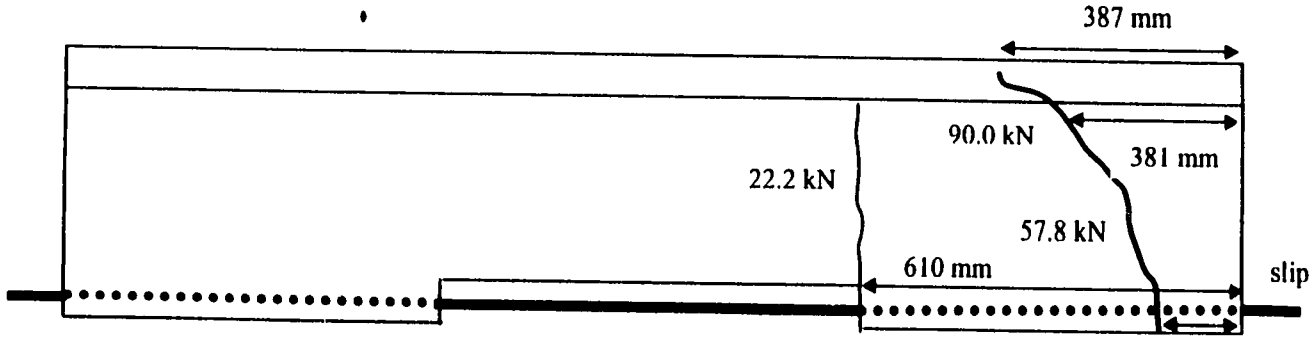

Figure F.9: Crack pattern of beam D1-D9.70-C24

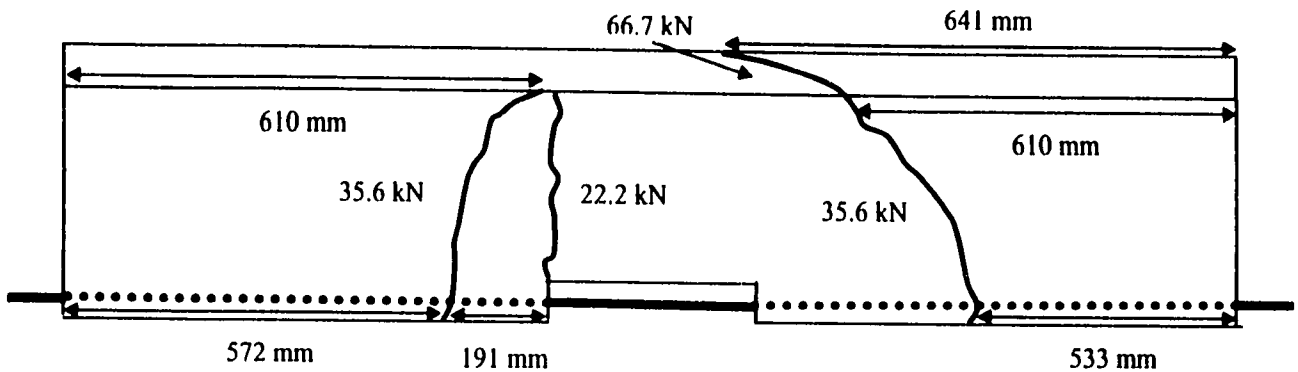

Figure F.10: Crack pattern of beam D1-D9.70-A30

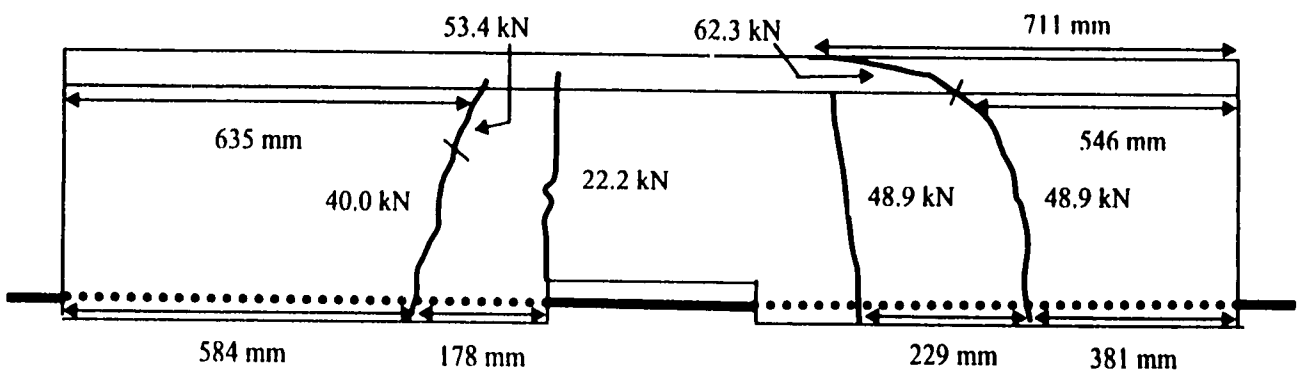

Figure F.11: Crack pattern of beam D1-D9.70-B30

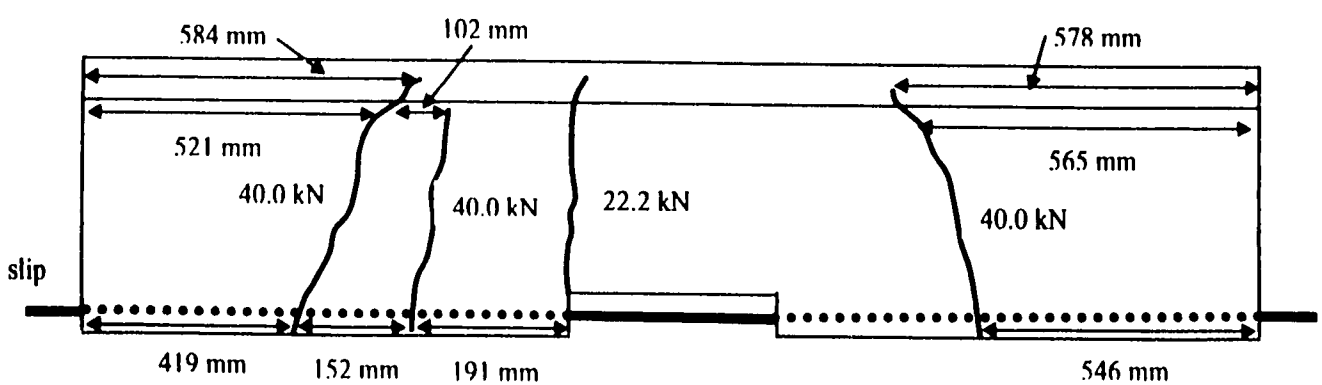

Figure F.12: Crack pattern of beam D1-D9.70-C30

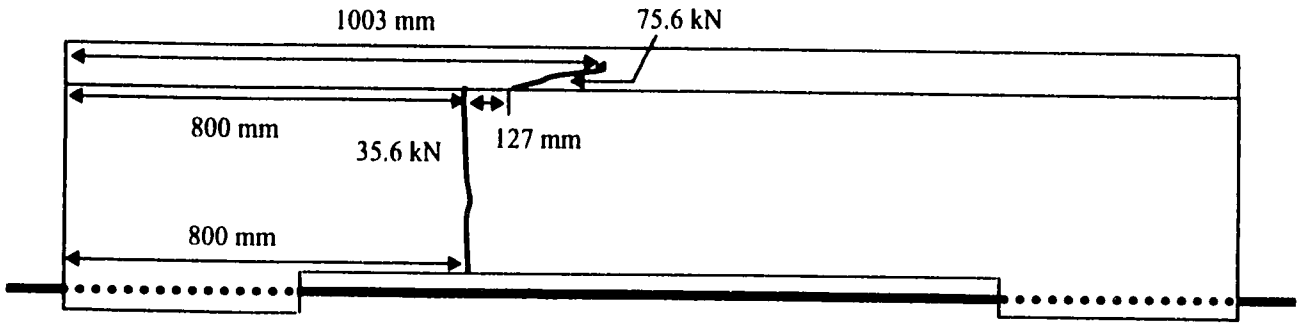

Figure F.13: Crack pattern of beam D1-D9.70-B18C

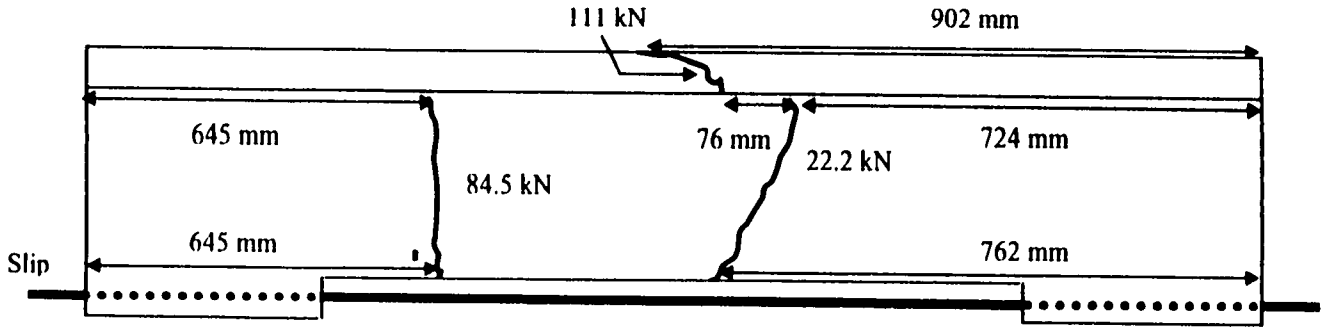

Figure F.14: Crack pattern of beam D1-D9.70-C18C

Appendix G

Applied Load vs. Slip Curve (G1-D8 Bar)

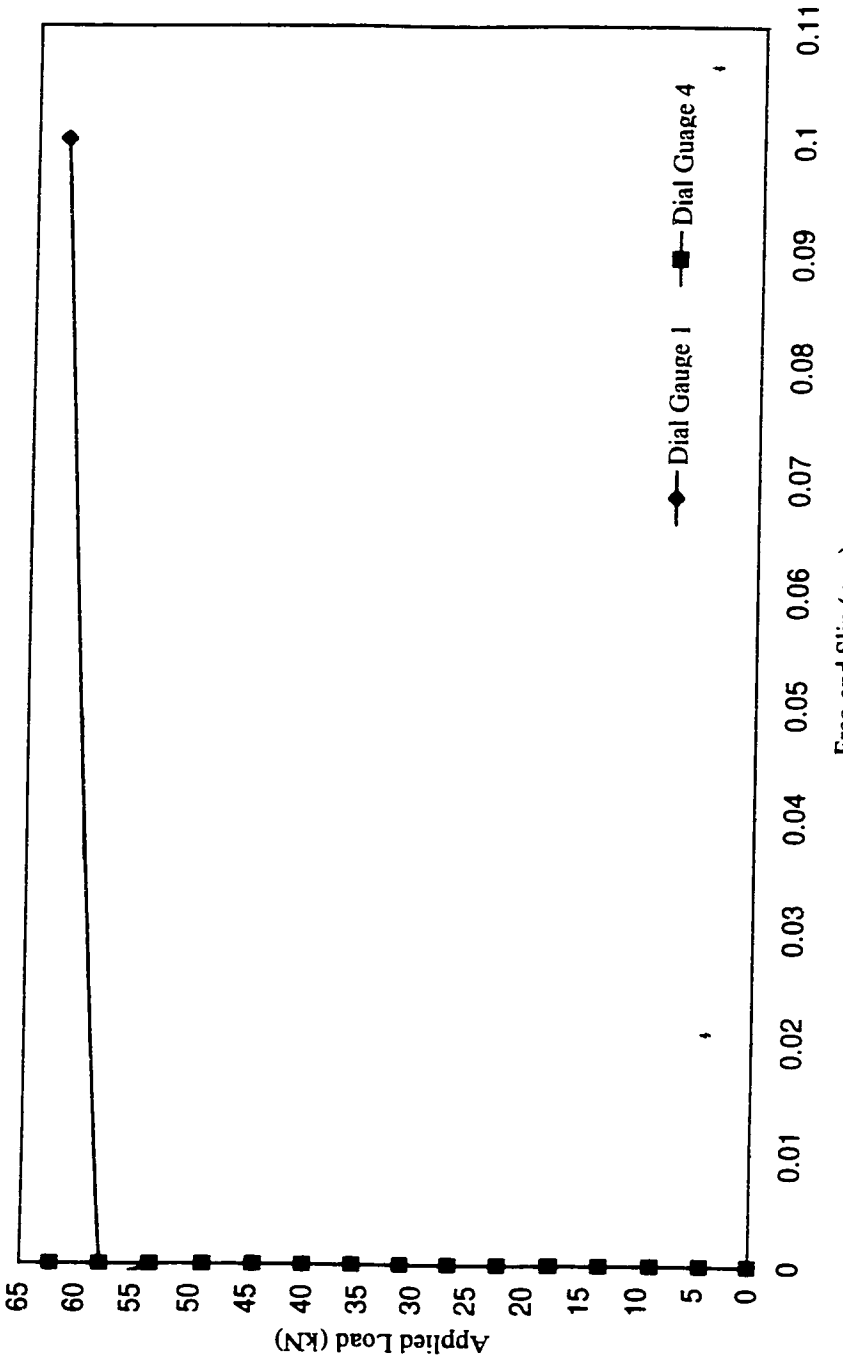

Figure G.1: Applied load vs. free-end slip of beam G1-D8-B12

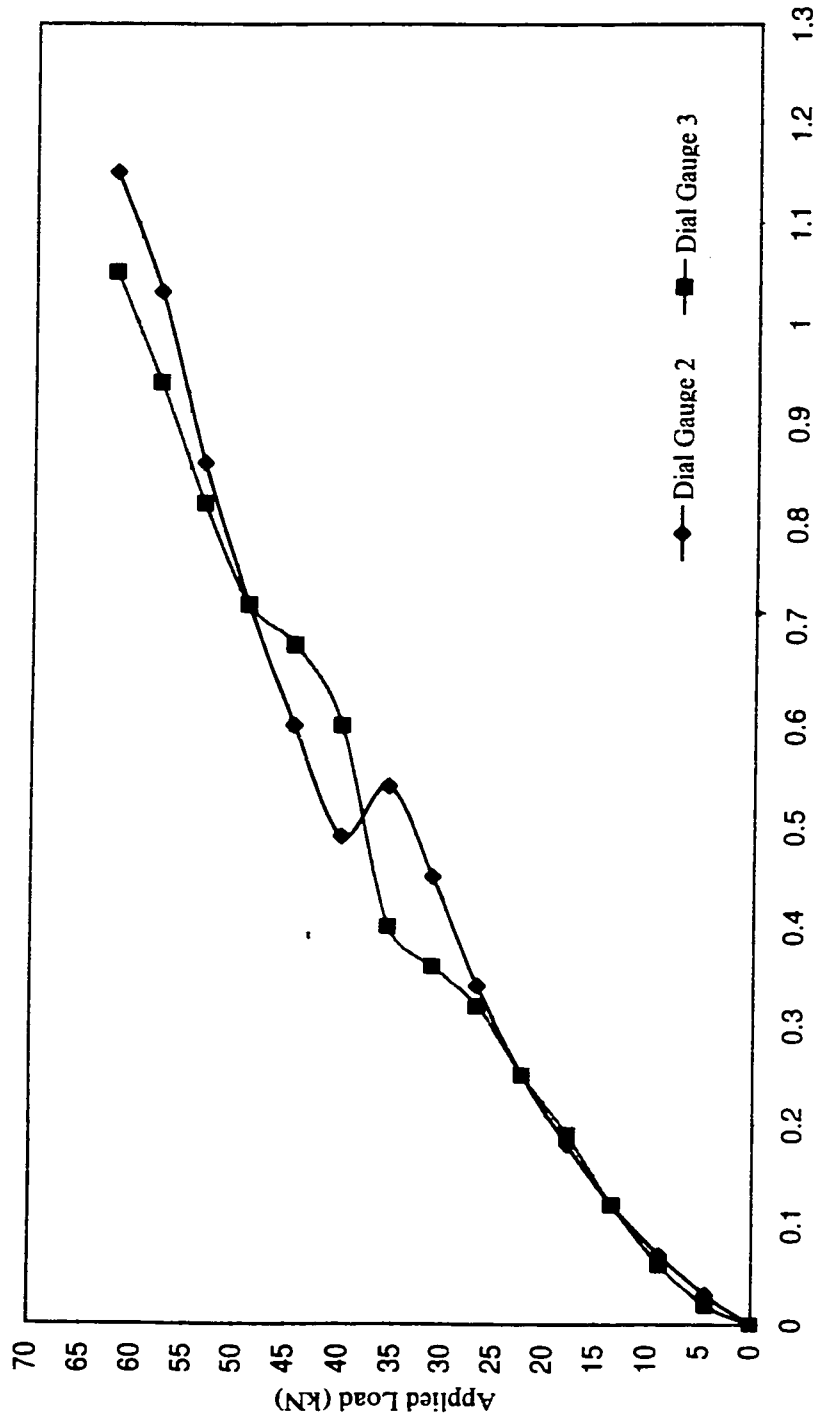

Figure G.2: Applied load vs. loaded-end slip of beam G1-D8-B12

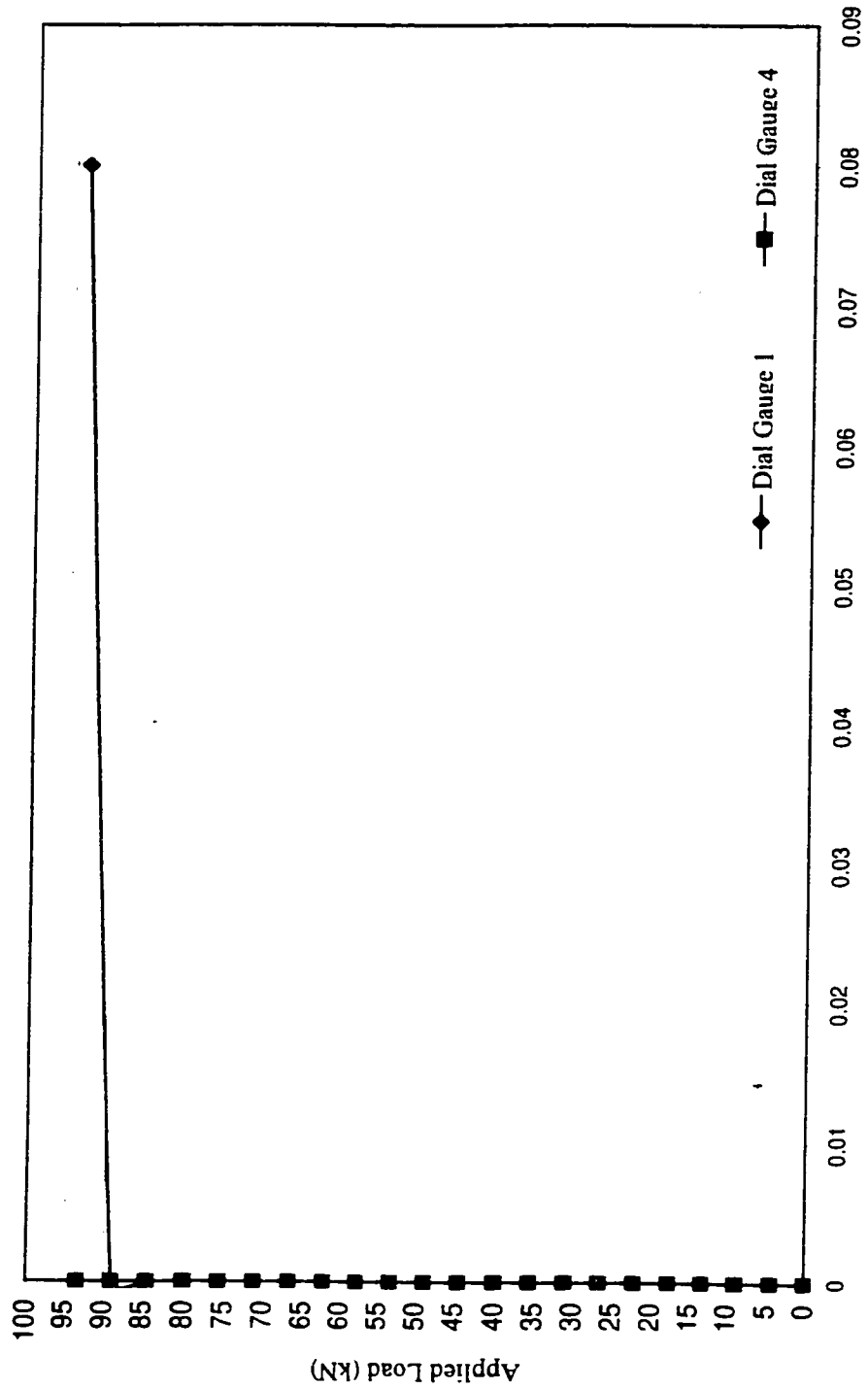

Figure G.3: Applied load vs. free-end slip of beam G1-D8-B13

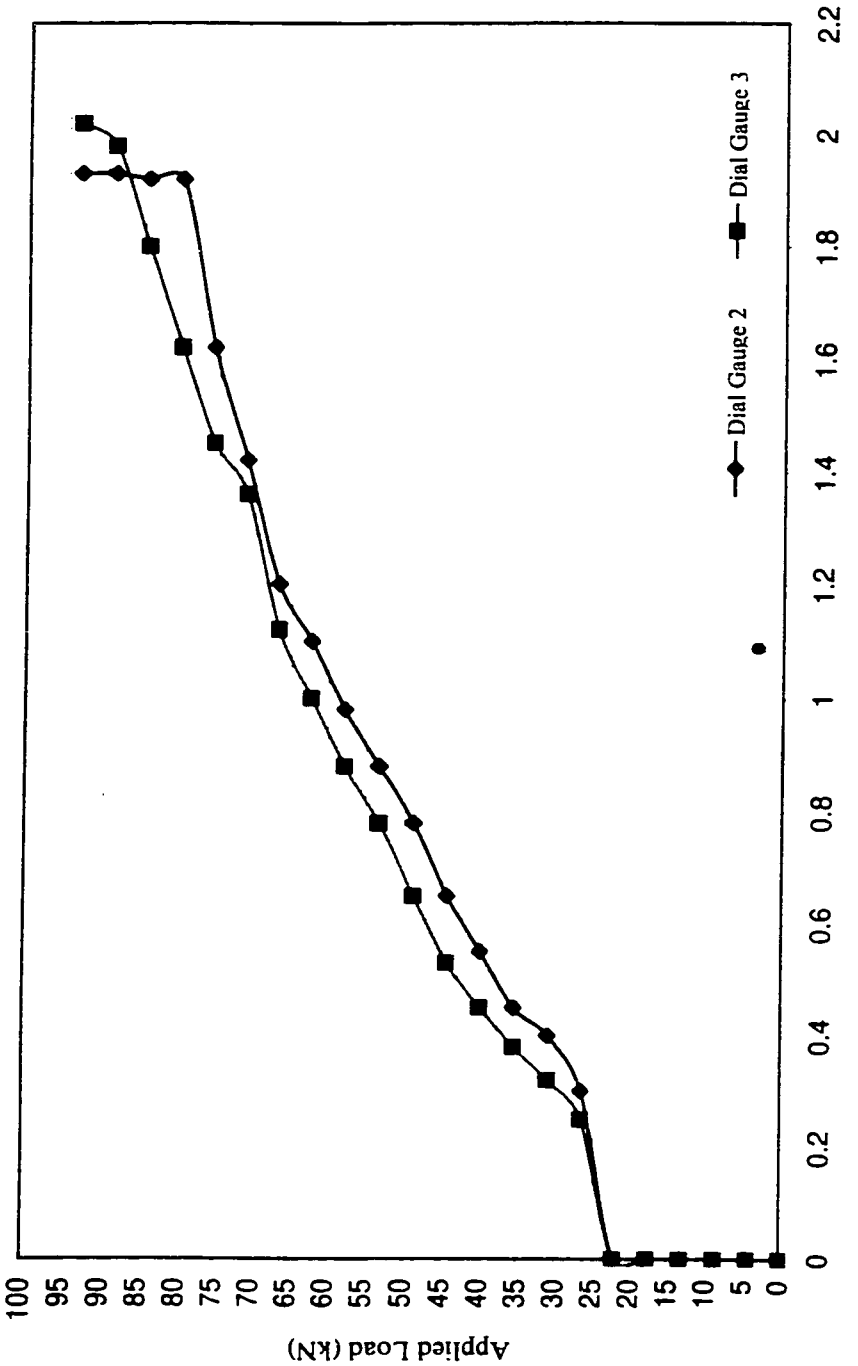

Figure G.4: Applied load vs. loaded-end slip of beam G1-D8-B13

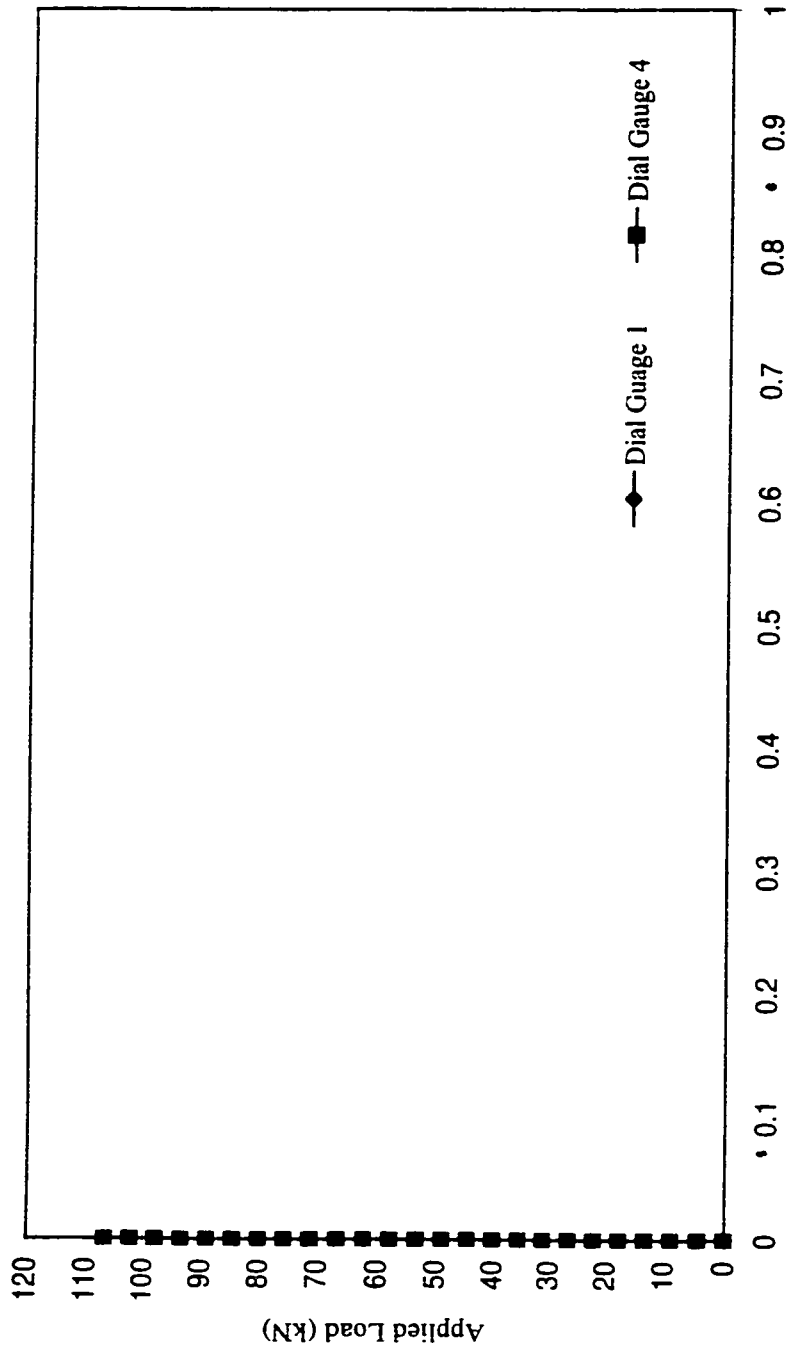

Figure G.5: Applied load vs. free-end slip of beam G1-D8-B14

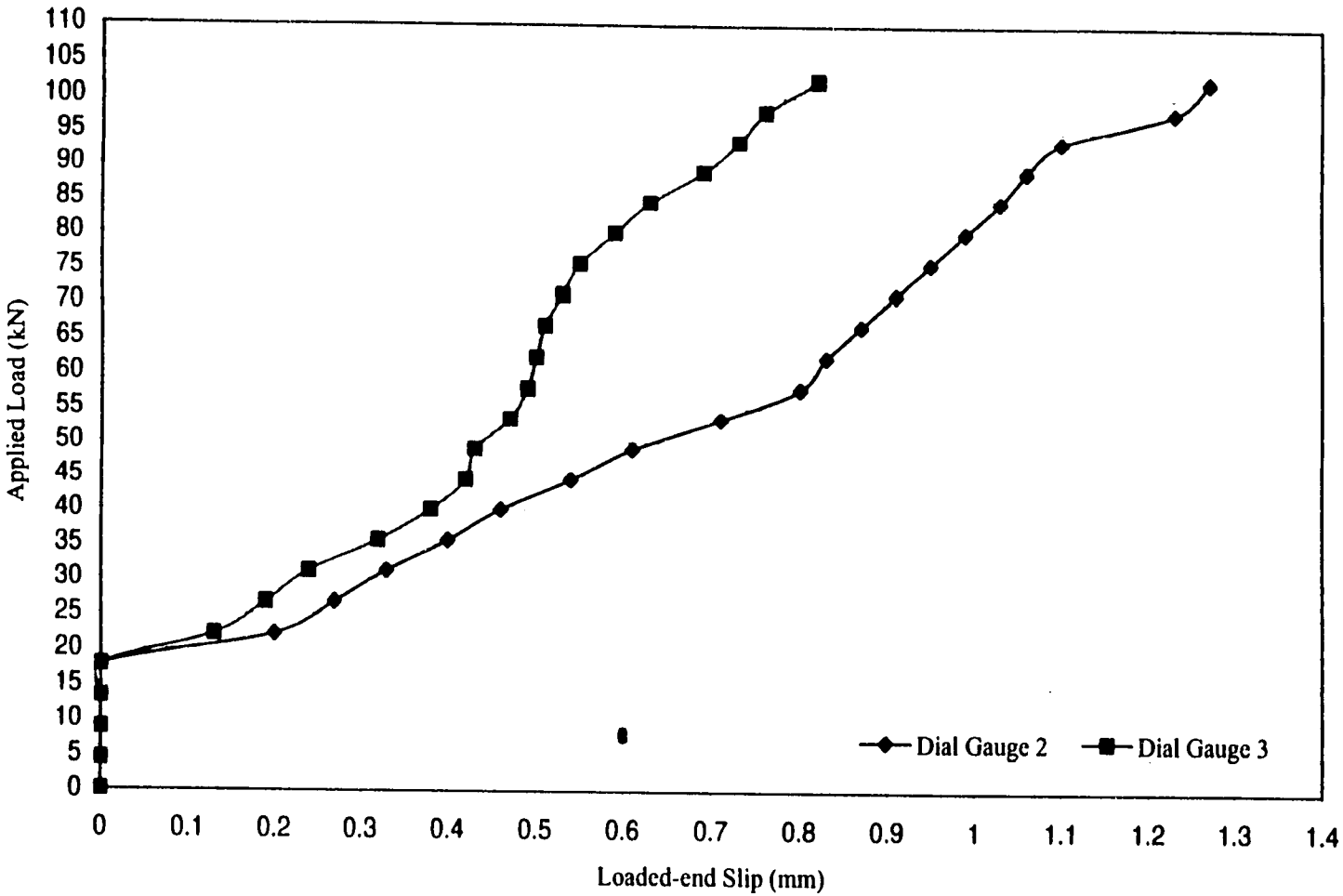

Figure G.6: Applied load vs. loaded-end slip of beam G1-D8-B14

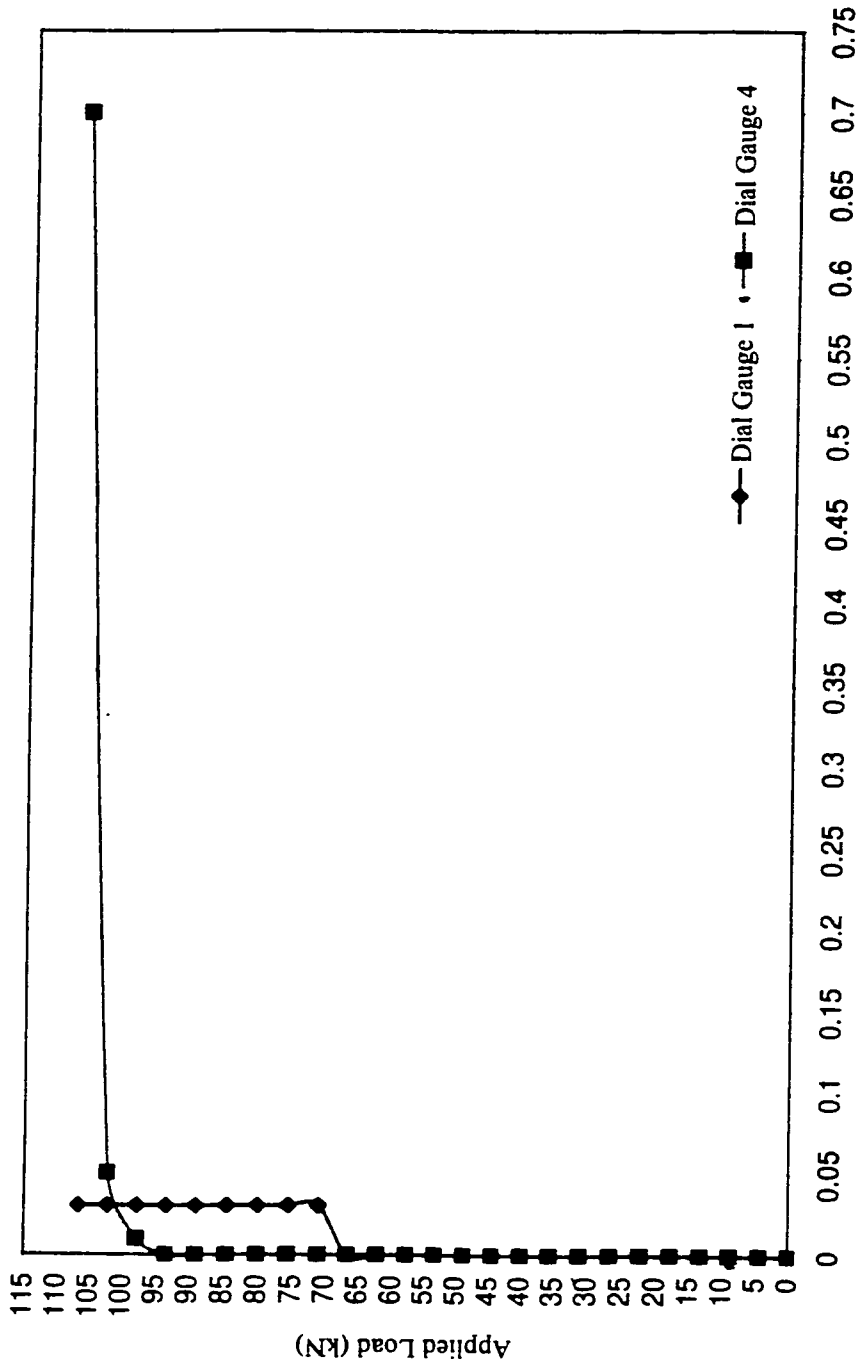

Figure G.7: Applied load vs. free-end slip of beam G1-D8-B15

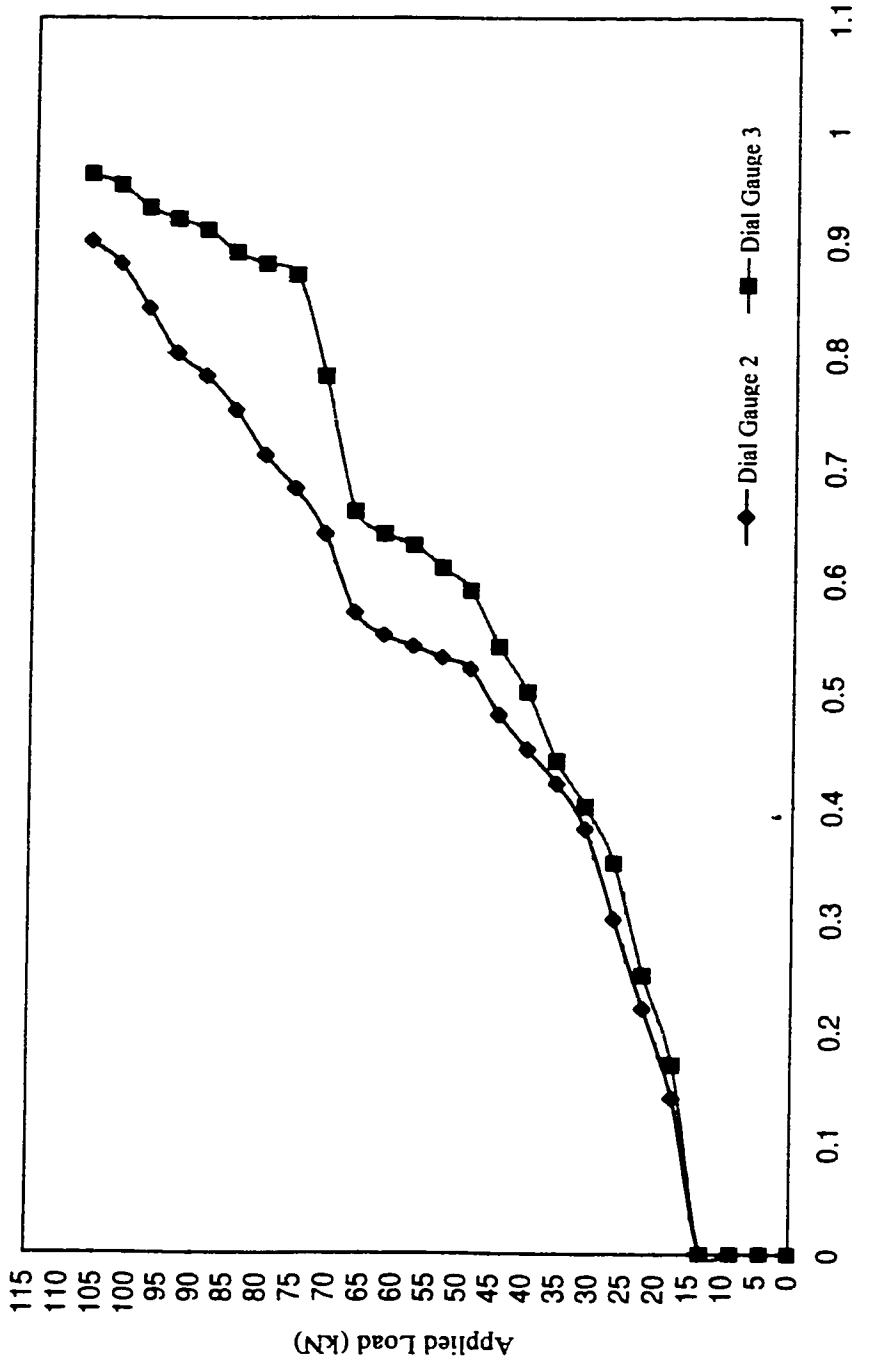

Figure G.8: Applied load vs. loaded-end slip of beam G1-D8-B15

Appendix H

Applied Load vs. Slip Curve (G2-D9.79 Bar)

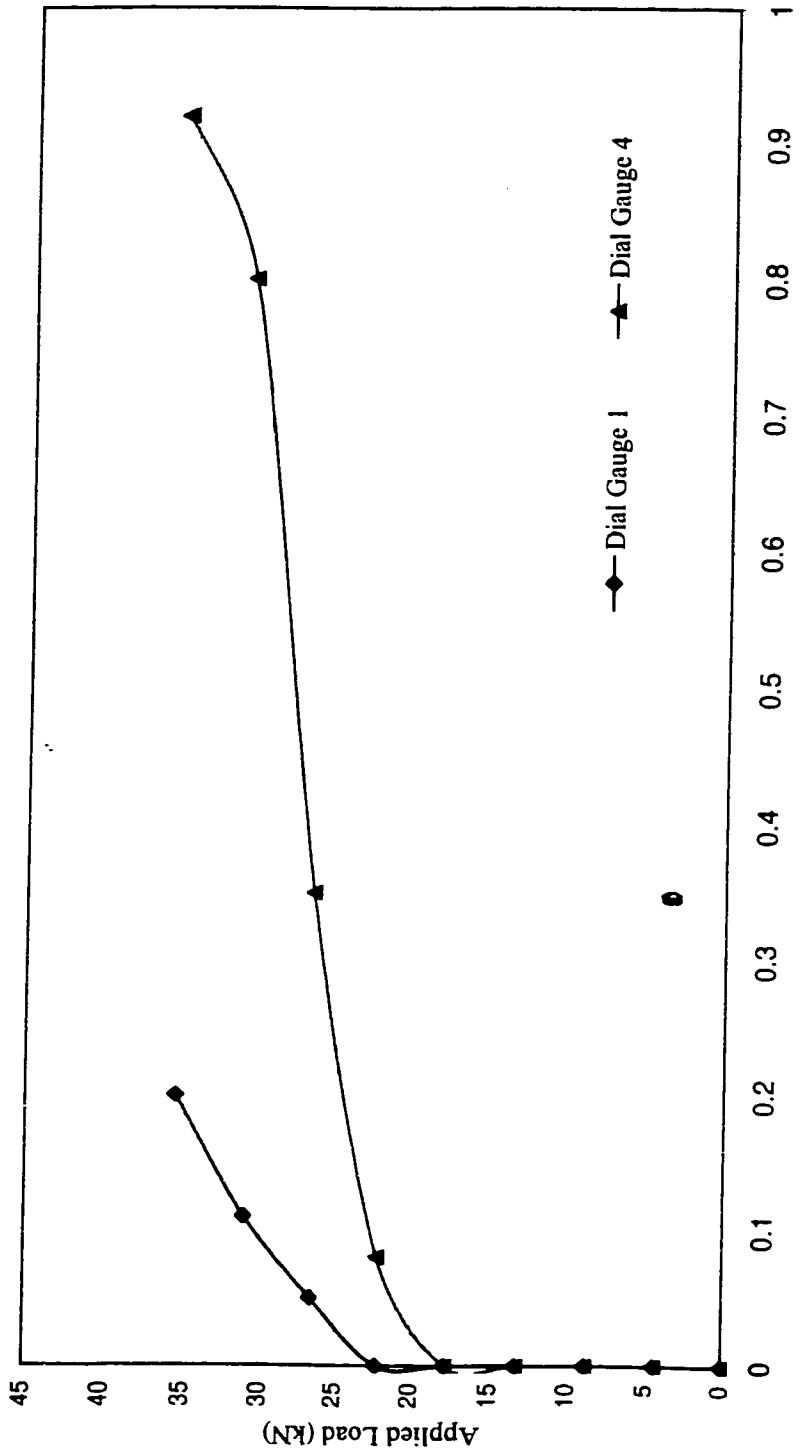

Figure H.1: Applied load vs. free-end slip of beam G2-D9.79-A18

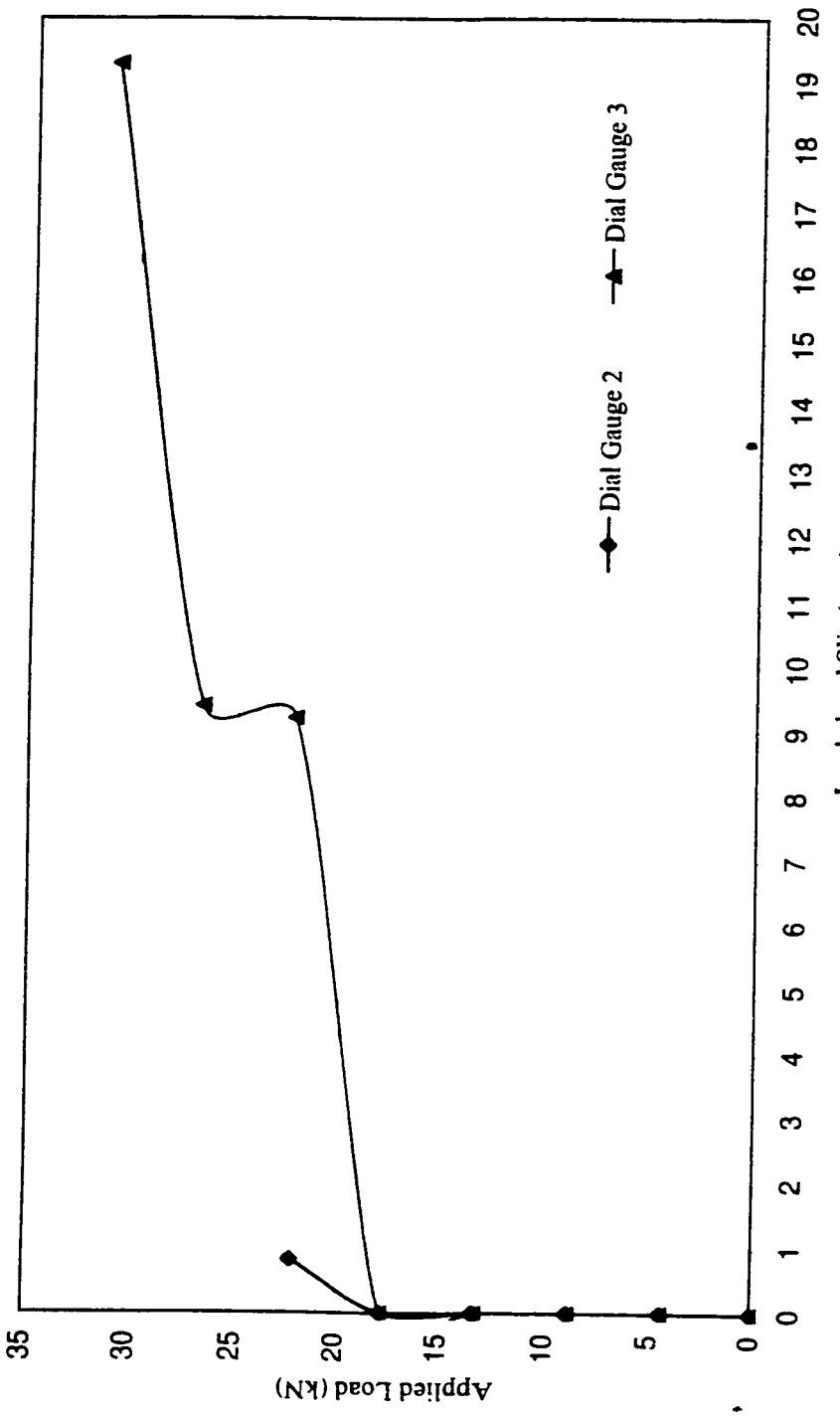

Figure H.2: Applied load vs. loaded-end slip of beam G2-D9.79-A18

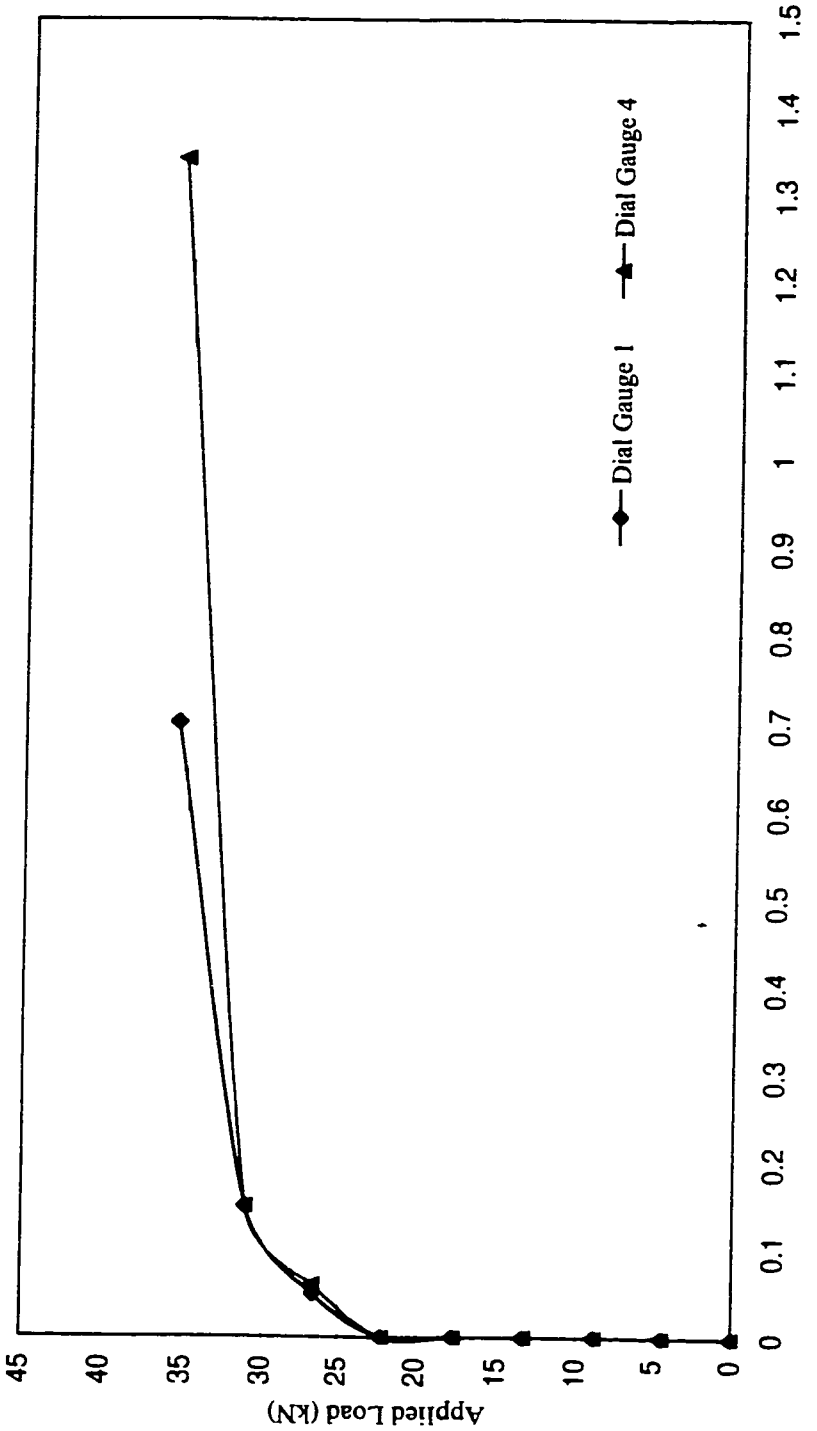

Figure H.3: Applied load vs. free-end slip of beam G2-D9.79-B18

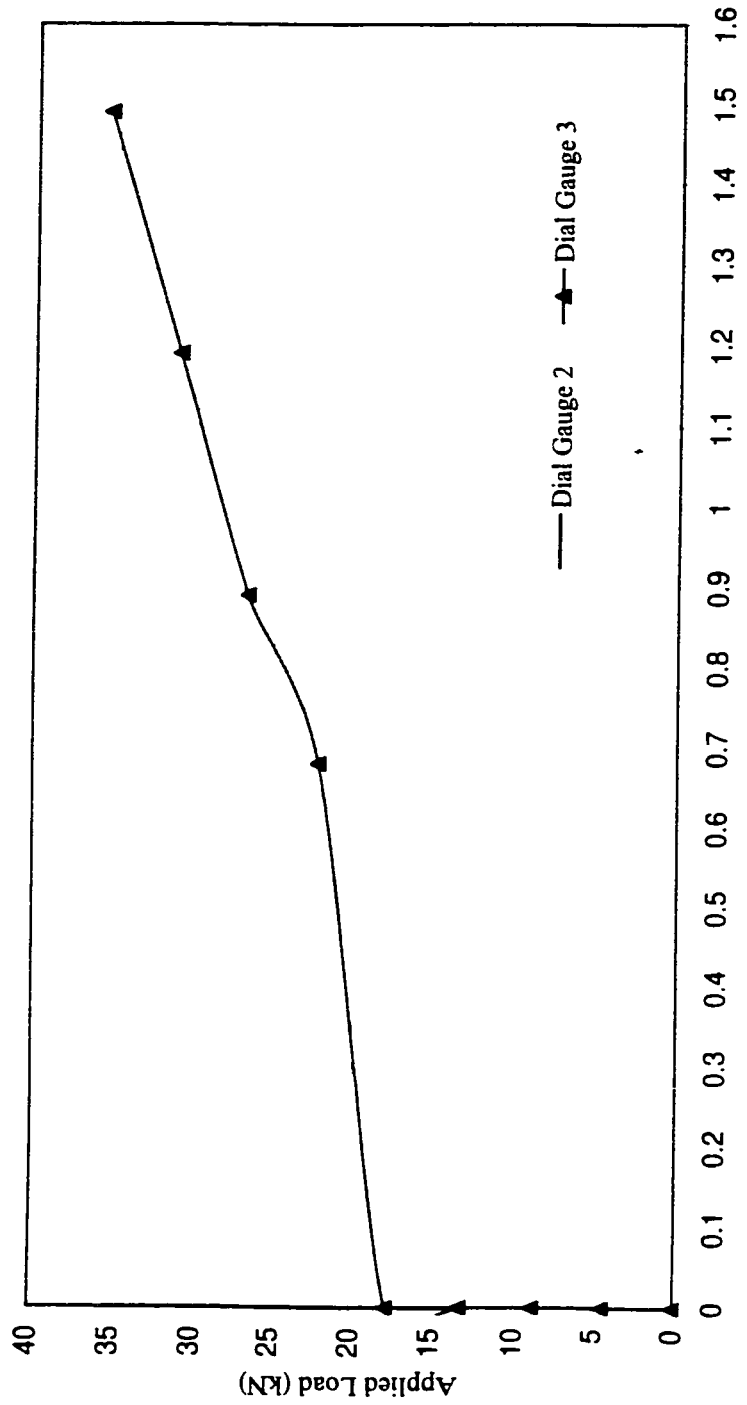

Figure H.4: Applied load vs. loaded-end slip of beam G2-D9.79-B18

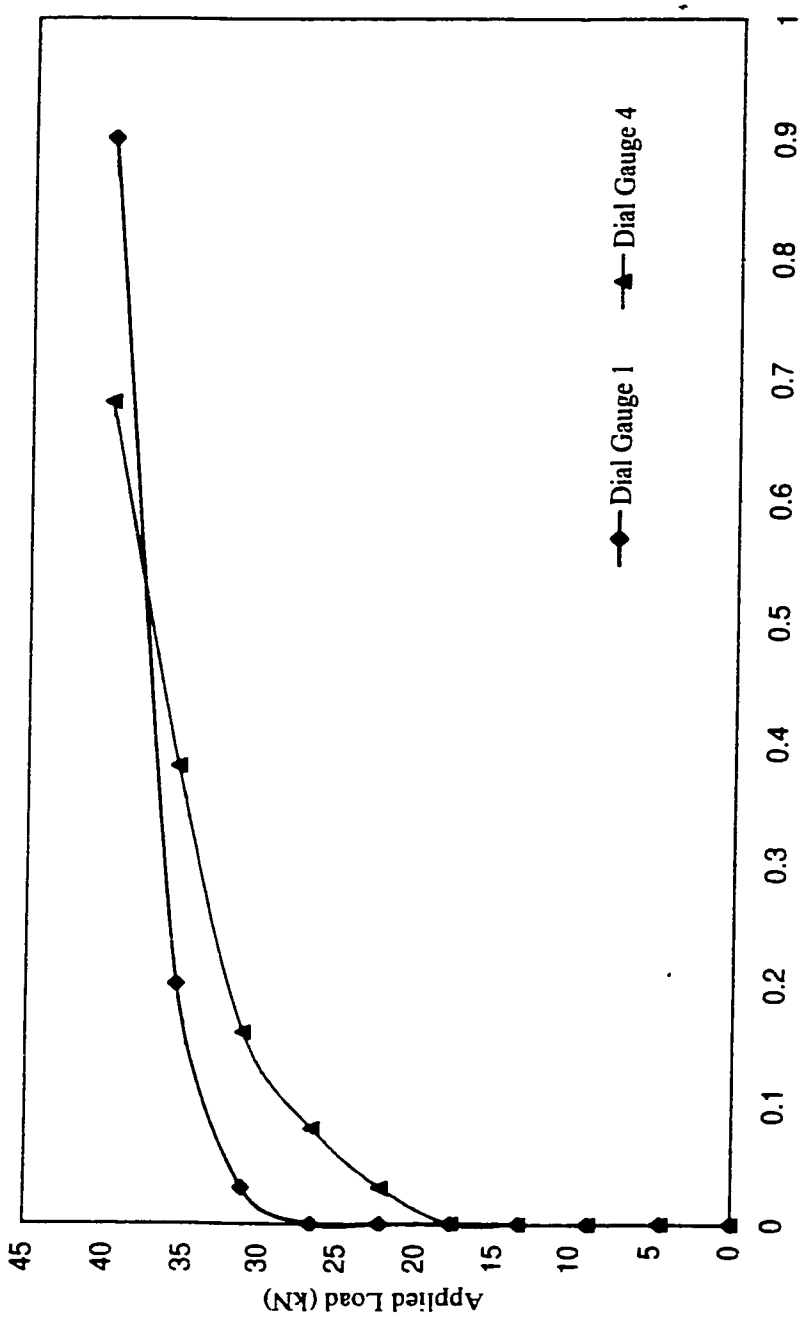

Figure H.5: Applied load vs. free-end slip of beam G2-D9.79-C18

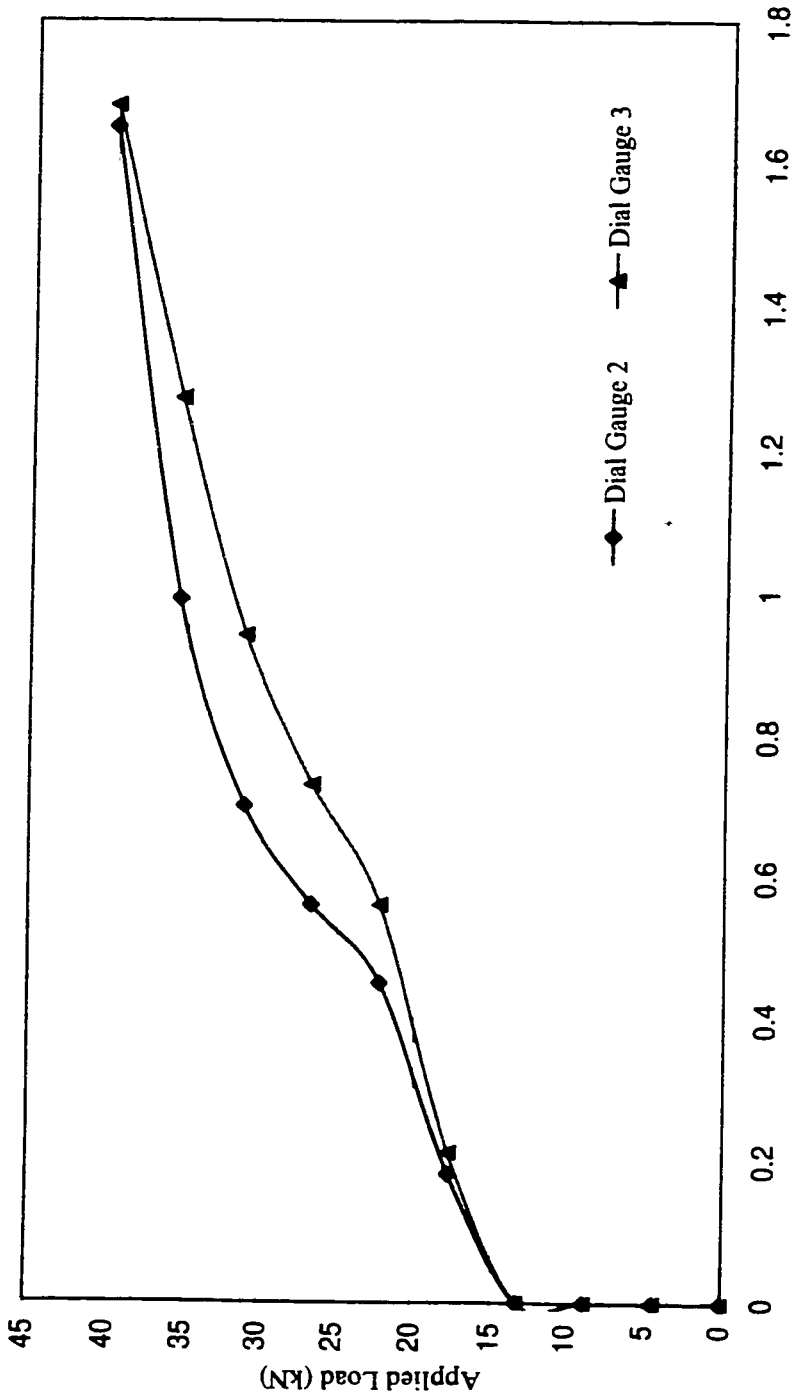

Figure H.6: Applied load vs. loaded-end slip of beam G2-D9.79-C18

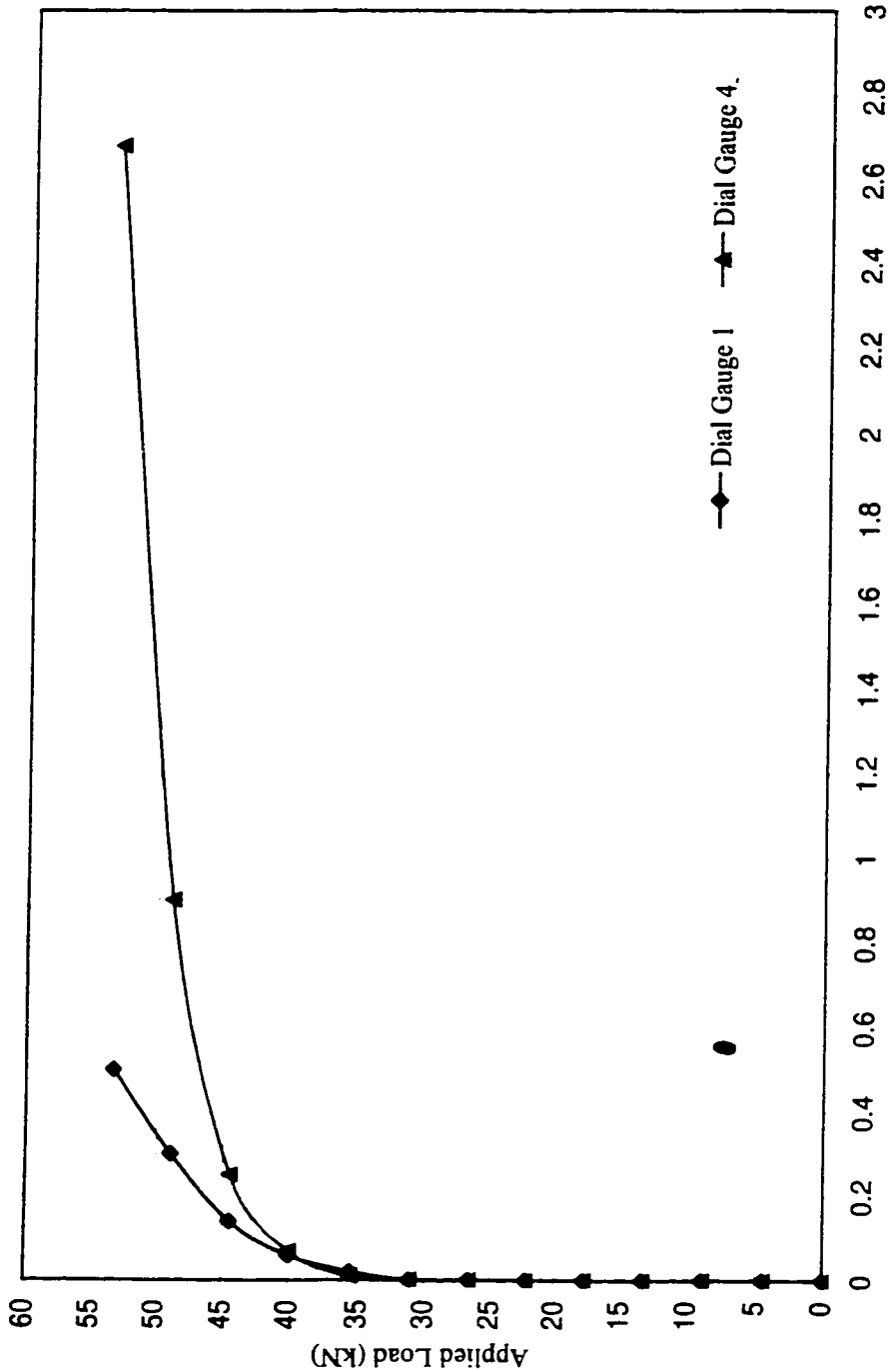

Figure H.7: Applied load vs. free-end slip of beam G2-D9.79-A24

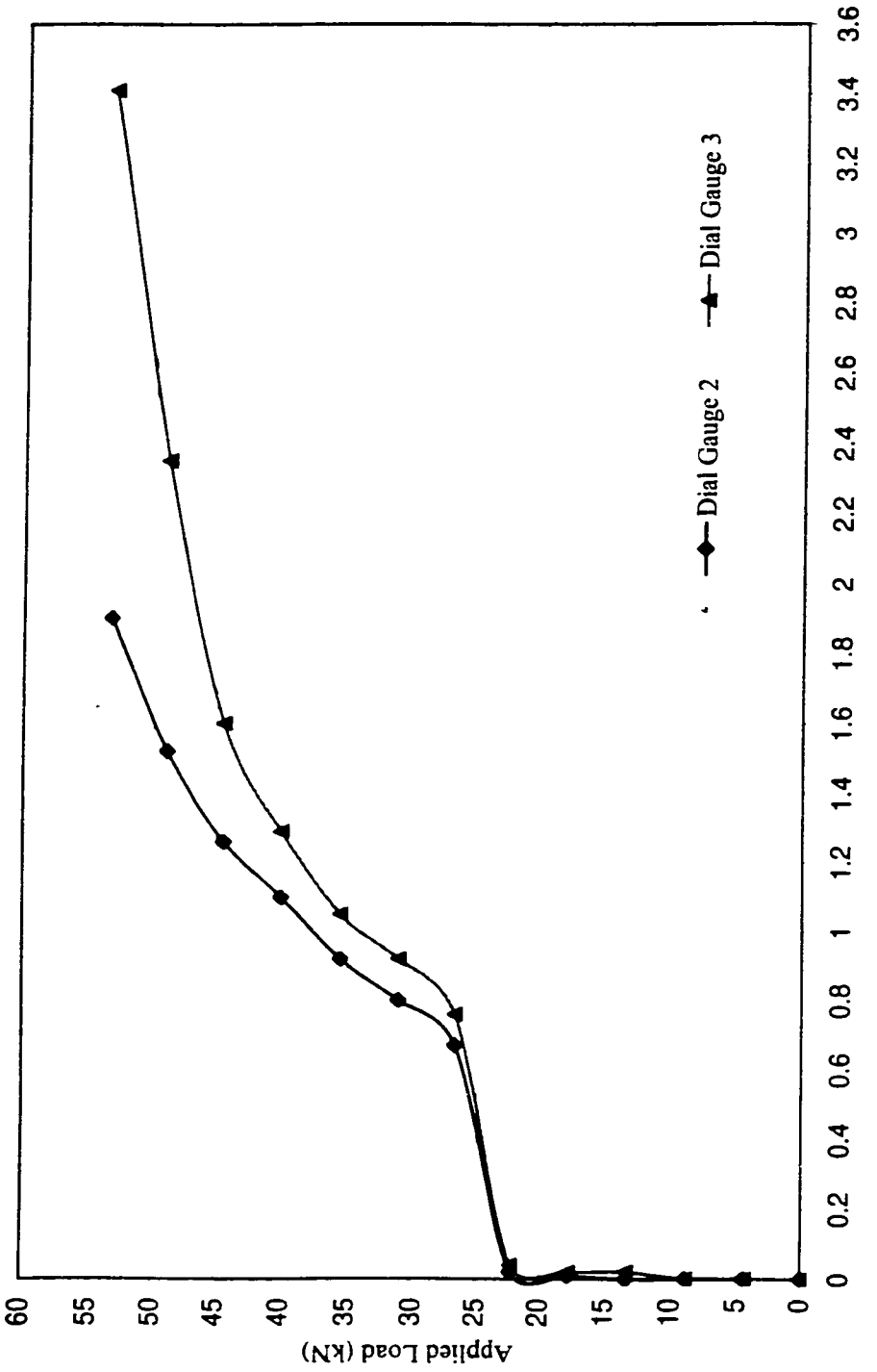

Figure H.8: Applied load vs. loaded-end slip of beam G2-D9.79-A24

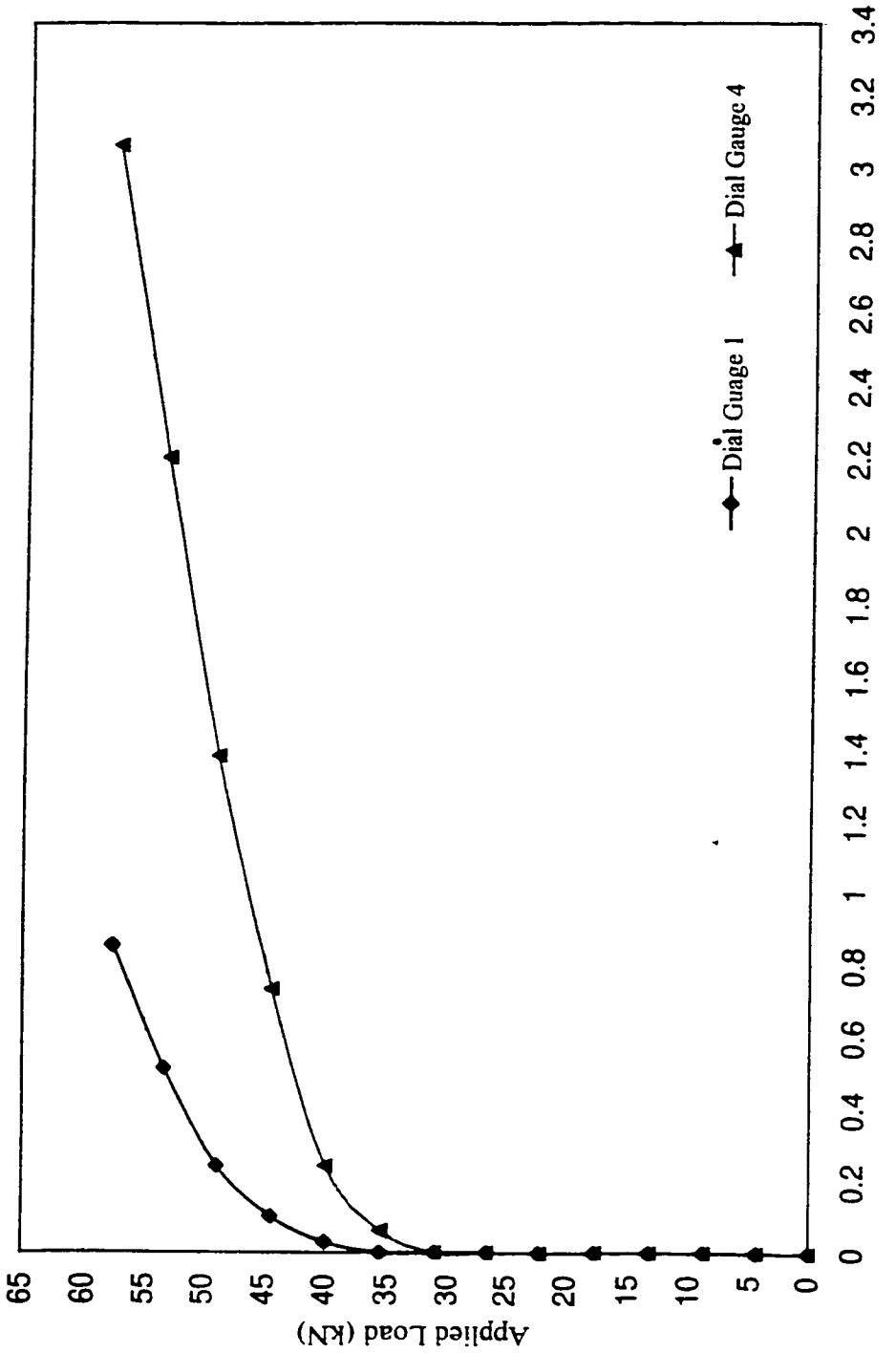

Figure H.9: Applied load vs. free-end slip of beam G2-D9.79-B24

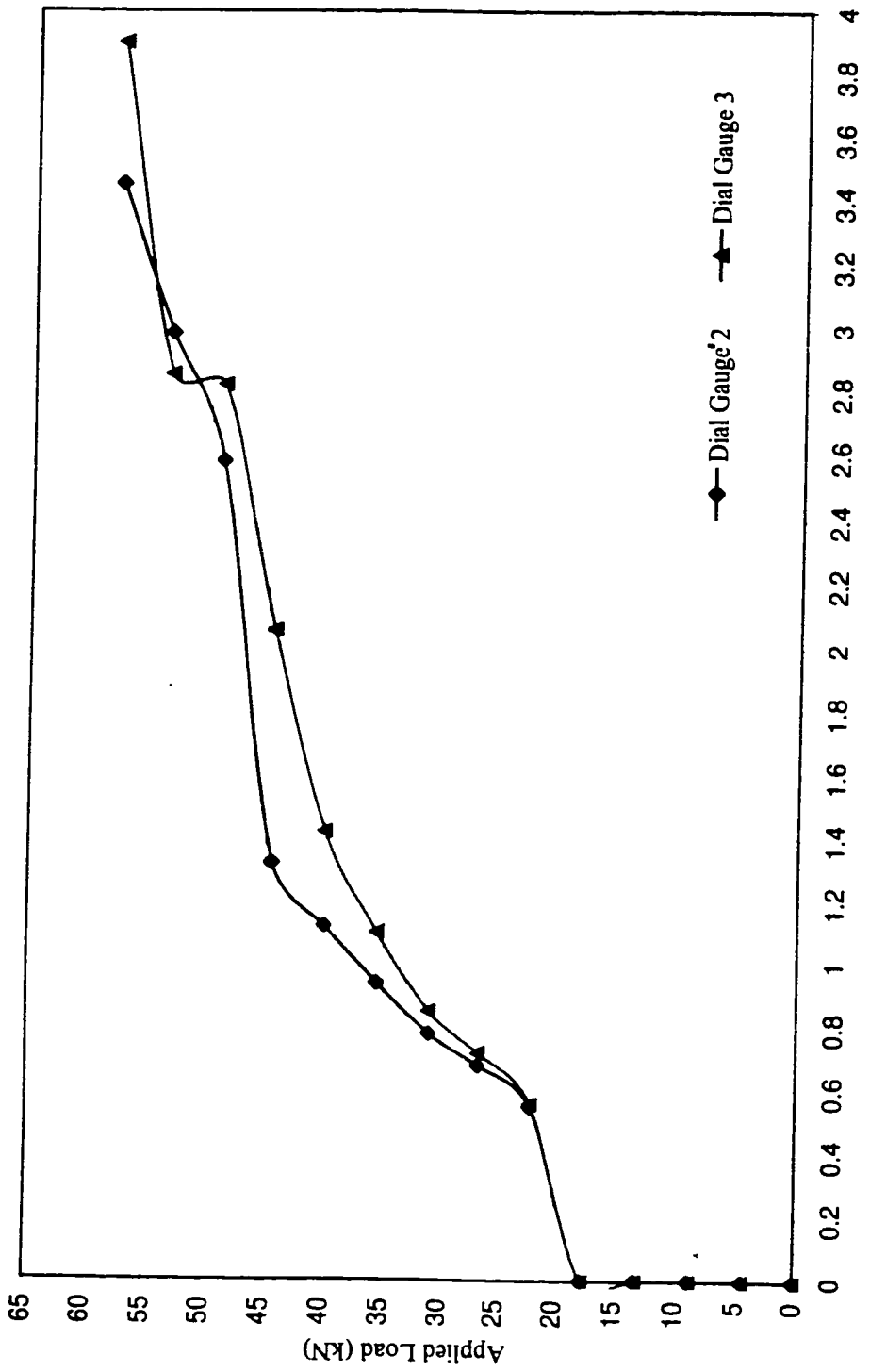

Figure H.10: Applied load vs. loaded-end slip of beam G2-D9.79-B24

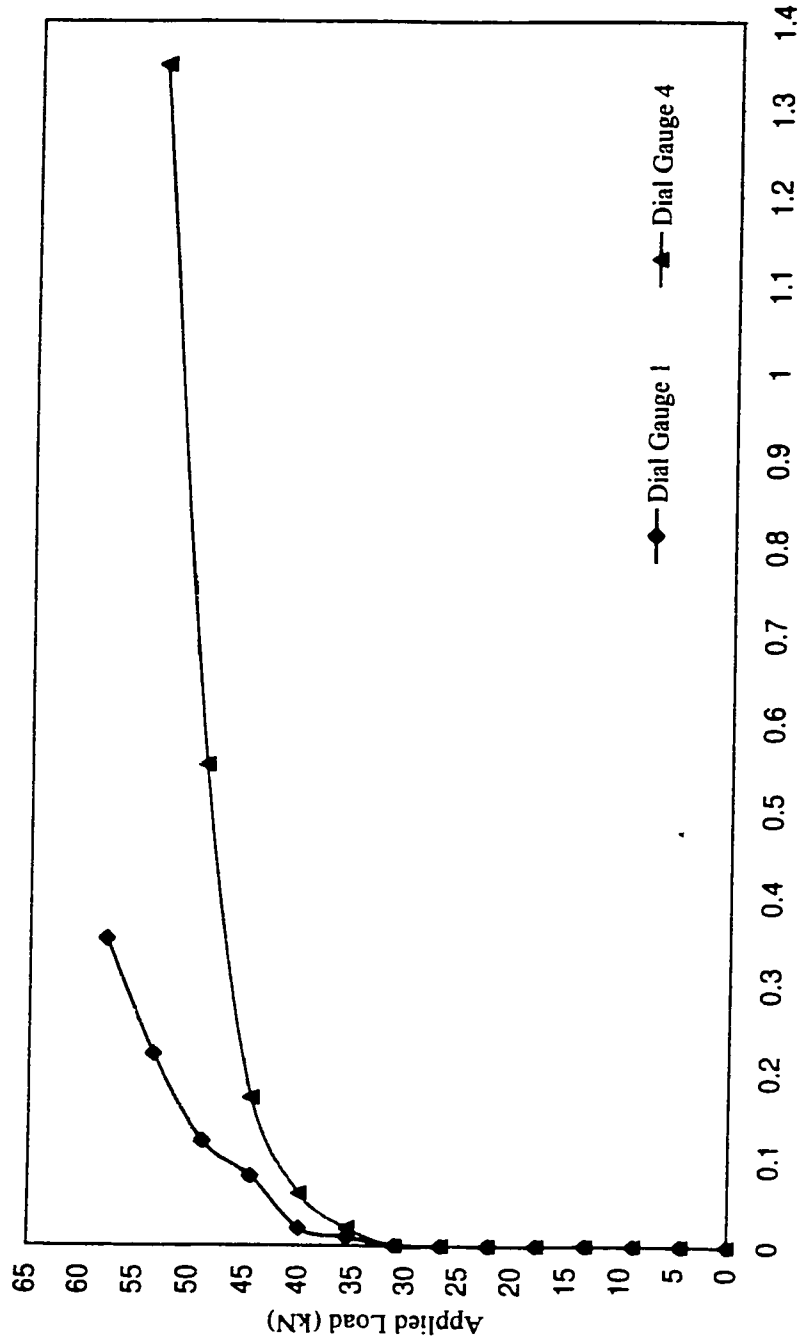

Figure H.11: Applied load vs. free-end slip of beam G2-D9.79-C24

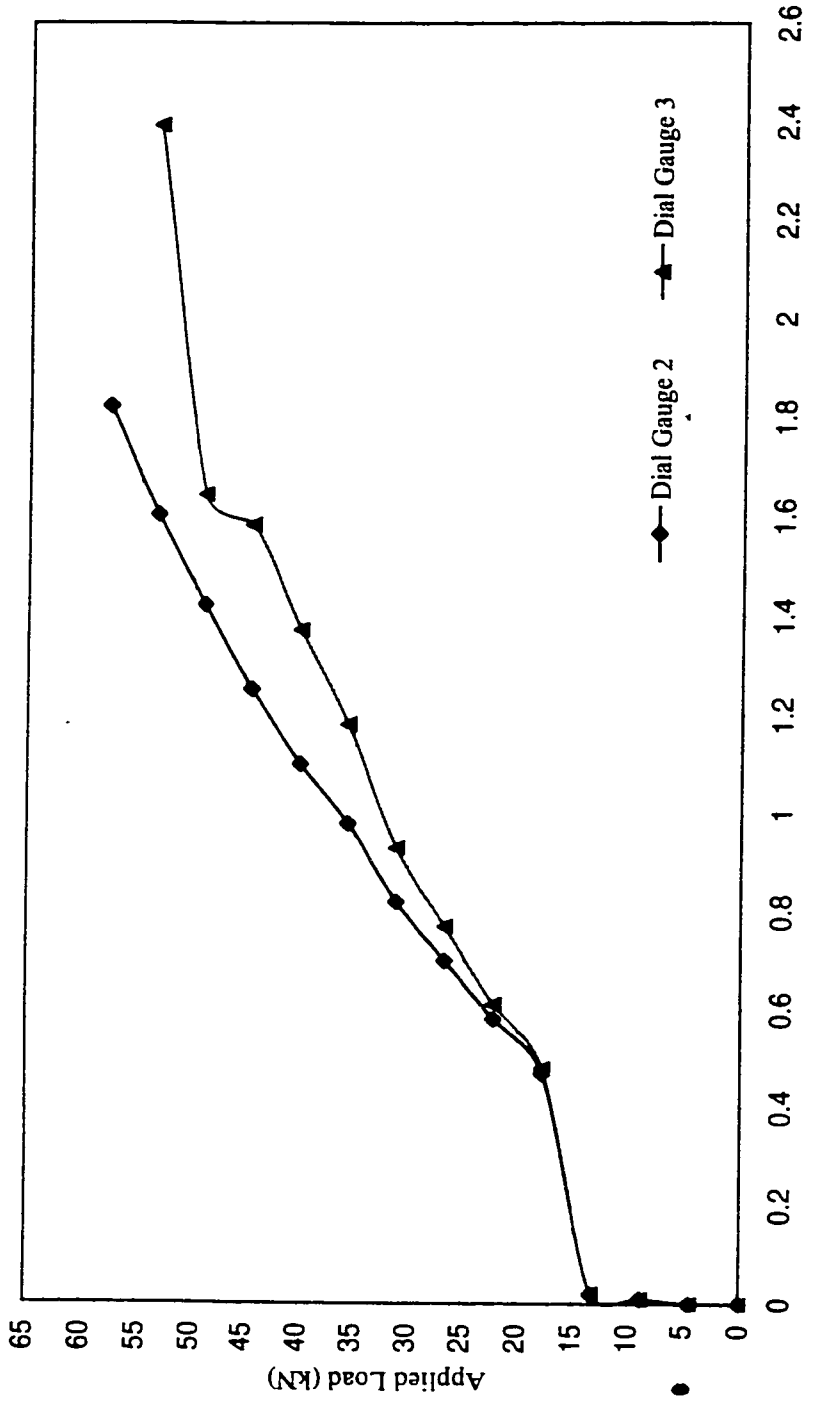

Figure H.12: Applied load vs. loaded-end slip of beam G2-D9.79-C24

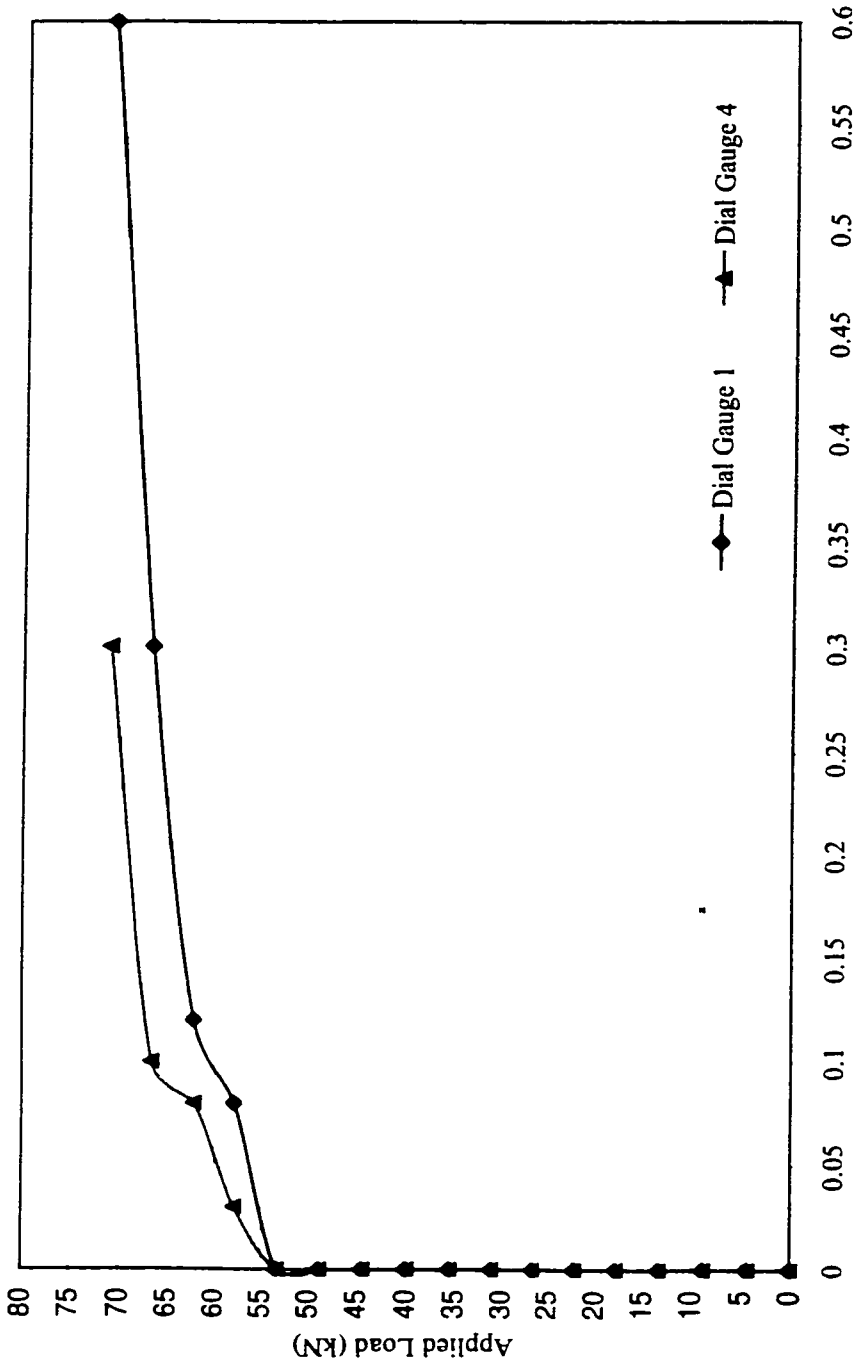

Figure H.13: Applied load vs. free-end slip of beam G2-D9.79-A30

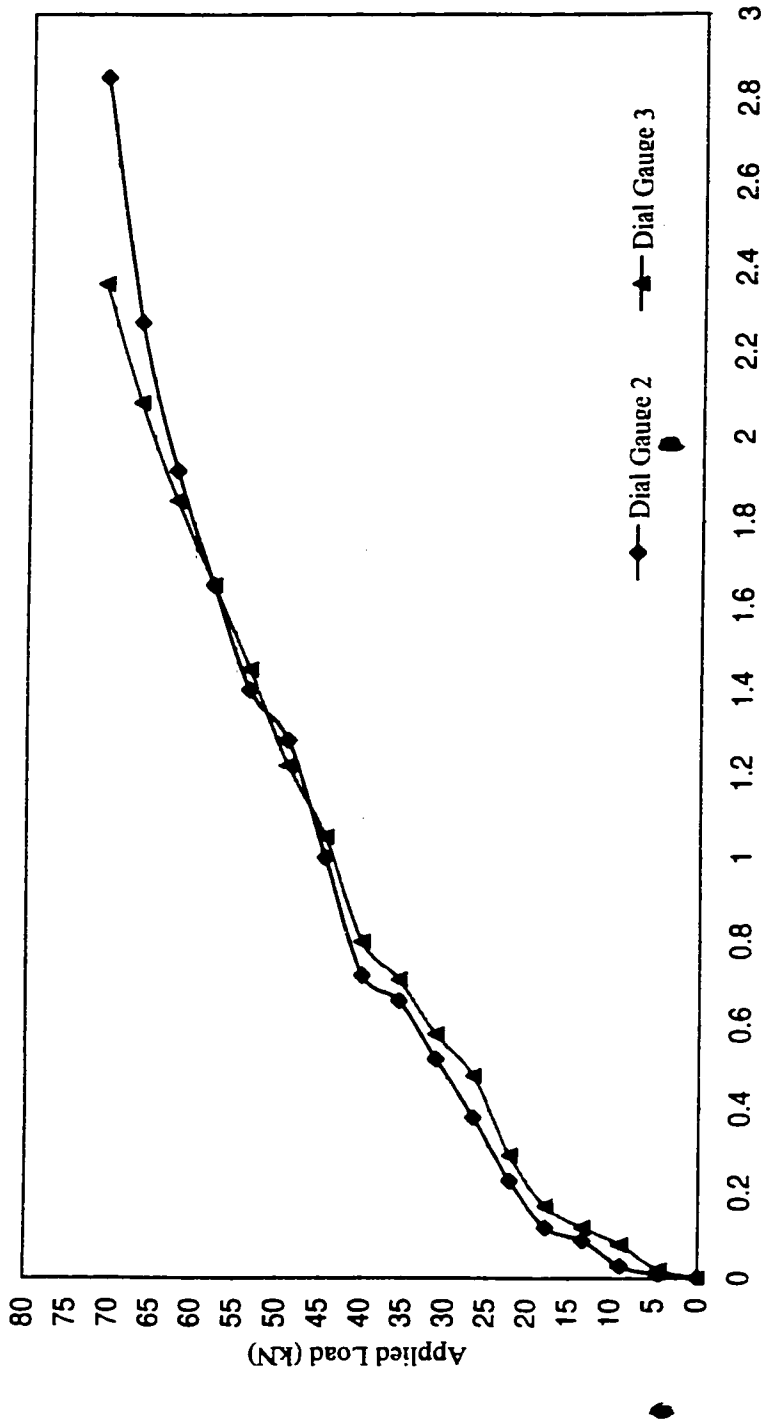

Figure H.14: Applied load vs. loaded-end slip of beam G2-D9.79-A30

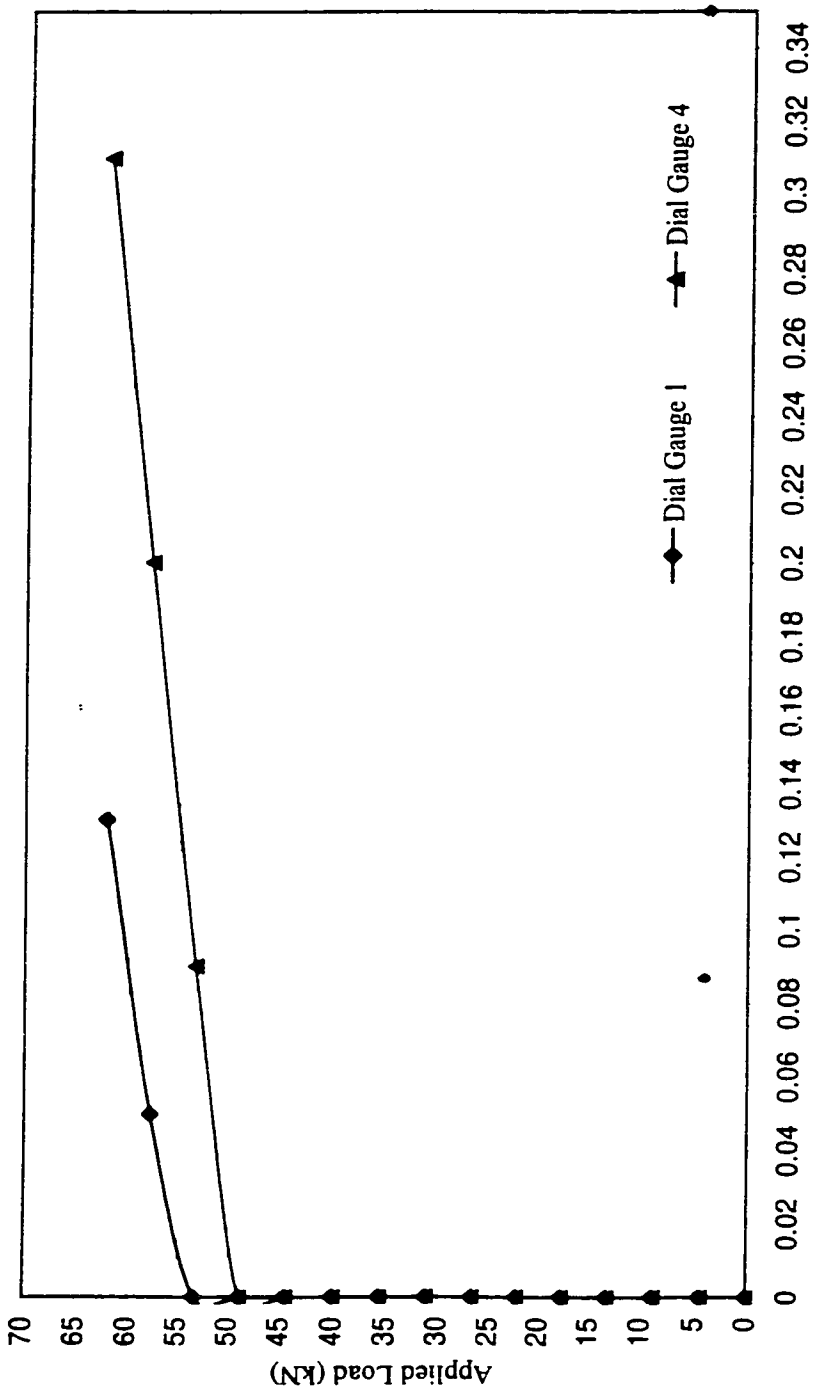

Figure H.15: Applied load vs. free-end slip of beam G2-D9.79-B30

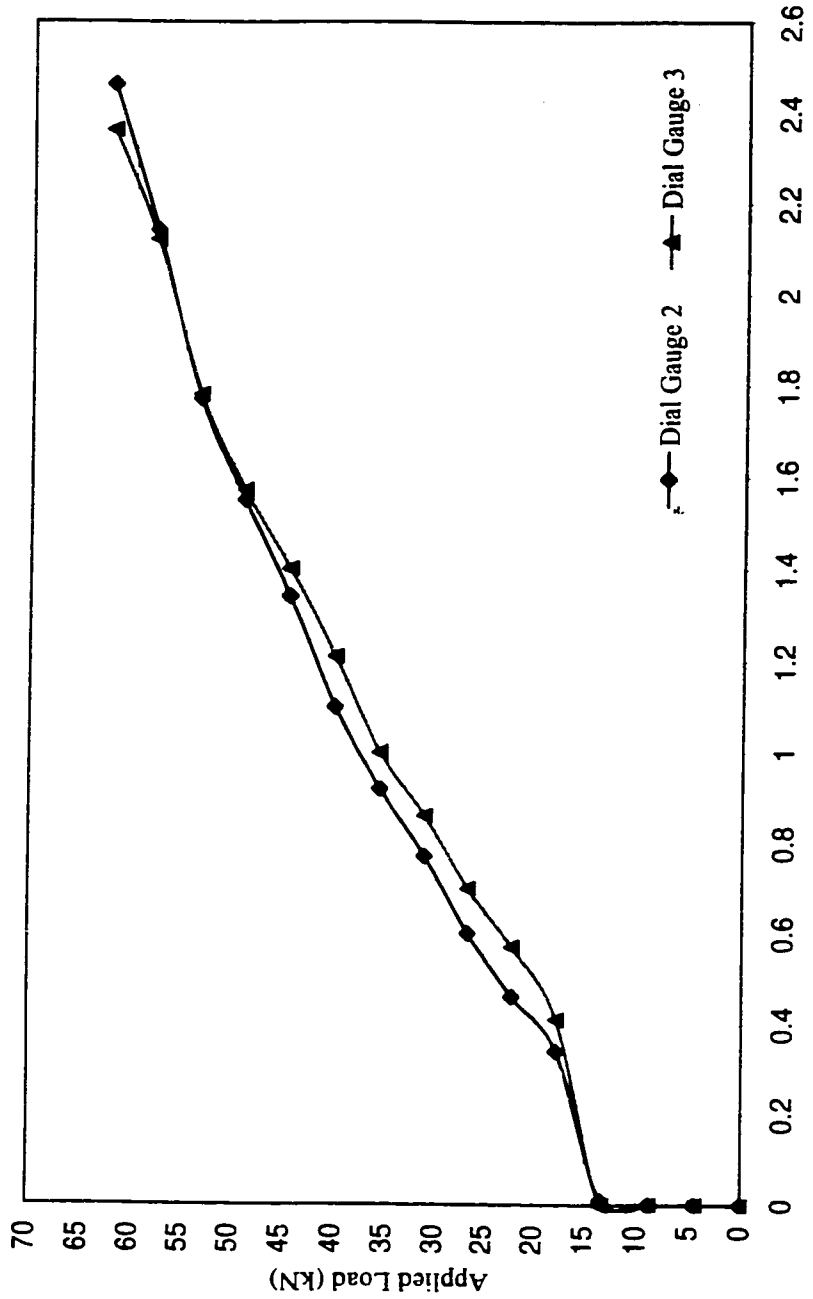

Figure H.16: Applied load vs. loaded-end slip of beam G2-D9.79-B30

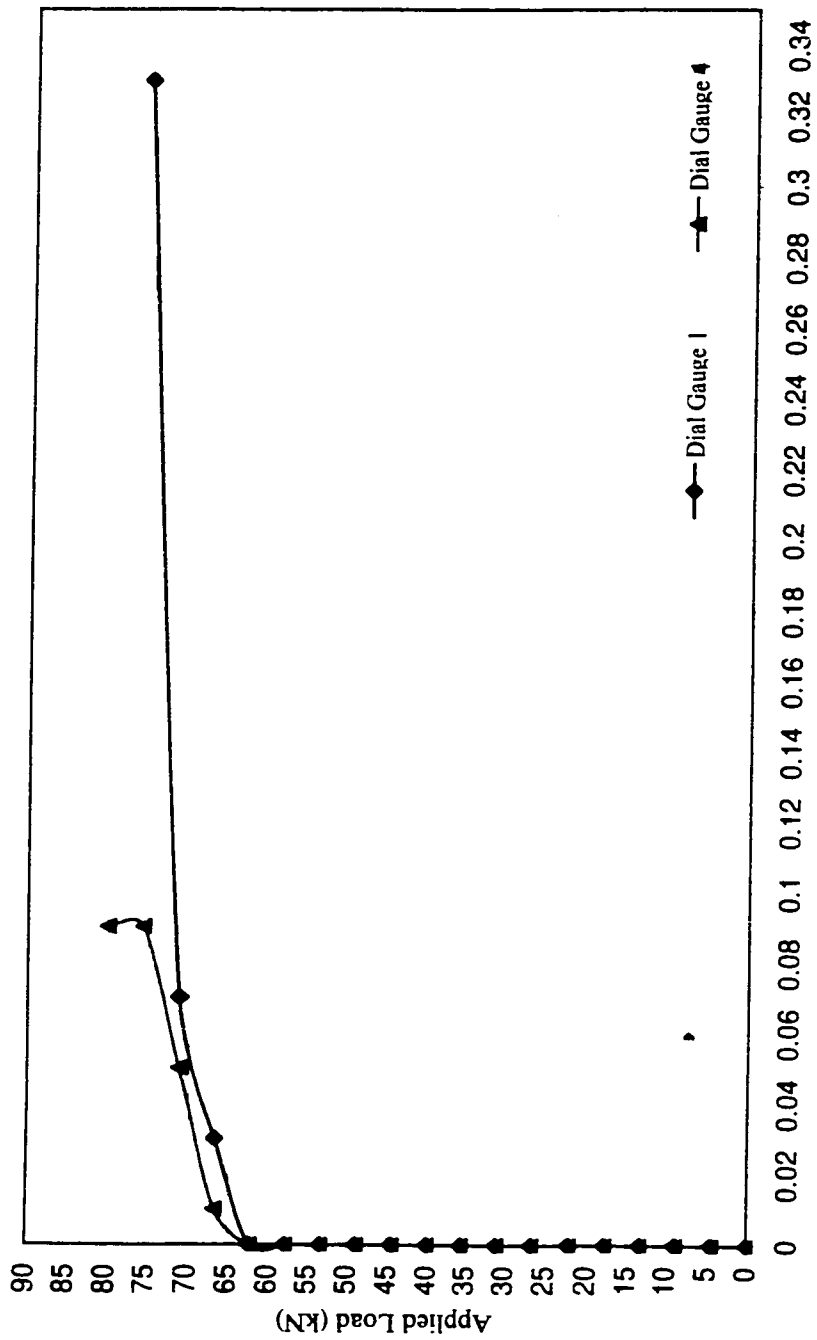

Figure H.17: Applied load vs. free-end slip of beam G2-D9.79-C30

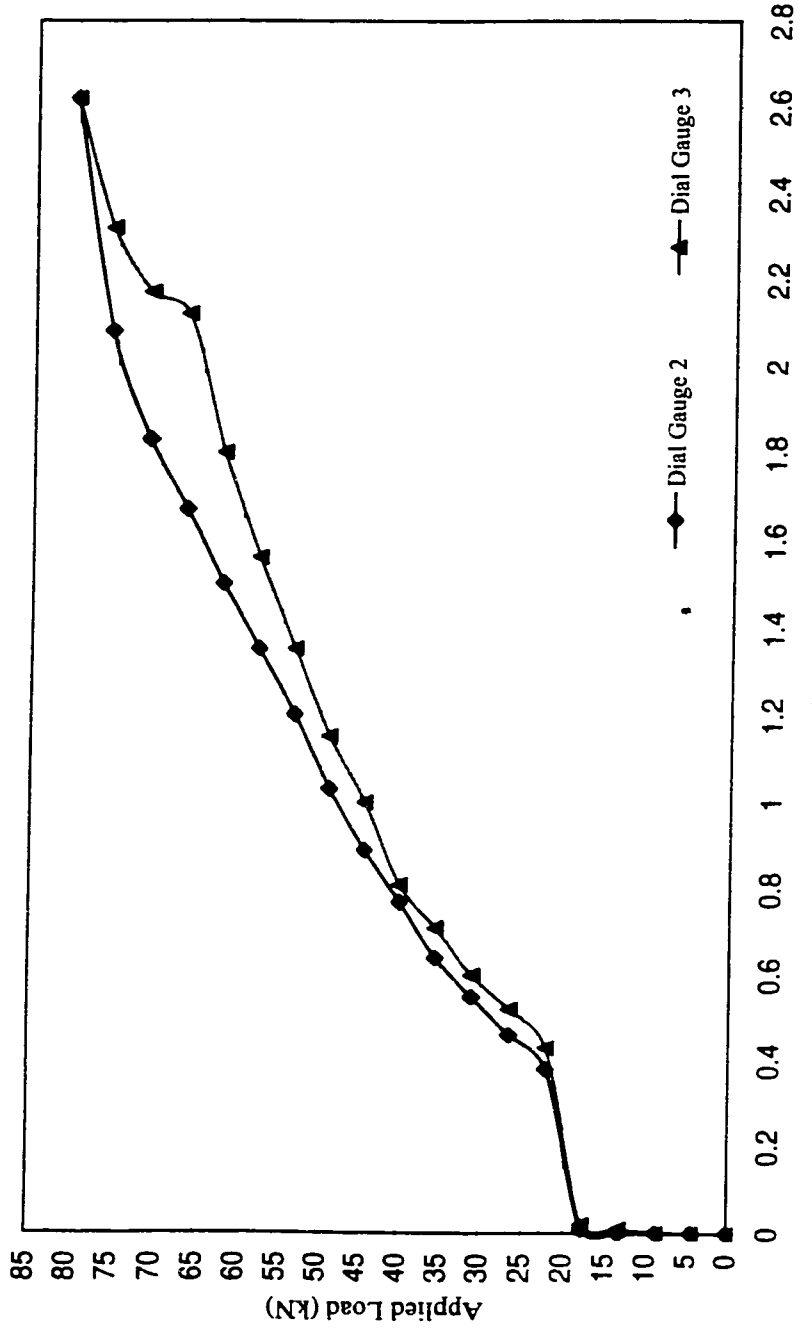

Figure H.18: Applied load vs. loaded-end slip of beam G2-D9.79-C30

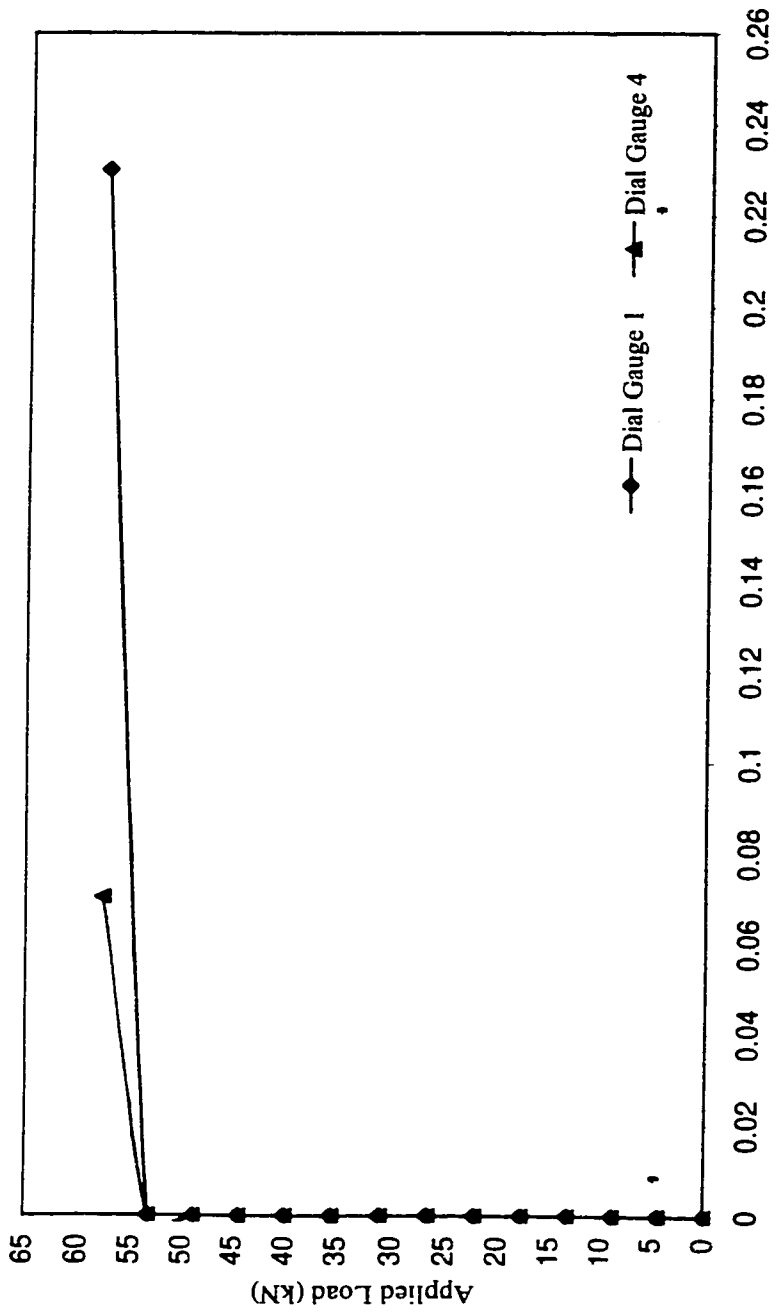

Figure H.19: Applied load vs. free-end slip of beam G2-D9.79-A36

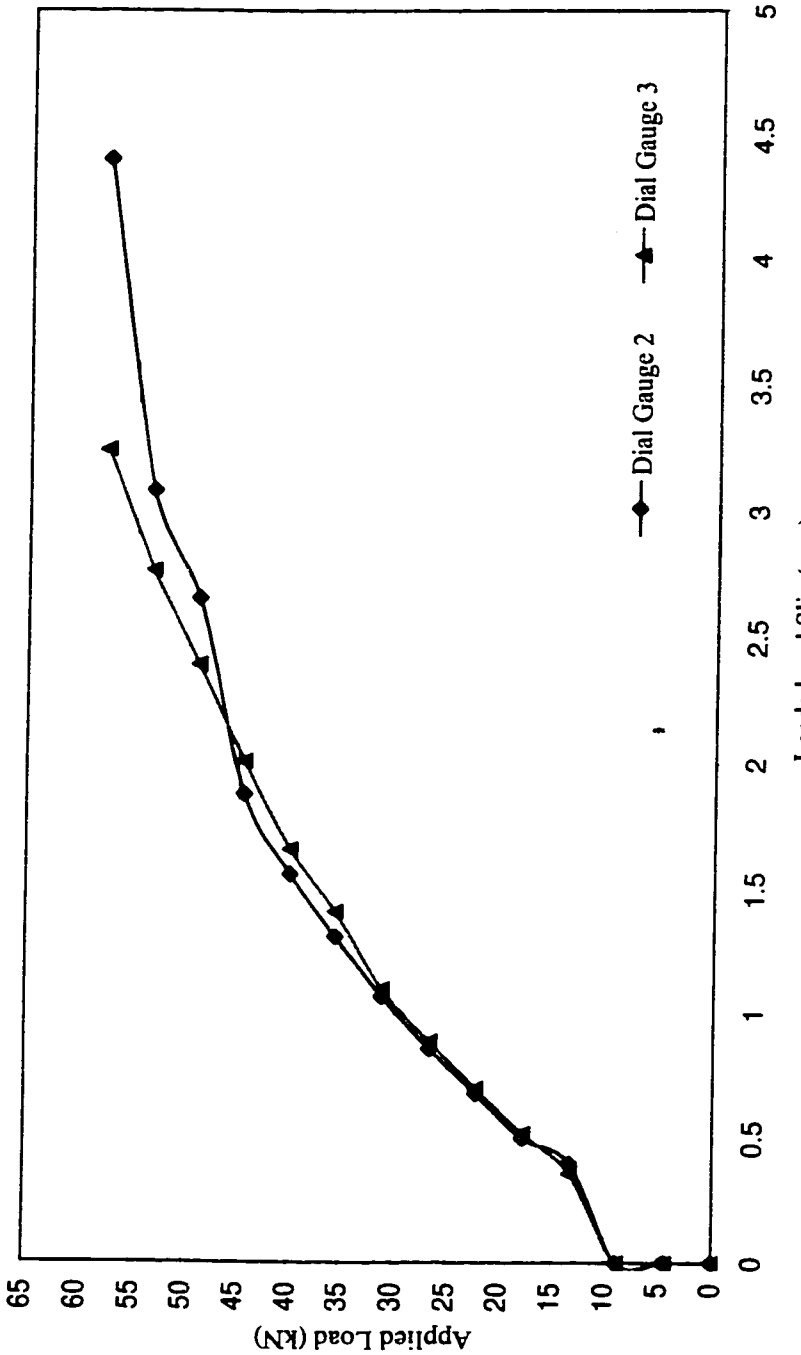

Figure H.20: Applied load vs. loaded-end slip of beam G2-D9.79-A36

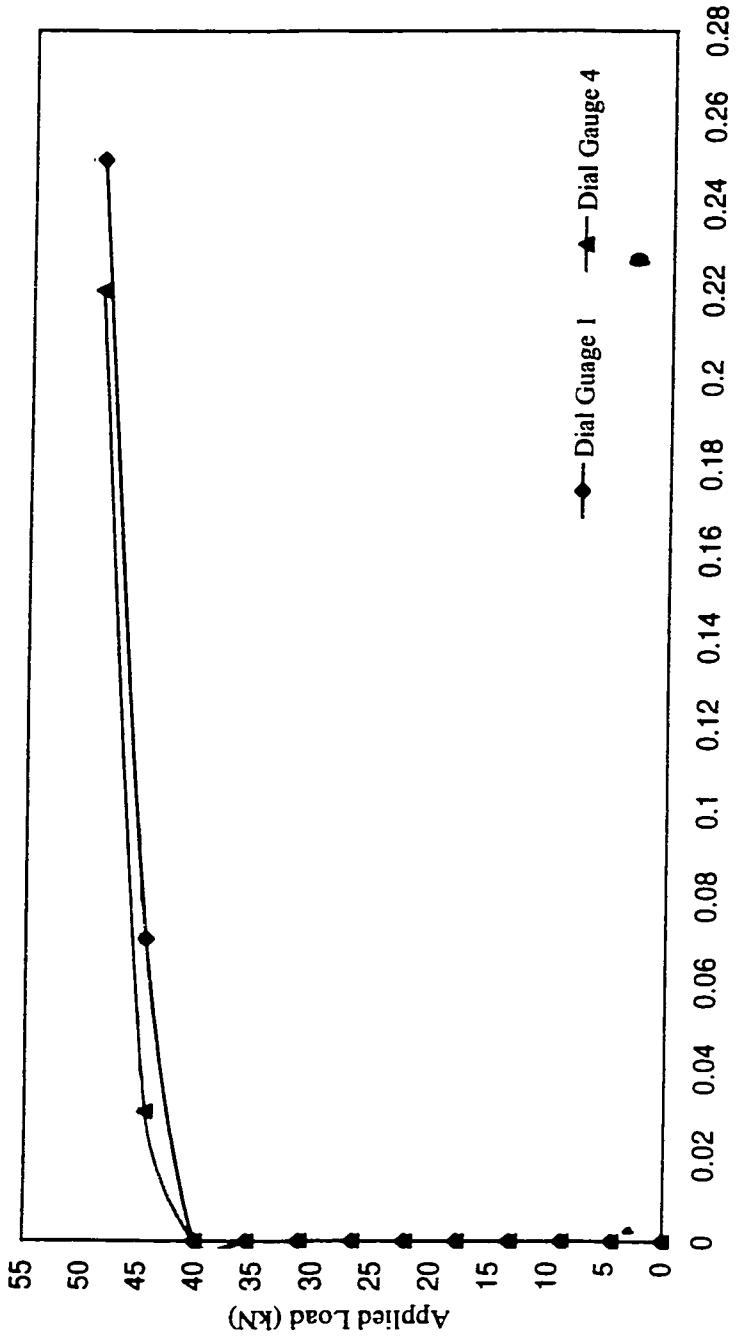

Figure H.21: Applied load vs. free-end slip of beam G2-D9.79-B36

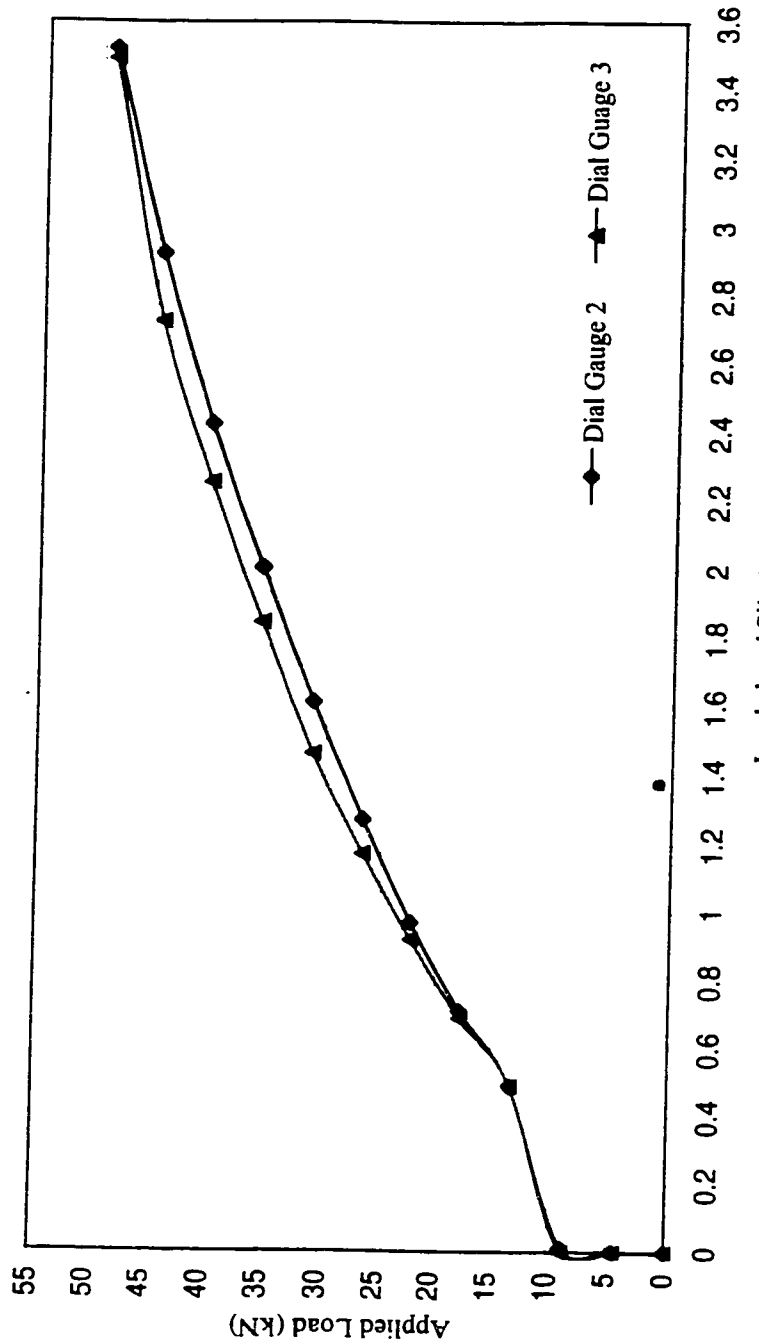

Figure H.22: Applied load vs. loaded-end slip of beam G2-D9.79-B36

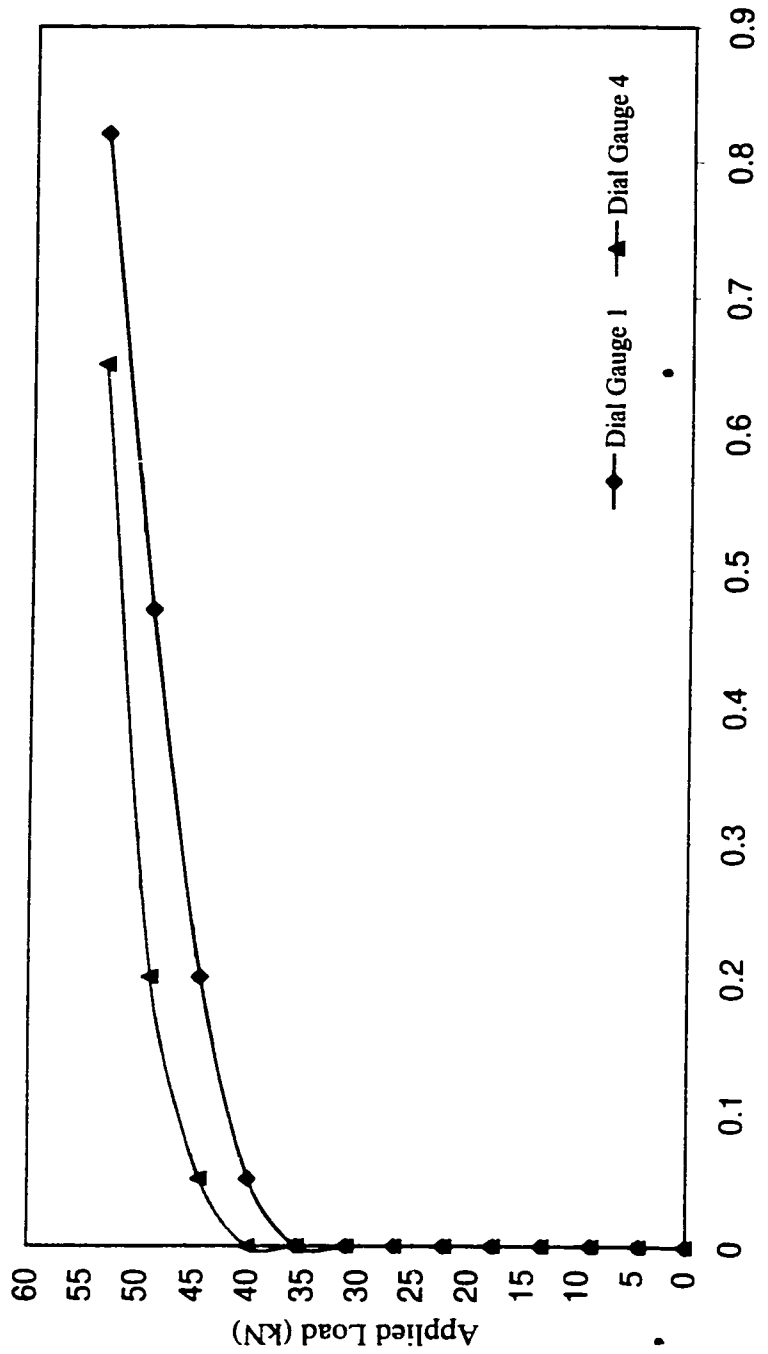

Figure H.23: Applied load vs. free-end slip of beam G2-D0.79-C36

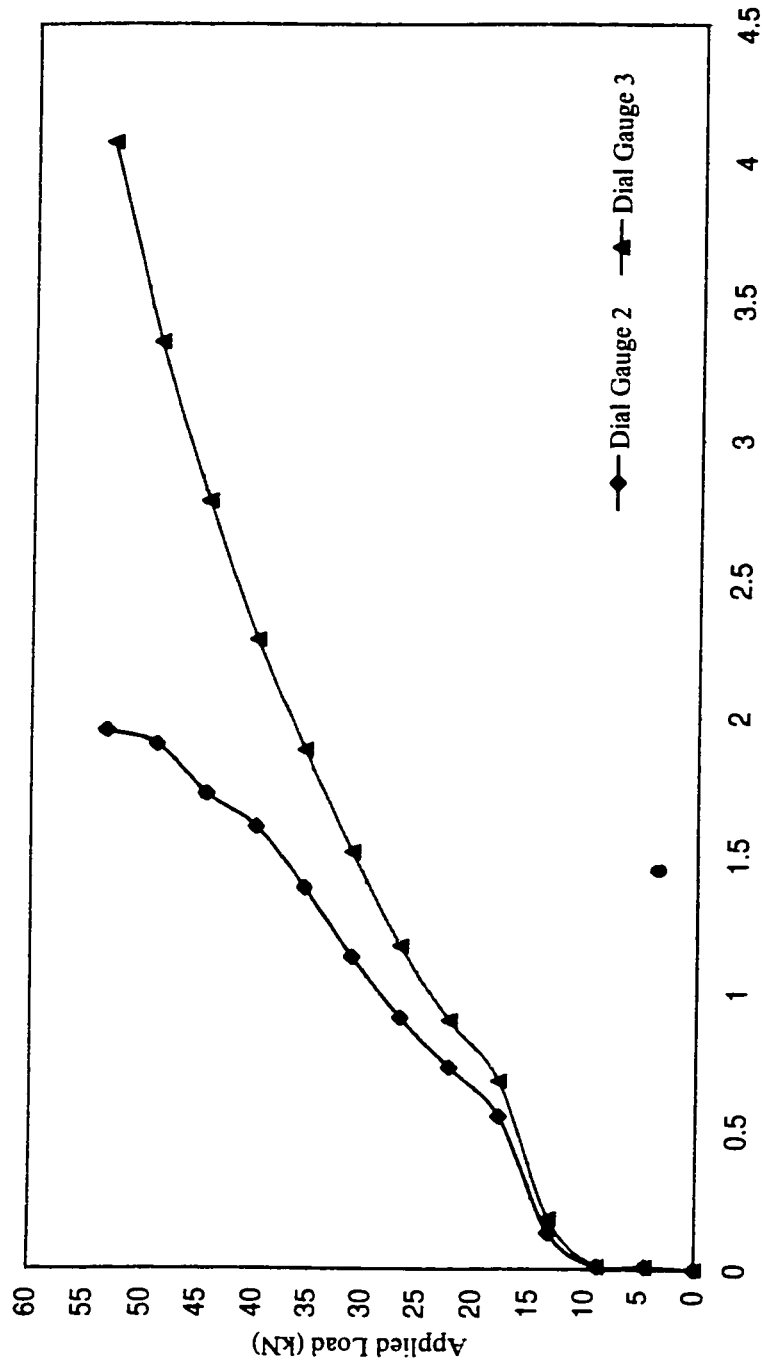

Figure H.24: Applied load vs. loaded-end slip of beam G2-D9.79-C36

Appendix I

Applied Load vs. Slip Curve (D1-D9.70 Bar)

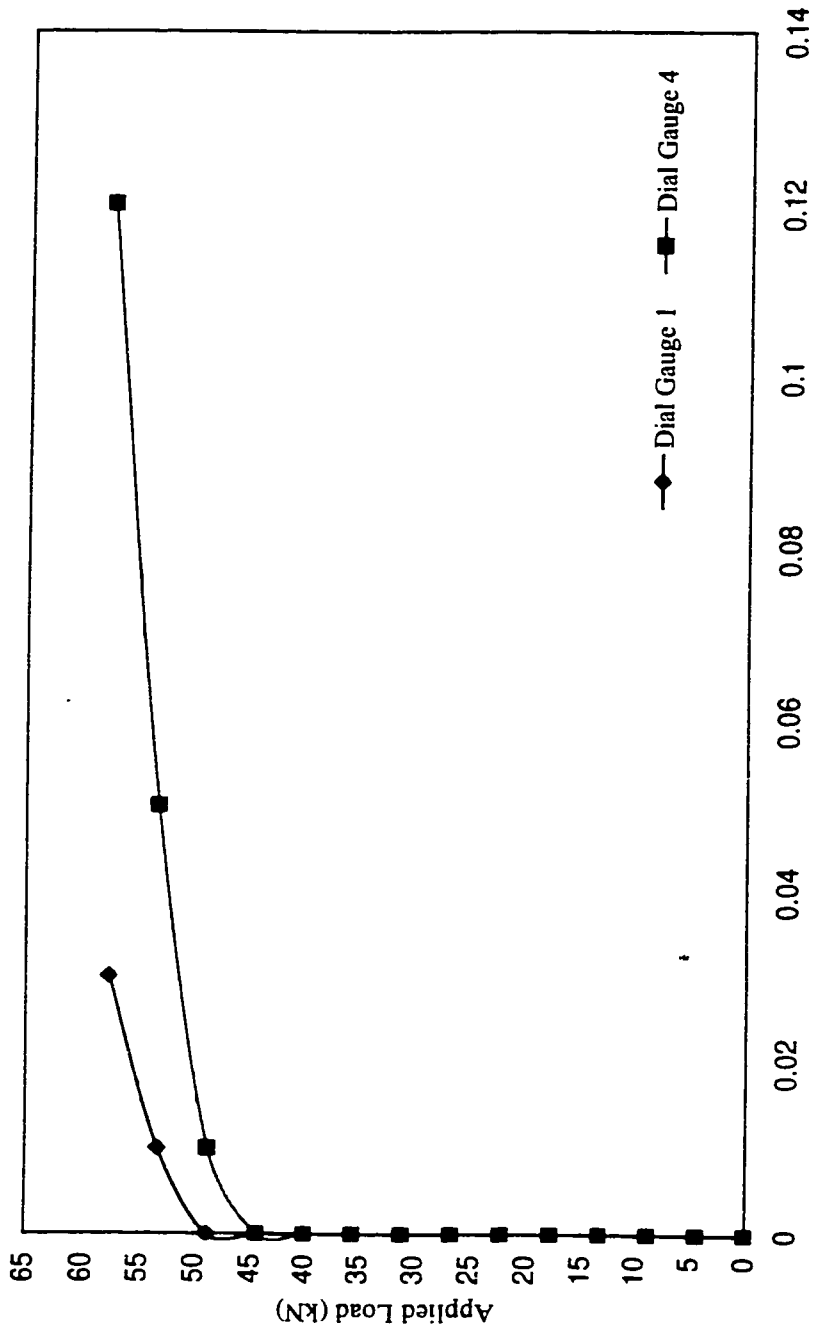

Figure I.1: Applied load vs. free-end slip of beam D1-D9.70-A12

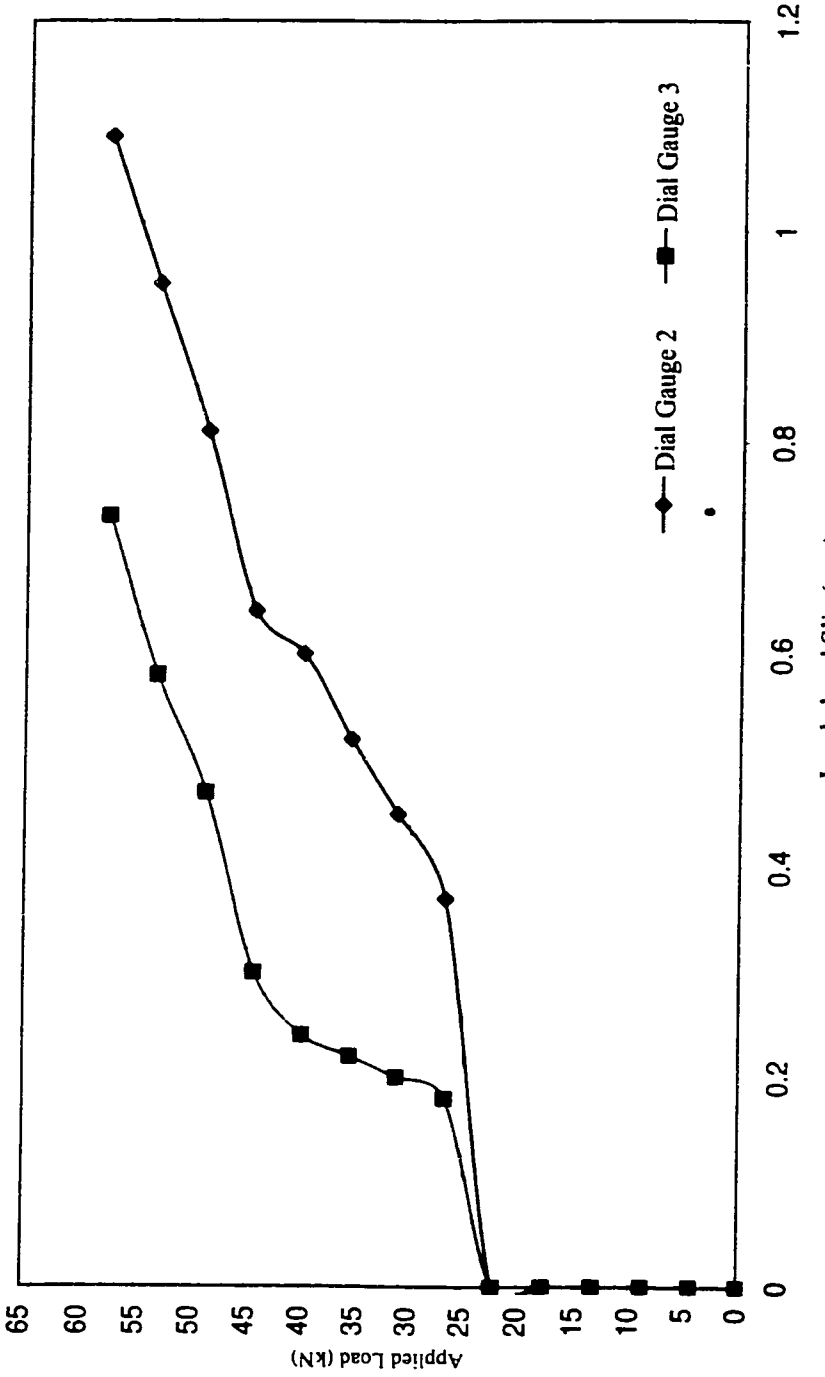

Figure I.2: Applied vs. loaded-end slip of beam D1-D9.70-A12

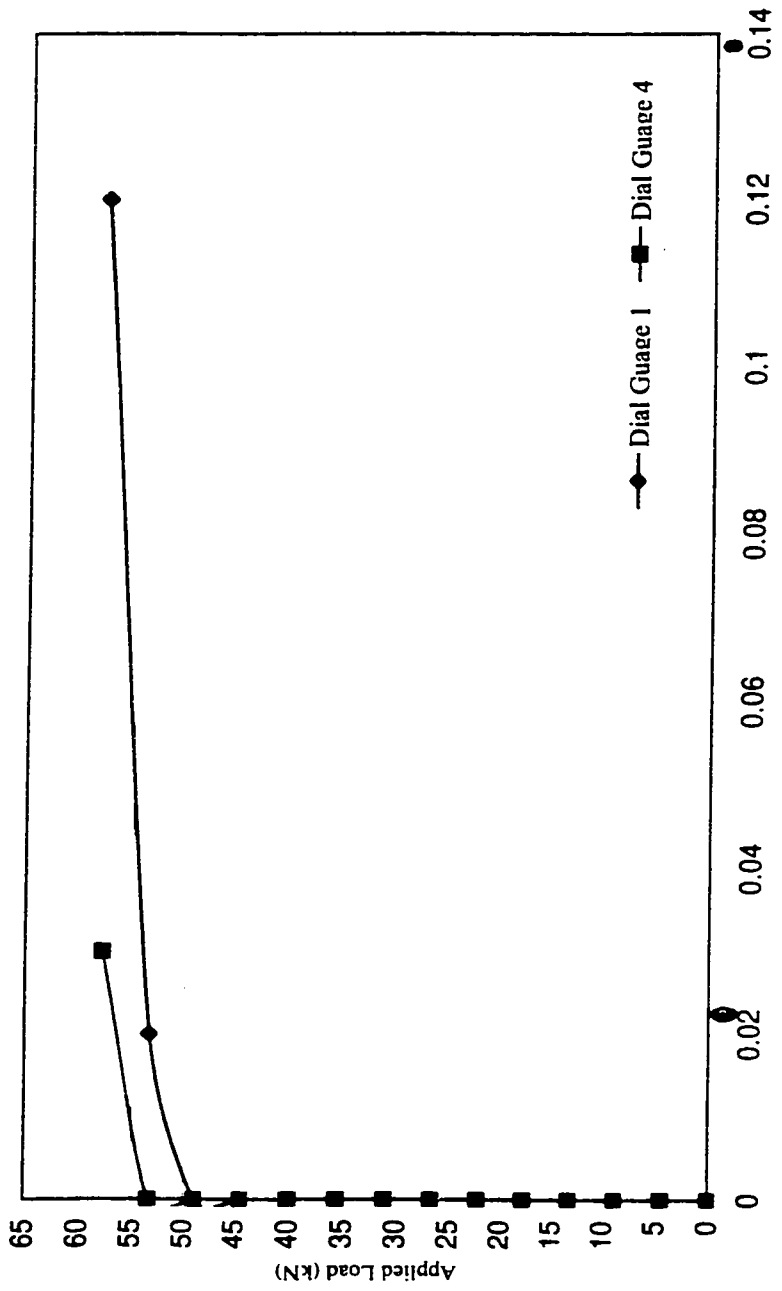

Figure I.3: Applied load vs. free-end slip of beam D1-D9.70-B12

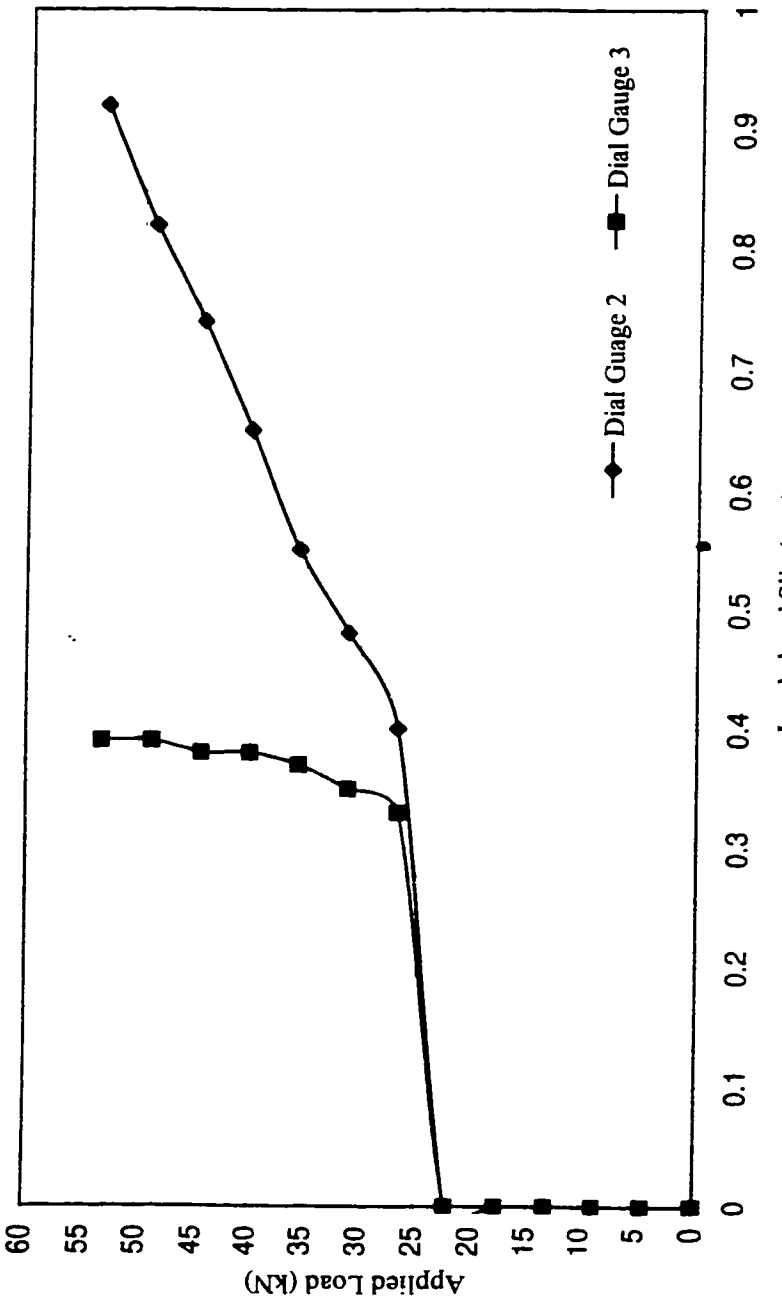

Figure I.4: Applied load vs. loaded-end slip of beam D1-D9.70-B12

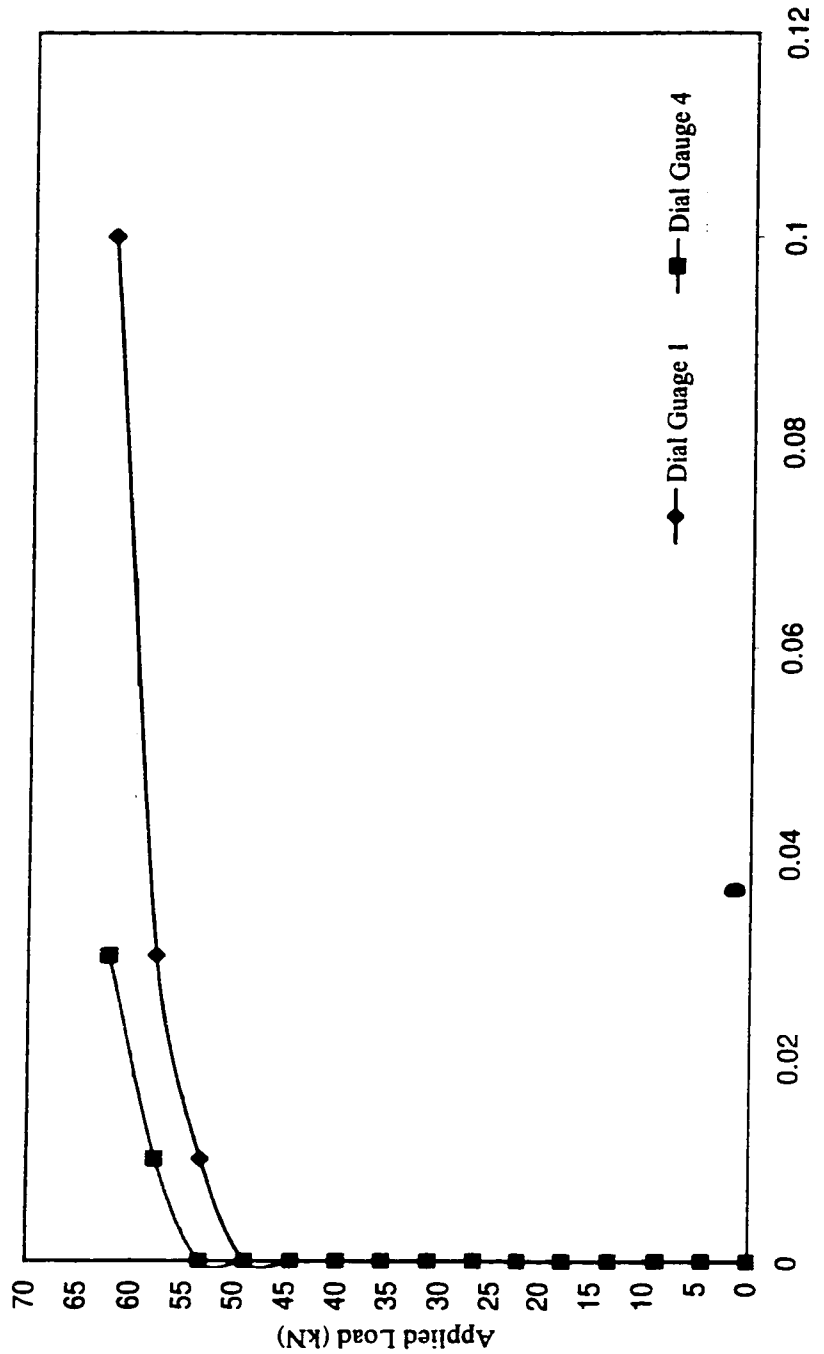

Figure I.5: Applied load vs. free-end slip of beam D1-D9.70-C12

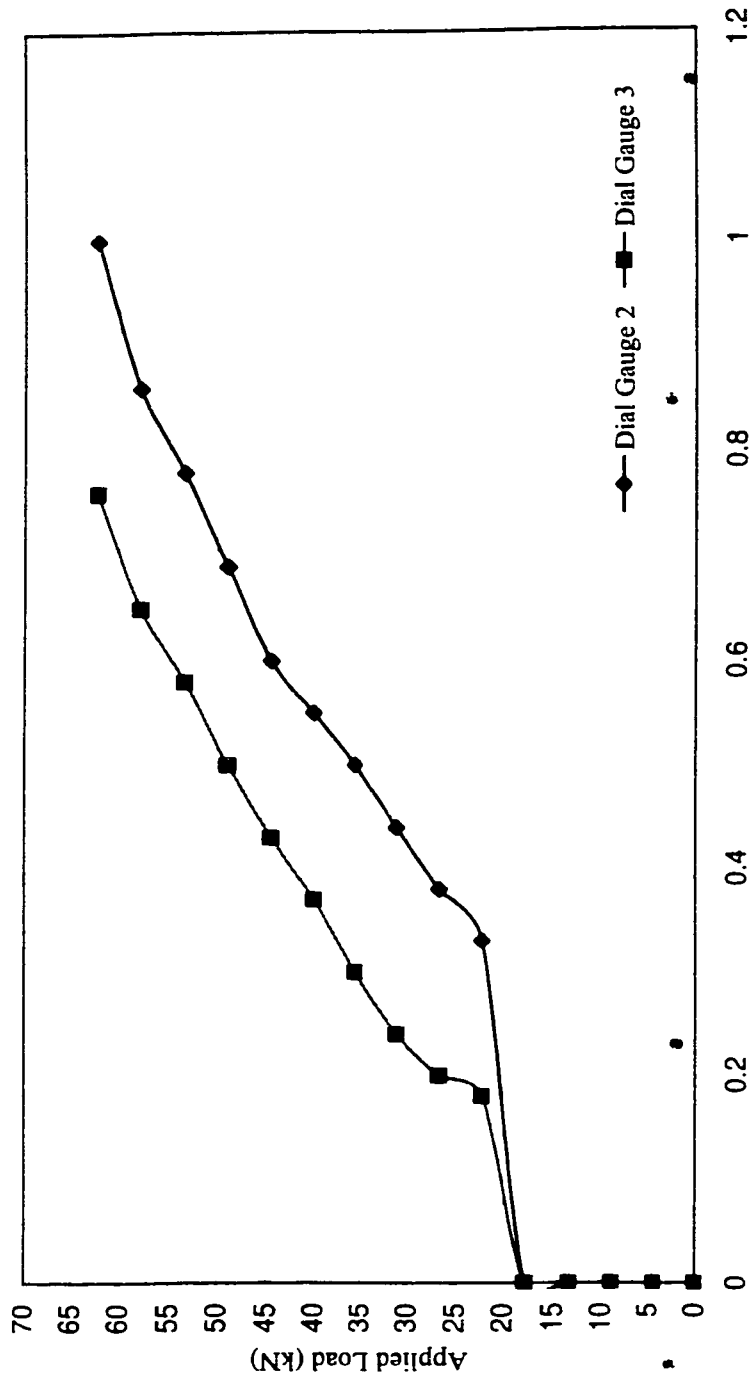

Figure I.6: Applied load vs. loaded-end slip of beam D1-D9.70-C12

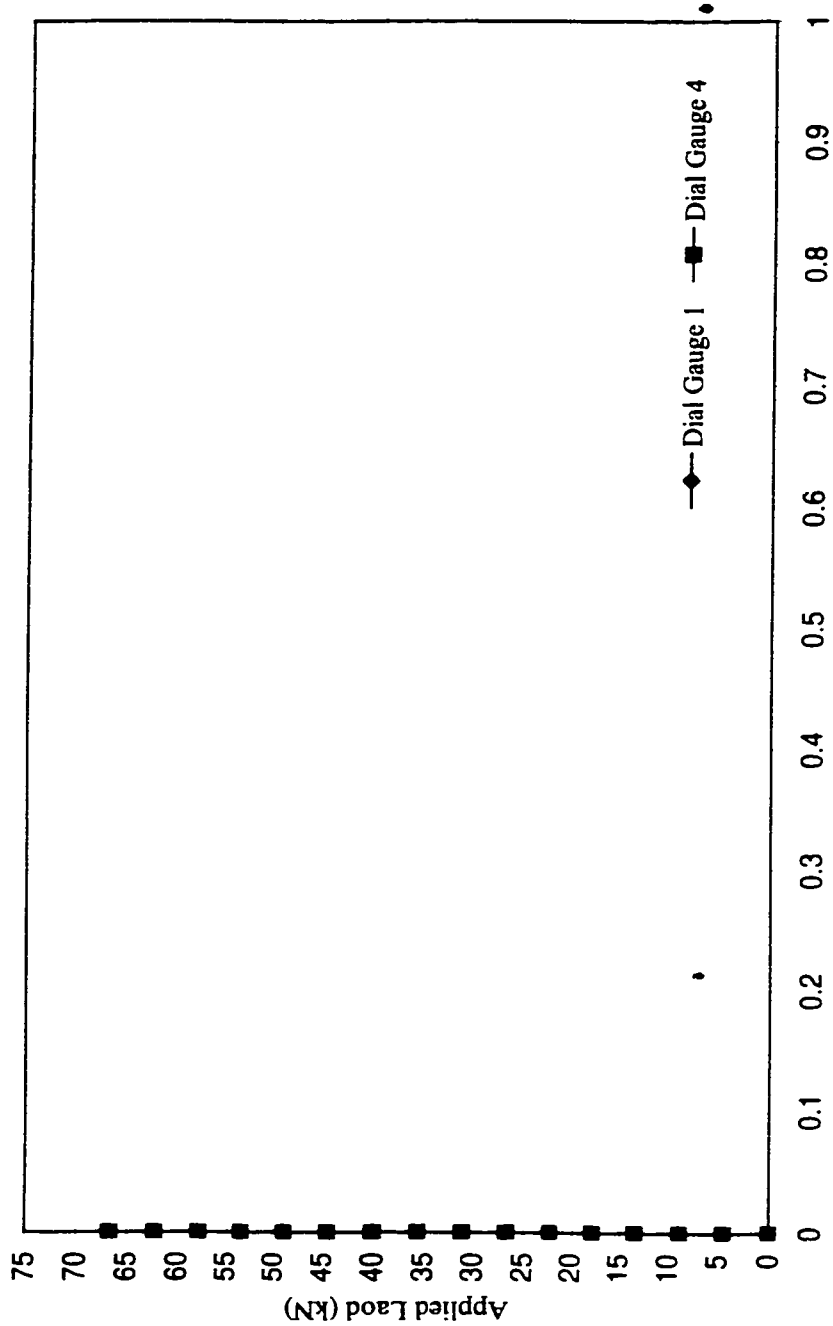

Figure I.7: Applied load vs. free-end slip of beam D1-D9.70-A18

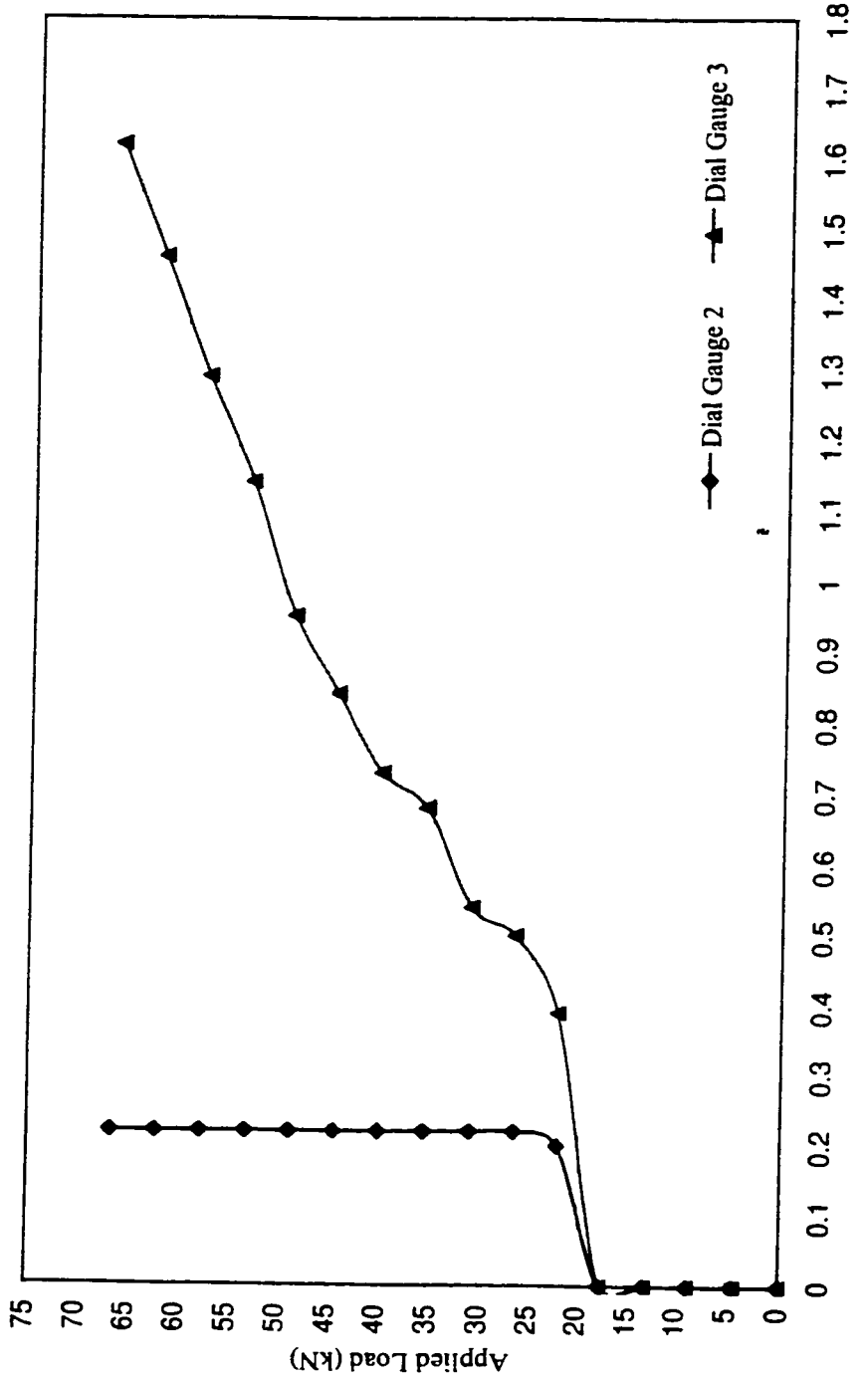

Figure I.8: Applied load vs. loaded-end slip of beam D1-D9.70-A18

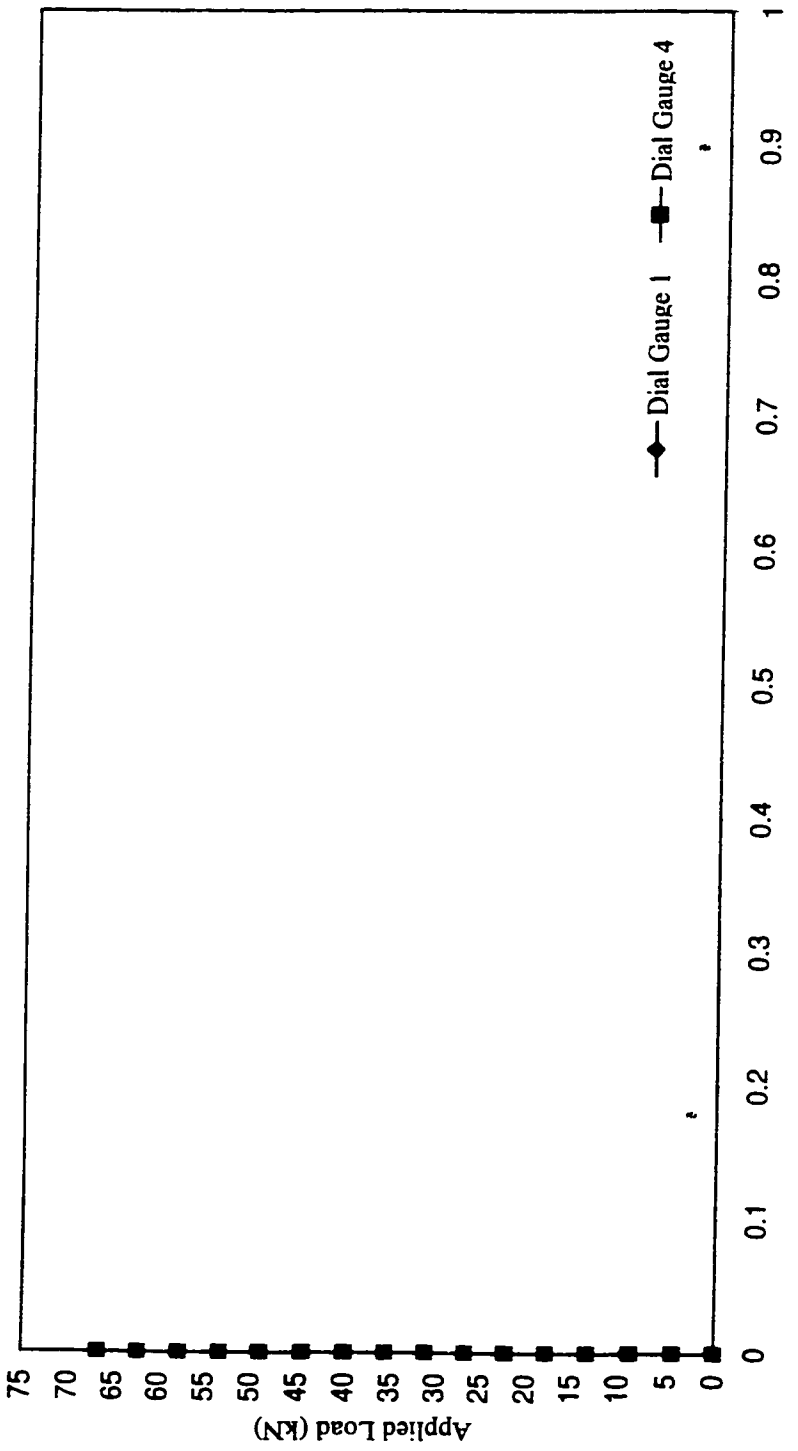

Figure I.9: Applied load vs. free-end slip of beam D1-D9.70-B18

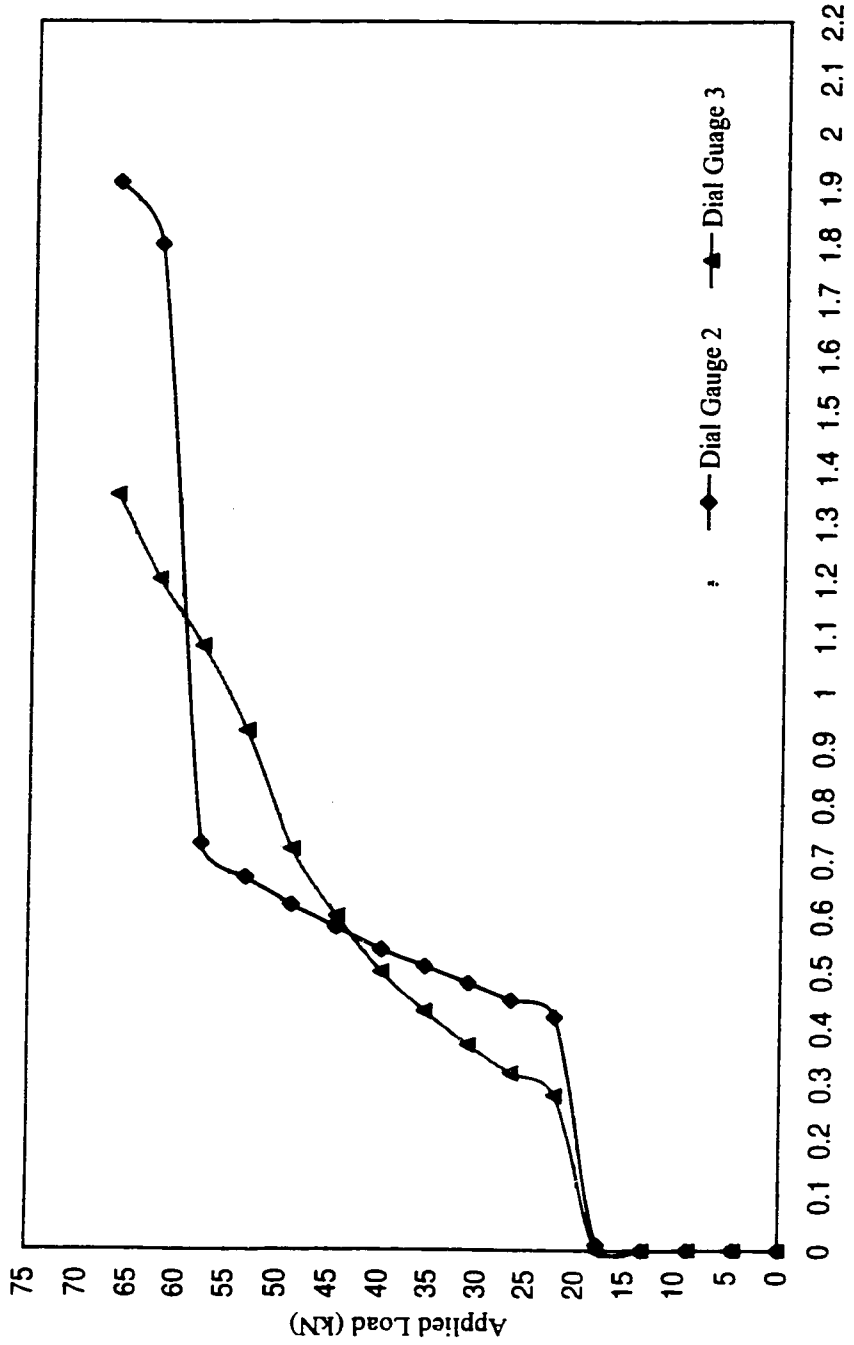

Figure I.10: Applied load vs. loaded-end slip of beam D1-D9.70-B18

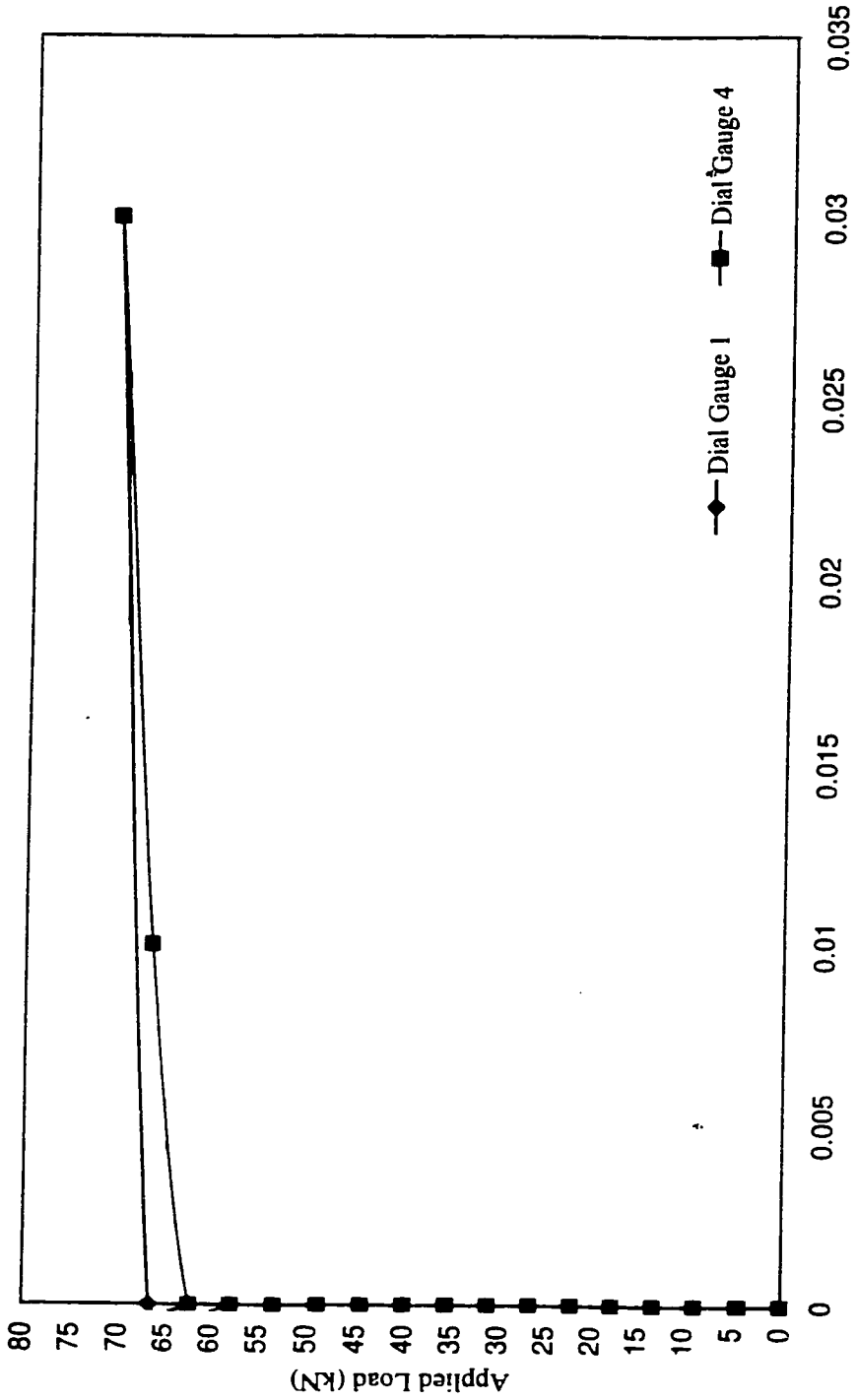

Figure I.11: Applied load vs. free-end slip of beam D1-D9.70-C18

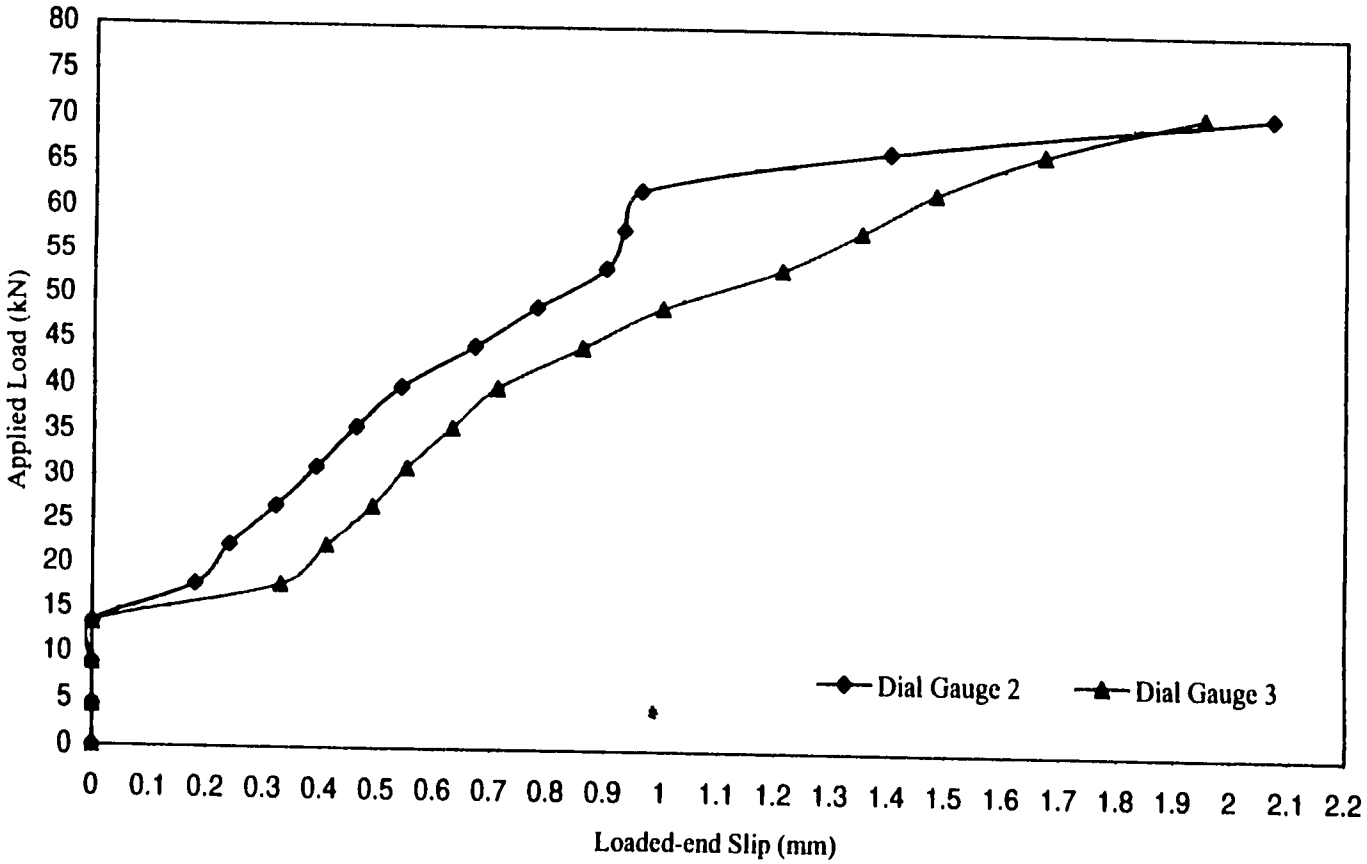

Figure I.12: Applied load vs. loaded-end slip of beam D1-D9.70-C18

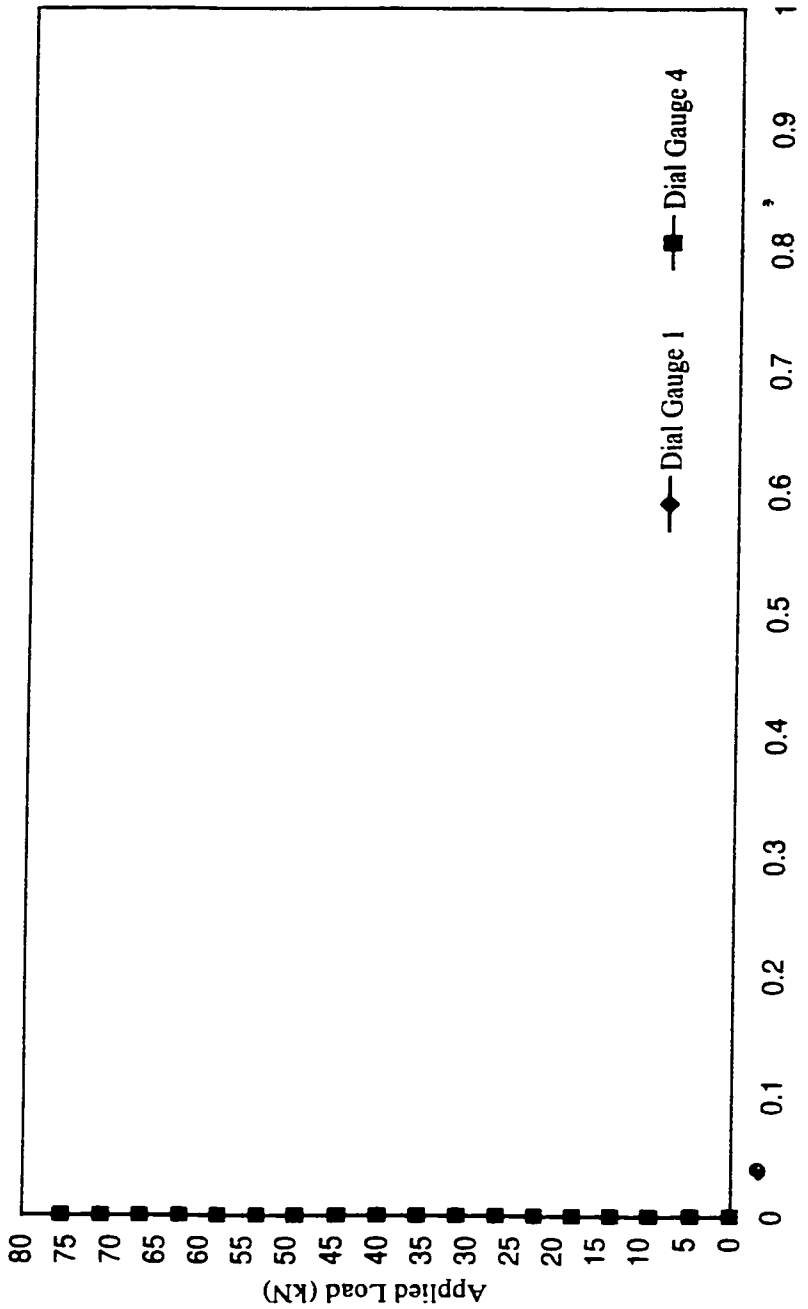

Figure I.13: Applied load vs. free-end slip of beam D1-D9.70-A24

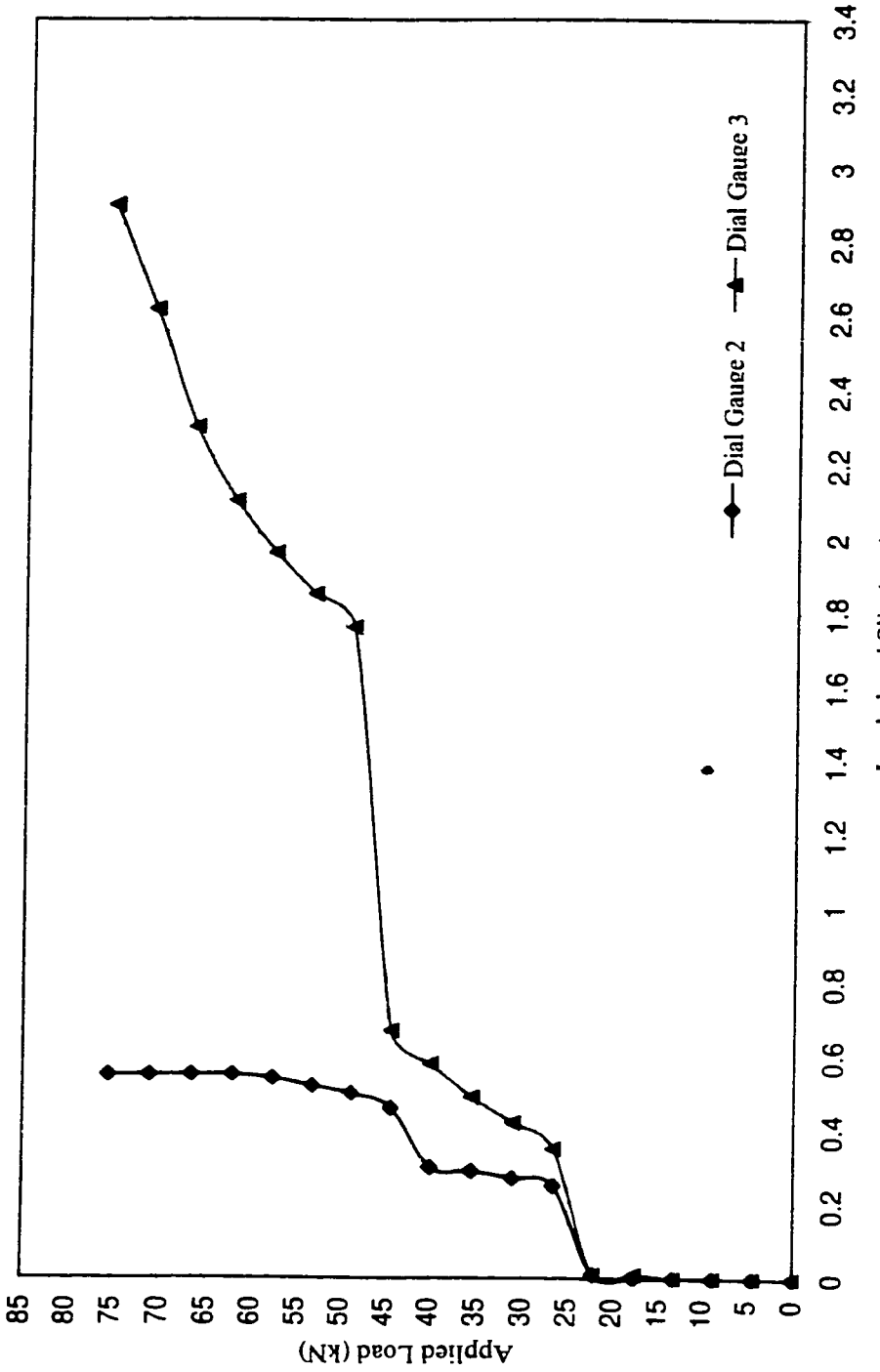

Figure I.14: Applied load vs. loaded-end slip of beam D1-D9.70-A24

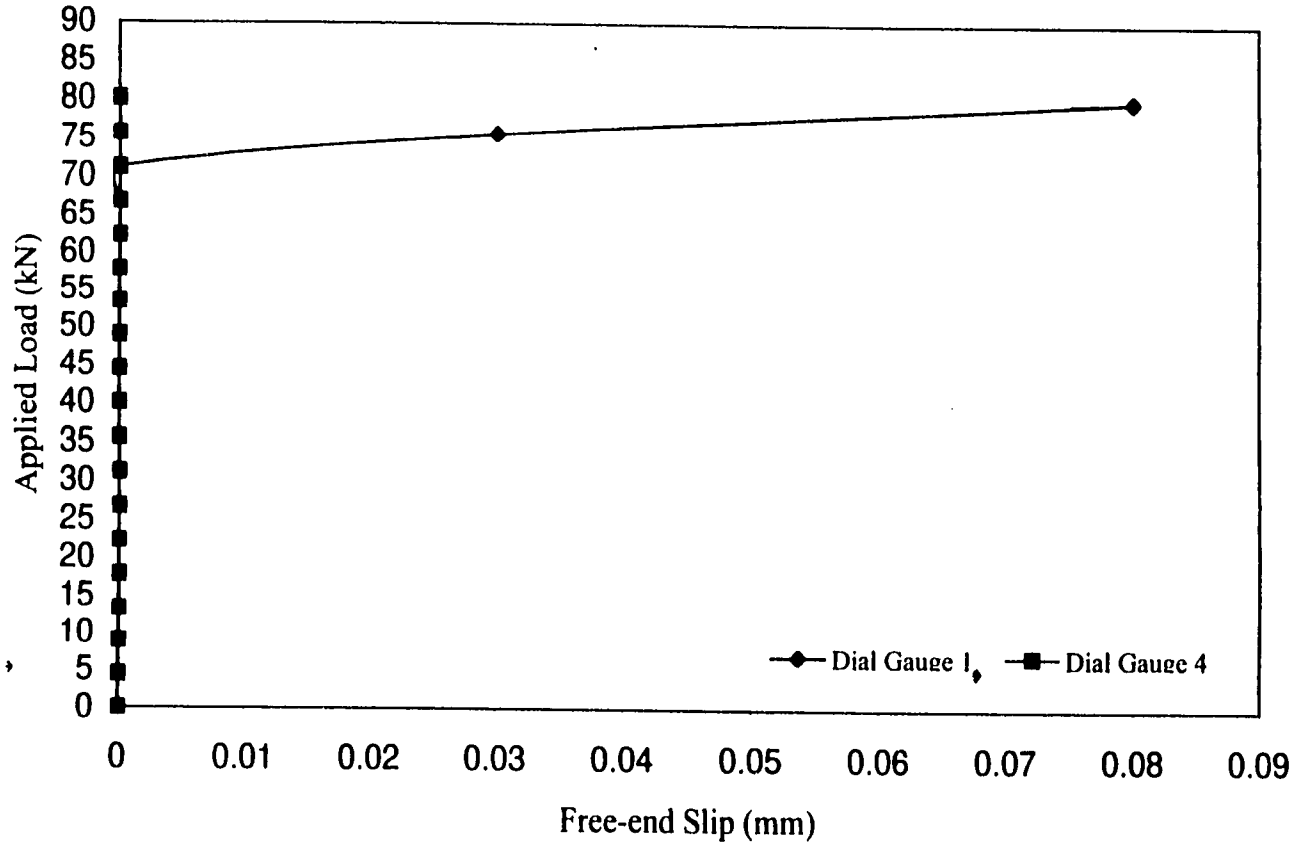

Figure I.15: Applied vs. free-end slip of beam D1-D9.70-B24

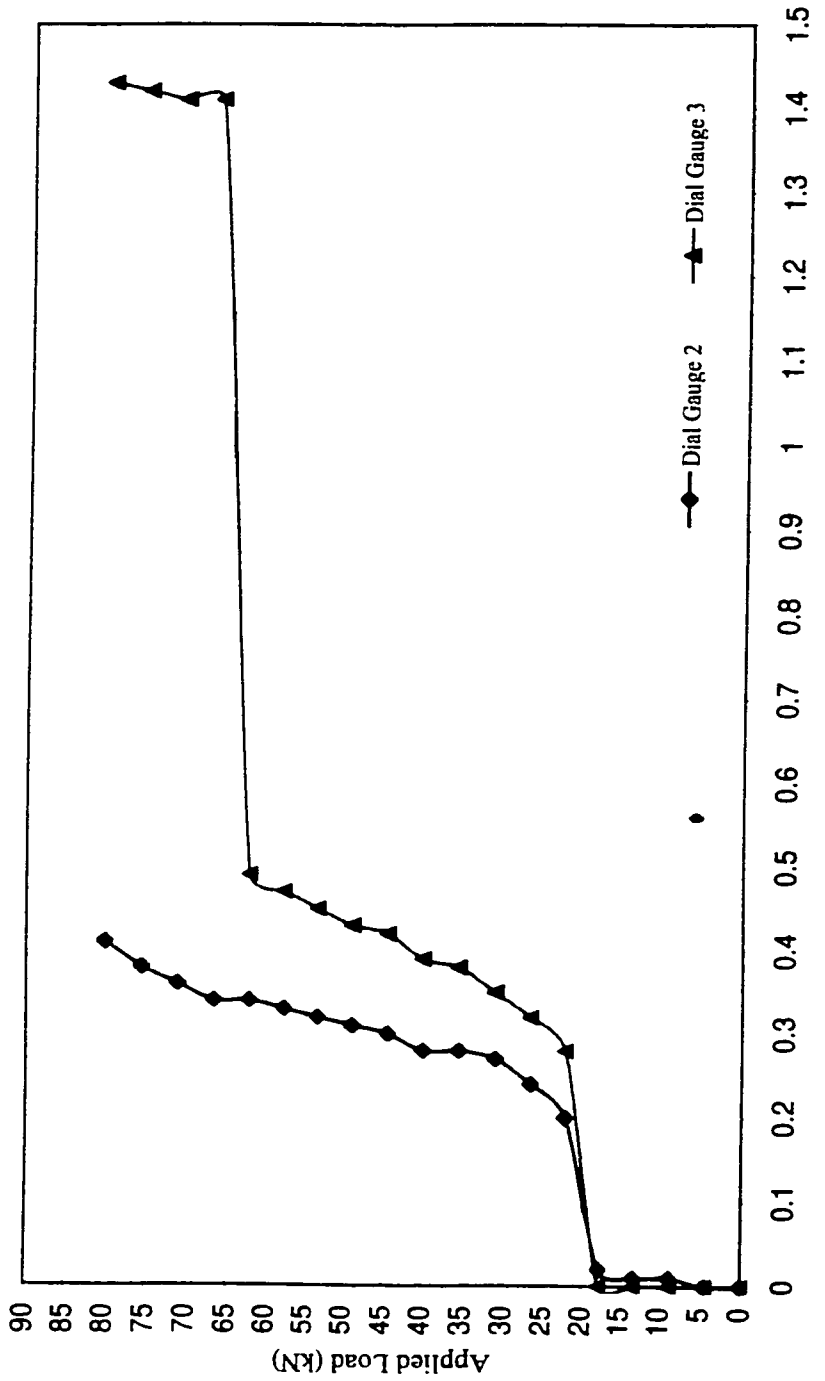

Figure I.16: Applied load vs. loaded-end slip of beam D1-D9.70-B24

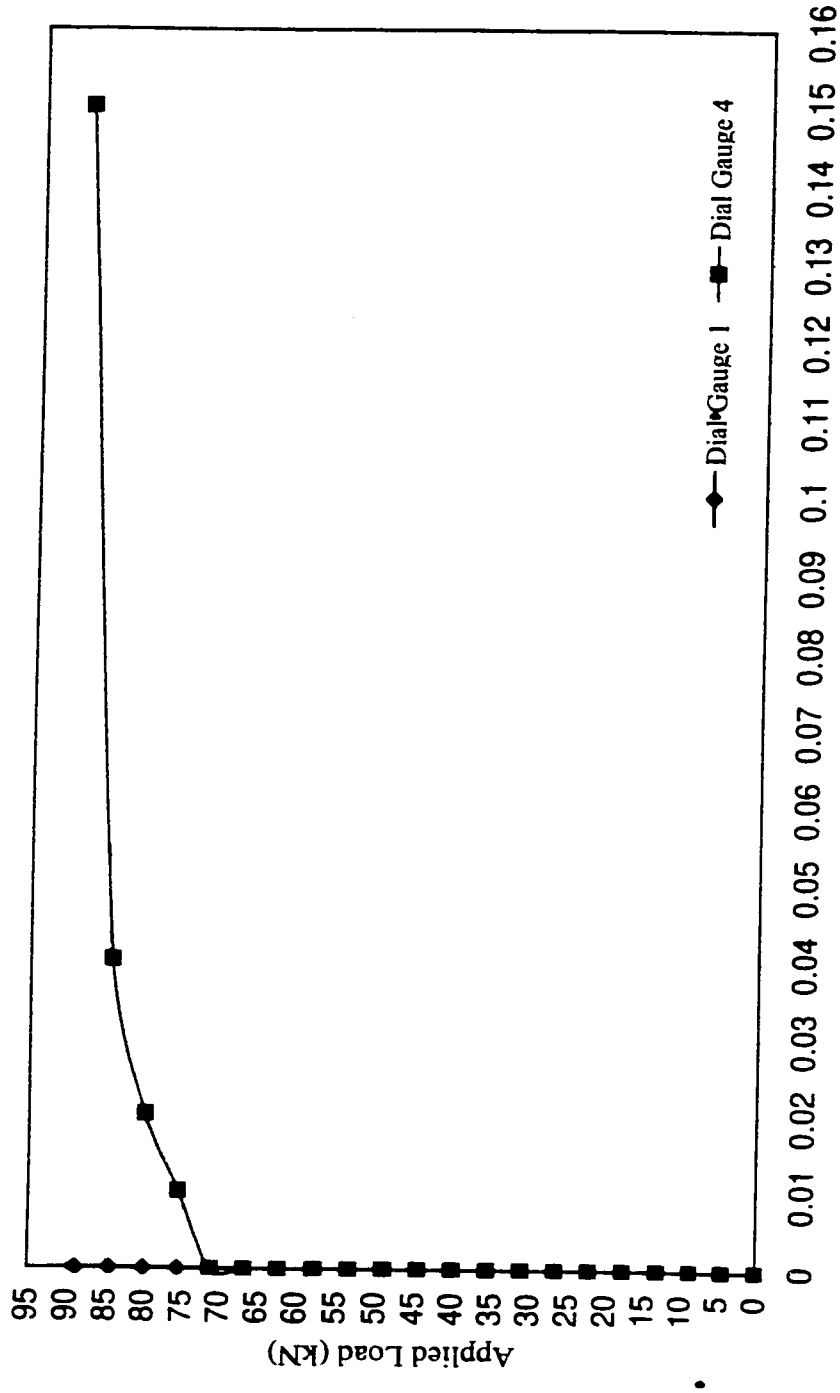

Figure I.17: Applied load vs. free-end slip of beam D1-D9.70-C24

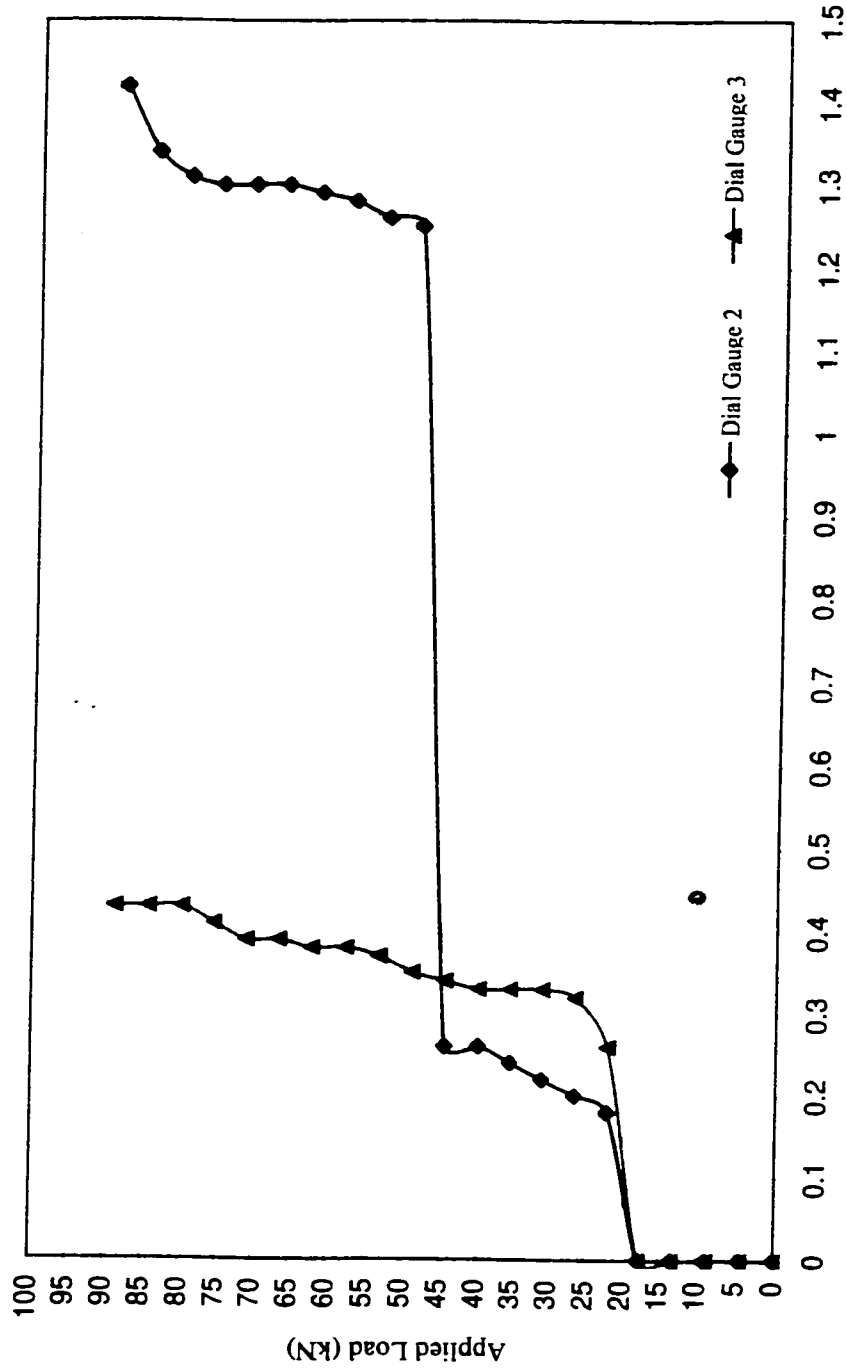

Figure I.18: Applied load vs. loaded-end slip of beam D1-D9.70-C24

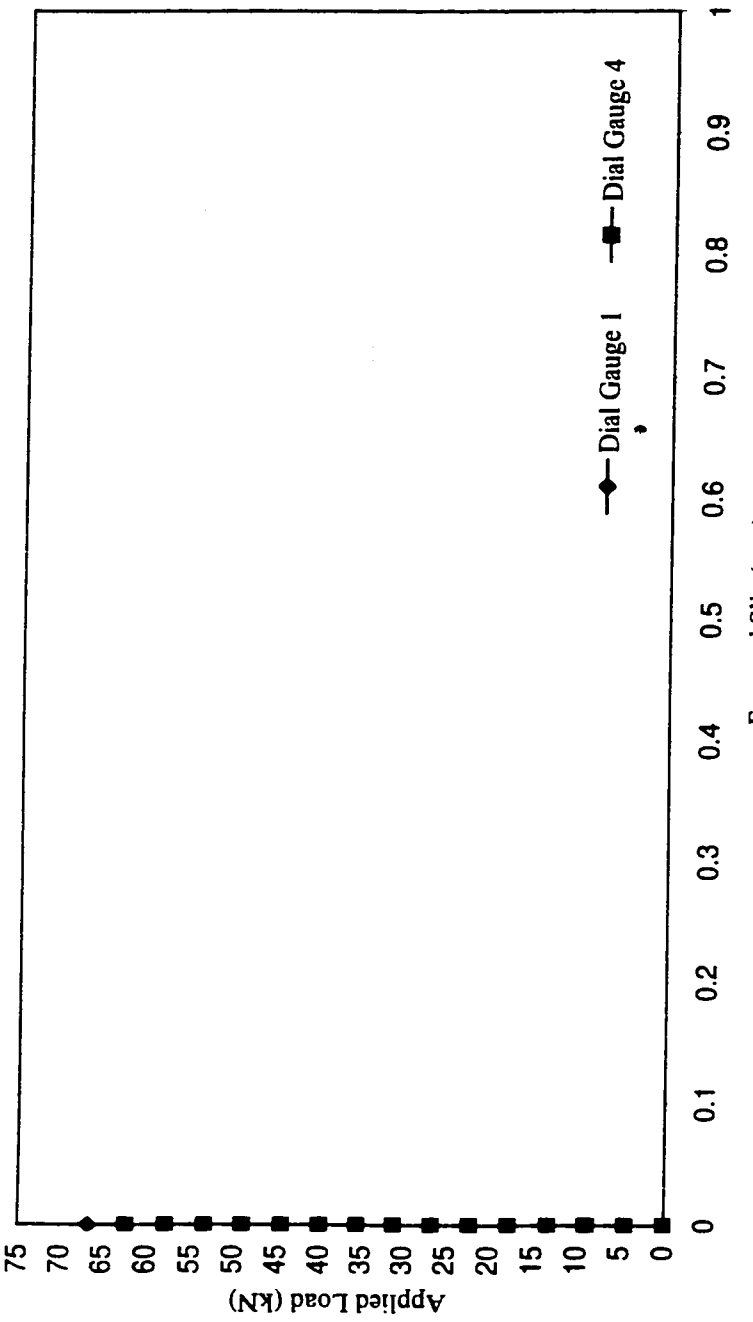

Figure I.19: Applied load vs. free-end slip of beam D1-D9.70-A30

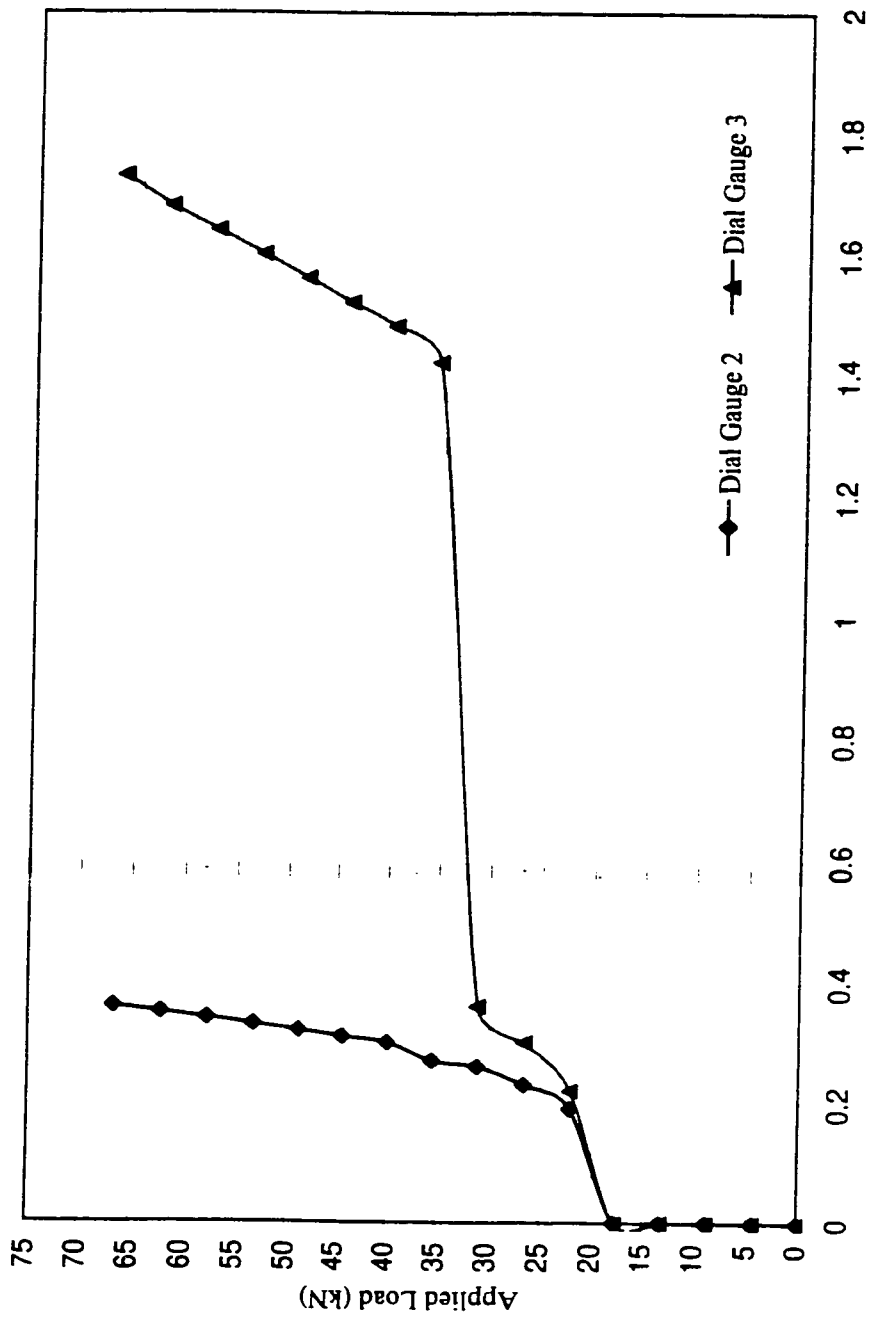

Figure I.20: Applied load vs. loaded-end slip of beam D1-D9.70-A30

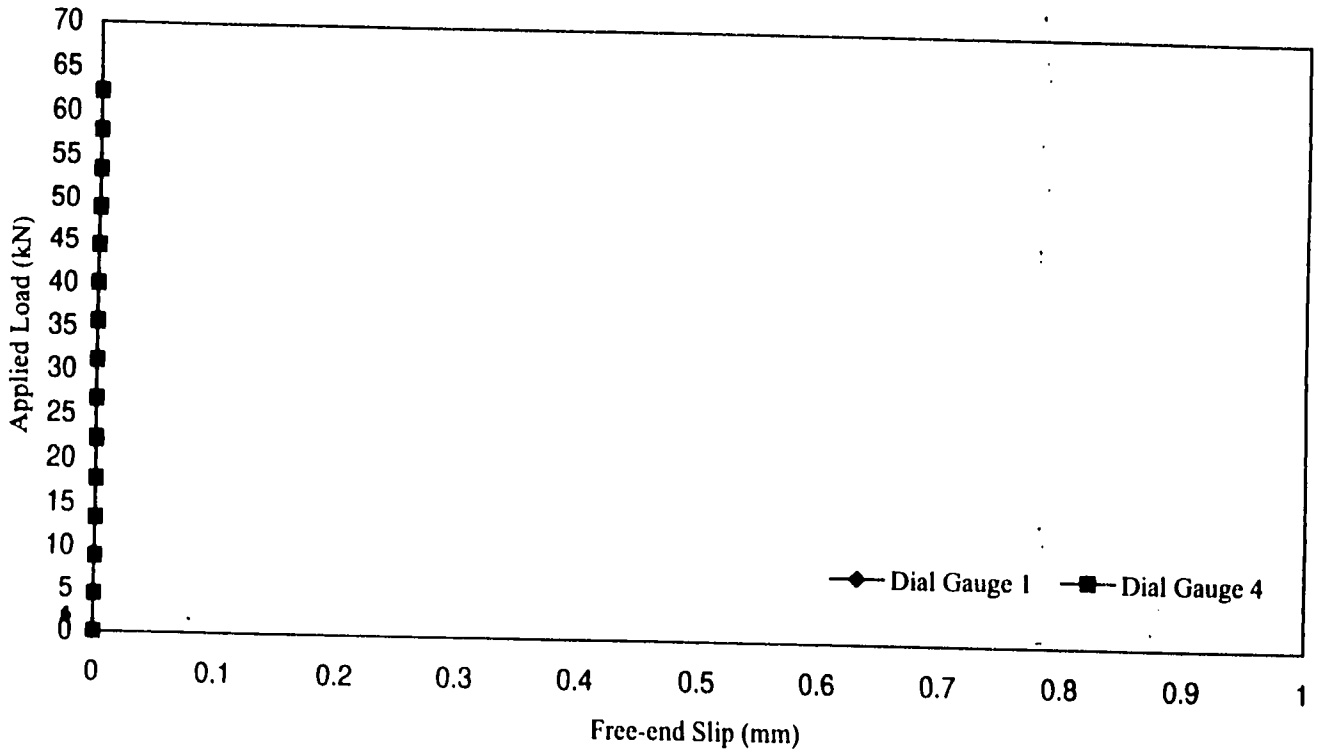

Figure I.21: Applied load vs. free-end slip of beam D1-D9.70-B30

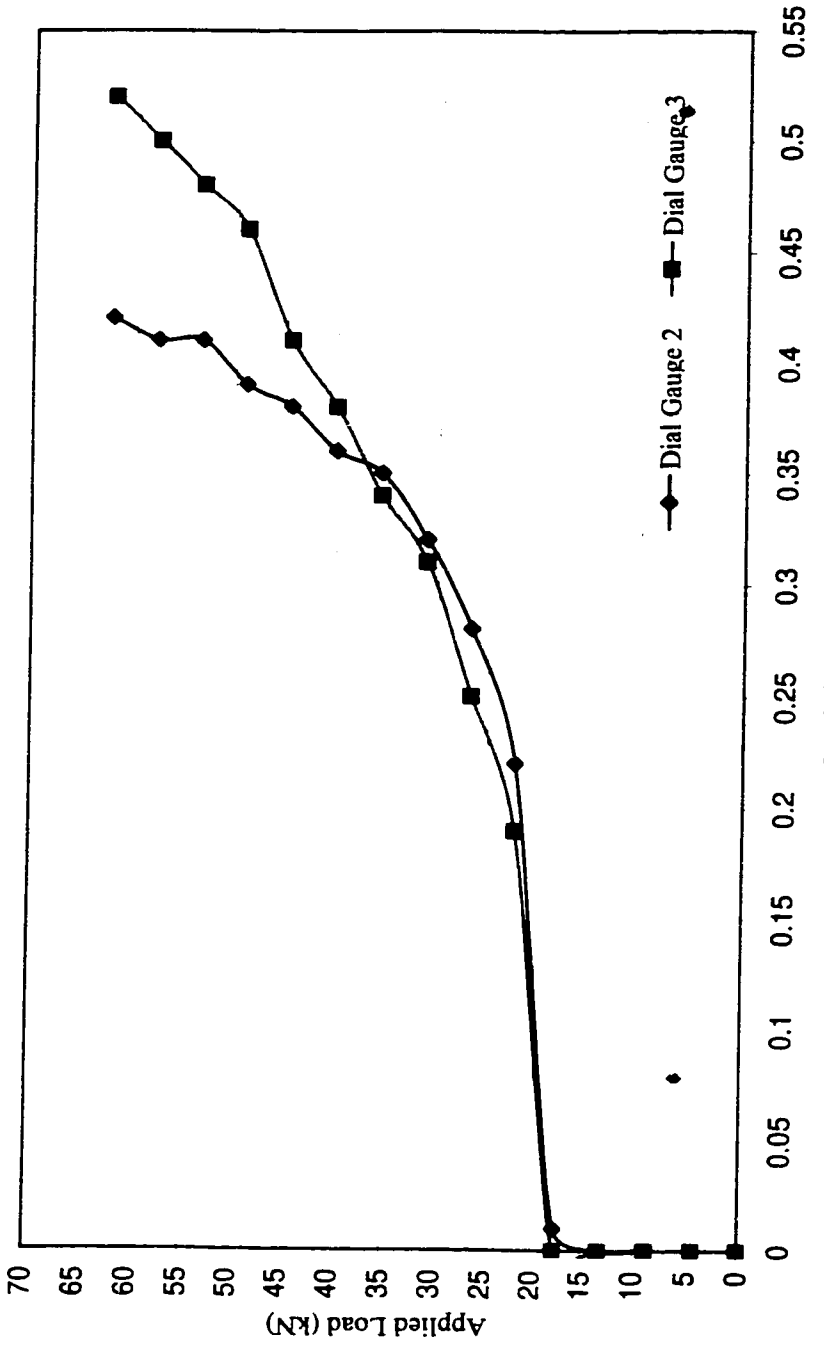

Figure I.22: Applied load vs. loaded-end slip of beam D1-D9.70-B30

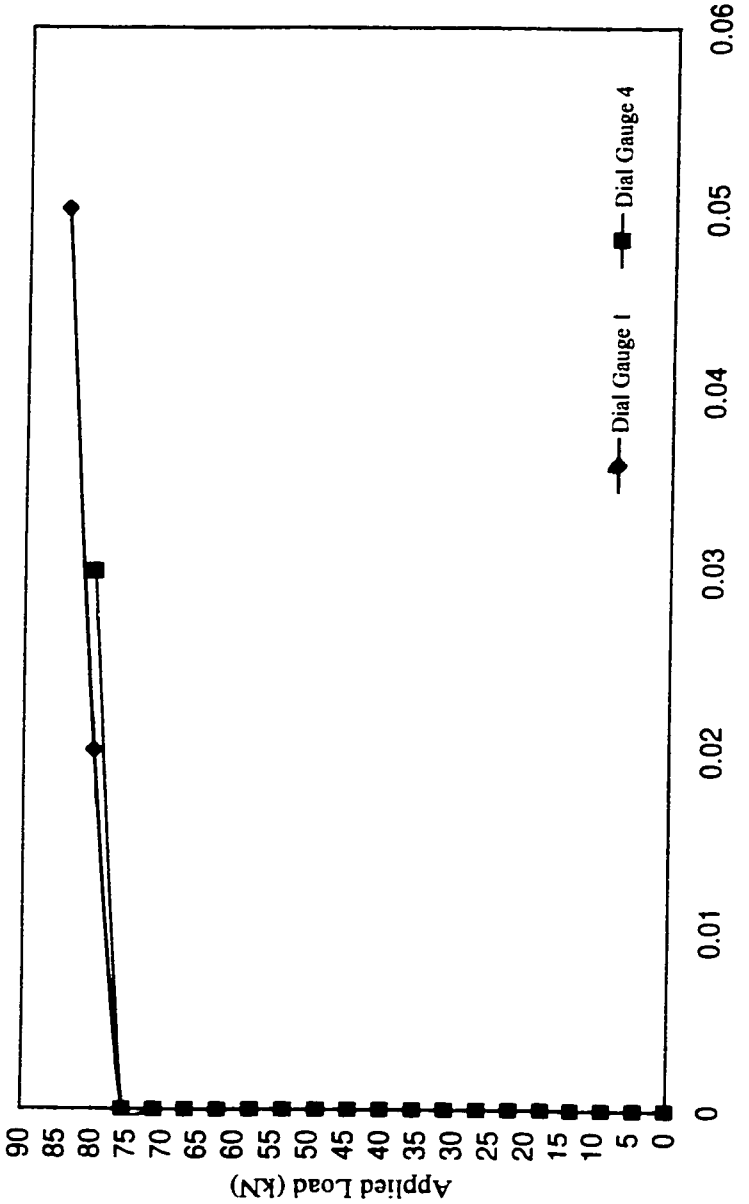

Figure I.23: Applied load vs. free-end slip of beam D1-D9.70-C30

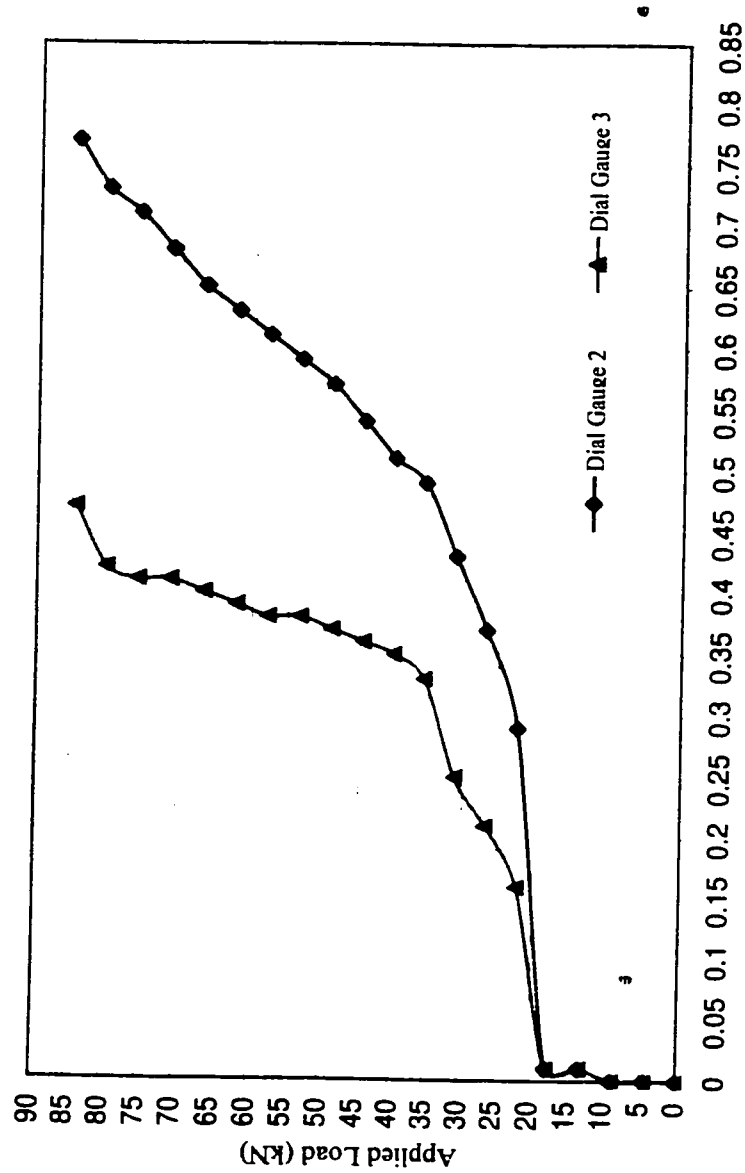

Figure I.24: Applied load vs. loaded-end slip of beam D1-D9.70-C30

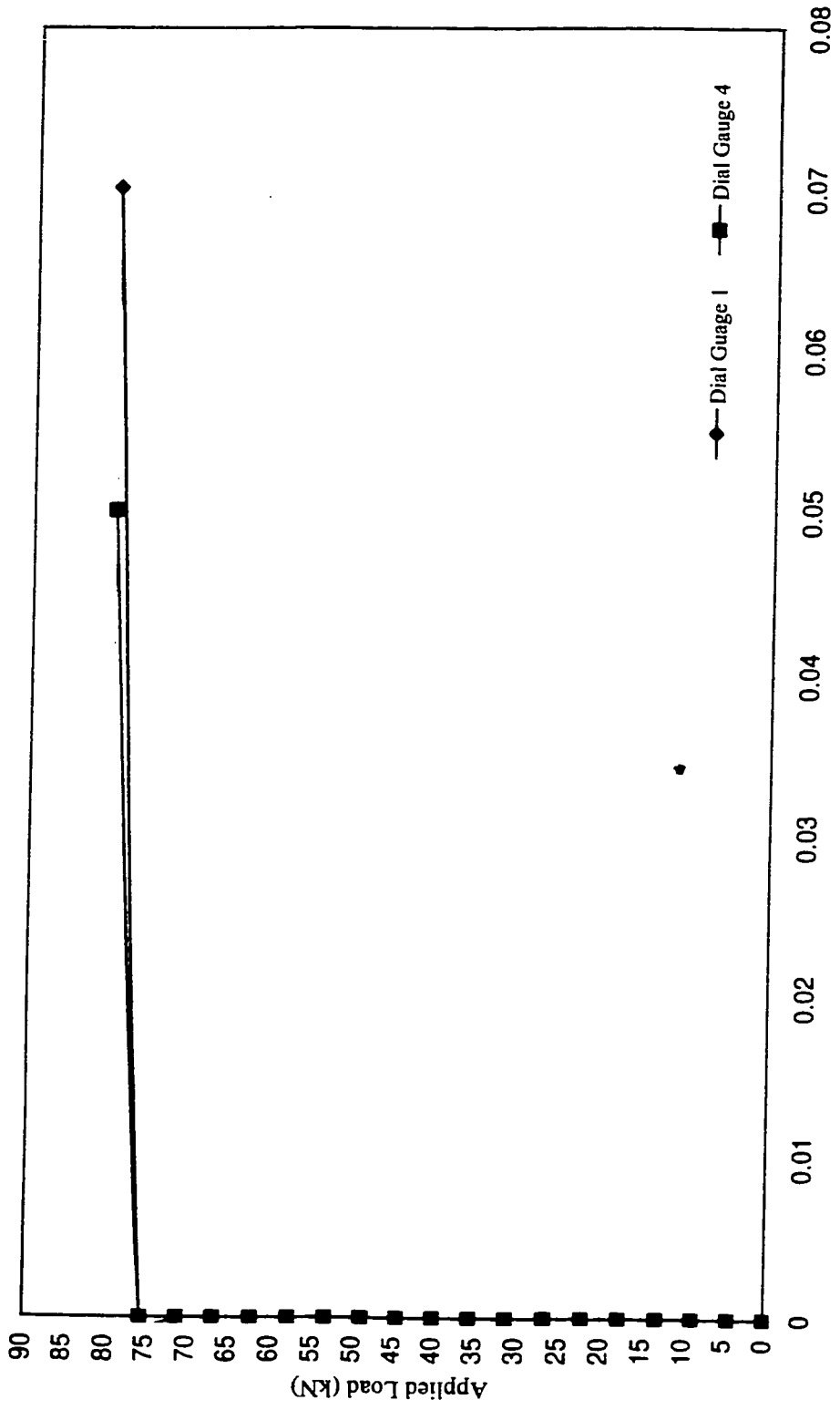

Figure I.25: Applied load vs. free-end slip of beam D1-D9.70-B18Comp

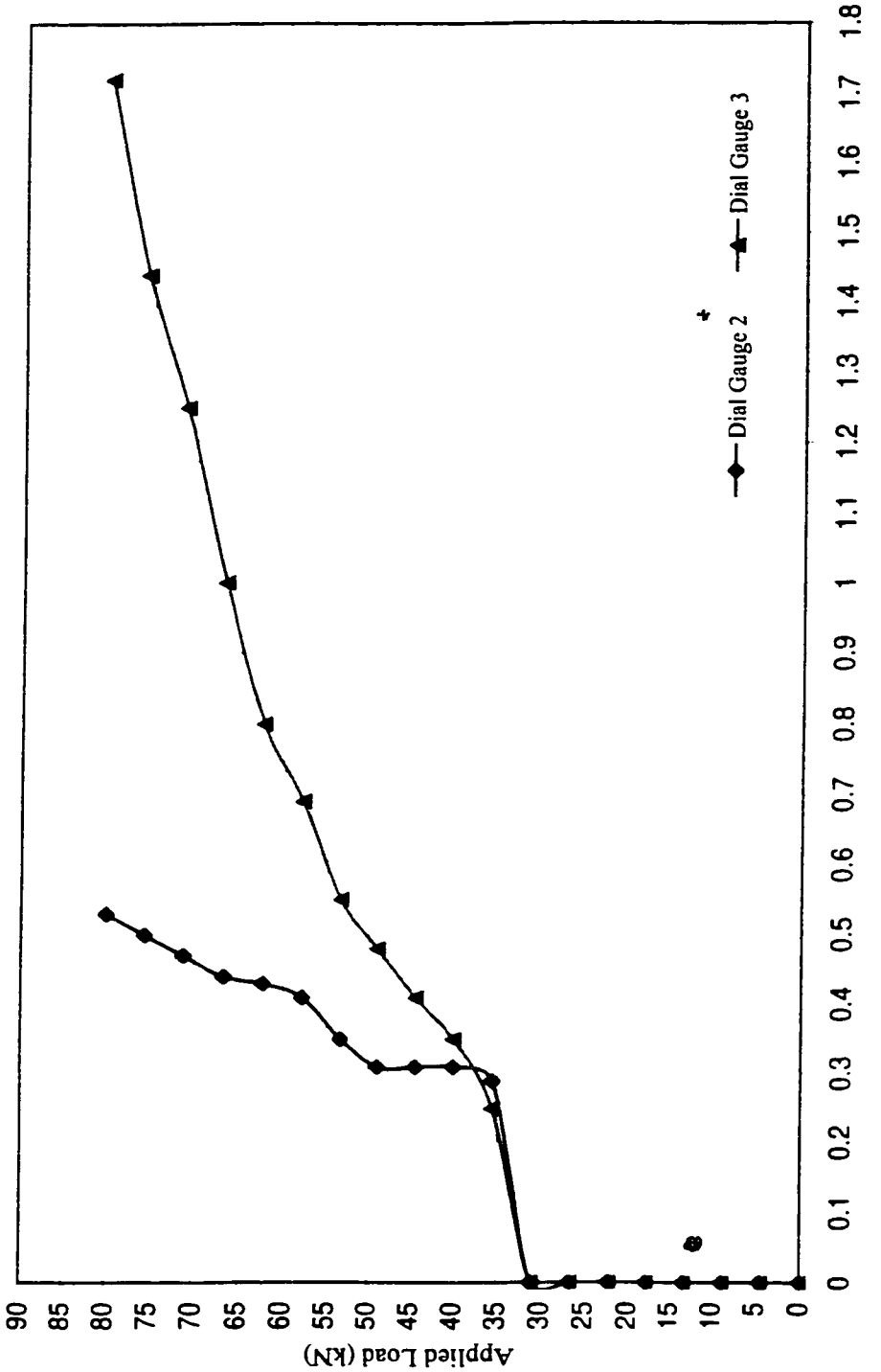

Figure I.26: Applied load vs. loaded-end slip of beam D1-D9.70-B18Comp

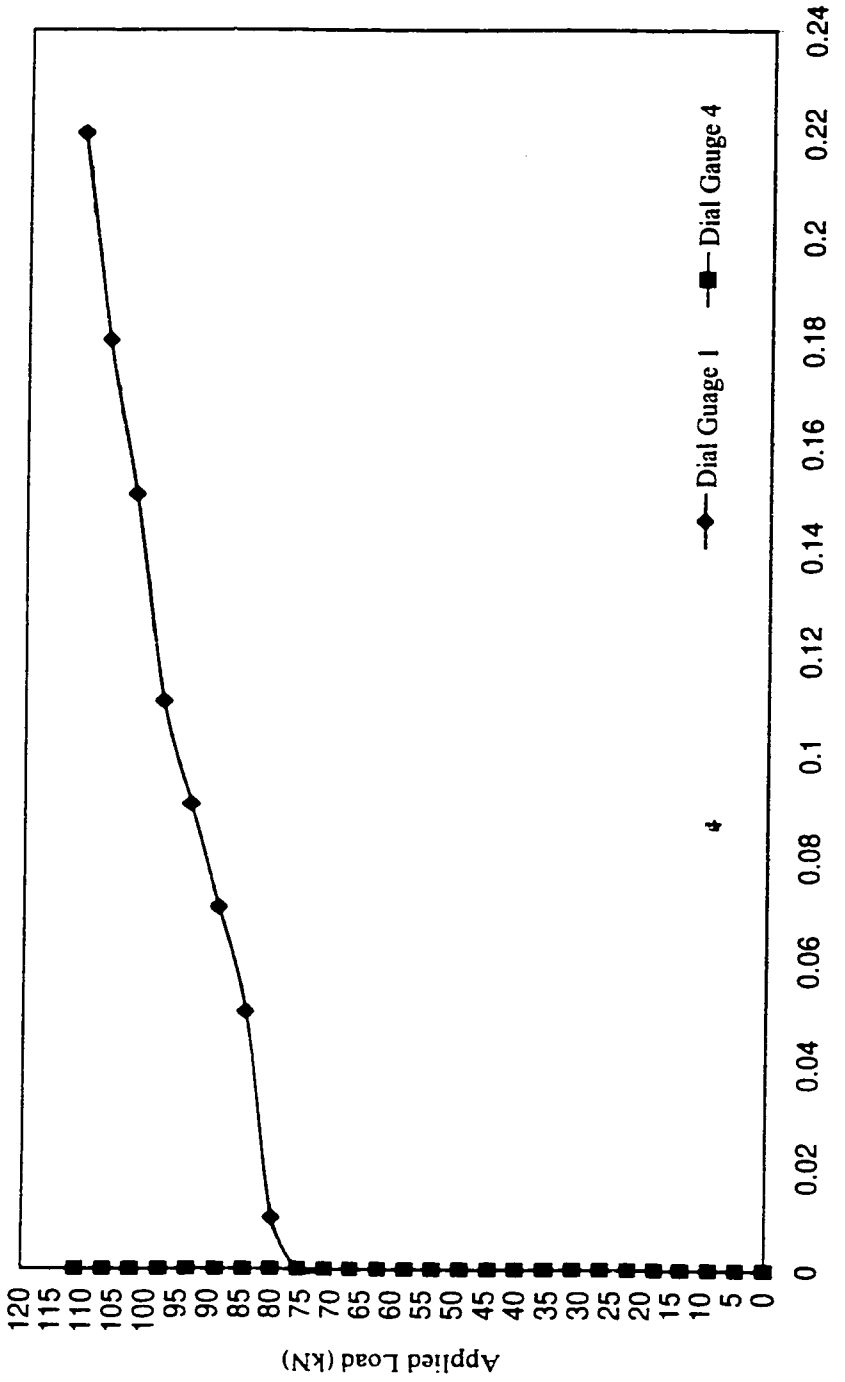

Figure I.27: Applied load vs. free-end slip of beam D1-D9.70-C18Comp

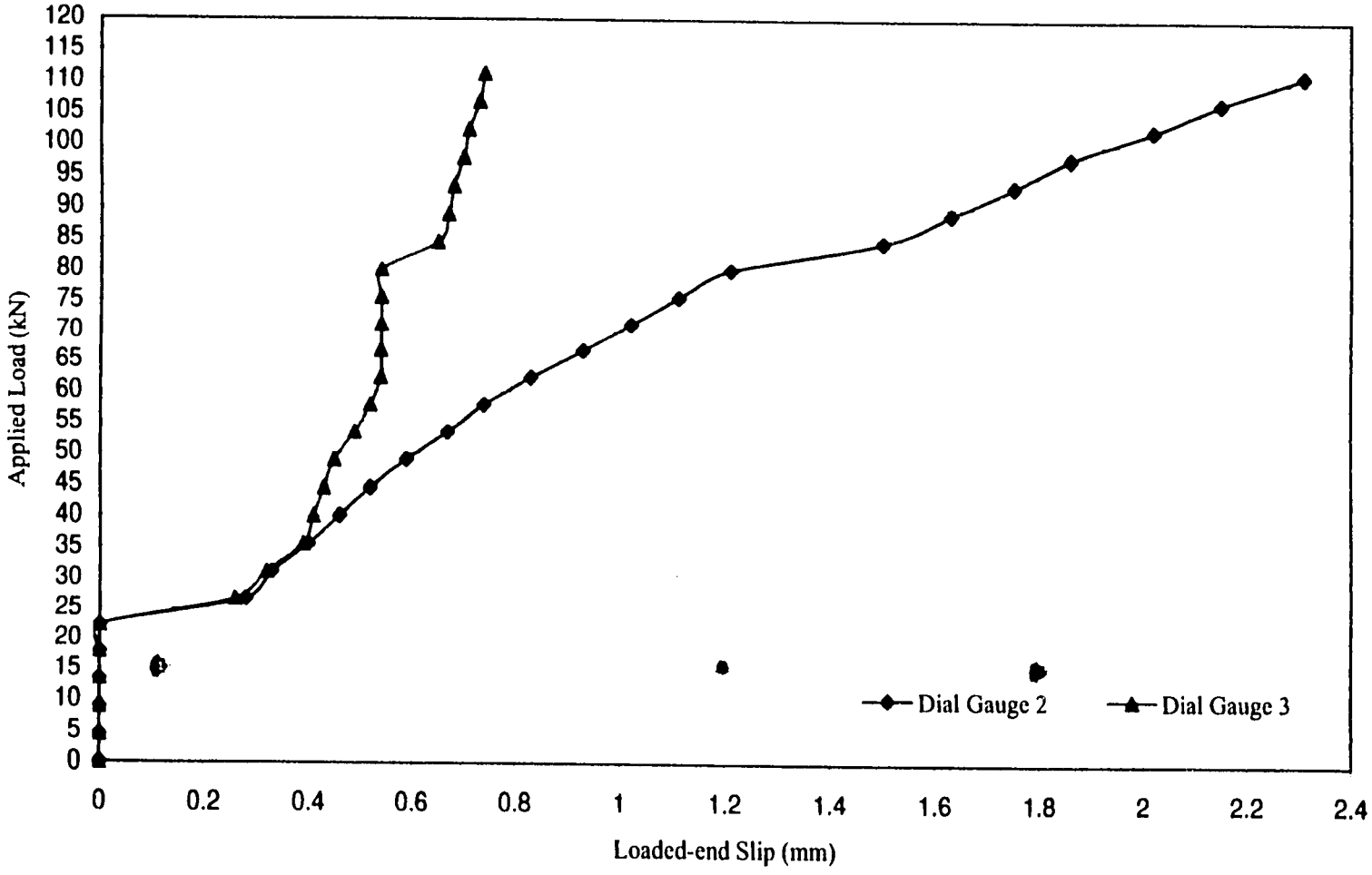

Figure I.28: Applied load vs. loaded-end slip of beam D1-D9.70-C18Comp

Appendix J

Load-Deflection Curve (G2-D9.79 Bar)

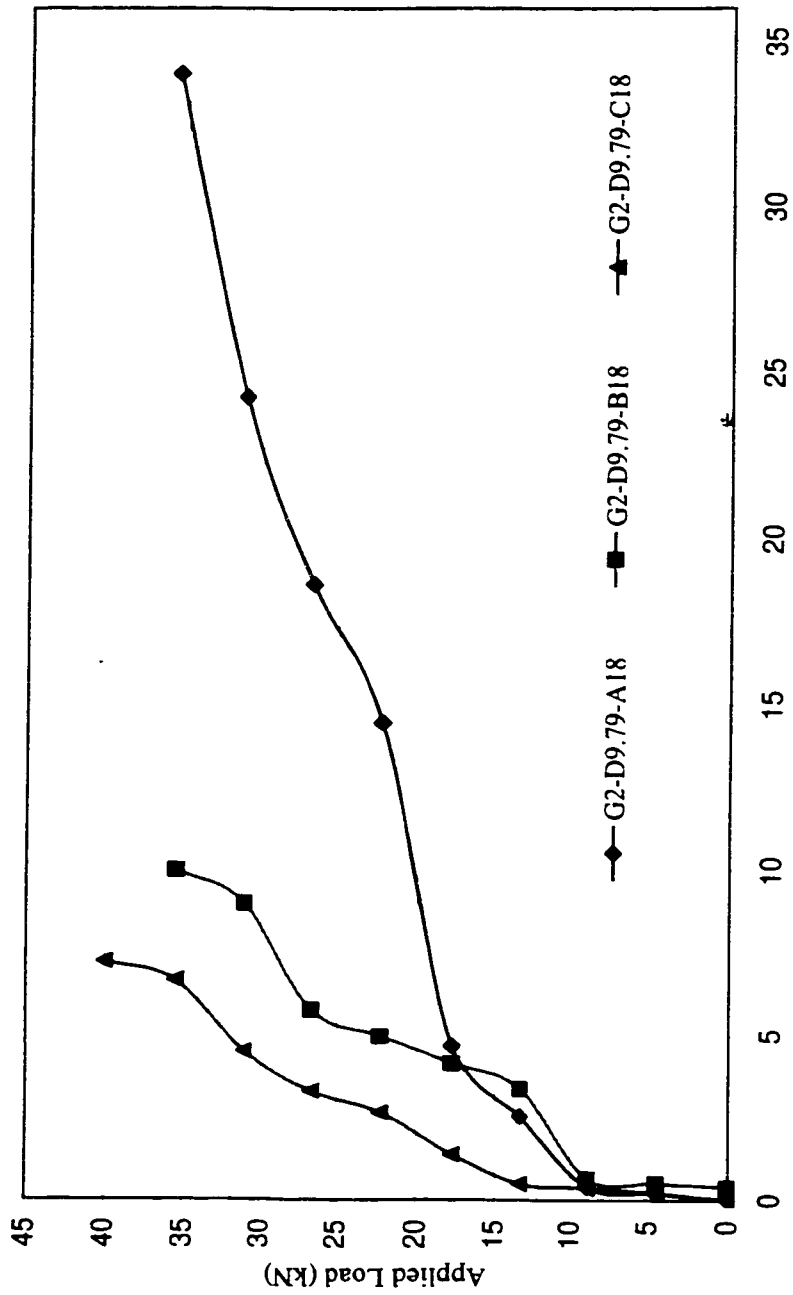

Figure J.1: Load-Deflection curve of beams G2-D9.79-A18, G2-D9.79-B18 and G2-D9.79-C18

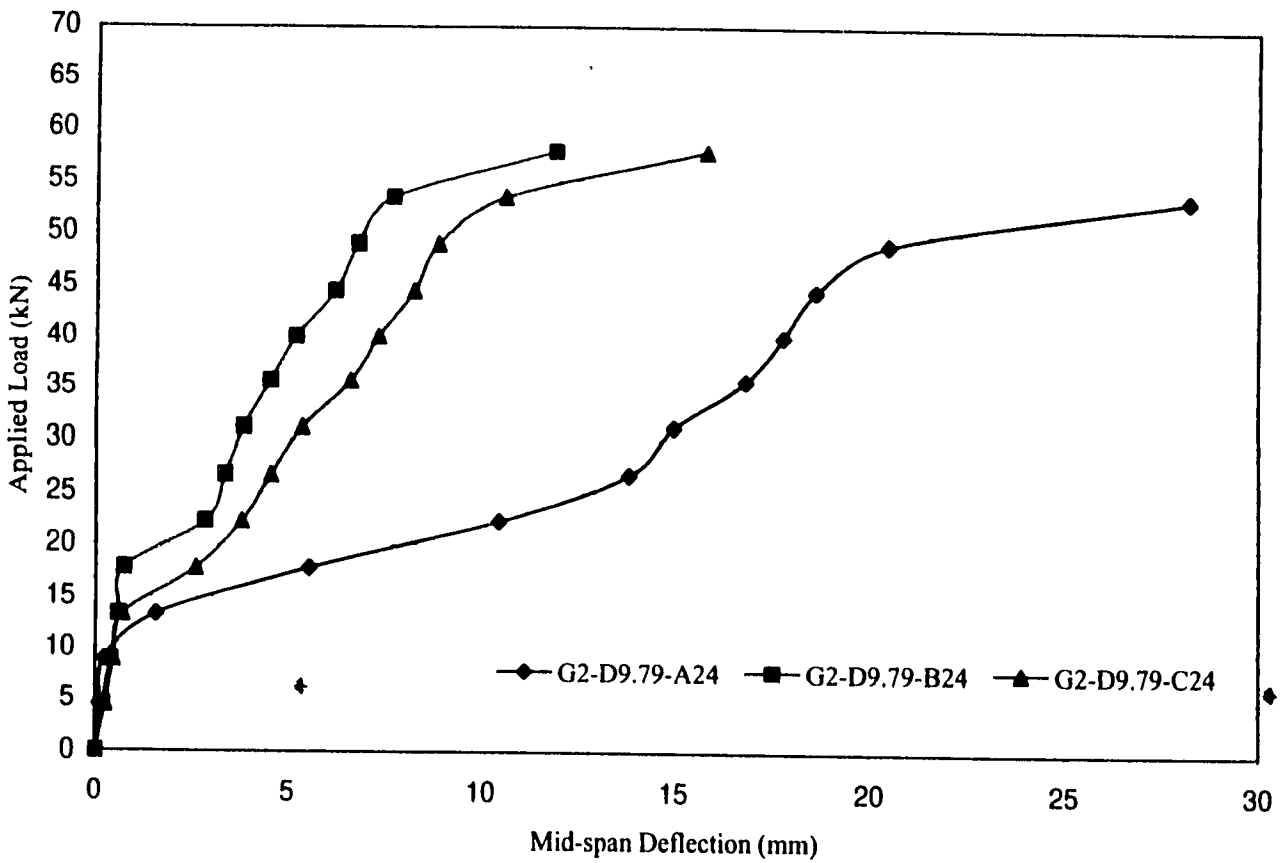

Figure J.2: Load-Deflection curve of beams G2-D9.79-A24, G2-D9.79-B24 and G2-D9.79-C24

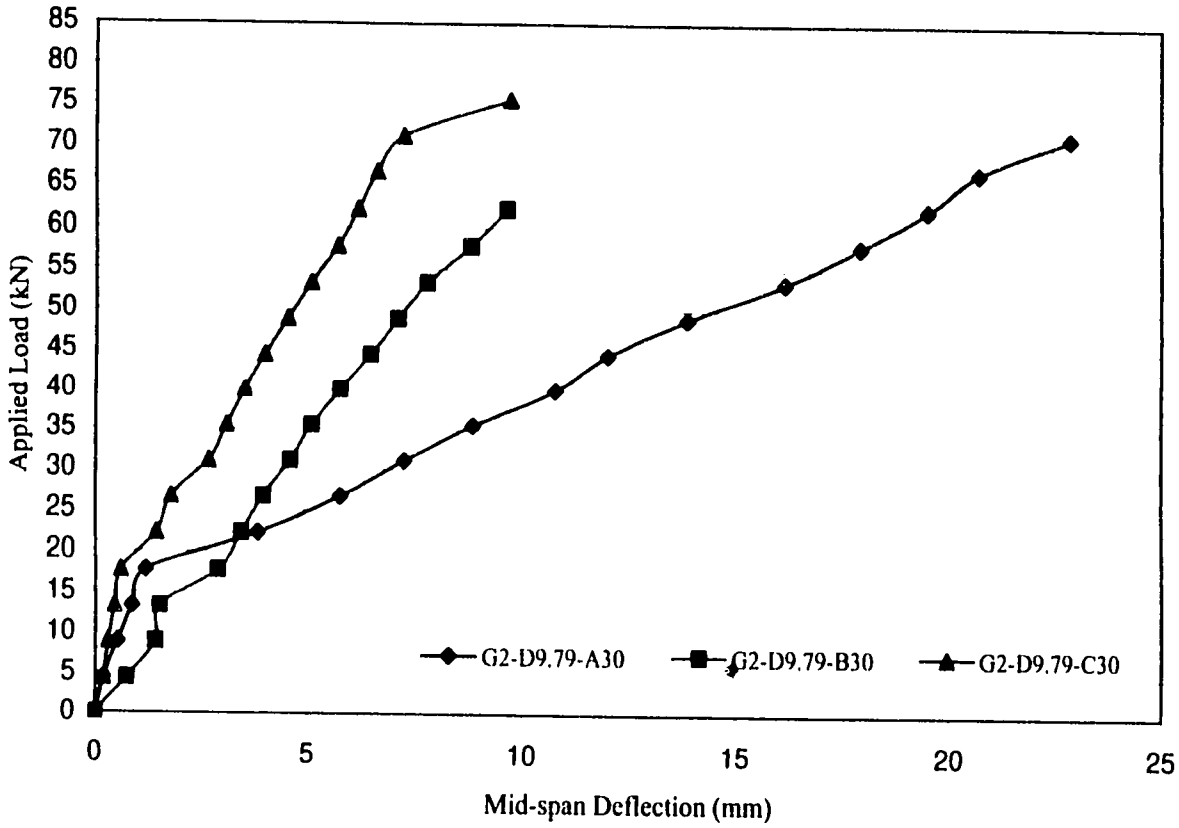

Figure J.3: Load-Deflection curve of beams G2-D9.79-A30, G2-D9.79-B30 and G2-D9.79-C30

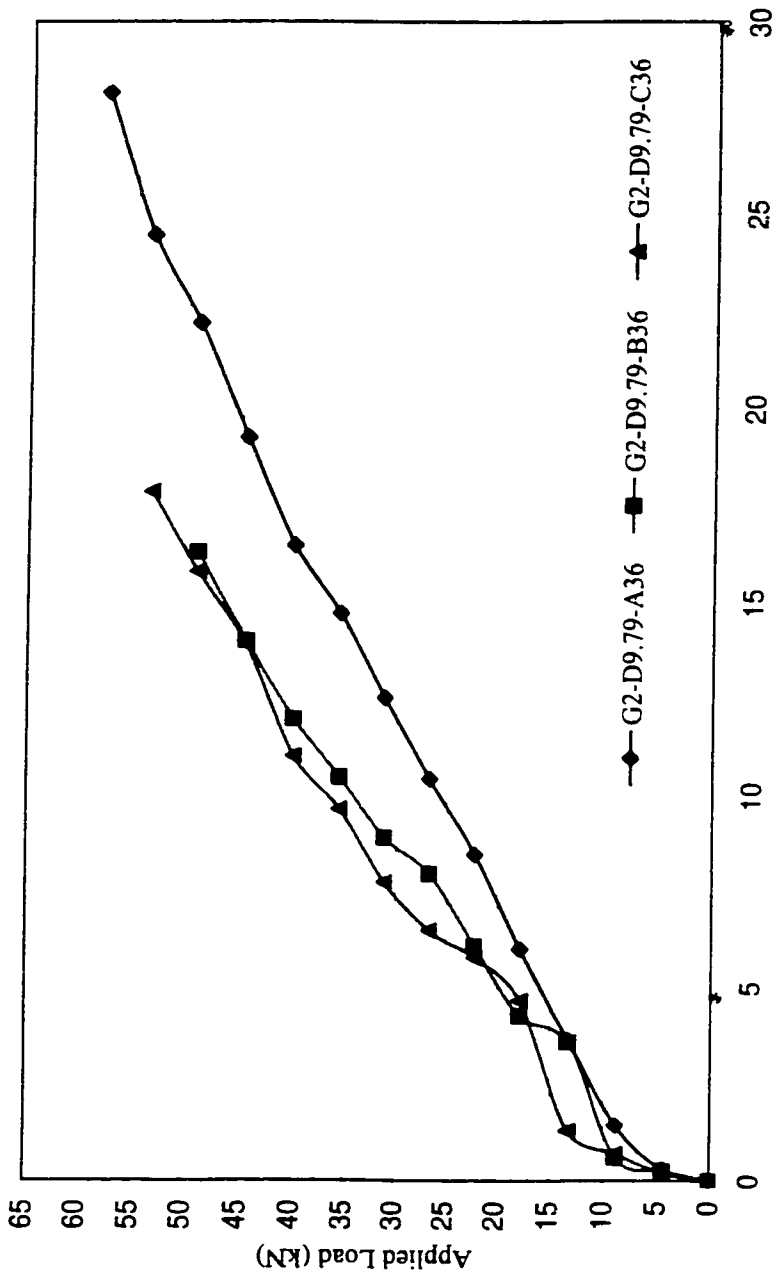

Figure J.4: Load-Deflection curve of beams G2-D9.79-A36, G2-D9.79-B36 and G2-D9.79-C36

Appendix K

Load-Deflection Curve (D1-D9.70 Bar)

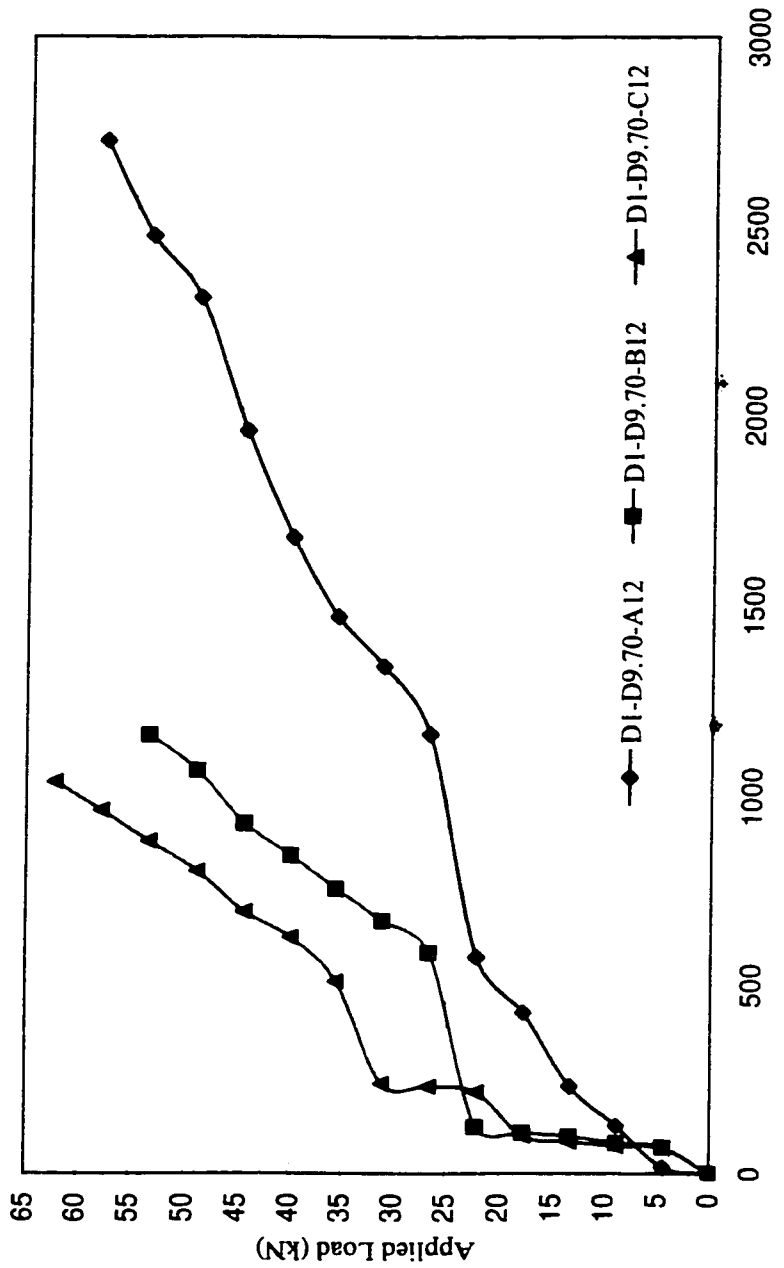

Figure K.1 Load-Delfection curve of beams D1-D9.70-A12, D1-9.70-B12 and D1-D9.70-C12

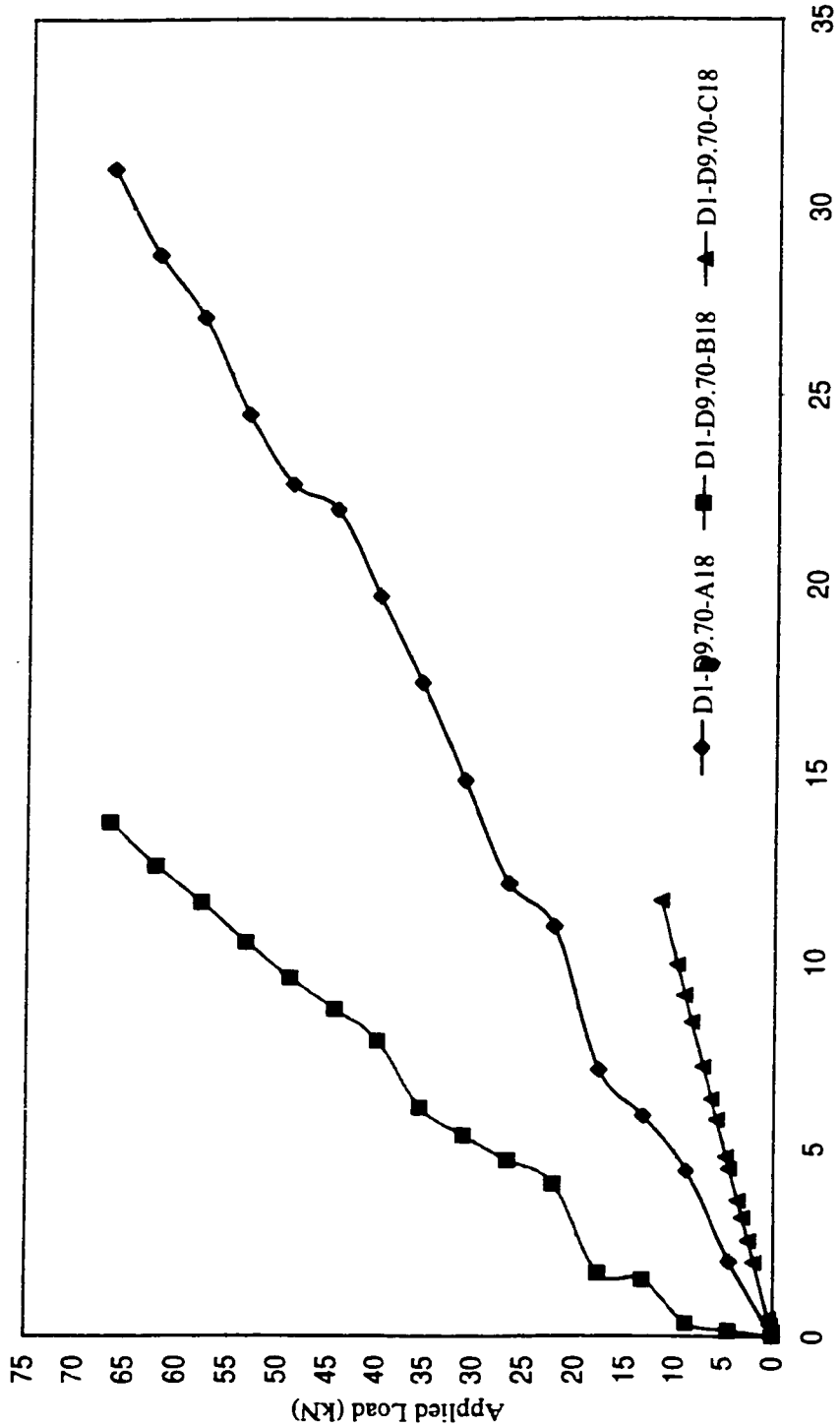

Figure K.2: Load-Deflection curve of beams D1-D9.70-A18, D1-D9.70-B18 and D1-D9.70-C18

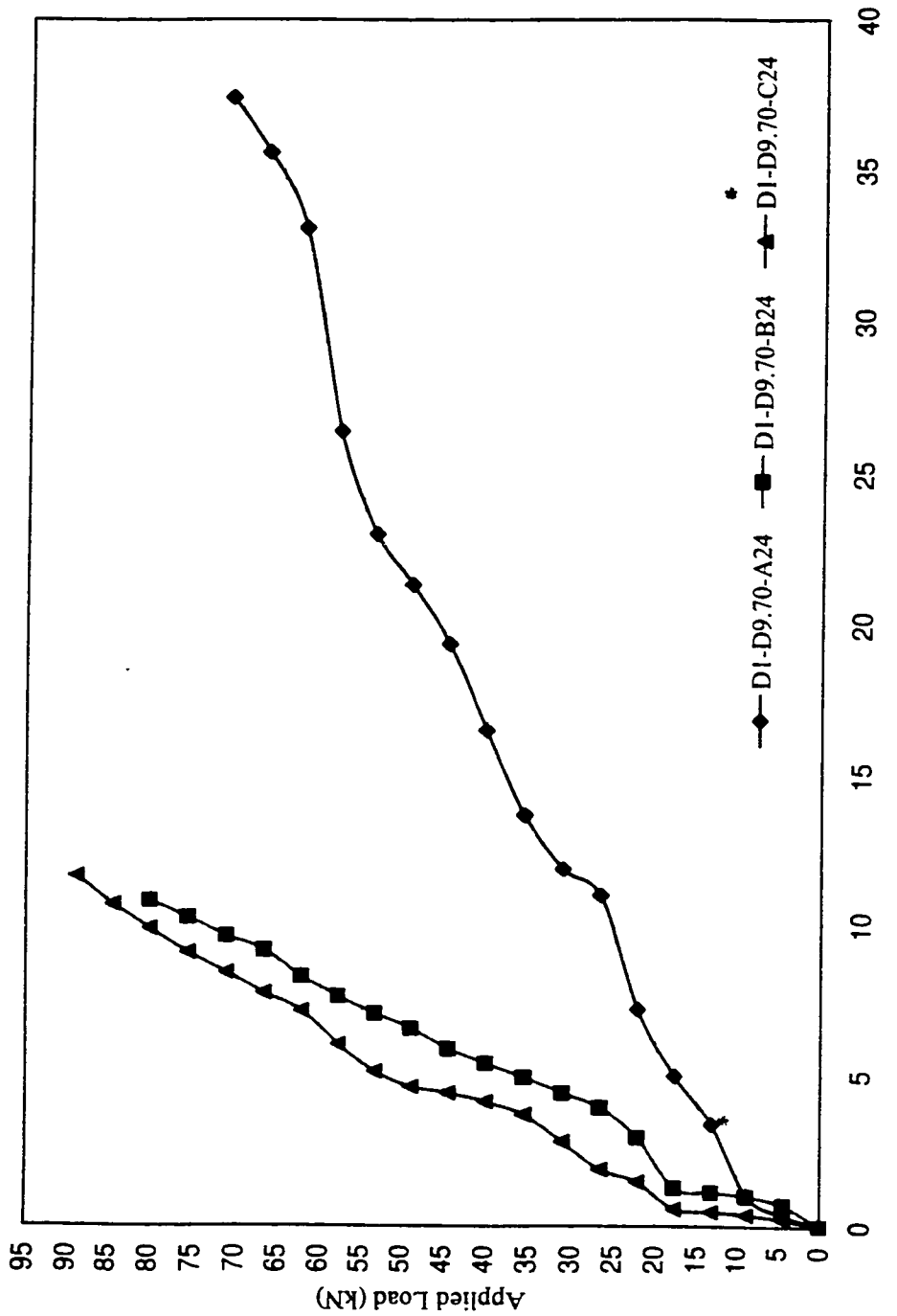

Figure K.3: Load-Deflection curve of beams D1-D9.70-A24, D1-D9.70-B24 and D1-D9.70-C24

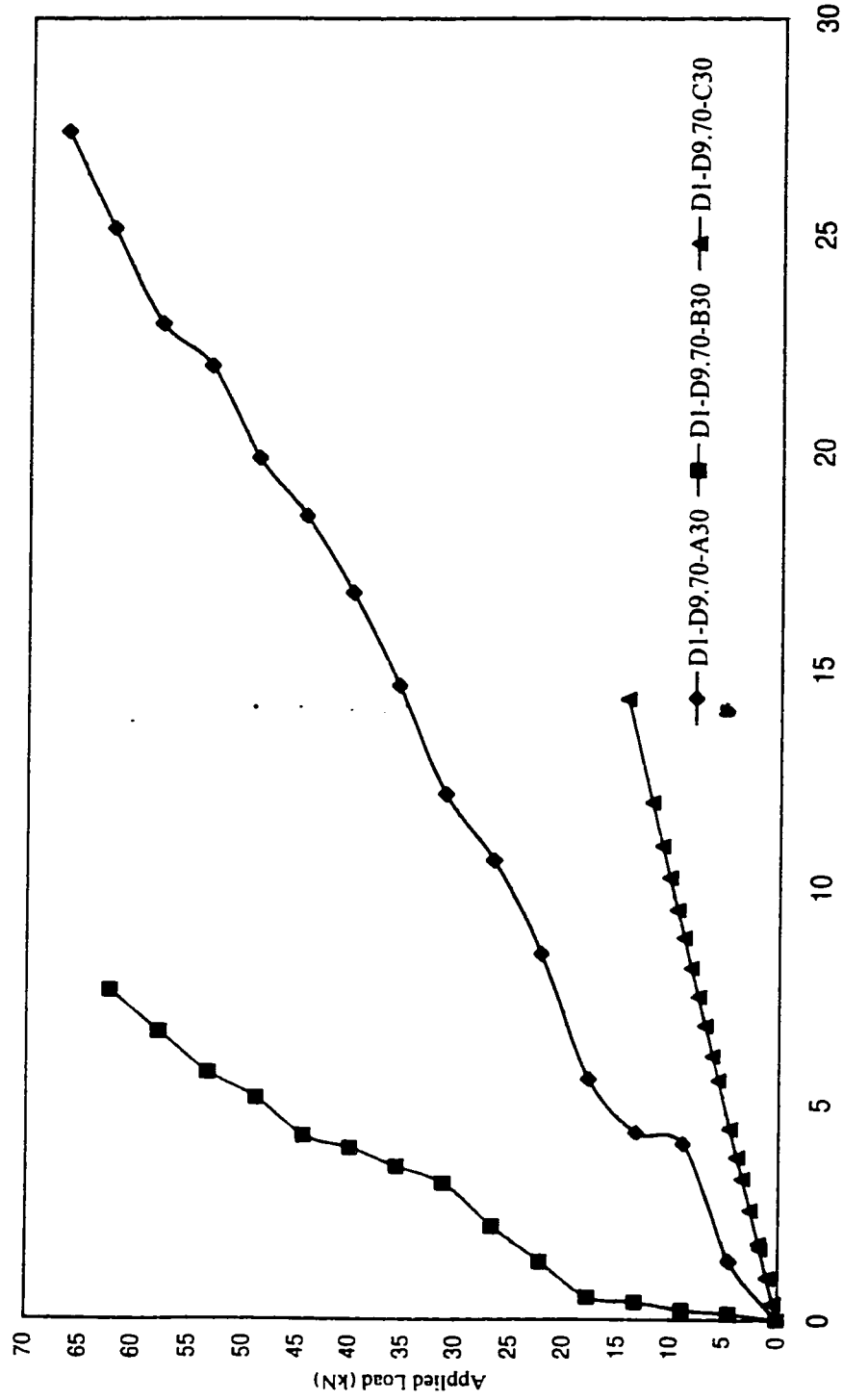

Figure K.4: Load-Deflection curve of beams D1-D9.70-A30, D1-D9.70-B30 and D1-D9.70-C30

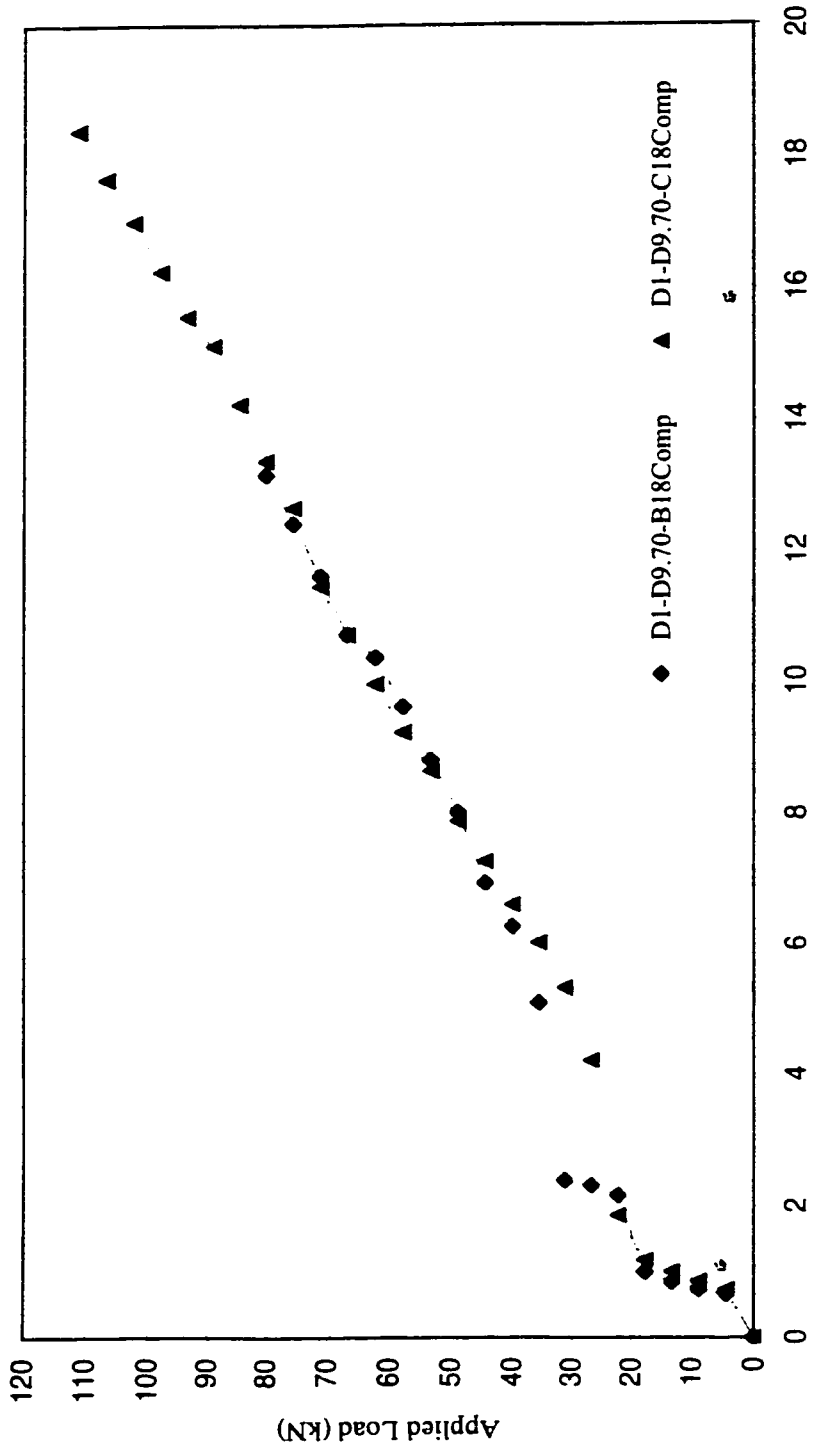

Figure K.5.: Load-Deflection Curve of beams D1-D9.70-B18Comp and D1-D9.70-B18Comp

Appendix L

Tensile Force vs. Bond Length (G2-D9.79 Bar, Free-end Slip)

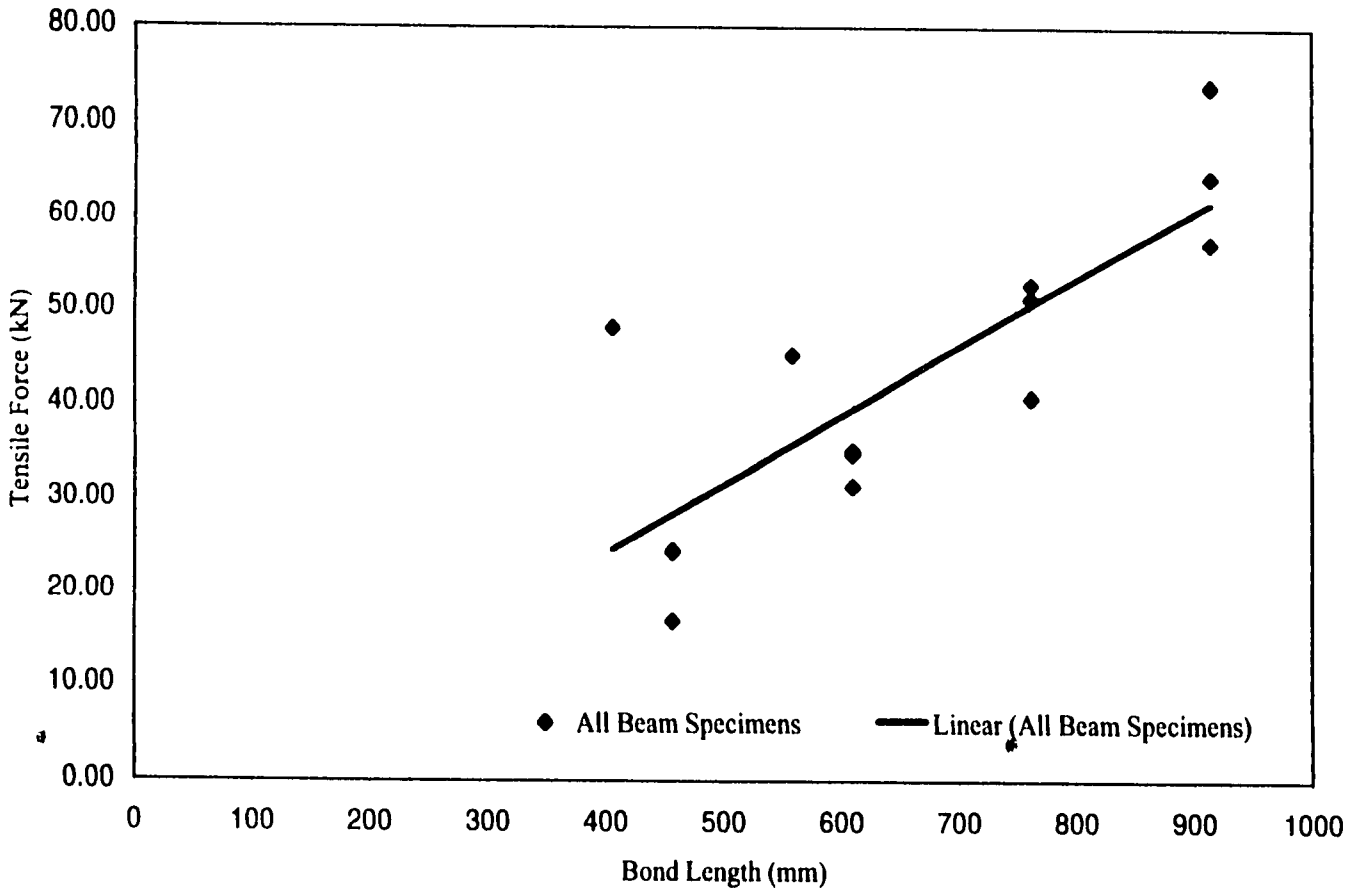

Figure L.1: Tensile force vs. bond length (G2-D9.79 bar, 0.05 mm free-end slip)

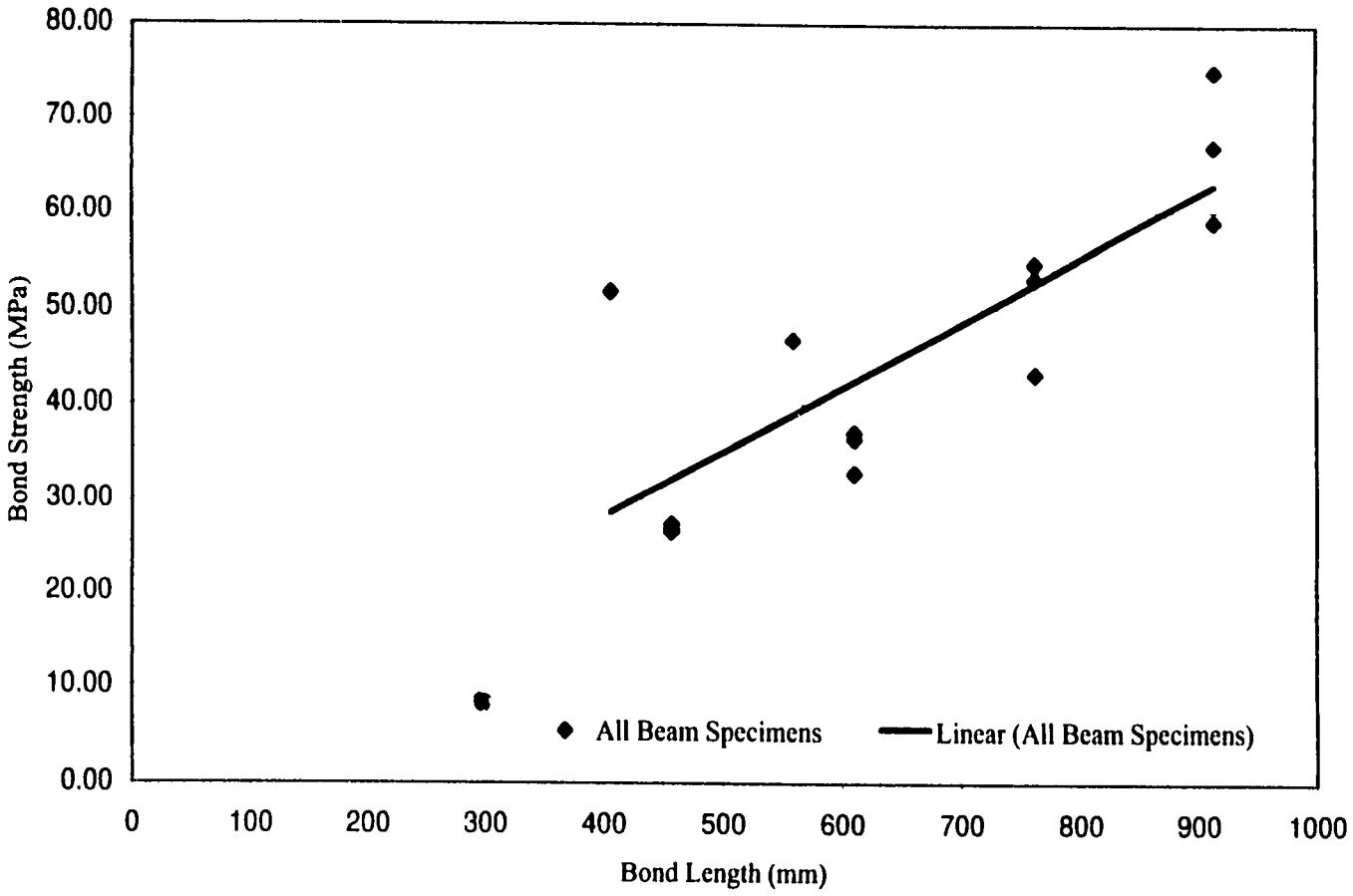

Figure L.2: Tensile force vs. bond length (G2-D9.79 bar, 0.10 mm free-end slip)

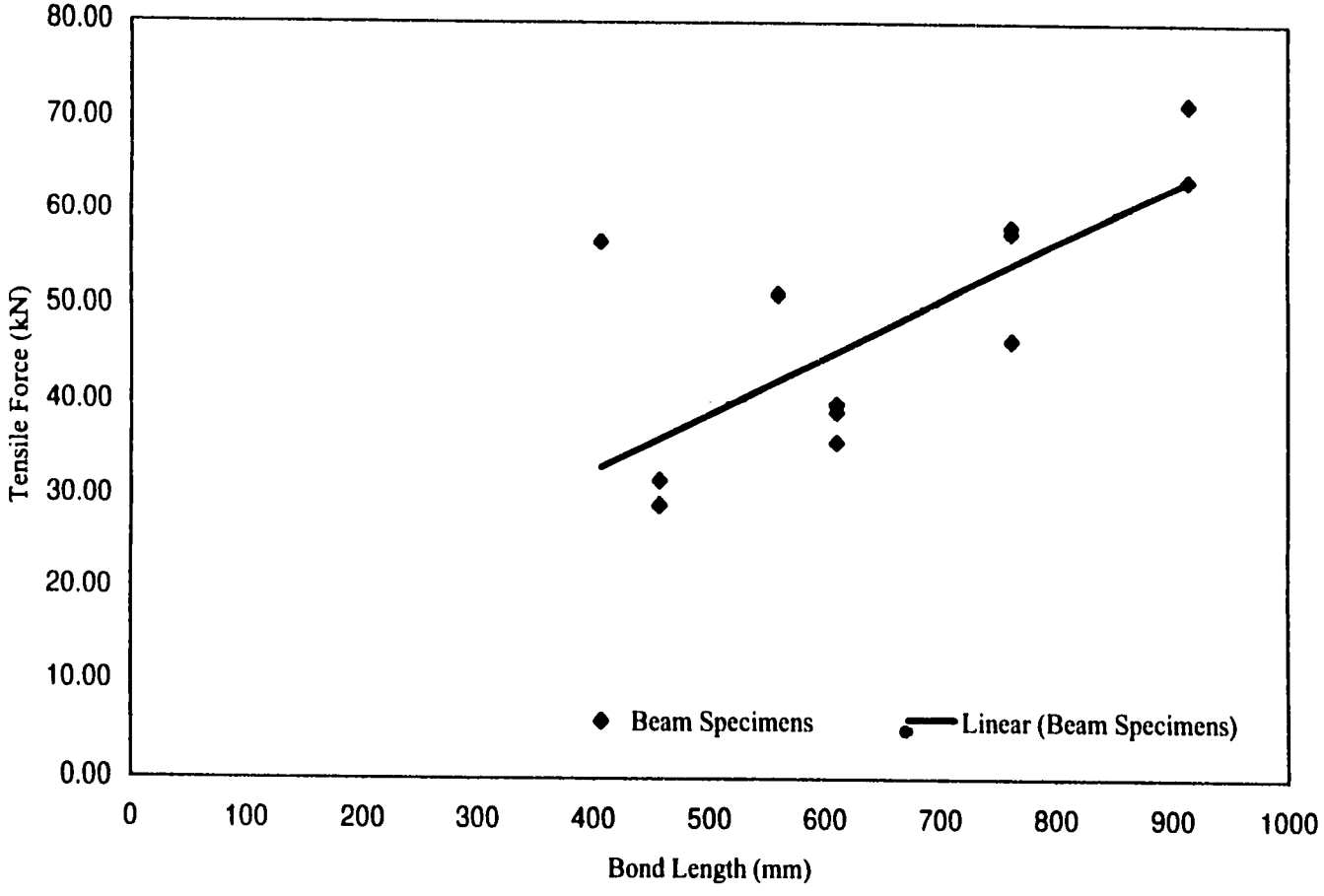

Figure L.3: Tensile force vs. bond length (G2-D9.79 bar, 0.25 mm free-end slip)

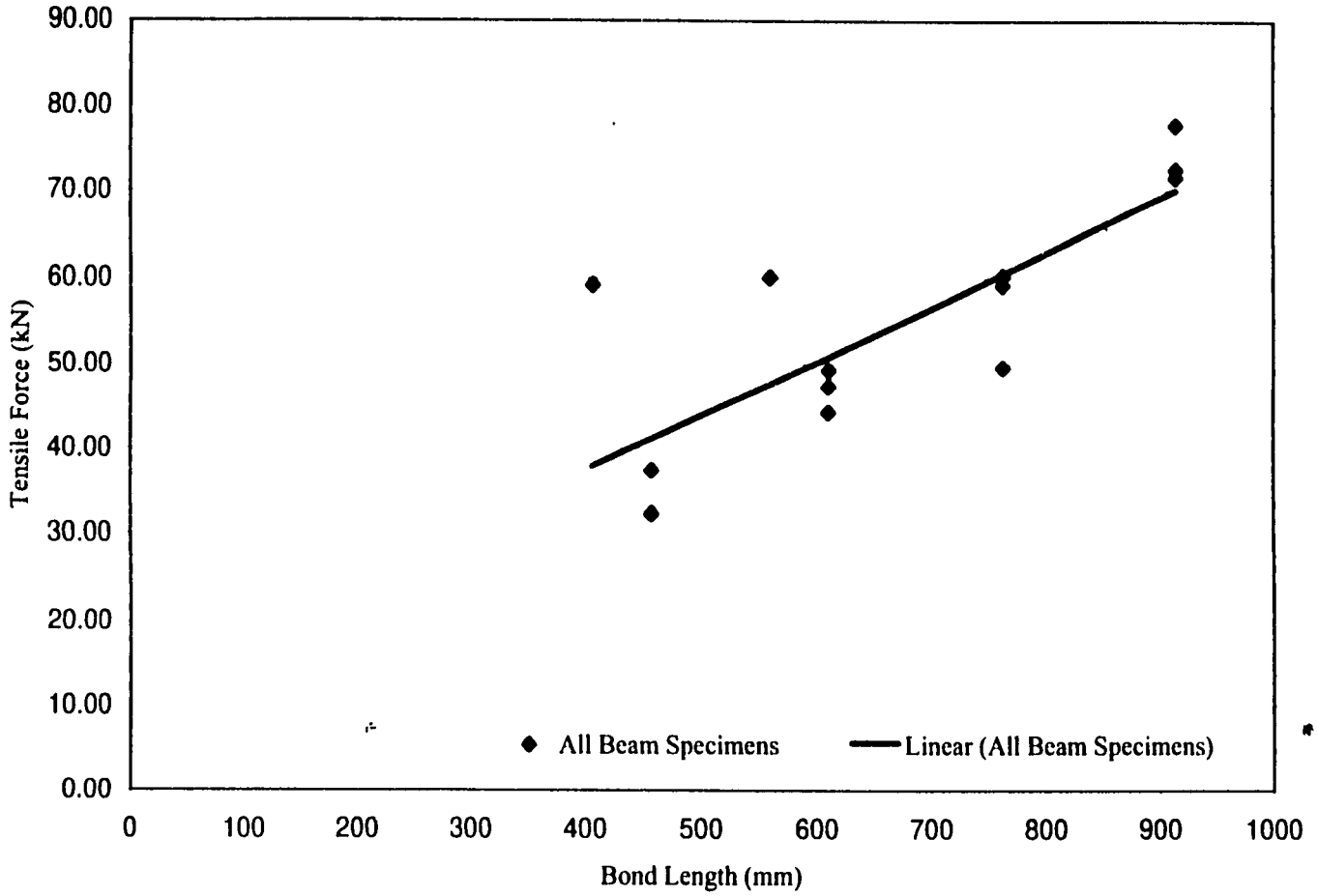

Figure L.4: Tensile force vs. bond length (G2-D9.79 bar, max. free-end slip)

Appendix M

Bond Strength vs. Bond Length (G2-D9.79 bar, Free-end Slip)

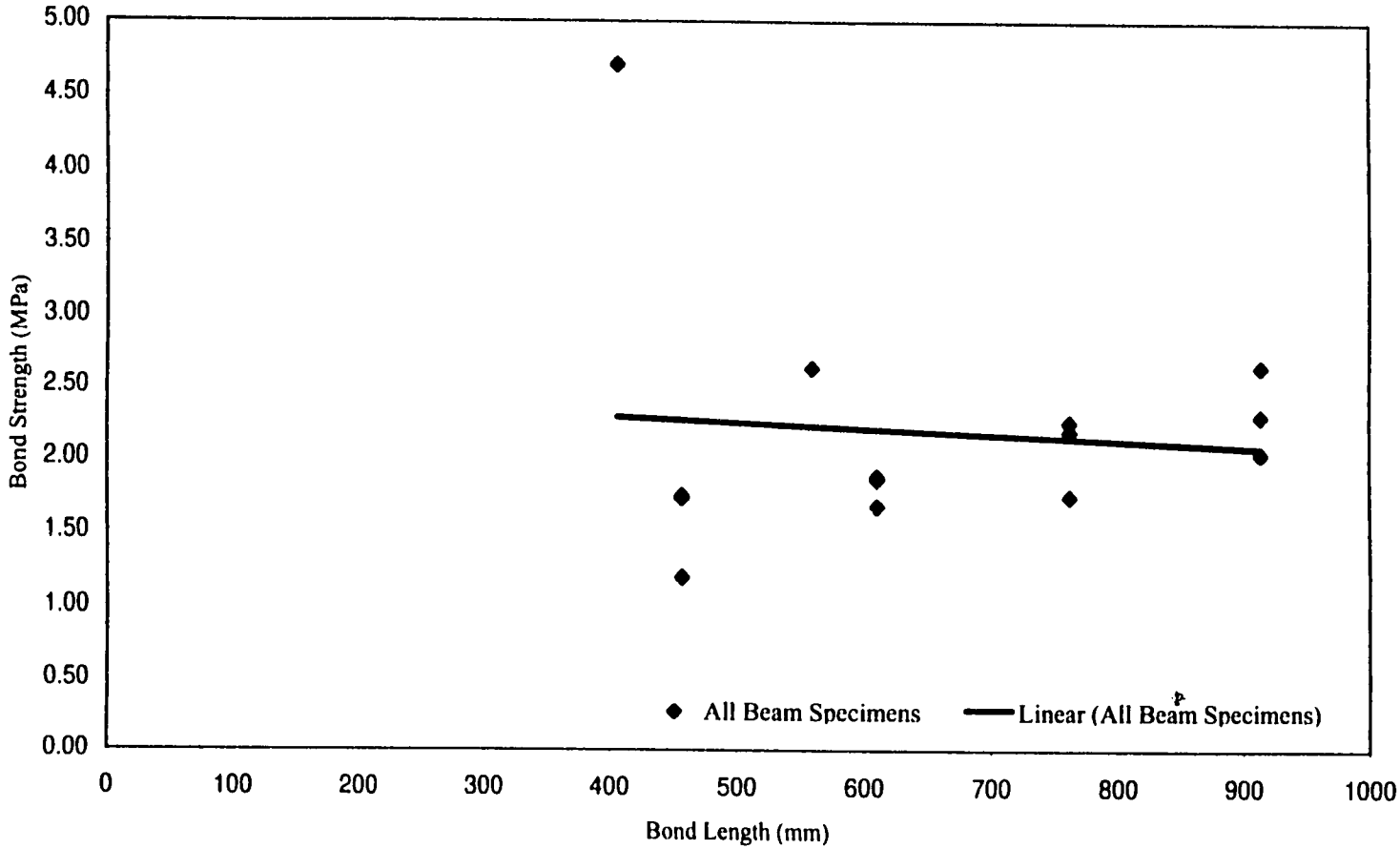

Figure M.1: Bond strength vs. bond length (G2-D9.79 bar, 0.05 mm free-end slip)

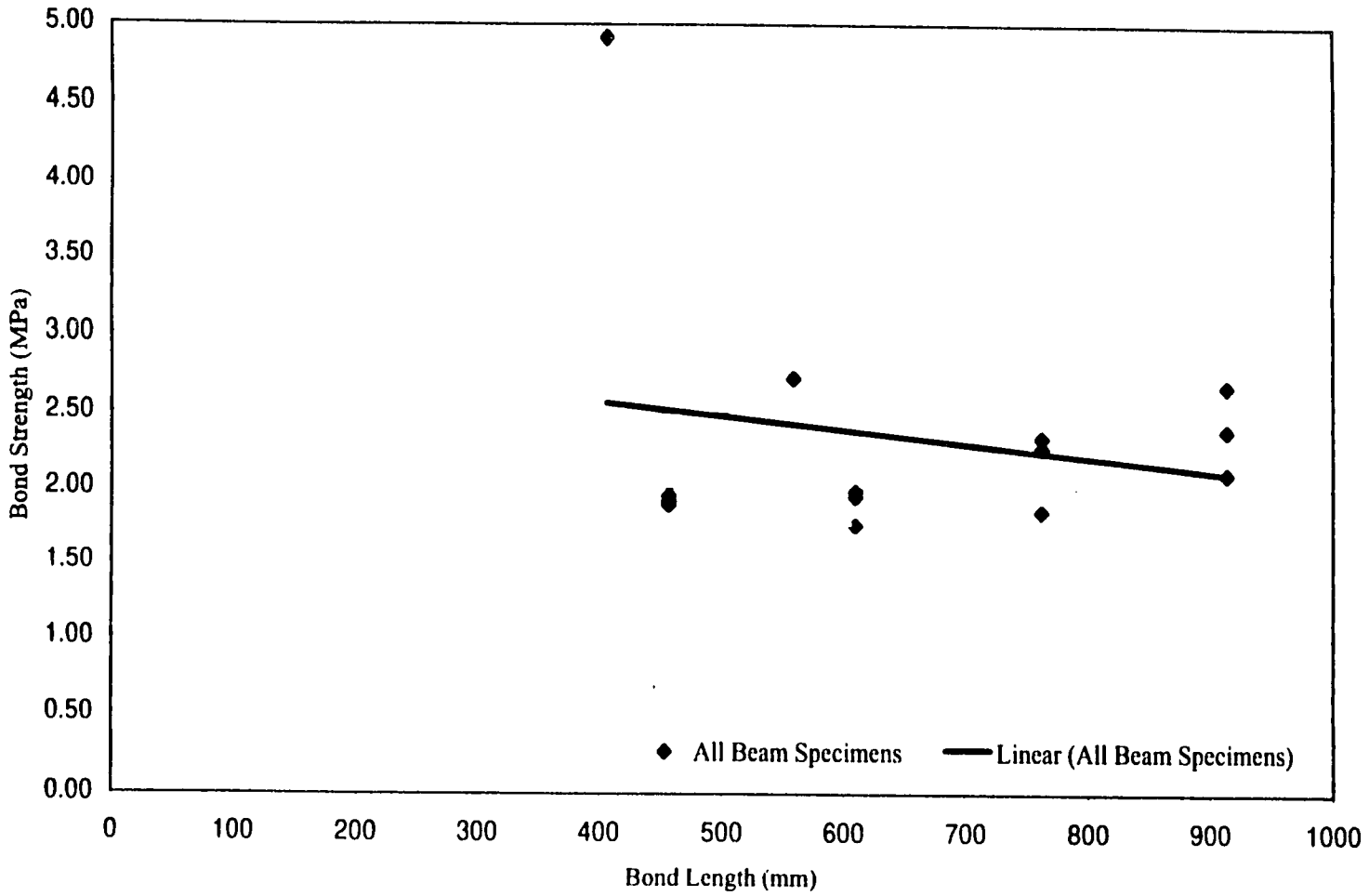

Figure M.2: Bond strength vs. bond length (G2-D9.79 bar, 0.10 mm free-end slip)

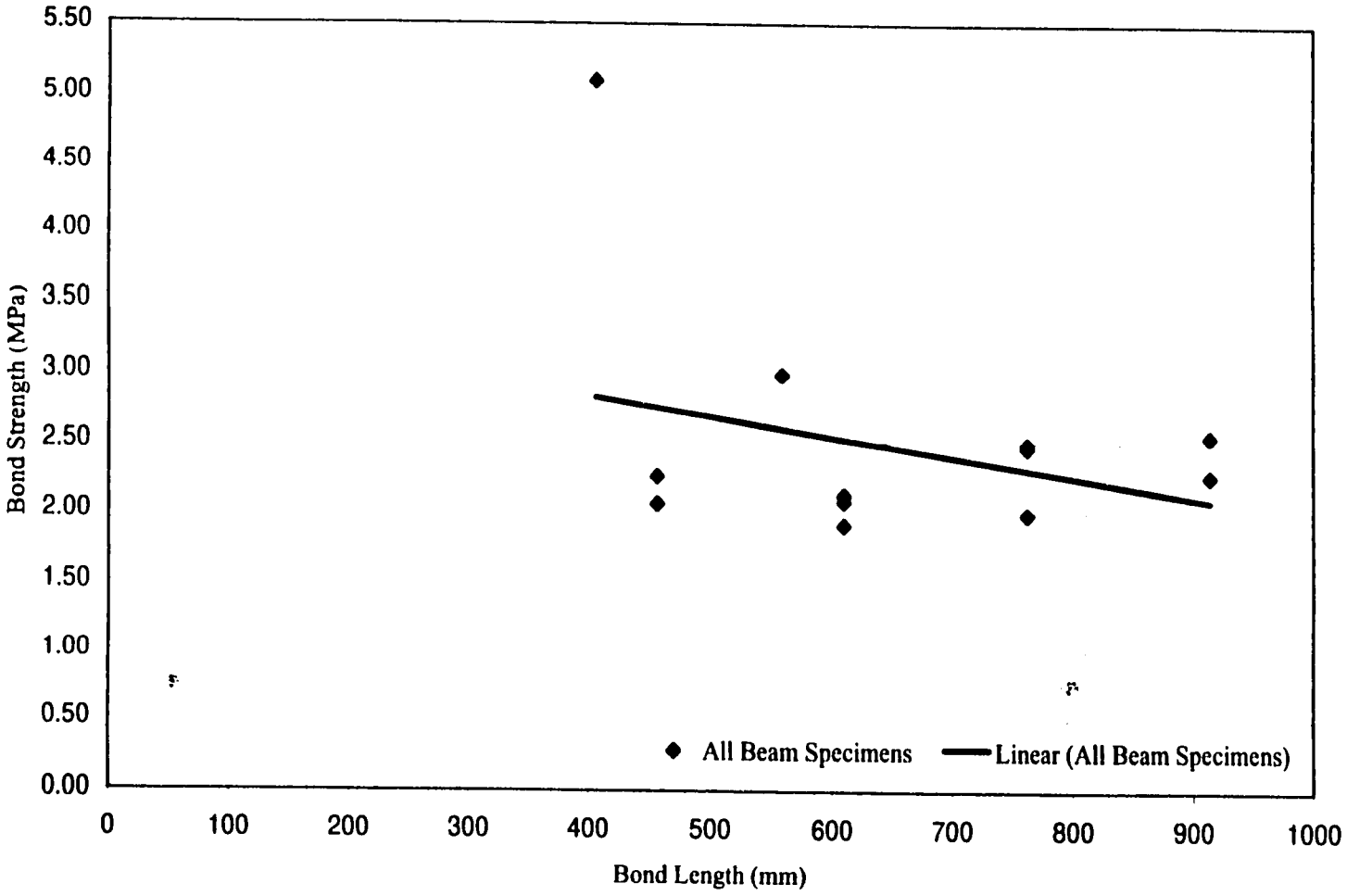

Figure M.3: Bond strength vs. bond length (G2-D9.79 bar, 0.25 mm free-end slip)

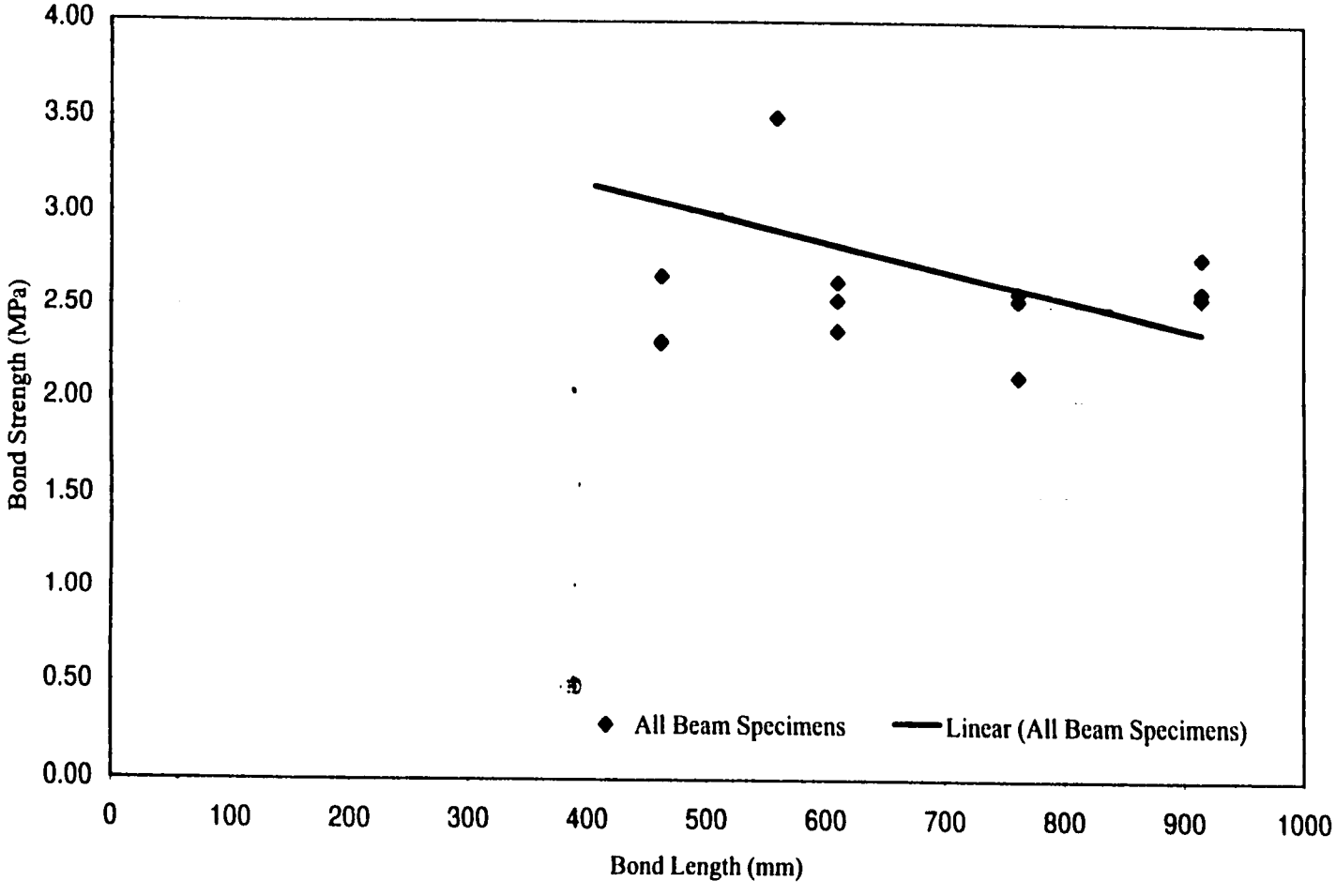

Figure M.4: Bond strength vs. bond length (G2-D9.79 bar, max. free-end slip)

Appendix N

Bond Strength vs. Free-end Slip (G2-D9.79 Bar)

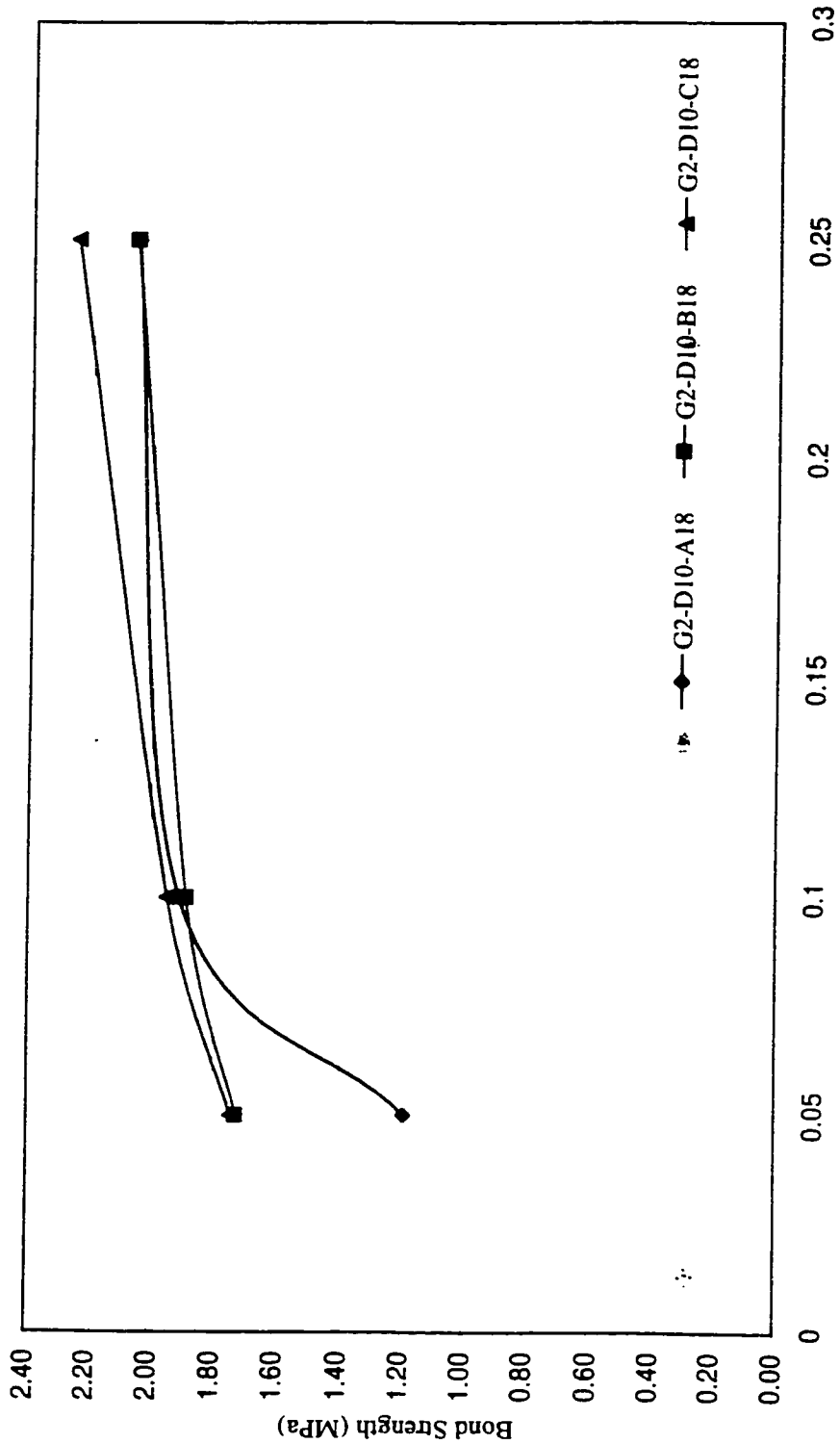

Figure N.1: Bond strength vs. free-end slip of beams G2-D9.79-A18, G2-D9.79-B18 and G2-D9.79-C18

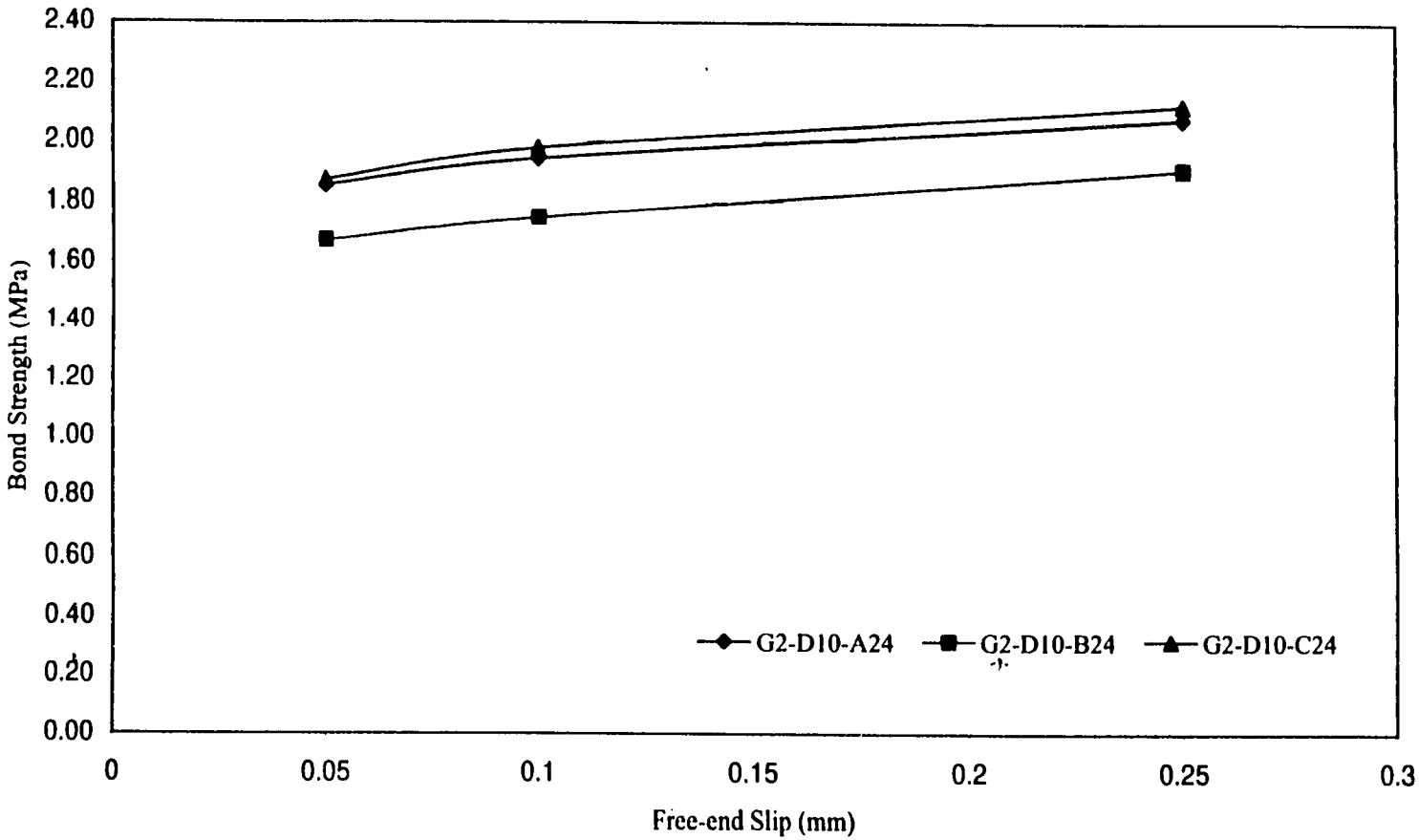

Figure N.2: Bond strength vs. free-end slip of beams G2-D9.79-A24, G2-D9.79-B24 and G2-D9.79-C24

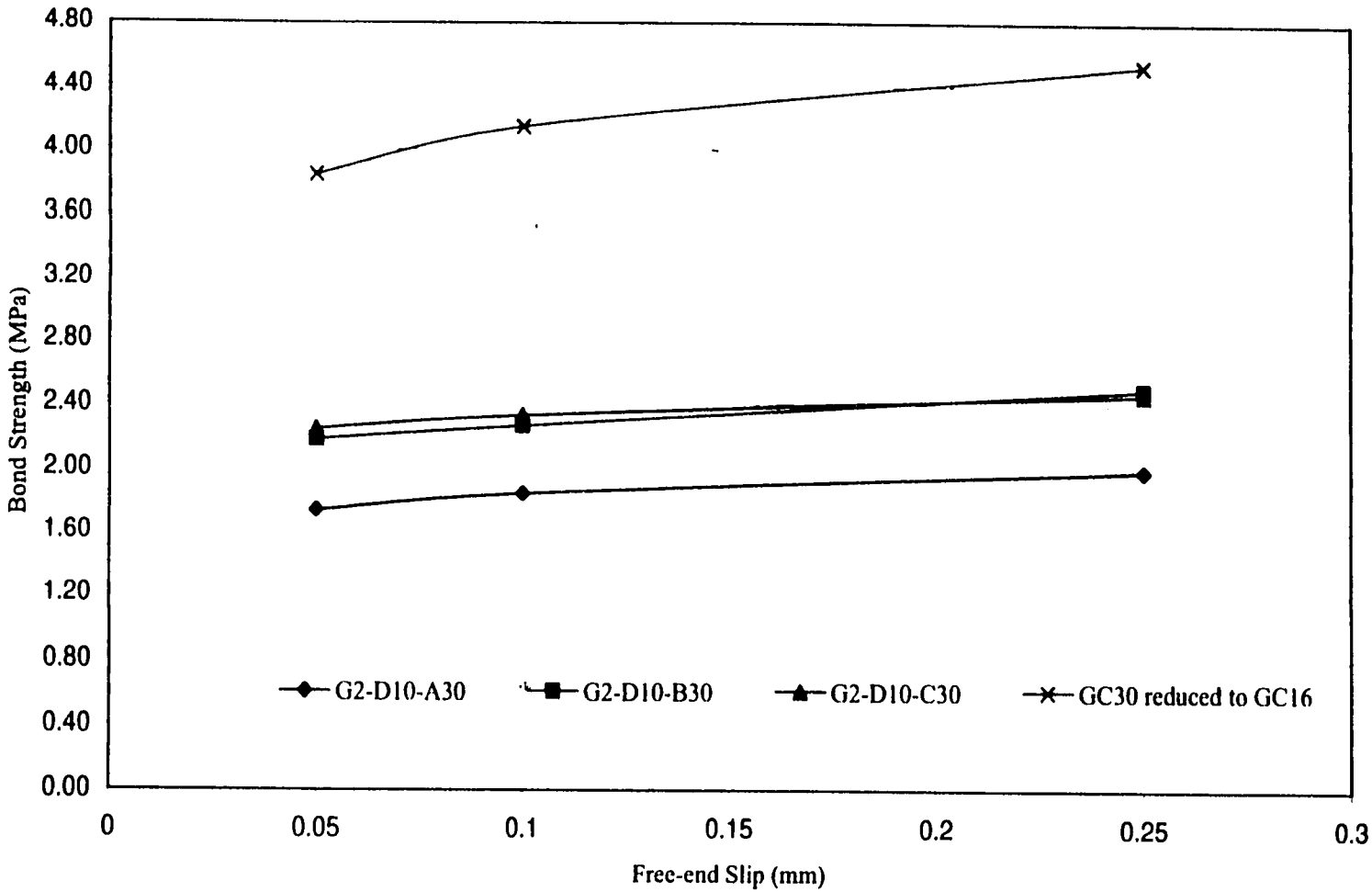

Figure N.3: Bond strength vs. free-end slip of beams G2-D9.79-A30, G2-D9.79-B30 and G2-D9.79-C30

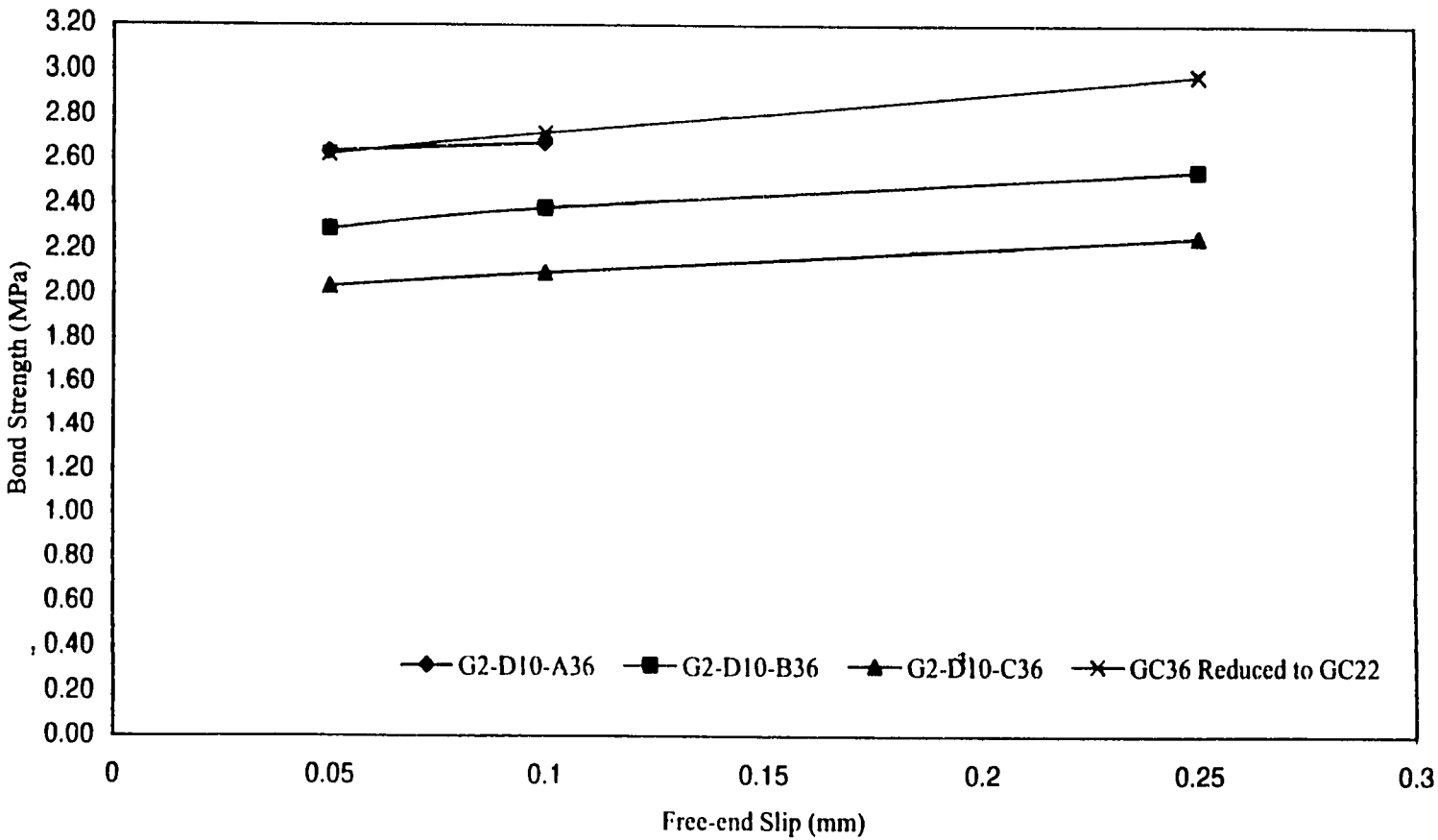

Figure N.4: Bond strength vs. free-end slip of beams G2-D9.79-A36, G2-D9.79-B36 and G2-D9.79-C36

Appendix O

Tensile Force vs. Bond Length (G2-D9.79 Bar, Loaded-end Slip)

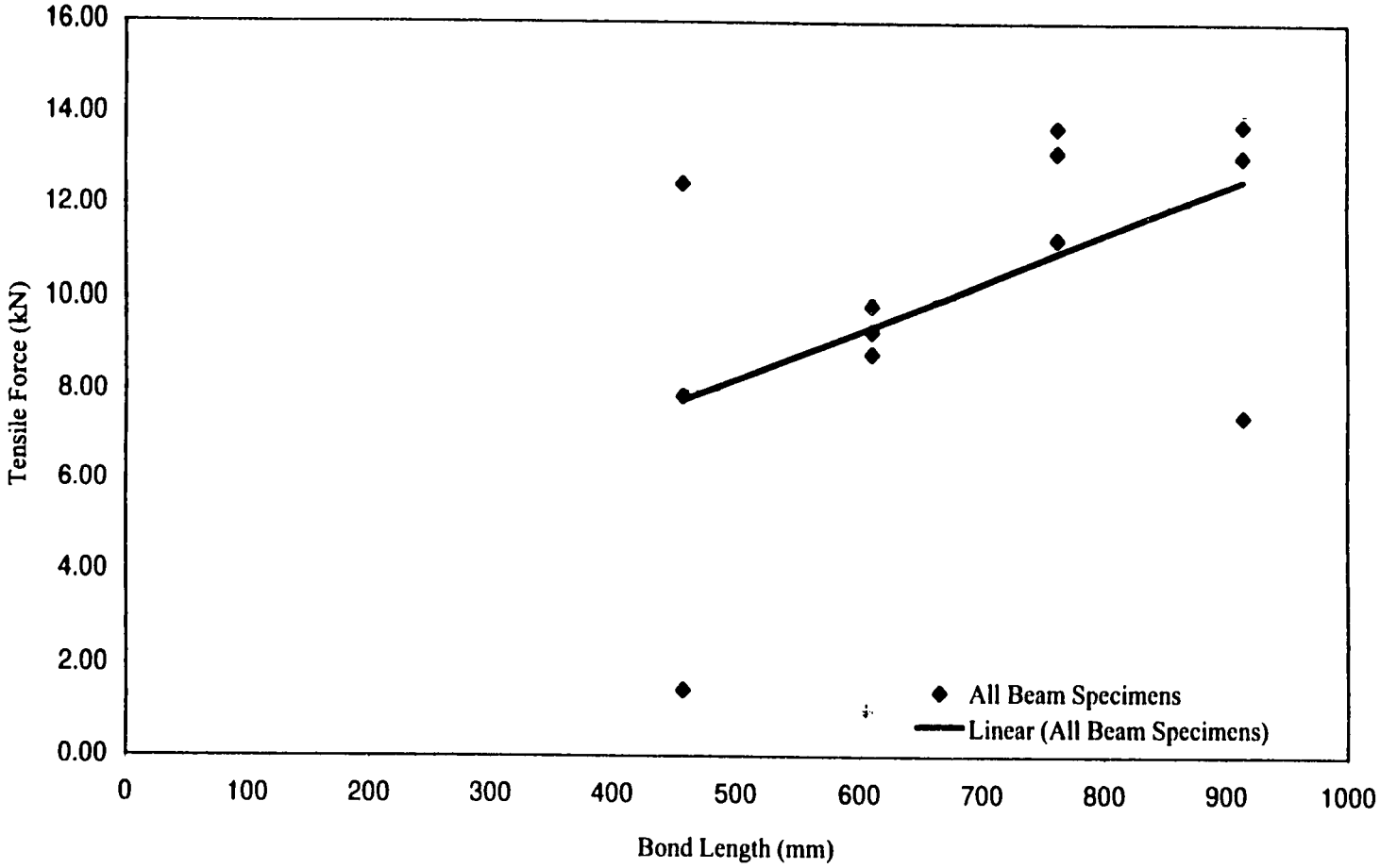

Figure O.1: Tensile force vs. bond length (G2-D9.79 bar, 0.25 mm loaded-end slip)

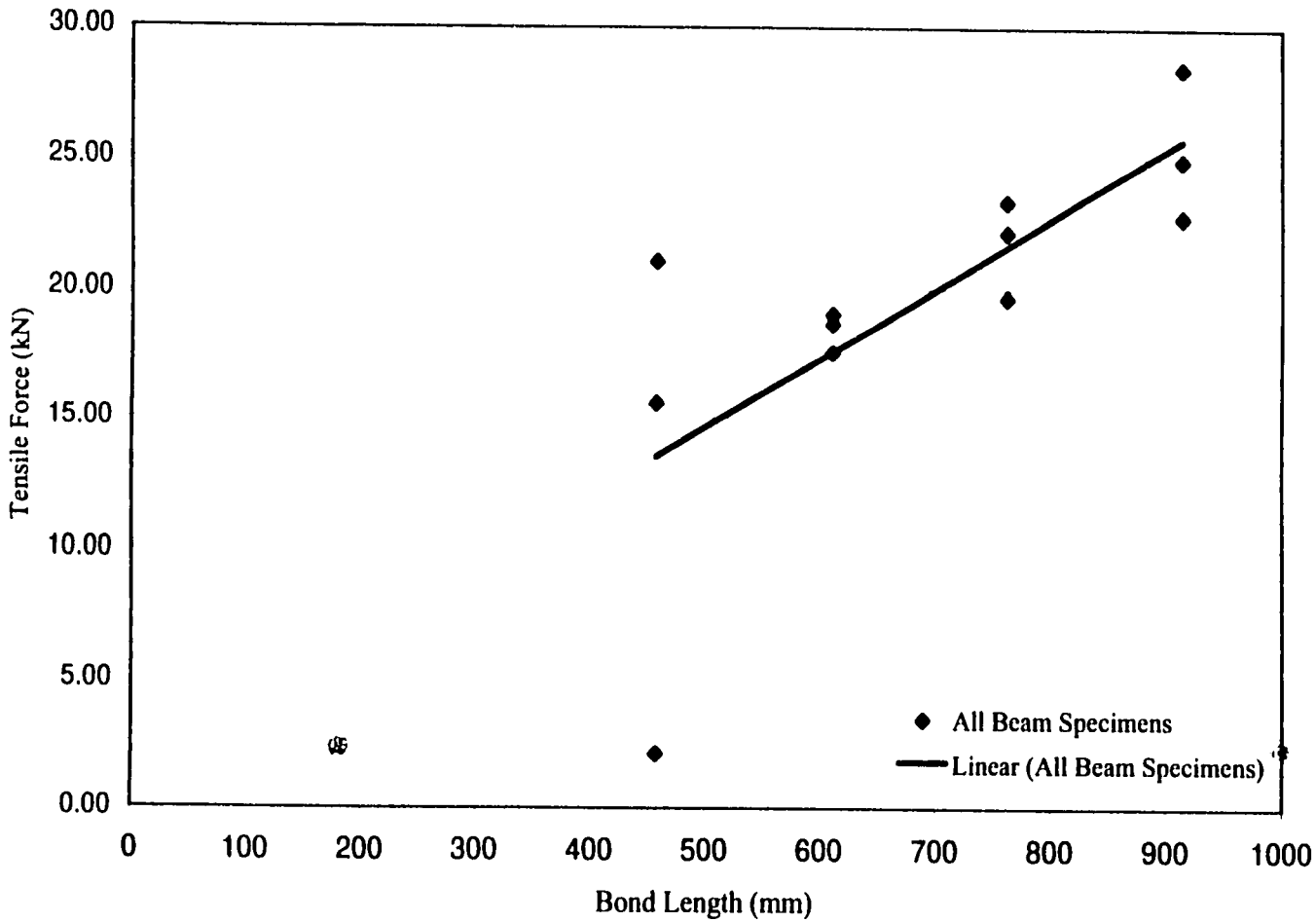

Figure O.2: Tensile force vs. bond length (G2-D9.79 bar, 0.50 mm loaded-end slip)

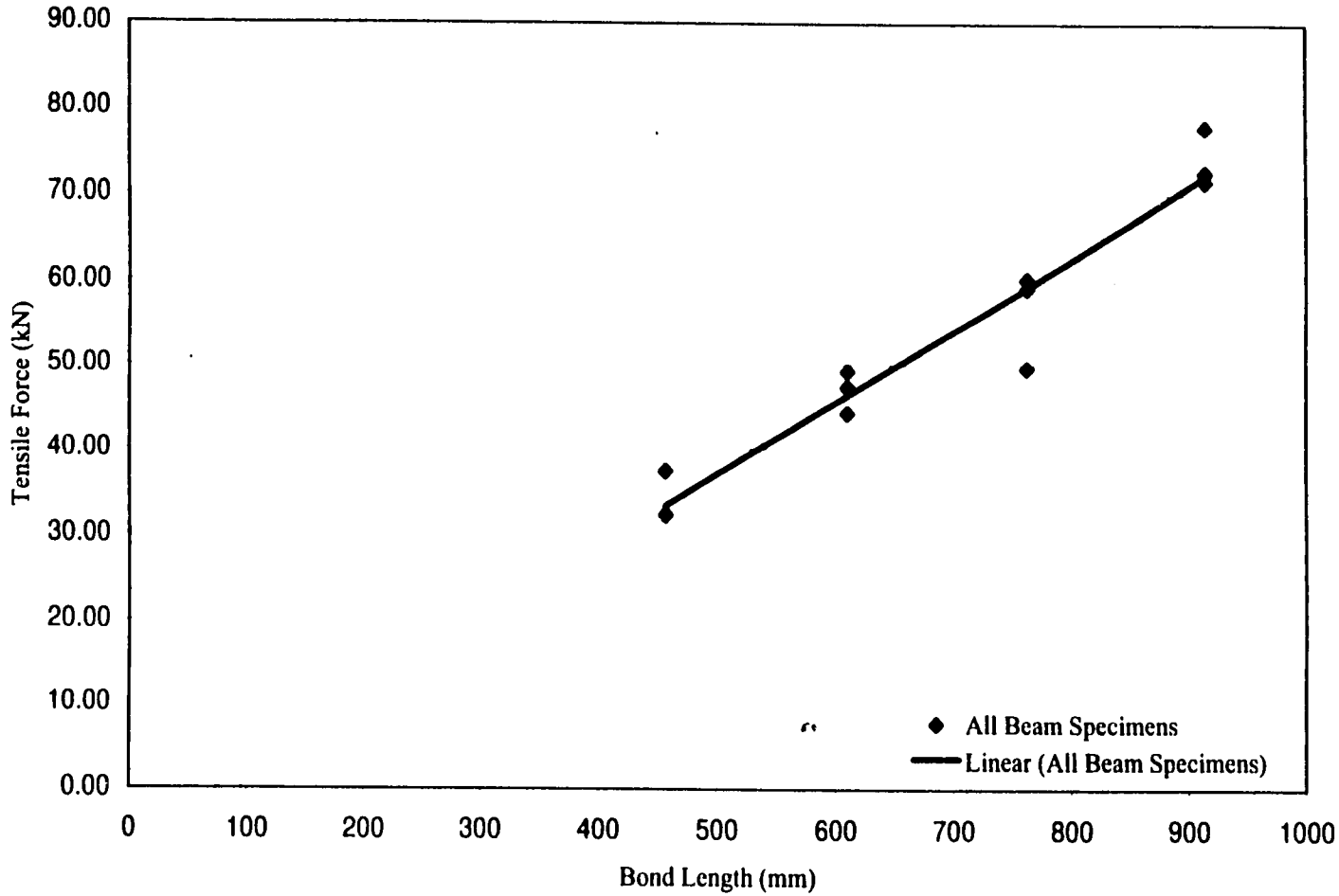

Figure O.3: Tensile force vs .bond length (G2-D9.79 bar, max. loaded-end slip)

Appendix P

Bond Strength vs. Bond Length (G2-D9.79 Bar, Loaded-end Slip)

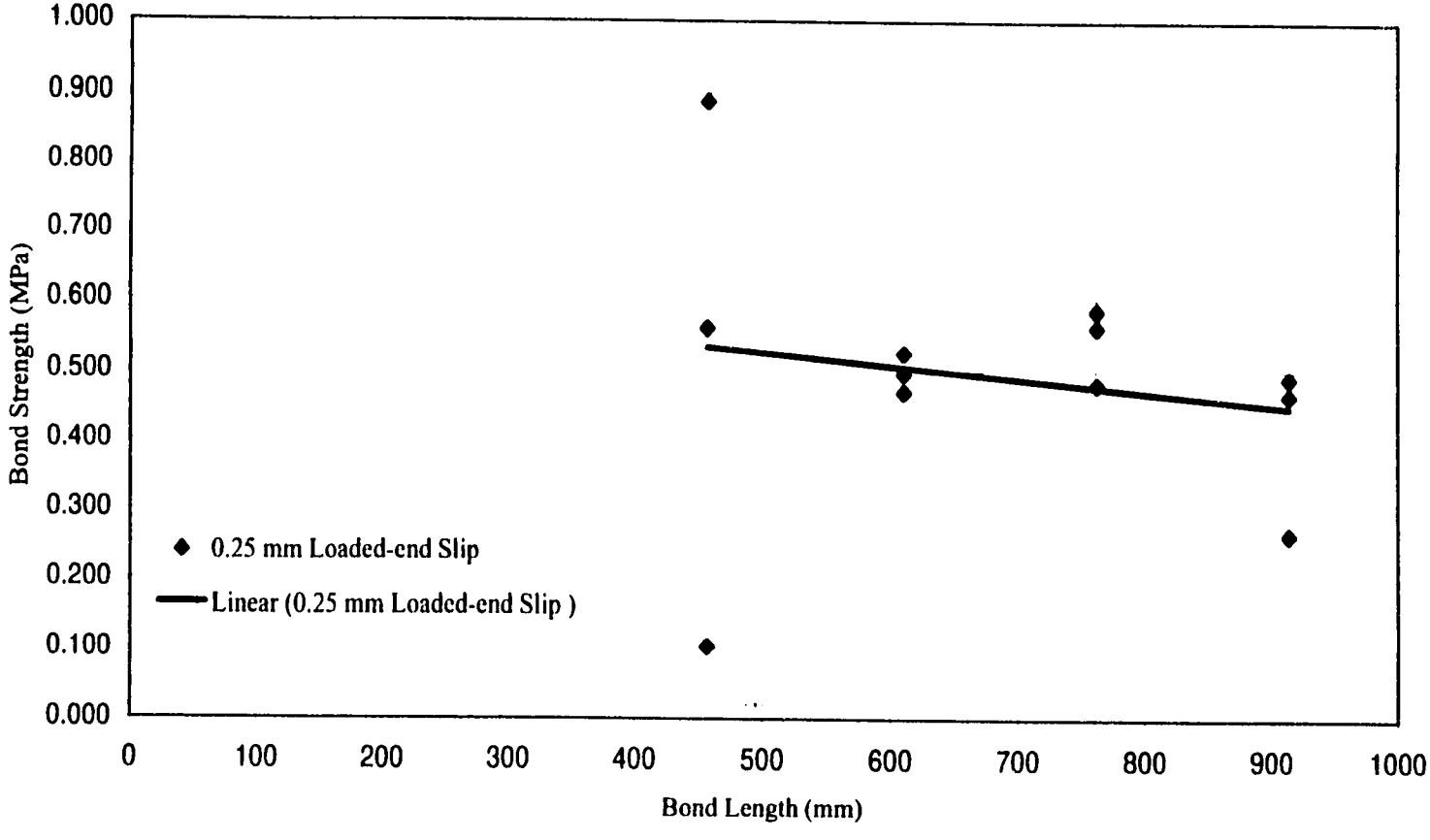

Figure P.1: Bond strength vs. bond length (G2-D9.79 bar, 0.25 mm loaded-end slip)

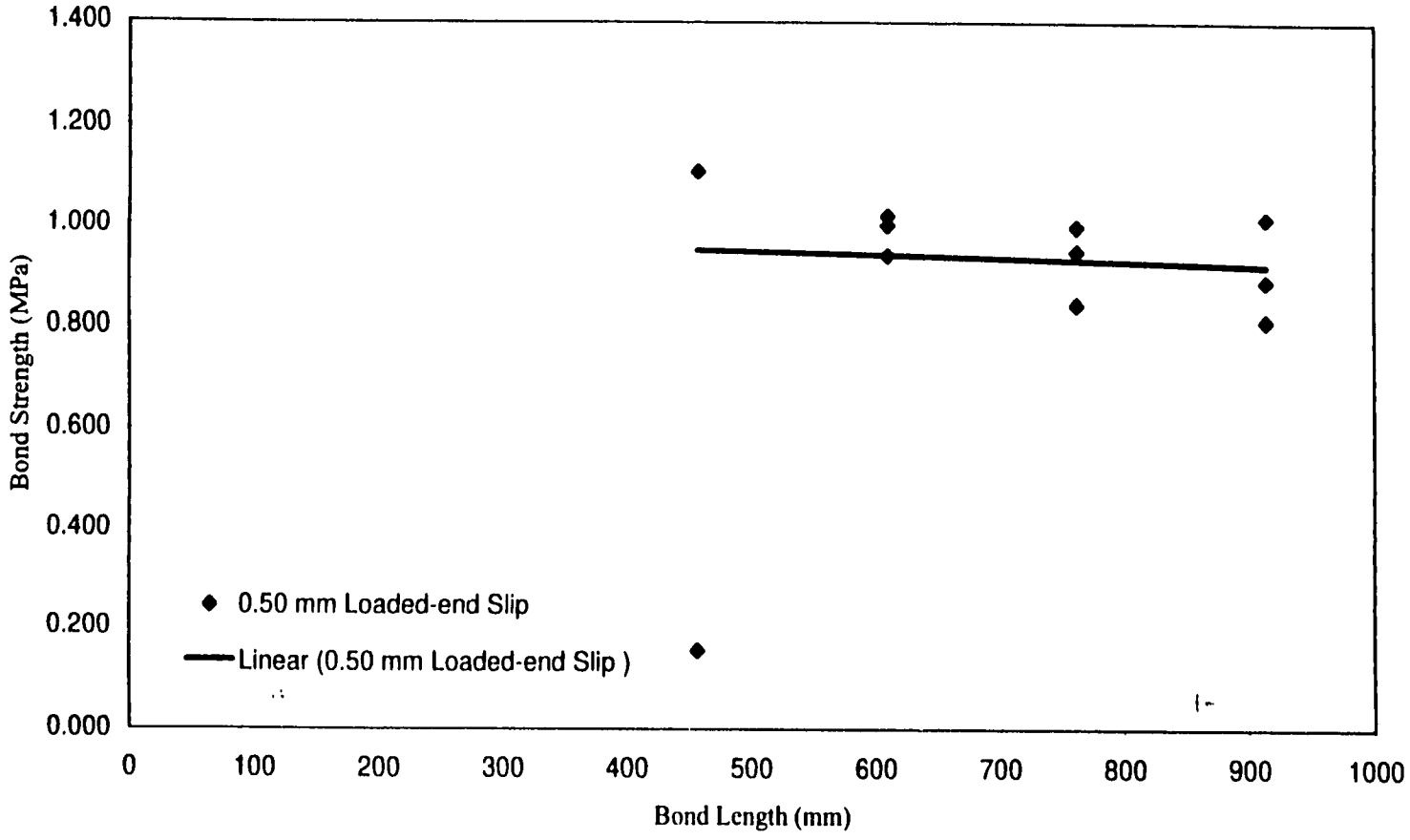

Figure P.2: Bond strength vs. bond length (G2-D9.79 bar, 0.50 mm loaded-end slip)

Appendix Q

Bond Strength vs. $\sqrt{f_c'}$ (G2-D9.79 Bar, Free-end Slip)

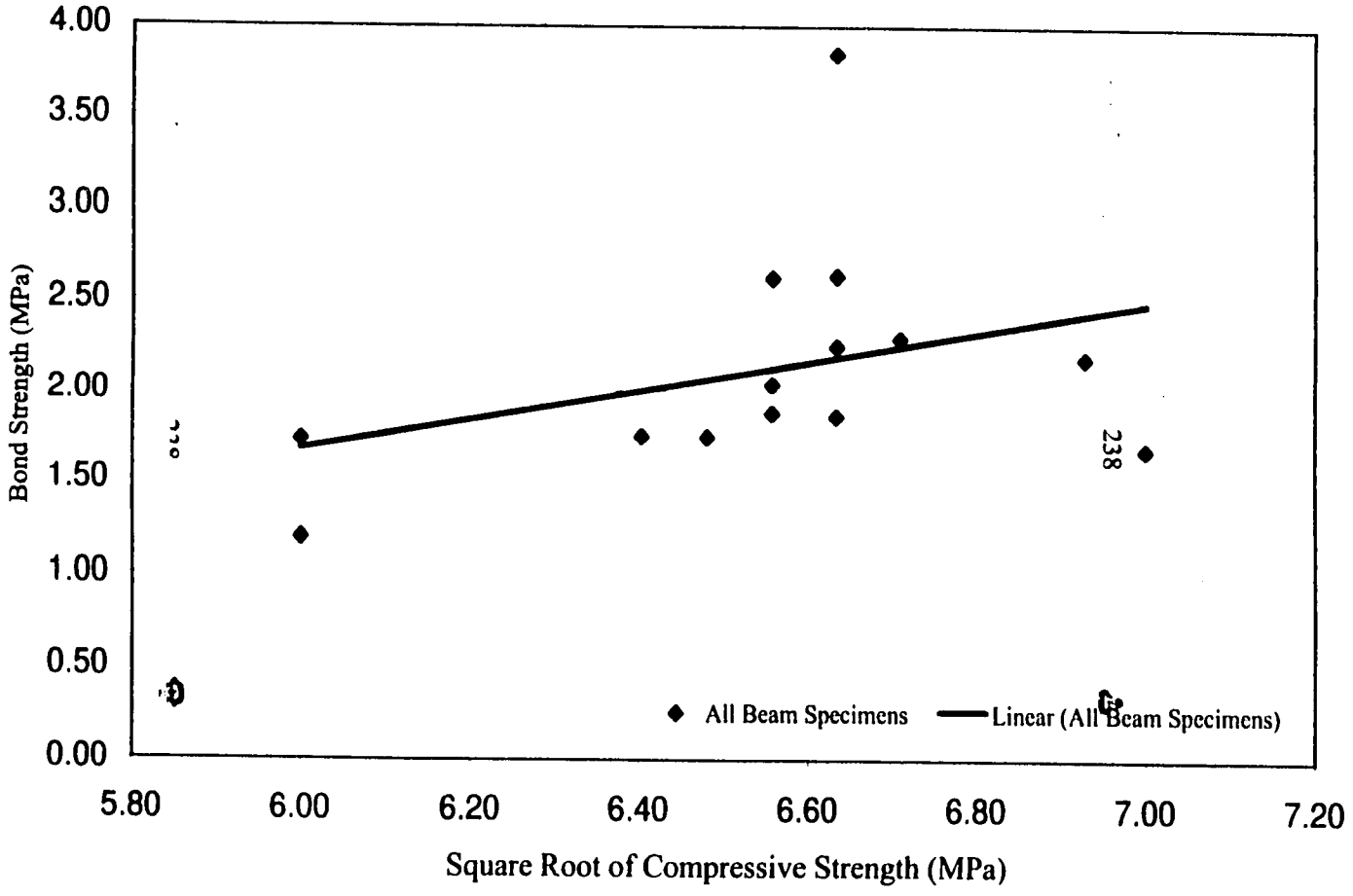

Figure Q.1: Bond strength vs. square root concrete compressive strength (G2-D9.79 bar, 0.05 mm free-end slip)

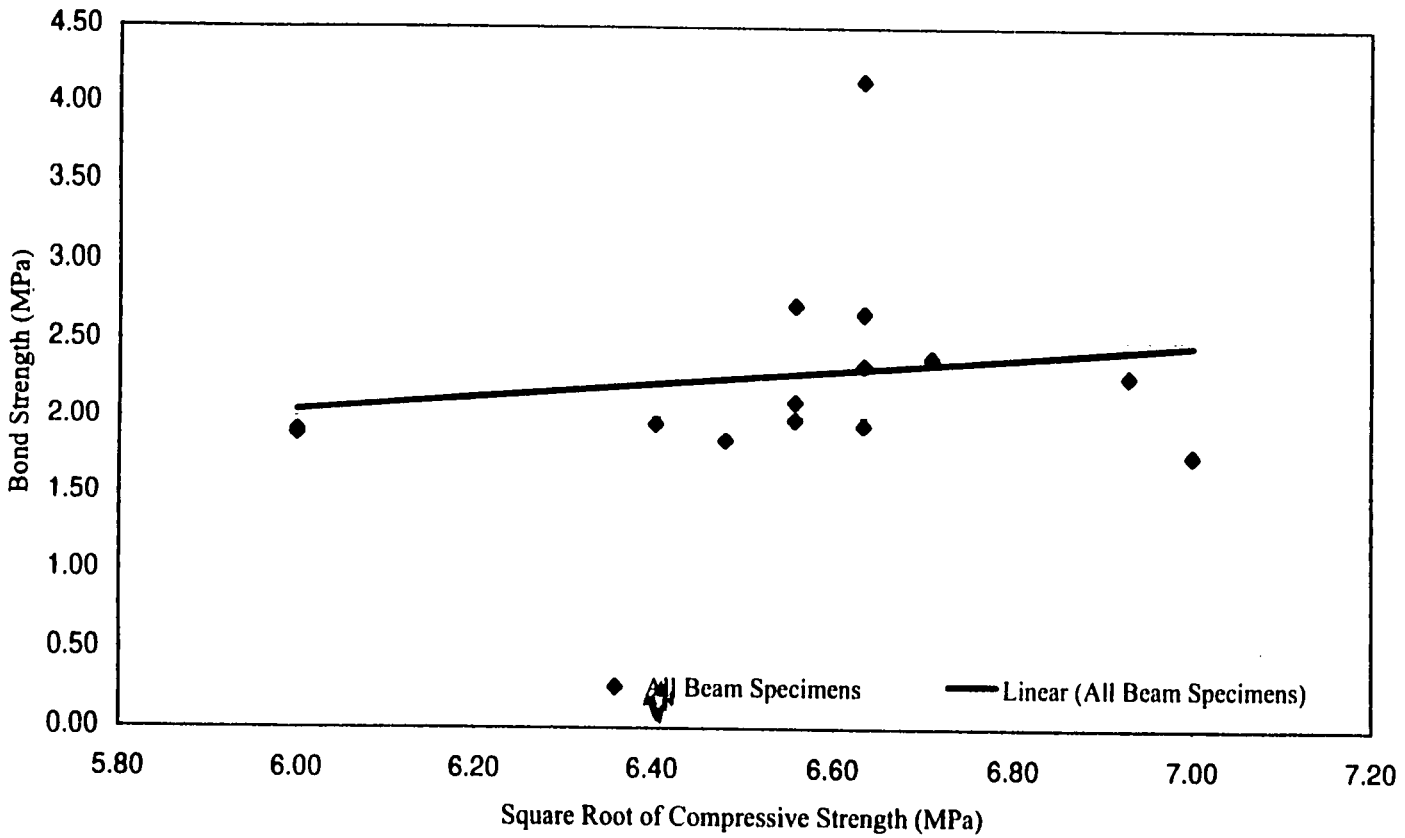

Figure Q.2: Bond strength vs. square root concrete compressive strength (G2-D9.79 bar, 0.10 mm free-end slip)

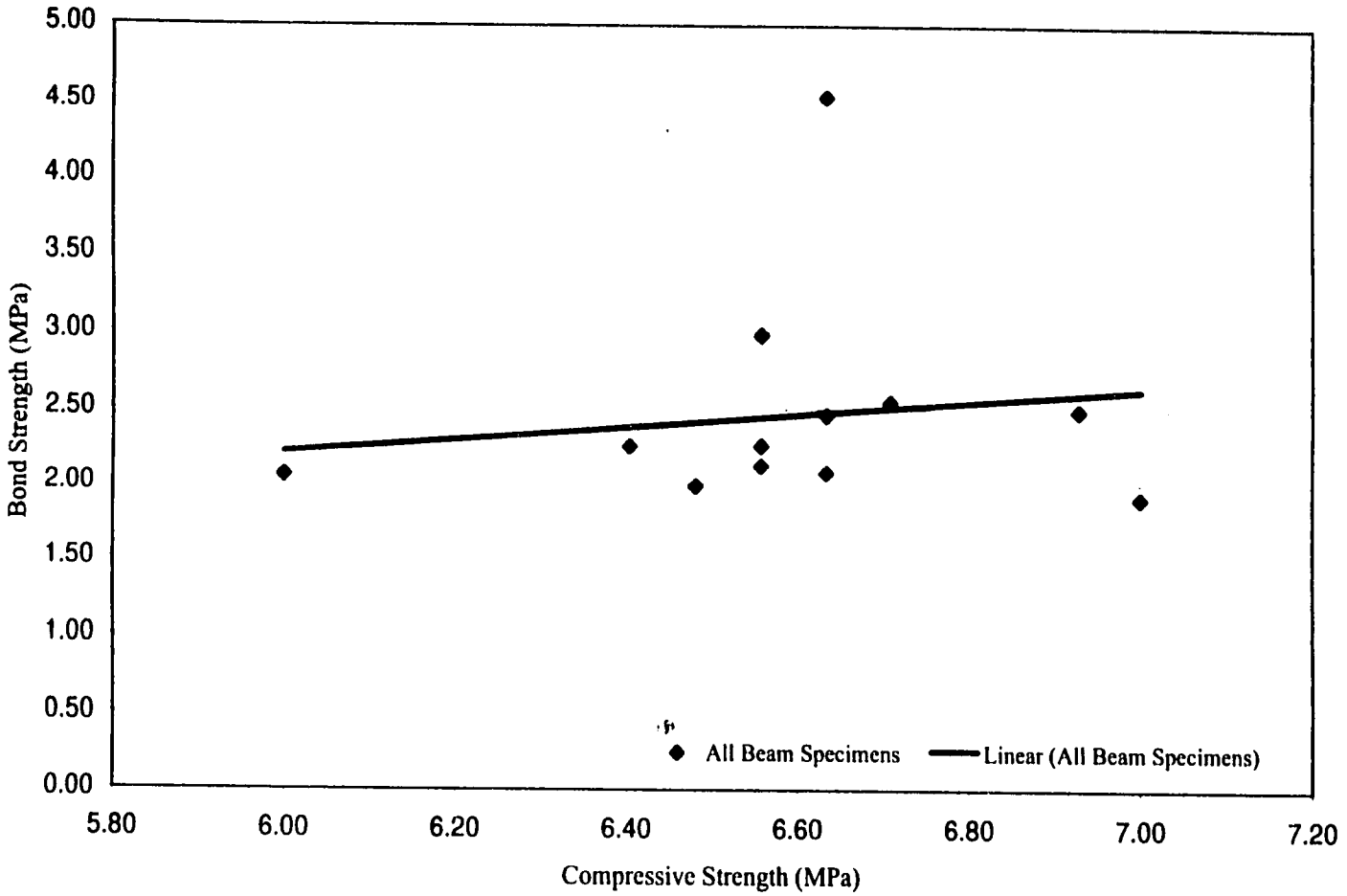

Figure Q.3: Bond strength vs. square root of concrete compressive strength
(G2-D9.79 bar, 0.25 mm free-end slip)

Appendix R

Effect of Transverse Reinforcement on Bond Strength (G2-D9.79 Bar)

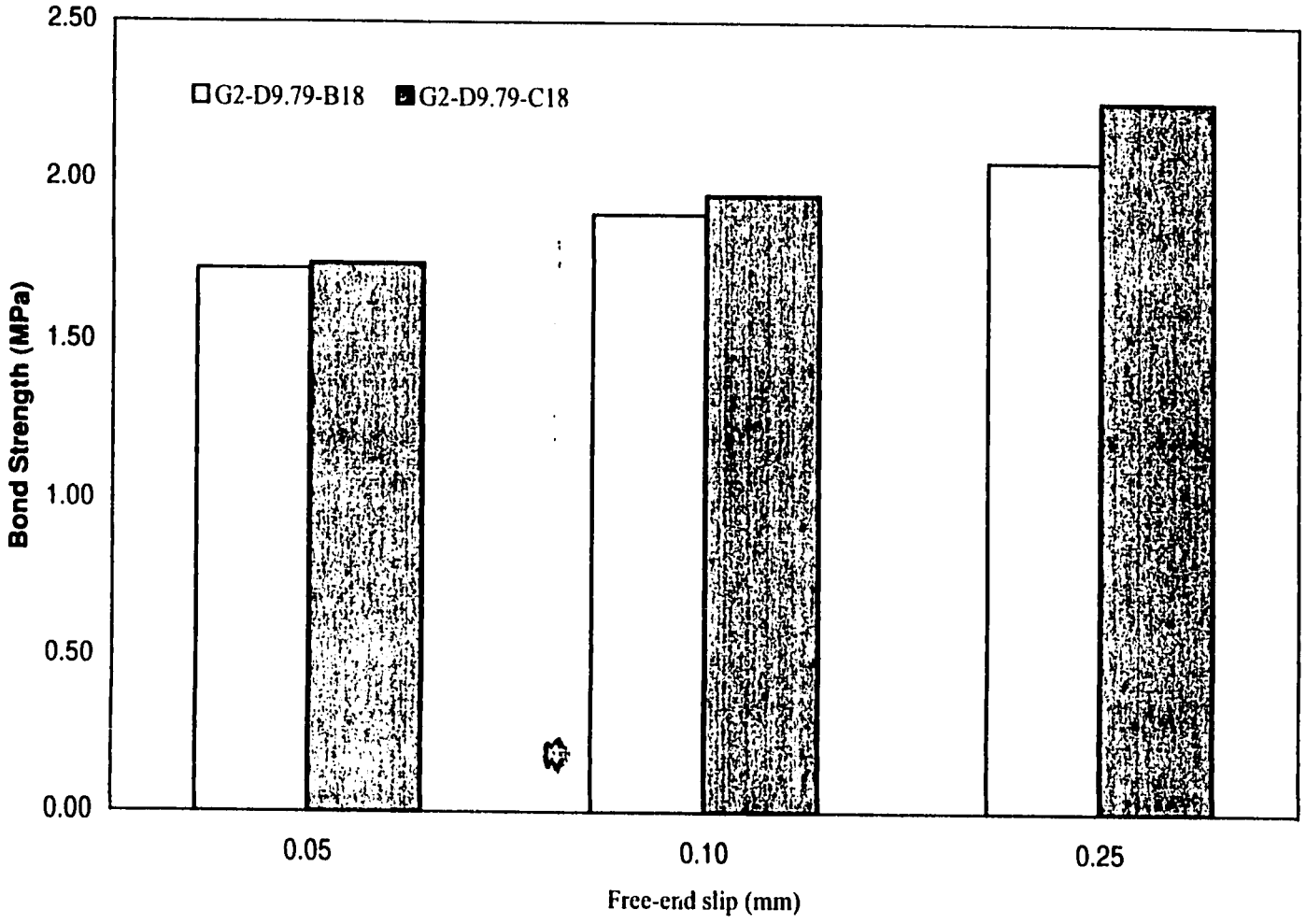

Figure R.1: Effect of trasnverse reinforcement on bond strength (beams G2-D9.79-B18 and G2-D9.79-C18)

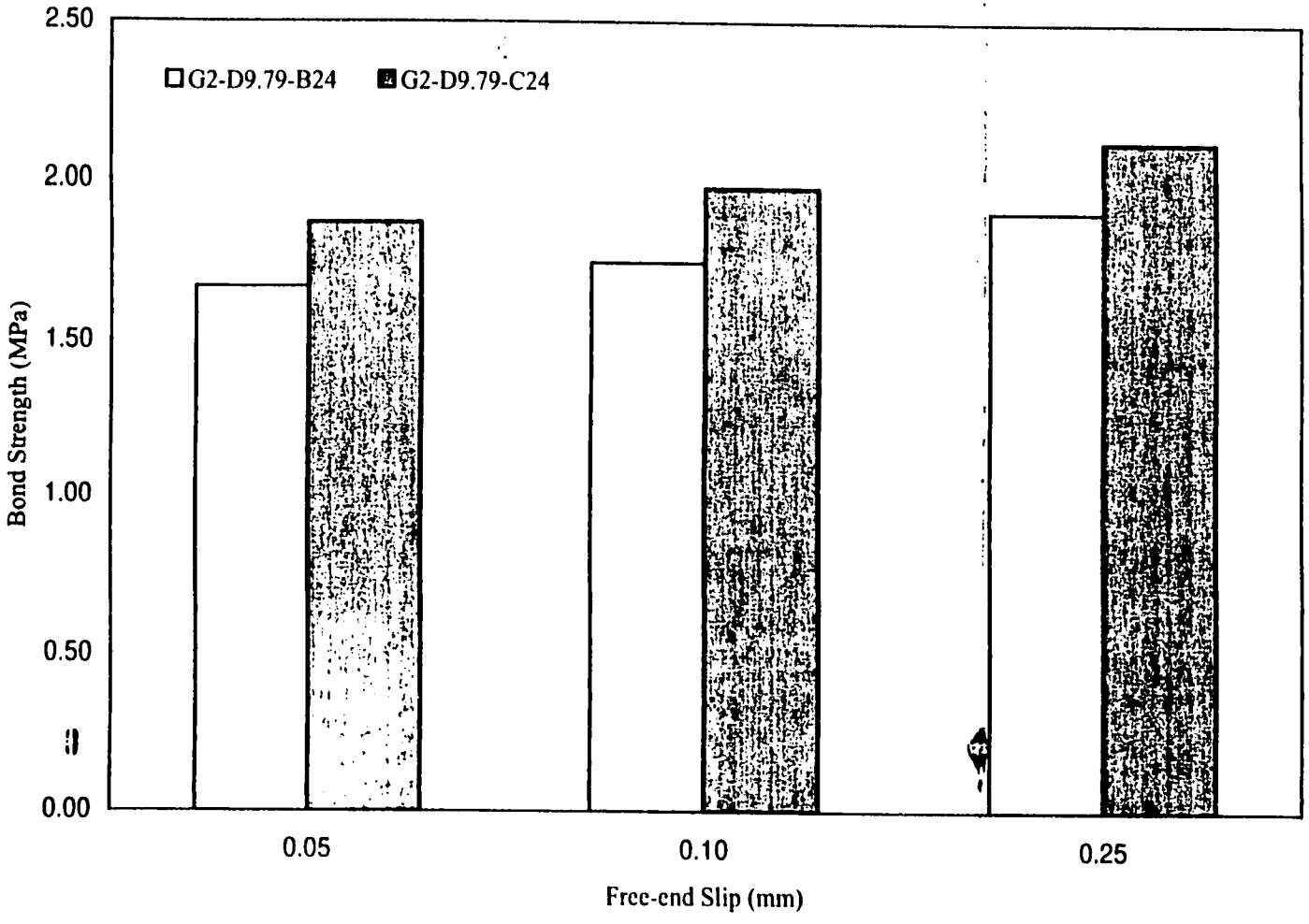

Figure R.2: Effect of transverse reinforcement on bond strength (beams G2-D9.79-B24 and G2-D9.79-C24)

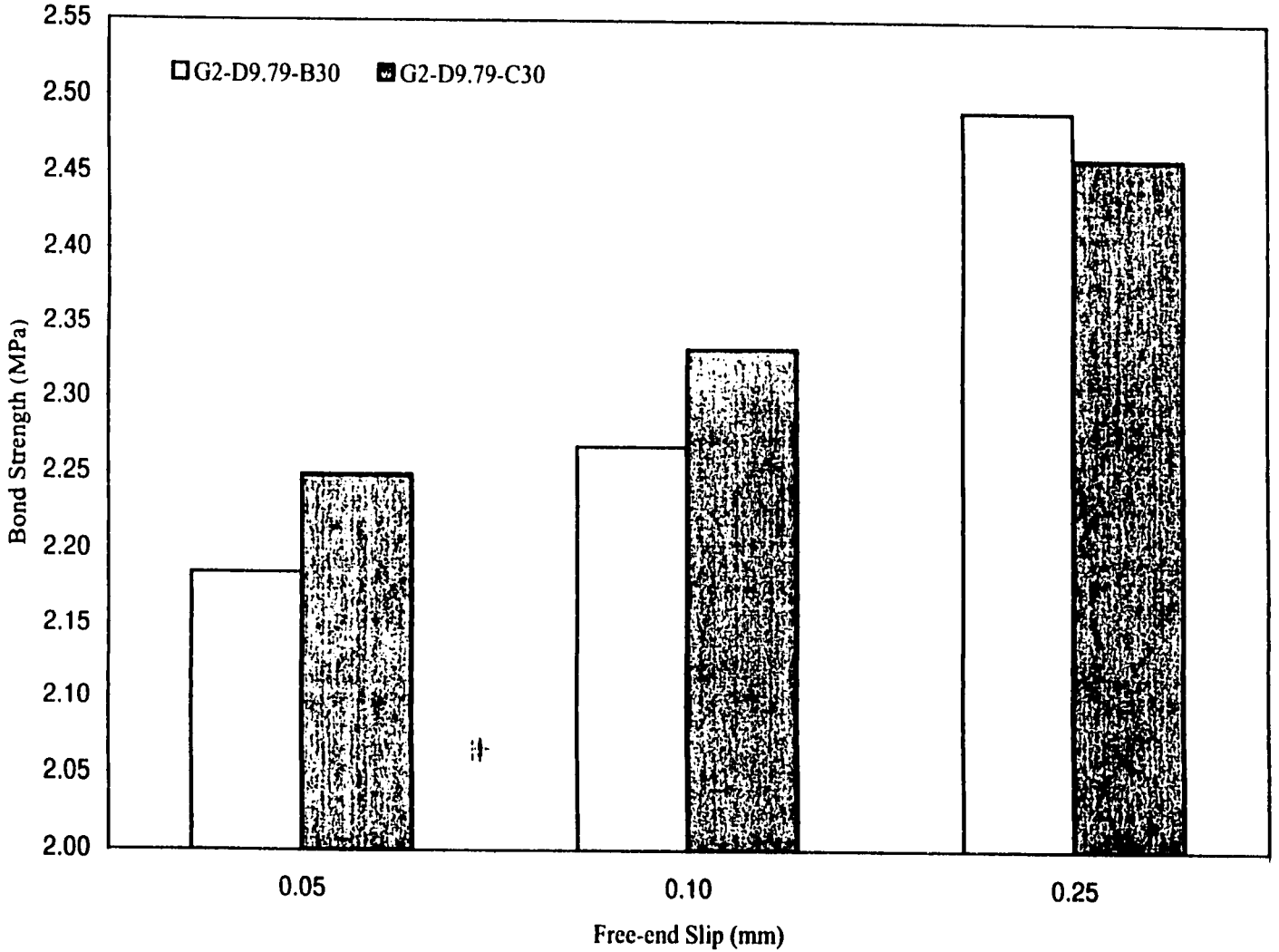

Figure R.3: Effect of transverse reinforcement on bond strength (beams G2-D9.79-B30 and G2-D9.79-C30)

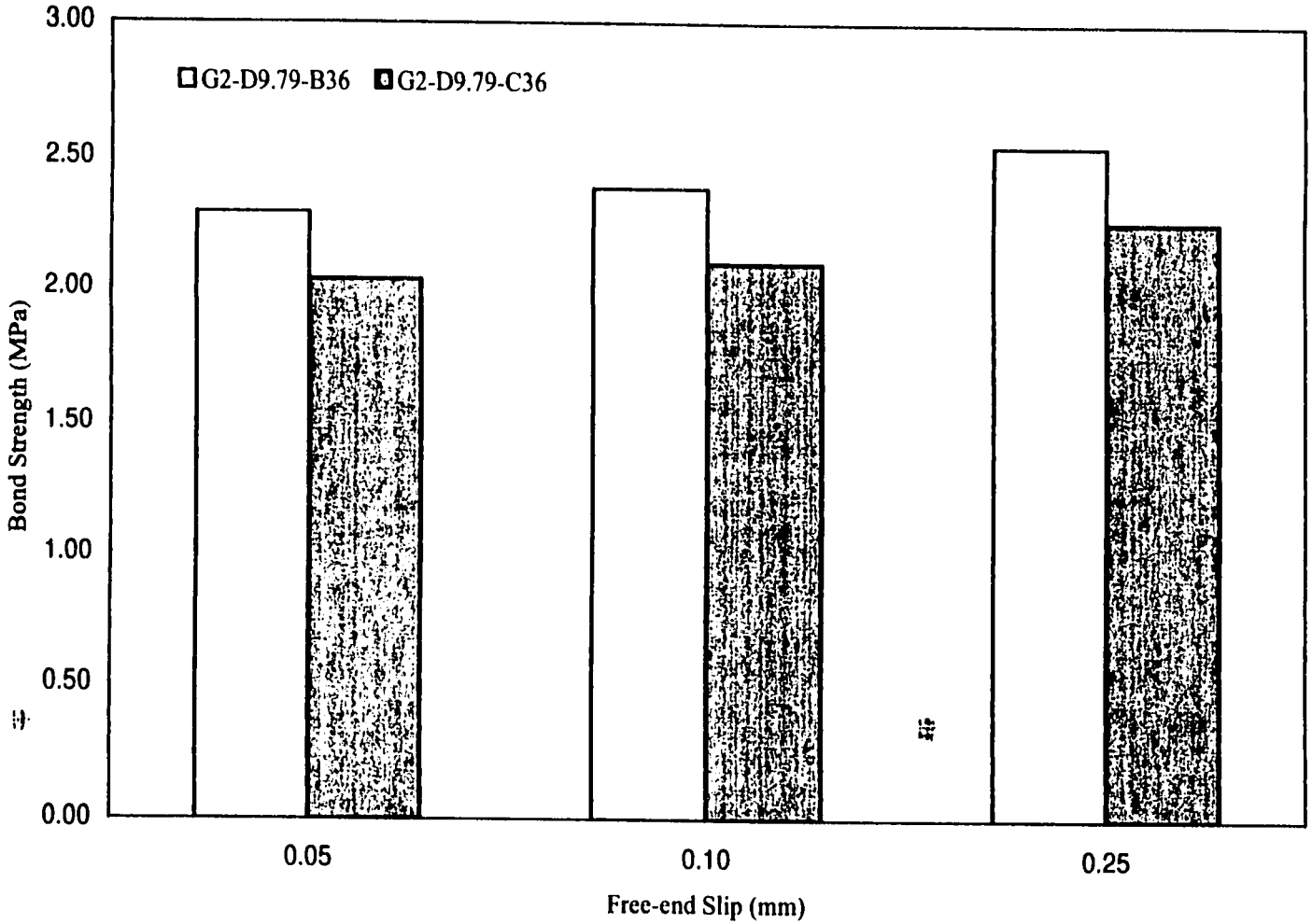

Figure R.4: Effect of transverse reinforcement on bond strength (beams G2-D9.79-B36 and G2-D9.79-C36)

Appendix S

Tensile Force vs. Bond Length (D1-D9.70 Bar, Free-end Slip)

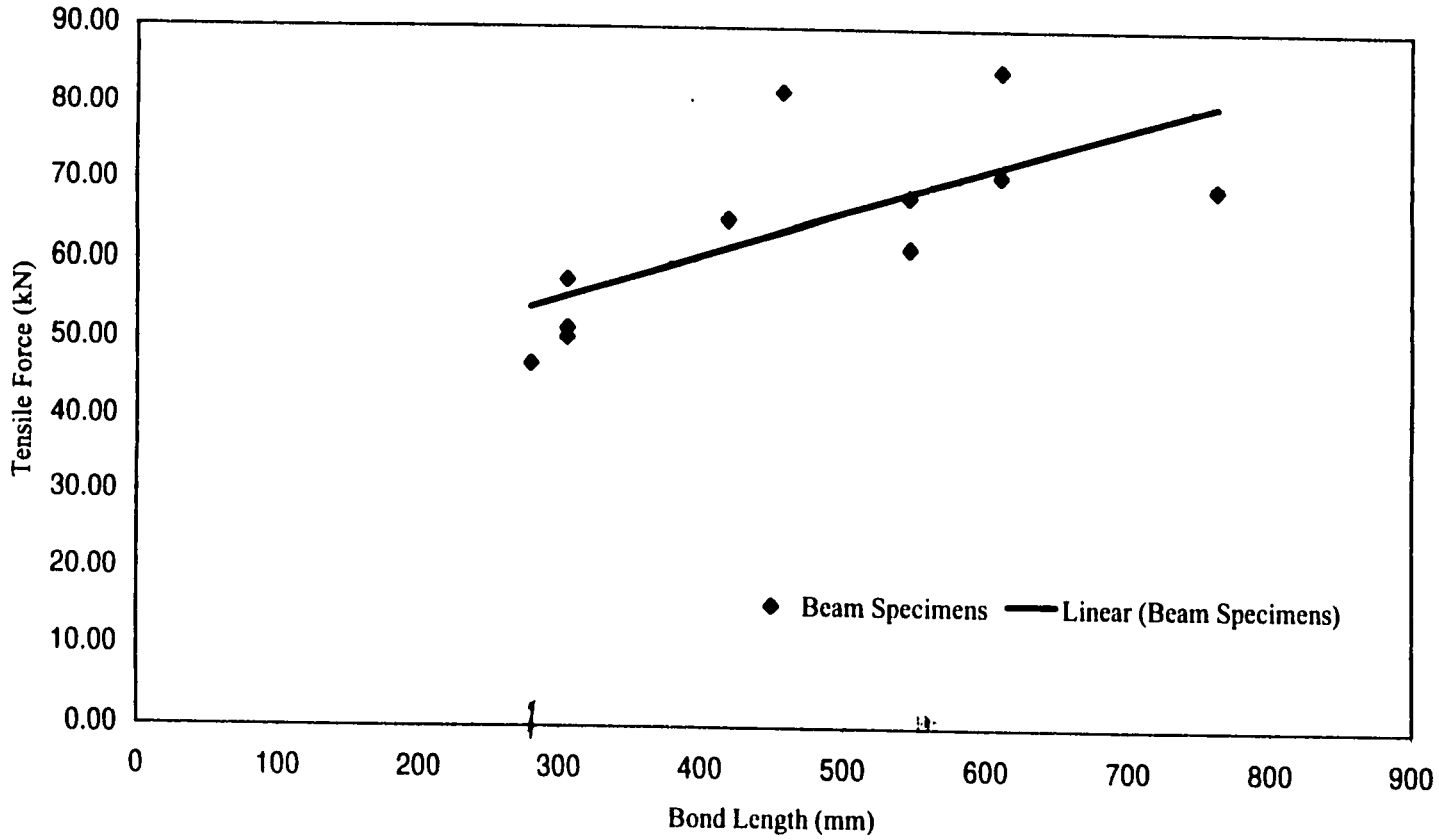

Figure S.1: Tensile force vs. bond length (D1-D9.70 bar, 0.05 mm free-end slip)

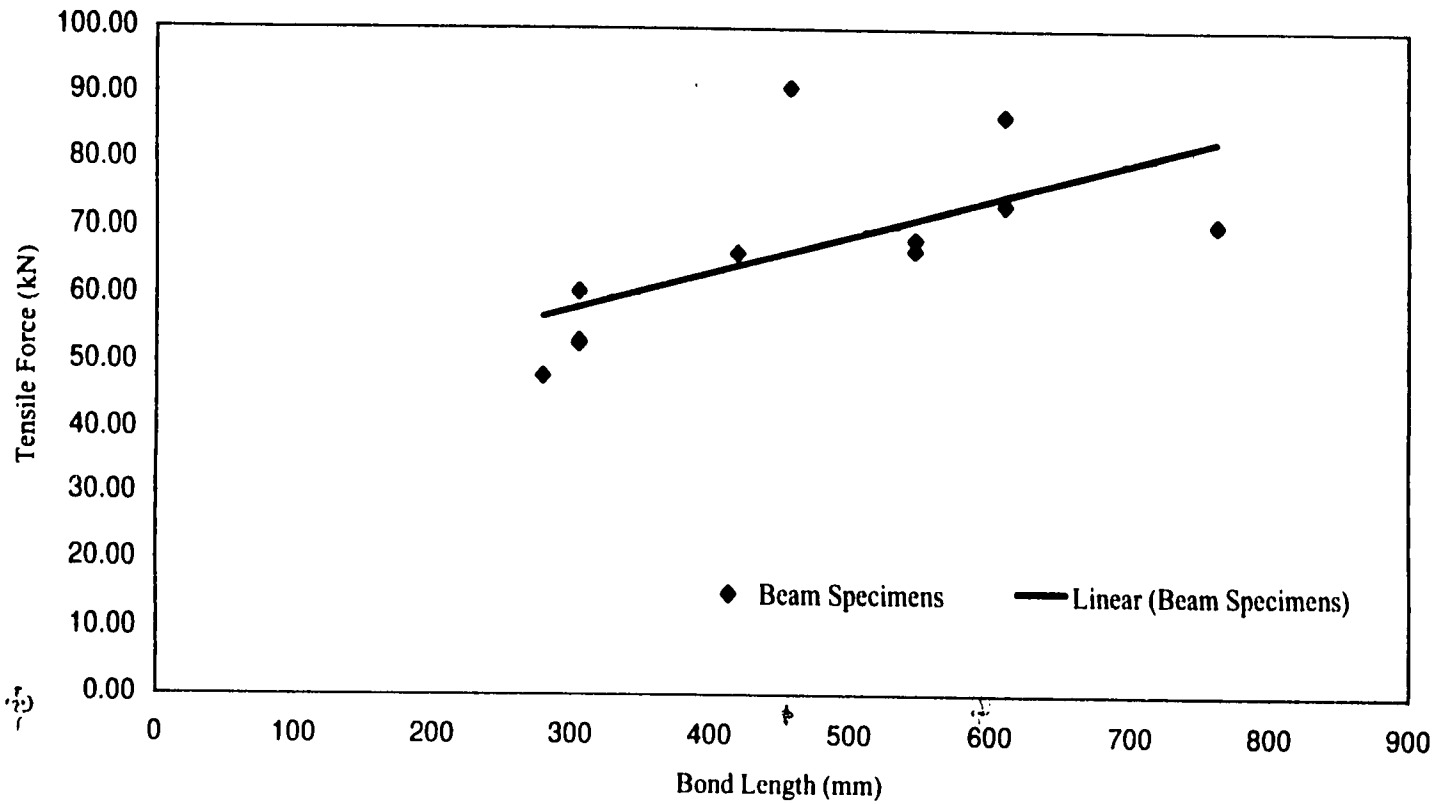

Figure S.2: Tensile force vs. bond length (D1-D9.70 bar, 0.10 mm free-end slip)

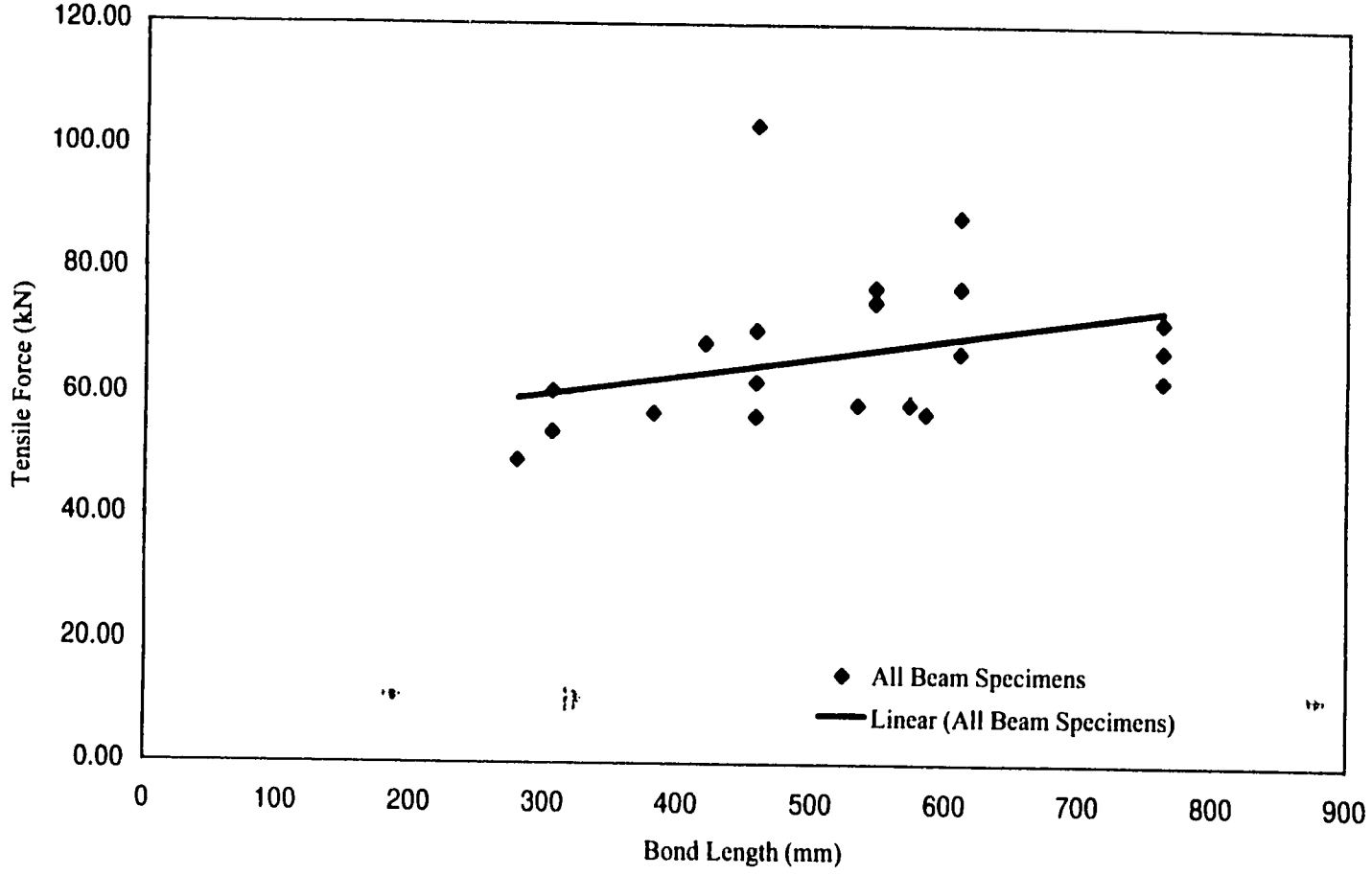

Figure S.3: Maximum tensile force vs. bond length (D1-D9.70 bar, free-end slip)

Appendix T

Bond Strength vs. Bond Length (D1-D9.70 Bar, Free-end Slip)

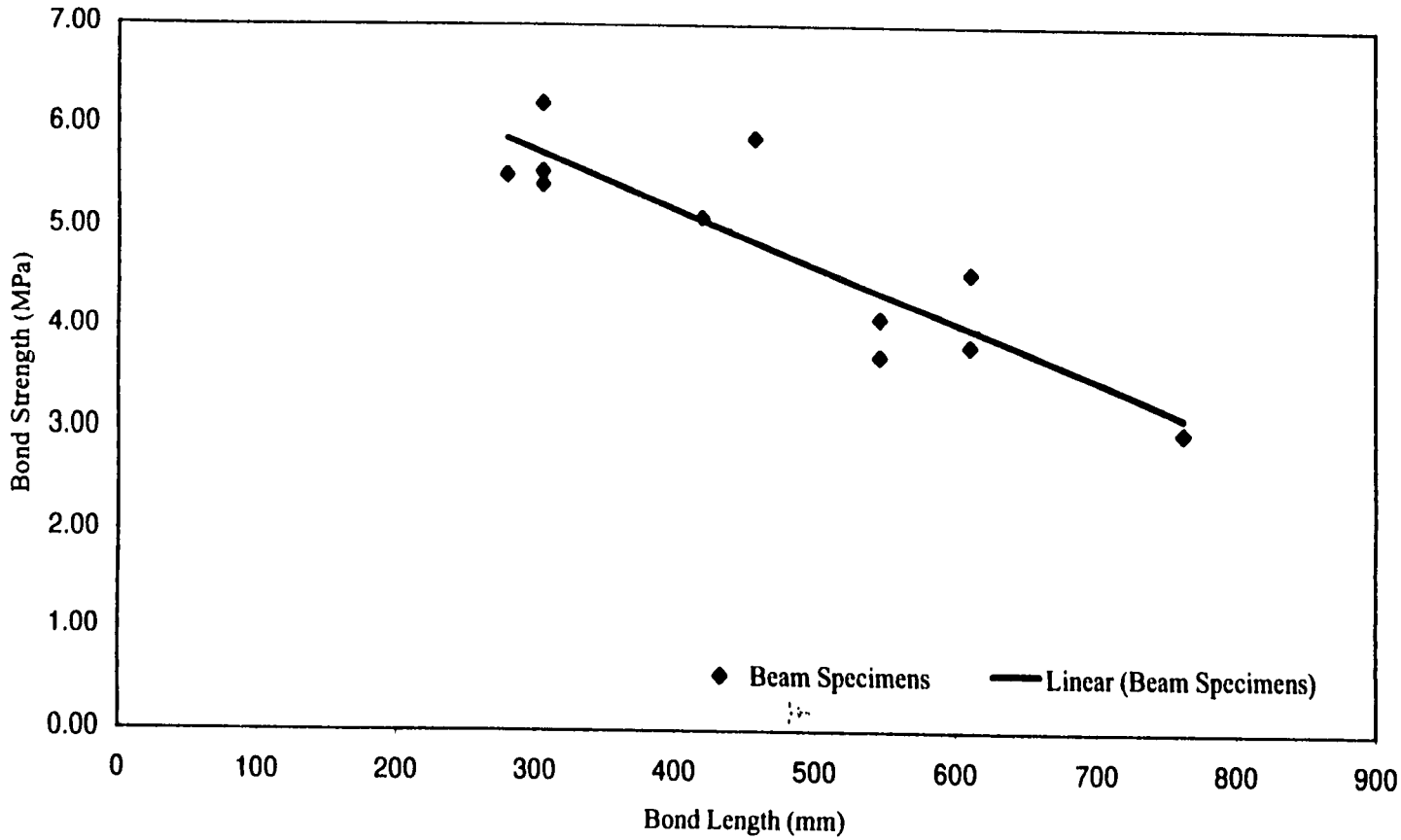

Figure T.1: Bond strength vs. bond length (D1-D9.79 bar, 0.05 mm free-end slip)

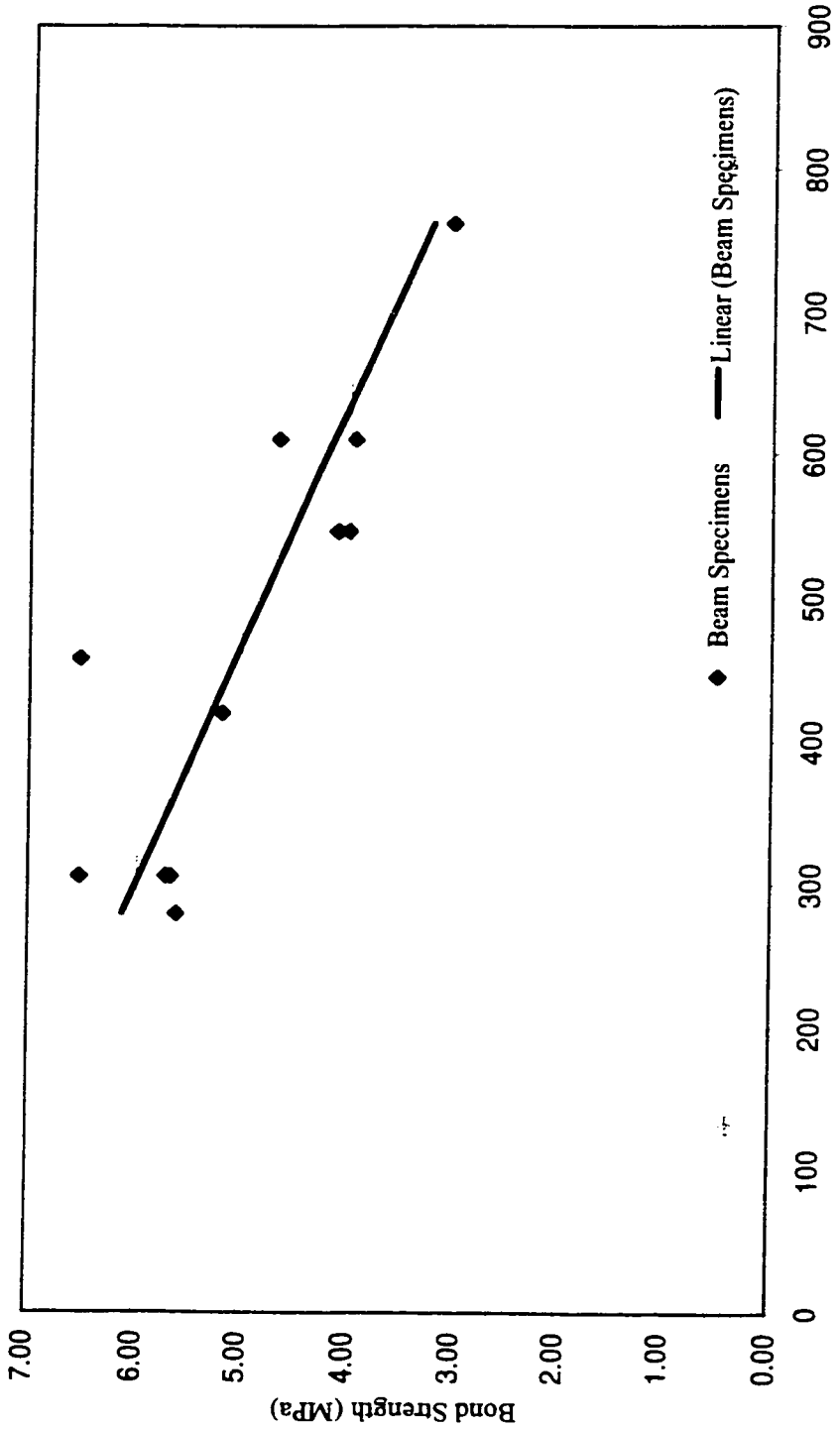

Figure T.2: Bond strength vs. bond length (D1-D9.70 bar, 0.10 mm free-end slip)

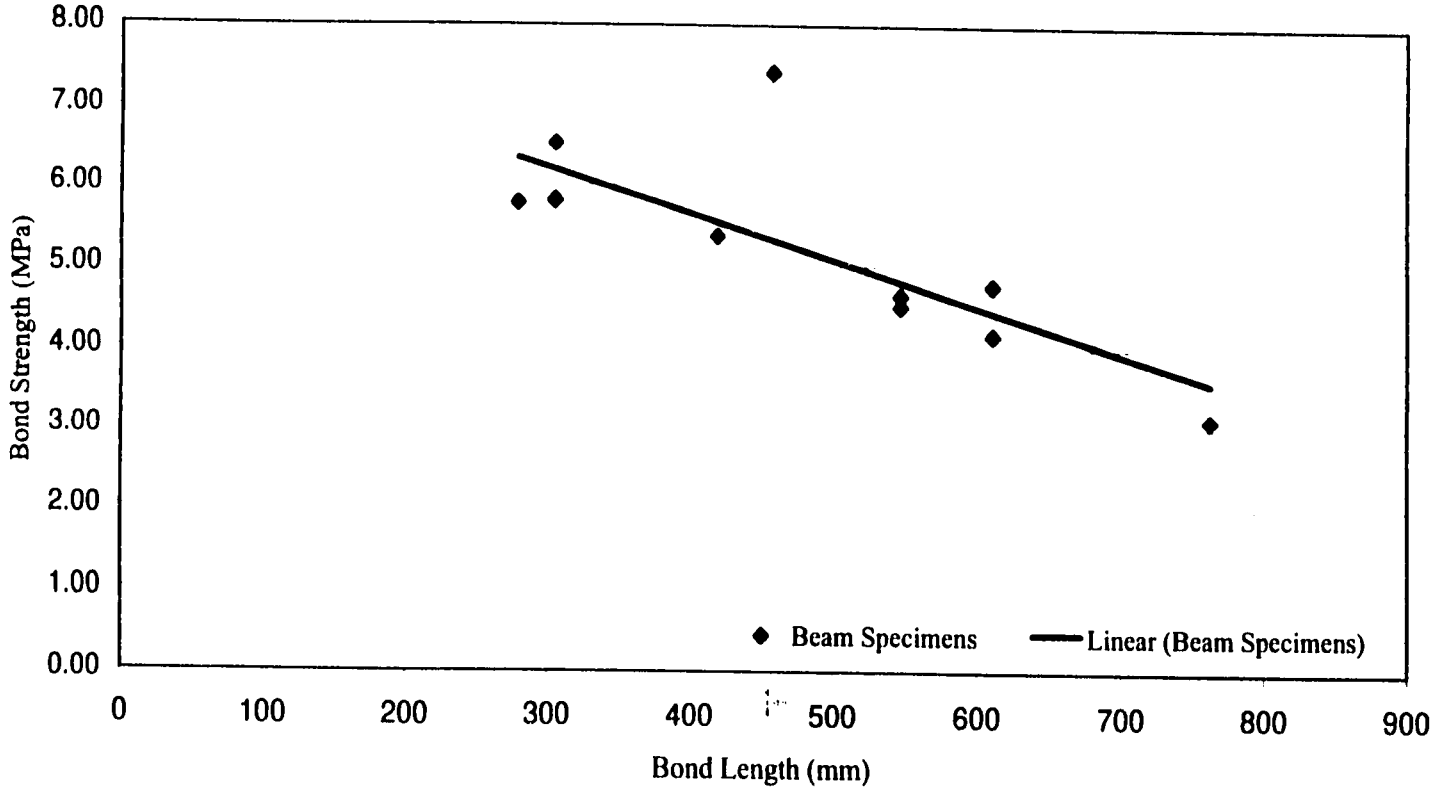

Figure T.3: Maximum bond strength vs. bond length (D1-D9.70 bar, free-end slip)

Appendix U

Bond Strength vs. Free-end Slip (D1-D9.70 Bar)

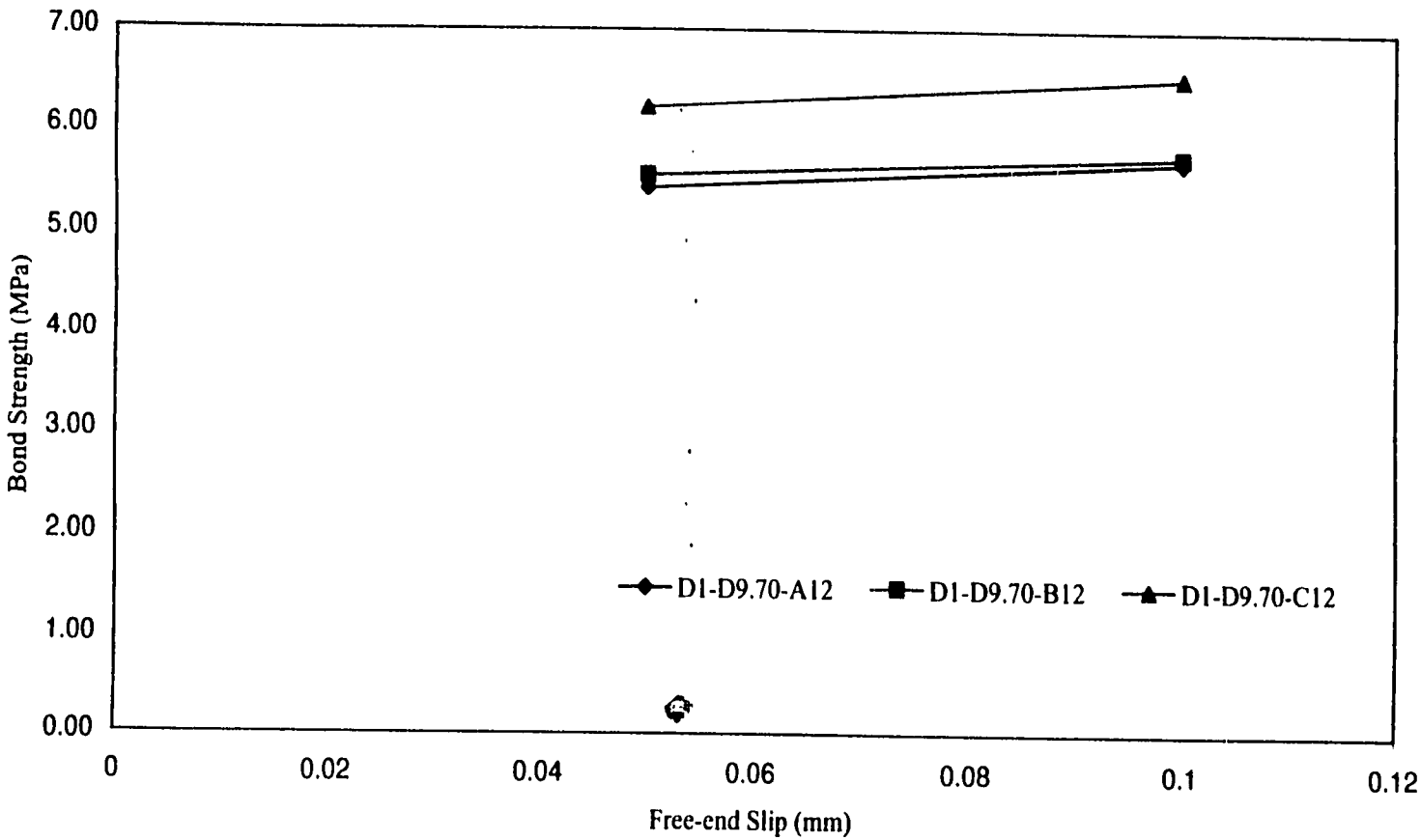

Figure U.1: Bond strength vs. free-end slip of beams D1-D9.70-A12, D1-D9.70-B12 and D1-D9.70-C12

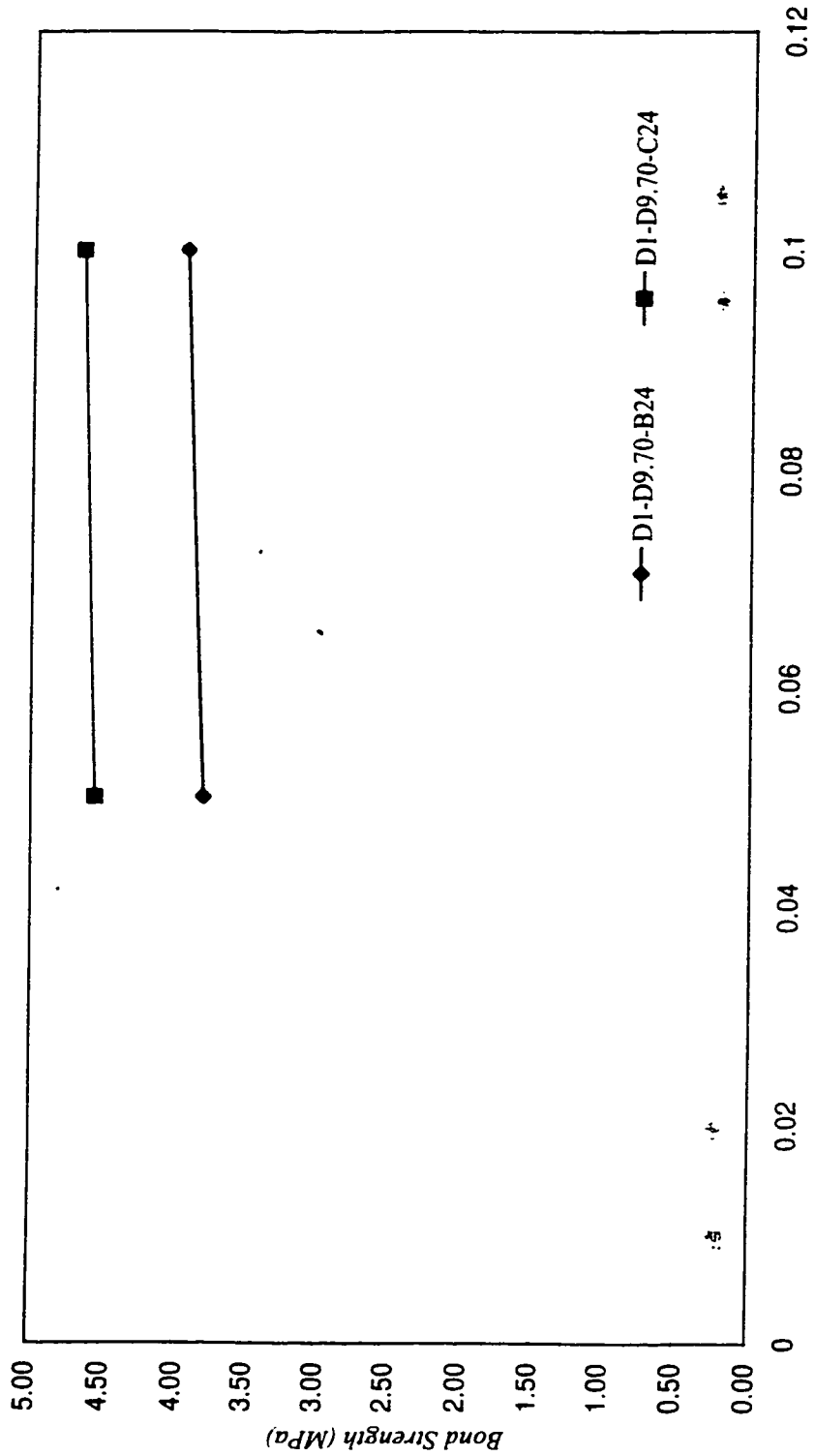

Figure U.2: Bond strength vs. free-end slip of beams D1-D9.70-b24 and D1-D9.70-C24

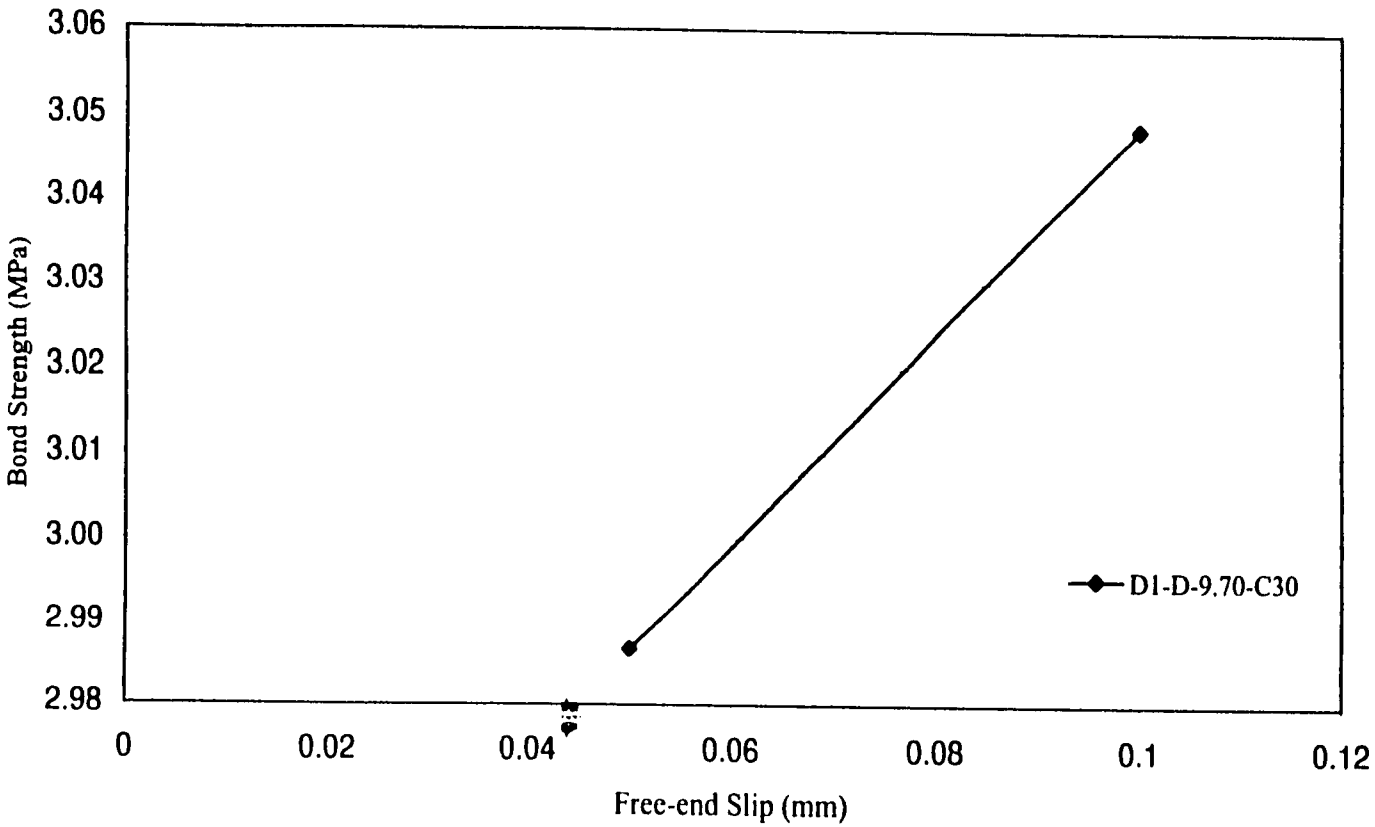

Figure U.3: Bond strength vs. free-end slip of beam D1-D9.70-C30

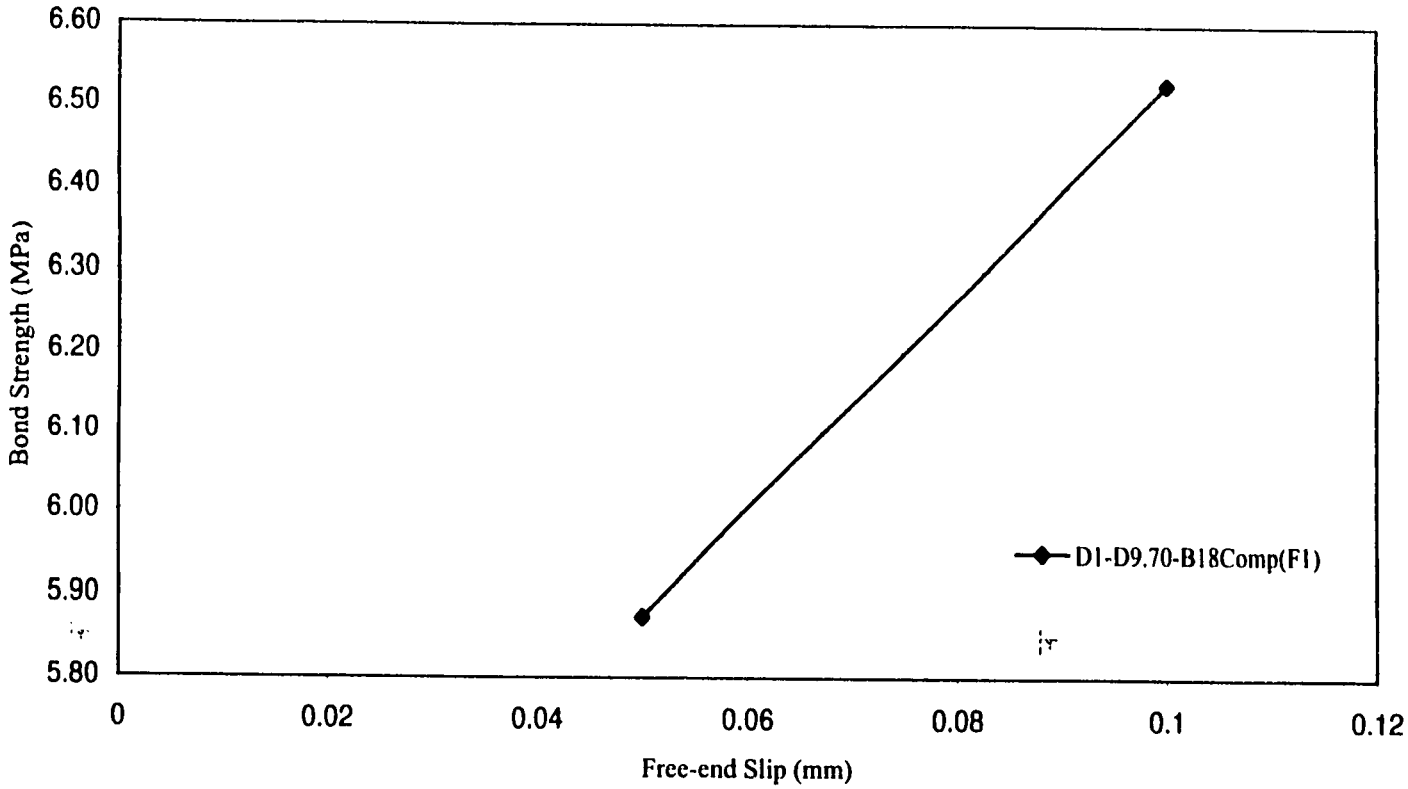

Figure U.4: Bond strength vs. free-end slip of beam D1-D9.70-B18Comp(F1)

Appendix V

Bond Strength vs. $\sqrt{f_c'}$ (D1-D9.70 Bar, Free-end Slip)

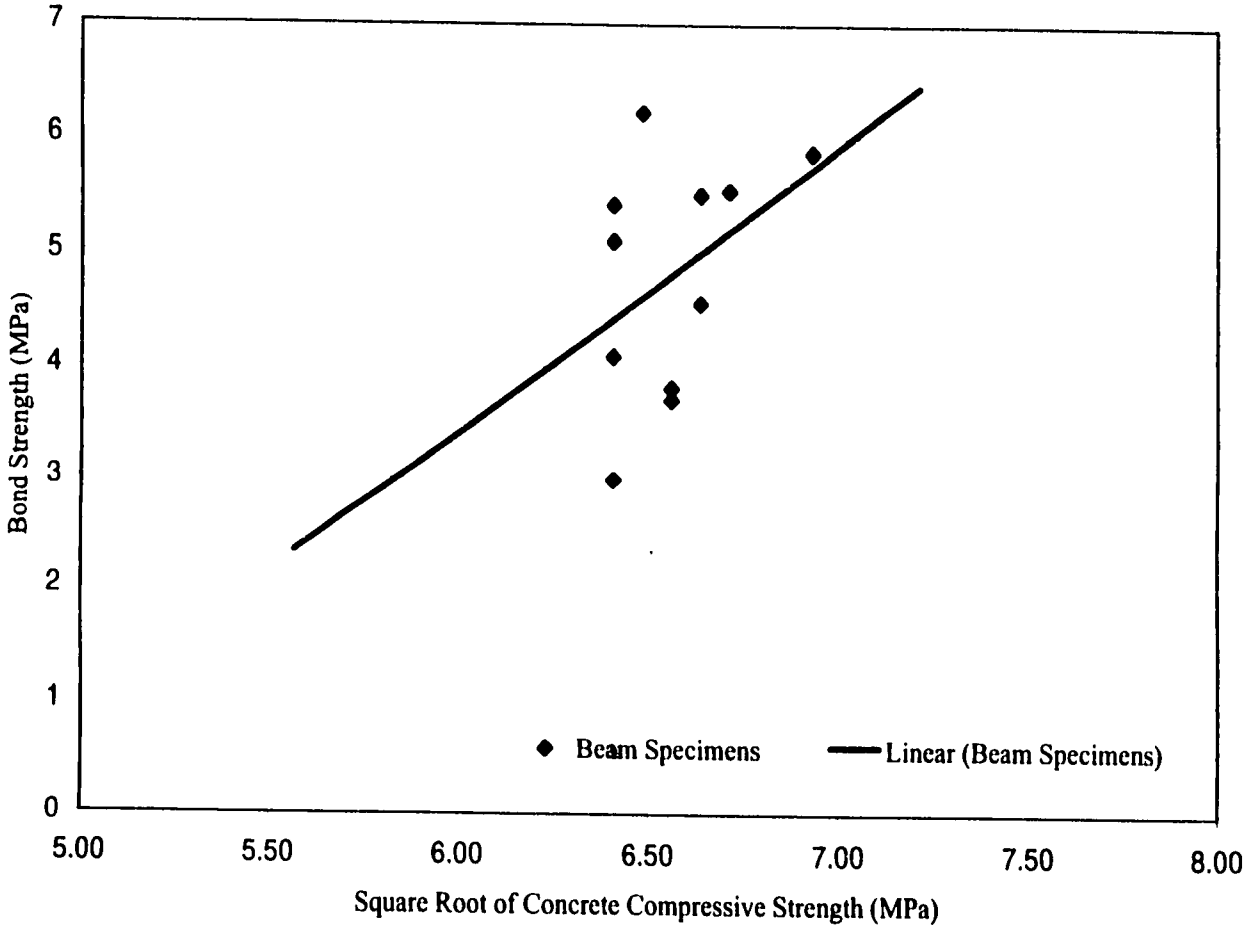

Figure V.1: Bond strength vs. square root of concrete compressive strength (D1-D9.70 bar, 0.05 mm free-end slip)

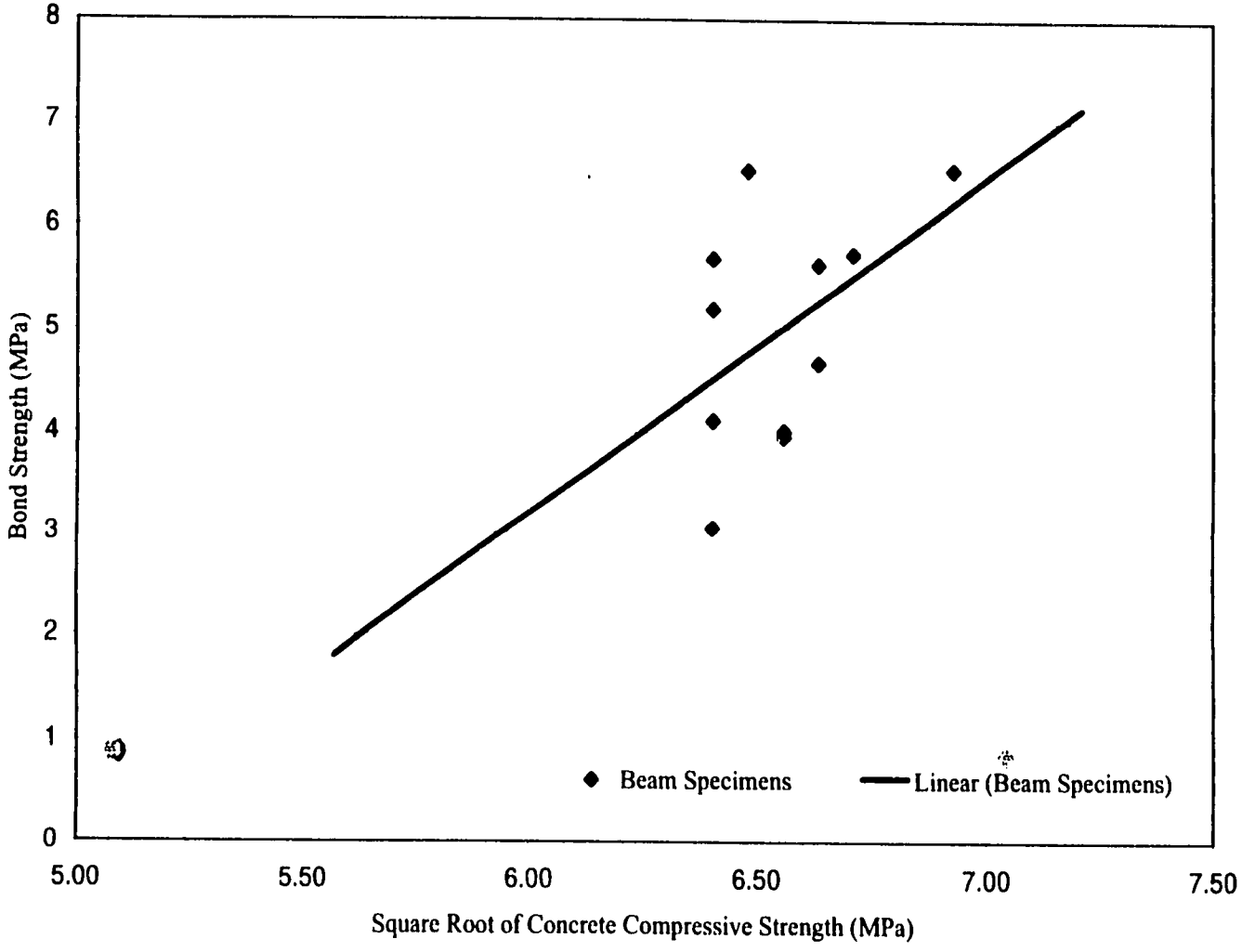

Figure V.2: Bond strength vs. square root of concrete compressive strength
(D1-D9.70 bar, 0.10 mm free-end slip)

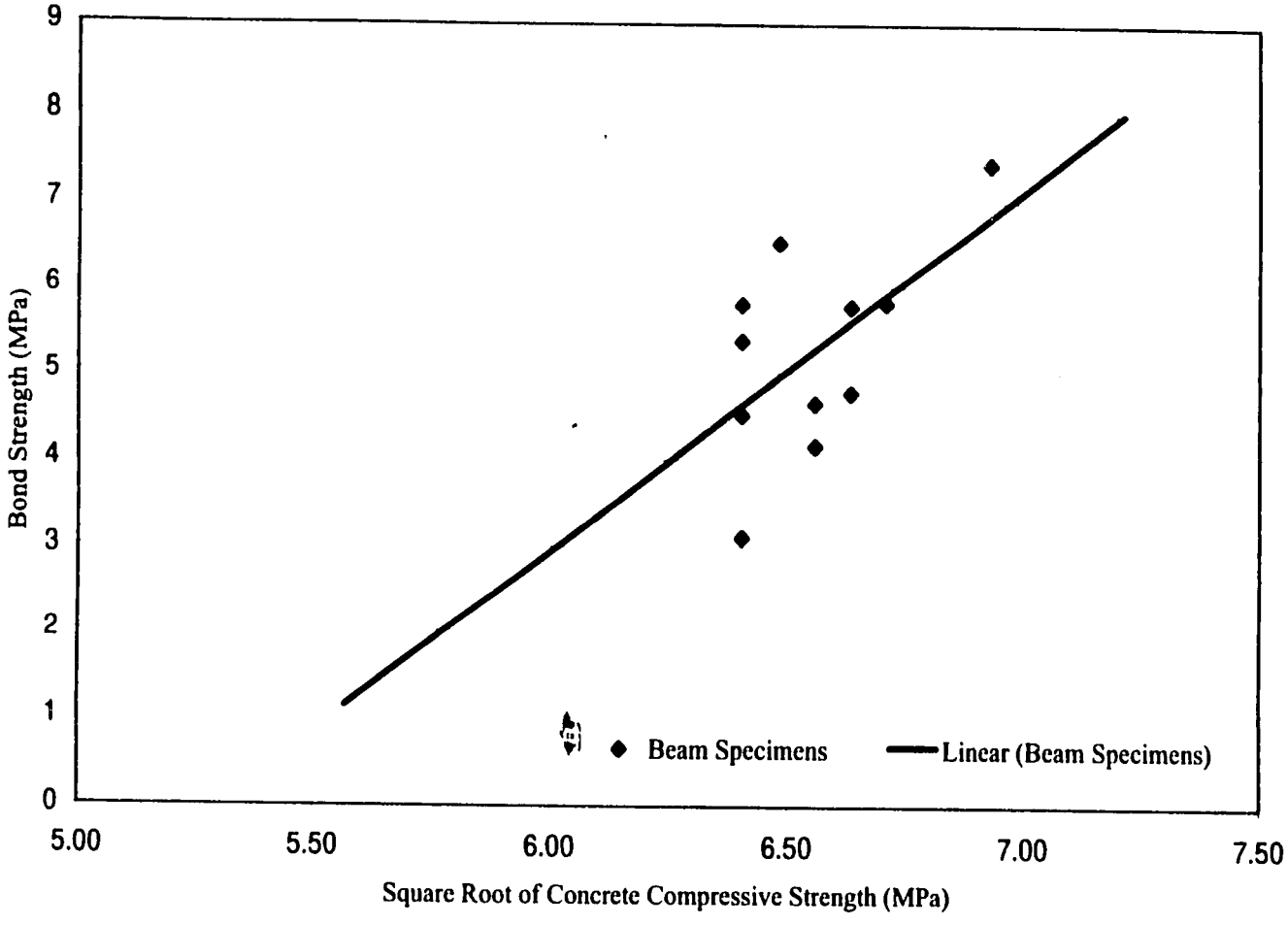

Figure V.3: Maximum bond strength vs. square root of concrete compressive strength (D1-D9.70 bar, free-end slip)

Appendix W

Effect of Transverse Reinforcement on Bond Strength (D1-D9.70 Bar)

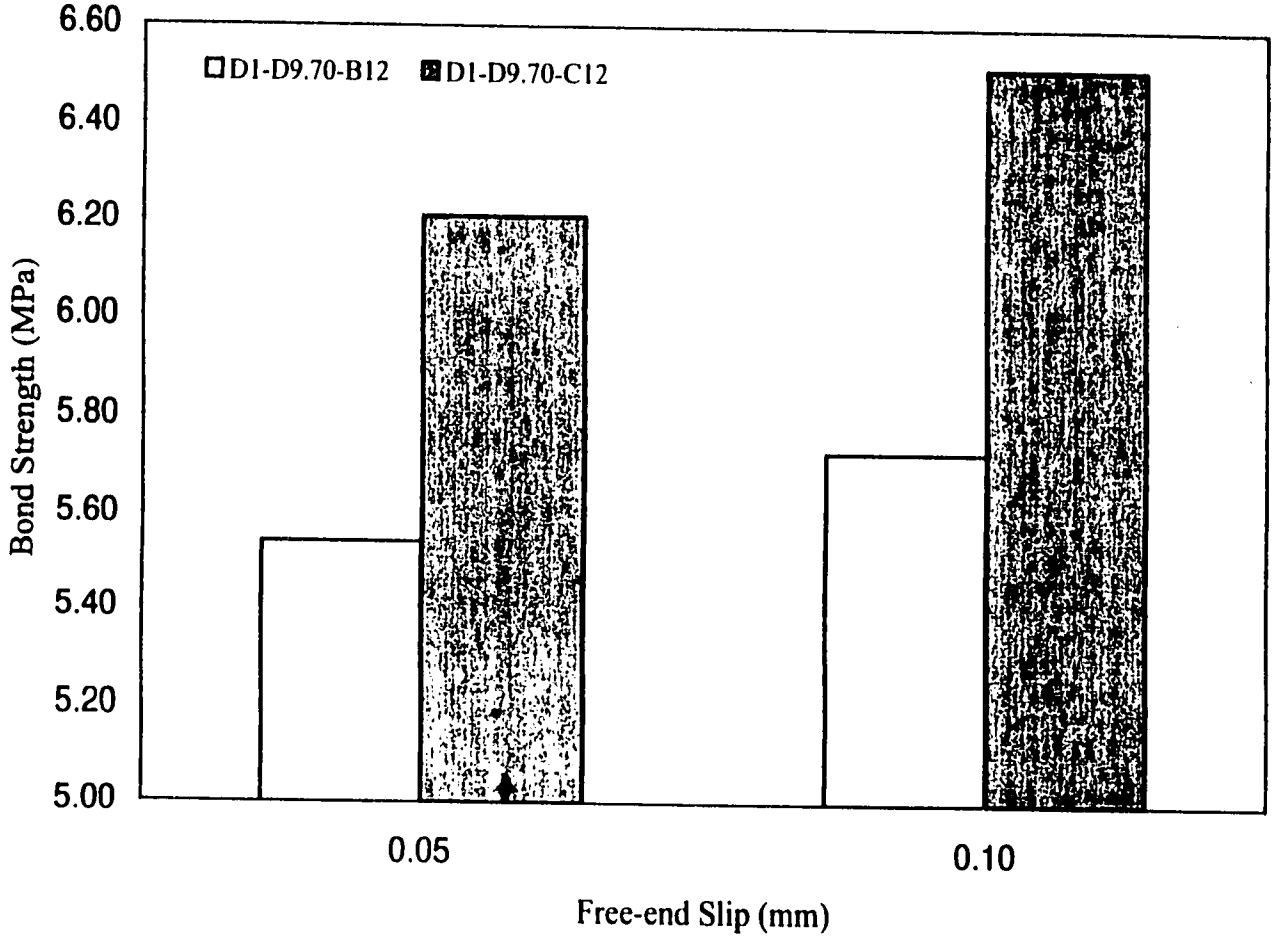

Figure W.1: Effect of transverse reinforcement on bond strength (beams D1-D9.70-B12 and D1-D9.70-C12)

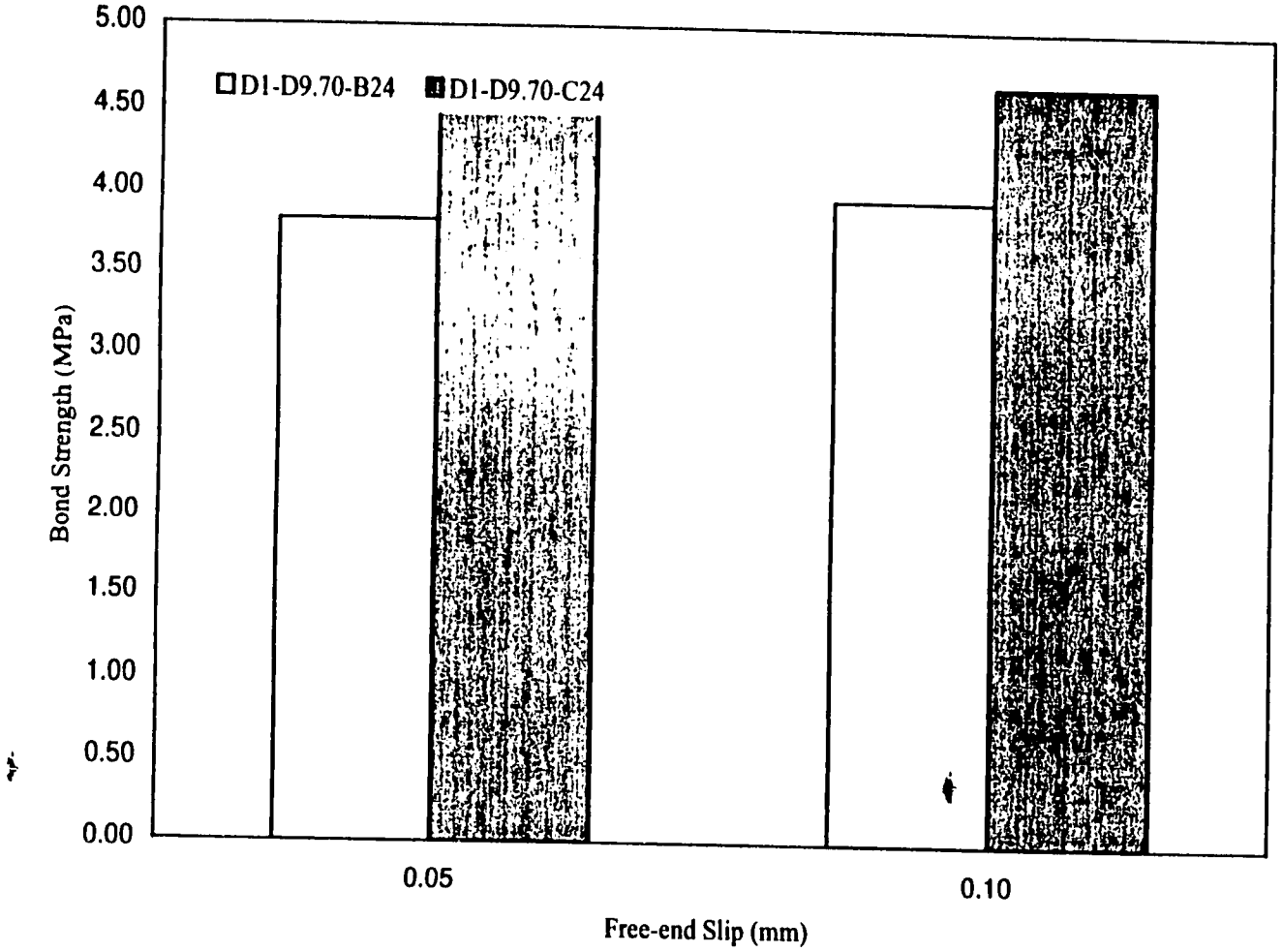

Figure W.2: Effect of transverse reinforcement on bond strength (beams D1-D9.70-B24 and D1-D9.70-C24)

Appendix X

Results of the CFRP Bond Test (Jerrett and Ahmad 1995)

Table X.1: Results of the CFRP bond test by Jerrett and Ahmad (1995)

Test Specimen[1]	Loading Rate, N/ min (lbs/min)	Load at Initial Free-end Displacement[2], kN (kips)	Ave. Load at Initial Free-end Displacement, KN (kips)	Max Load, kN (kips)	Ave. Max Load, kN (kips)	Free-end Displacement at the Max Load[3], mm (in)
6S1	890 (200)	1.80 (0.40)	1.85 (0.42)	1.80 (0.40)	1.85 (0.42)	0.0
6S2	180 (40)	1.47 (0.33)		1.47 (0.33)		0.0
6S3	65 (15)	2.31 (0.52)		2.31 (0.52)		0.0
12S1	130 (30)	2.40 (0.54)	2.43 (0.55)	2.40 (0.54)	2.43 (0.55)	0.0
12S2	130 (30)	1.51 (0.340		1.51 (0.340		0.0
12S3	130 (30)	3.38 (0.76)		3.38 (0.76)		0.0
18S1	130 (30)	4.36 (0.98)	5.20 (1.17)	4.36 (0.98)	5.20 (1.17)	0.0
18S2	200 (45)	5.96 (1.34)		5.96 (1.34)		0.0
18S3	200 (45)	5.25 (1.18)		5.25 (1.18)		0.0
6D1	130/670[4] (30/150)	3.47 (0.78)	3.38 (0.76)	28.0 (6.30)	29.9 (6.73)	6.25 (0.246)
6D2	670 (150)	2.67 (0.6)		29.8 (6.70)		5.13 (0.2020
6D3	670 (150)	4.00 (0.90)		32.0 (7.20)		8.13 (0.327)
12D1	1330/670[4] (300/150)	12.5 (2.8)	14.6 (3.30)	54.3 (12.2)	57.8 (13.0)	6.83 (0.269)
12D2	670 (150)	19.1 (4.3)		57.4 (12.9)		6.82 (0.269)
12D3	1330 (3000)	12.5 (2.8)		62.3 (14.0)		6.64 (0.2610
18D1	1330 (300)	20.5 (4.6)	24.0 (5.40)	74.7 (16.8)	84.5 (19.0)	7.19 (0.283)
18D2	1330 (300)	24.0 (5.40)		84.5 (19.0)		7.10 (0.279)
18D3	1330 (300)	27.6 (6.20)		94.3 (21.2)		8.36 (0.329)

Note:

1. Test specimen nomenclature: 6S1
   - 6 → specimen number
   - S → surface characteristic; S =smooth, D = deformed
   - 1 → embedment length (slab thickness) in inches
2. Defined as the load at which 0.0051 mm (0.002 in.) free end displacement is recorded.
3. Free end displacement recorded immediately prior to bpnd failure.
4. First number indicates an initial load rate up initial free end displacement, the second number is the load rate after initial free end displacement.

VITA AUCTORIS

Ee Yeong Lim was born on October 19, 1976 in Kluang, Johor, Malaysia. He came to Columbia International College, Hamilton, Ontario on January 1995 and obtained OSSD on July 1995. From there he attended the University of Windsor, Windsor, Ontario in the Fall of 1995 and graduated in 1999 with a Bachelor's of Applied Science in Civil Engineering. He began his Master's of Applied Science in Structural Engineering at the University of Windsor in the Fall of 1999.